Characterization of the transcription factor *ANAC058* and its role in suberin regulation

Dissertation

zur

Erlangung des Doktorgrades (Dr. rer. nat.)

der

Mathematisch-Naturwissenschaftlichen Fakultät

der

Rheinischen Friedrich-Wilhelms-Universität Bonn

vorgelegt von

Katharina Markus

aus

Köln

Bonn, Februar 2018

Angefertigt mit Genehmigung der Mathematisch-Naturwissenschaftlichen Fakultät der Rheinischen Friedrich-Wilhelms-Universität Bonn.

1. Gutachter: Dr. Rochus Franke
2. Gutachter: Prof. Dr. Volker Knoop

Tag der Promotion: 14. 06. 2018

Erscheinungsjahr: 2018

Contents

List of abbreviations

Physical variables and respective dimensions are abbreviated according to the International System of Units (SI).

The symbols of the chemical elements and the chemical formula of compounds use a molecular formula describing the atom, its abundance and occasionally its charge.

Aliphatic compounds are described with a simplified nomenclature using the number of carbon atoms and the respective substance class the compound belongs to. For example, for icosanoic acid with the formula $C_{20}H_{40}O_2$ C20 acid, C20 fatty acid is used. If aliphatic compounds are unsaturated such as (Z)-octadec-9-enedioic acid and (E)-18-hydroxyoctadec-9-enoic acid (IUPAC), these are abbreviated to C18:1 α,ω-dicarboxylic acid (or C18:1 α,ω-diacid) and C18:1 ω-hydroxy fatty acid (or C18:1 ω-OH acid), respectively.

aa	Amino acid
ABA	Abscisic acid
AME	Analysis of Motif Enrichment
amiRNA	artificial microRNA
approx.	approximately
att	attachment site (recombination sequences attB, -P, -L, -R)
bp	base pair
*ccd*B	control of cell death, DNA gyrase inhibitor
cDNA	complementary DNA
CDS	coding sequence
ChIP	chromatin immunoprecipitation
Col	Columbia
CS	Casparian strip
C_T	cycle threshold
d	day
DBD	DNA binding domain
deion	de-ionized
ΔΔ C_T method	comparative C_T method
DNA	Desoxyribonucleic acid
DNase	DNA nuclease
dNTP	deoxynucleotide
DW	dry weight
ET	enhancer trap
FID	flame ionization detector analysis
FIMO analysis	Find Individual Motif Occurrences analysis
FW	Fresh weight
GC MS	gas chromatography mass spectrometry

GFP	green fluorescent protein
GUS	β-glucuronase
GOI	gene of interest
HLPC	high-performance liquid chromatography
ID	intrinsic disorder
LA-ICP-MS	laser ablation-inductively coupled plasma-mass spectrometry
LB	lysogeny broth
L*er*	Landsberg *erecta*
LRES	lateral root emergence sites
MEME	Multiple Em for Motif Elicitation
min	minute
MoRF	molecular recognition feature
MS	mass spectrometry
MS medium	Murashige Skoog medium
NACBS	NAC binding site
PEG	polyethylene glycol
PCR	polymerase chain reaction
PTFE	polytetrafluoroethylene
qRT-PCR	quantitative reverse transcription polymerase chain reaction
RISC	RNA-induced silencing complex
RNA	ribonucleic acid
RNase	RNA nuclease
RT-PCR	reverse transcription PCR
SD	standard deviation
SOI	sequence of interest
Ta	annealing temperature
TAE buffer	TRIS-acetate-EDTA buffer
T-DNA	transfer DNA
TE buffer	TRIS-EDTA buffer
TF	transcription factor
Tm	Melting temperature
TPT	TRANSPLANTA
TRD	transcription regulatory domain
v/v	volume per volume
w	week
WT	wild type
w/v	weight per volume
X-Gluc	cyclohexylammonium salt

1 Introduction

Plants, being sessile organisms, are affected by various environmental stresses they cannot avoid by changing their location. Water and nutrient availability can be scarce for land plants. Additionally, compared to growth in aqueous conditions, special structures have to provide mechanical stability during plant development. With the evolutionary transition to land, plants started to accumulate lignin-like material (Renault et al., 2017) until various polymers have developed that are deposited in the space between cells, the apoplast. These allow preservation of water and nutrient homeostasis, mechanical stability as well as protection of plant organs (Nawrath et al., 2013). Nutrient and drought stress are predominant factors in agriculture which decrease crop growth and yield. Due to climate change especially abiotic stresses like salt, drought and heat stress are predicted to become more severe in vulnerable regions (Mittler and Blumwald, 2010). Consequently, there is a need for new tolerant crop varieties, able to withstand several stresses simultaneously. Knowledge about apoplastic polymers protecting the plant from water and nutrient deficiency and their transcription factors might provide the tools to enhance stress tolerance and resistance in crops.

1.1 Border tissues as apoplastic diffusion and uptake barriers in plants

Plant apoplastic barriers such as the cuticle, suberin lamella and the Casparian strip (CS) are present in different plant organs and tissues (Nawrath et al., 2013). While the cuticle is localized predominantly in aboveground plant organs, the Casparian Strip and suberin lamella adopt important functions in the root. Localization of the CS is exclusive to roots by definition of the CS structure (Caspary, 1865), whereas suberin is also present in the periderm of potato tubers and bark, in bundle sheaths of C4 plants, in the seed coat and the chalazal region of mature seeds and abscission zones (Nawrath et al., 2013). Suberin is well known for its presence in bark of the oak tree *Quercus suber* (Pereira, 1988). Furthermore, suberin is deposited in response to various biotic and abiotic stresses (Barberon et al., 2016; Krishnamurthy et al., 2009; Ranathunge et al., 2008).

1.1.1 Cuticle

The cuticle consists of the aliphatic polyester cutin and of cuticular wax. It is present in leaves, stems, fruits and flower organs. Specifically, it is deposited onto the outer side of epidermal cells, on top of the primary cell wall (Jeffree, 2006). Effectively, it serves as the barrier between plant and environment and protects the plant against uncontrolled water loss, strong ultraviolet irradiation and pathogens. During plant development it ensures proper organ development and morphology (Hoffmann-Benning and Kende, 1994; Sieber et al., 2000). Cutin is structurally similar to suberin, consisting of long chain fatty acids with different functional groups and glycerol interconnected by ester bonds (Heredia, 2003; Nawrath et al., 2013). The layer of the cuticle which is connected to the primary cell wall, thereby forming a structural continuum, is called the cuticular layer. It mainly consists of cutin and polysaccharides. Depending on the species, the cuticular layer is covered by the cuticle proper which is more hydrophobic due to cuticular wax being interspersed within the structural component cutin

(Jetter et al., 2000). Finally, the outermost layer of the cuticle is the epicuticular wax which can form an amorphous layer or wax crystals (Jeffree, 2006). Composition and ultrastructure of the cuticle can vary considerably between plant species. In general, cuticular wax consists of fatty acids, primary alcohols, aldehydes and alkanes with chain lengths of 20 to 40 carbons and alkyl esters with the chain lengths of 36 to 70 carbons (Nawrath et al., 2013; Samuels et al., 2008). These molecules are not interconnected and can be extracted with organic solvents. In addition to the presence of the cuticle in aboveground organs after germination, it was also observed to cover the surface of the embryo (Panikashvili et al., 2010; Szczuka and Szczuka, 2003; Tsuwamoto et al., 2008).

1.1.2 Casparian strip and suberin lamella in roots

Both the Casparian strip and the suberin lamella are present in the endodermis of roots which serves as the barrier for water and nutrients entering the central cylinder (Barberon, 2017; Naseer et al., 2012). The central cylinder contains the vascular tissue with xylem and phloem cells, necessary for transporting water and nutrients to the shoot. Surrounding the central cylinder is the pericycle, source of lateral root development. Outwards of the pericycle is the endodermis, the cortex and the epidermis (fig. 1.1 C, Dolan et al., 1993). The epidermis serves as the barrier between root and environment, except at the root tip where it is covered by the root cap. Single epidermis cells can grow outwards as root hair cells, allowing the root to increase its surface with which it can take up water and nutrients. The epidermis might also contain diffuse suberin as secondary cell wall modification. However, the diffuse suberin supposedly does not form a continuous lamella (Nawrath et al., 2013). In several plant species such as rice, an additional cell layer beneath the epidermis, called the hypodermis or exodermis provides another suberized and possibly lignified cell layer (Schreiber et al., 2005). Once the root enters the secondary growth stage, the vascular tissue of the central cylinder, including xylem vessels, expands and makes up most of the root (fig. 1.1 B). The pericycle cell layer becomes meristematic and is called cork cambium or phellogen (Dolan et al., 1993; Nieminen et al., 2015; Vishwanath et al., 2015). It serves as the boundary between the vascular tissue and the peridermal tissue. Presumably it has a similar function as in the shoot where it is essential to producing bark tissue (Martin and Crist, 1970). The phellogen gives rise to cork cells (phellem) towards the outside of the plant organ (Martin and Crist, 1970; Miguel et al., 2016). Either the phellem or the entire non-vascular tissue is called periderm or peridermis. The periderm serves as the protective barrier tissue in older roots and contains suberin (fig. 1.1 B, Höfer et al., 2008; Nawrath et al., 2013a; Ranathunge and Schreiber, 2011).

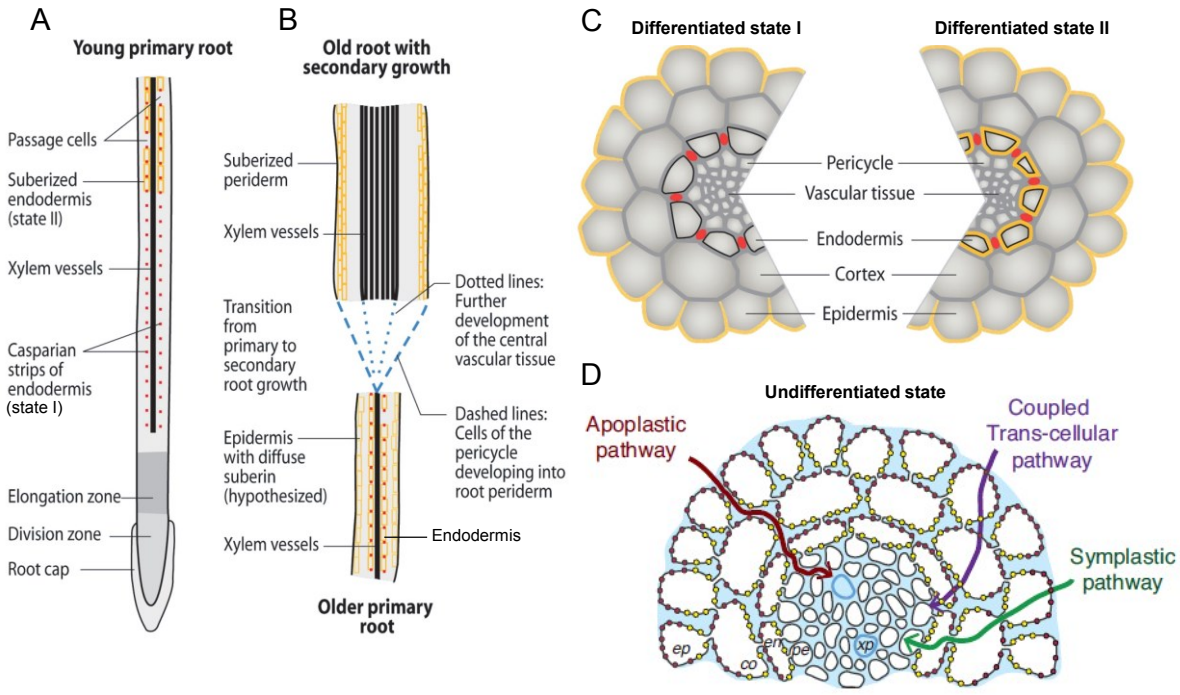

Fig. 1.1 Root structure at different developmental stages with suberin lamella, Casparian Strip and uptake pathways in dicots

Young roots in the primary growth phase (A and B, primary root) contain the endodermis in three different stages of differentiation (undifferentiated (D), state I and state II (C)). In the elongation zone (A) it is present in the undifferentiated state (D) where nutrients and water can cross the root and reach the central cylinder with the vascular tissue by way of three different pathways: the apoplastic pathway, the coupled transcellular pathway and the symplastic pathway. With deposition of Casparian strips (red dots in A - C) the endodermis reaches differentiation state I (A, C root on the left). Diffuse suberin in the epidermis (C) may already be present. The endodermal deposition of suberin marks the differentiation state II of the endodermis (yellow suberin lamella surrounding endodermis cells in A, B, C root on the right). With the transition of the root from the primary to secondary growth phase (B, secondary growth), vascular tissue with xylem vessels take up an increasing proportion of the root (see dotted lines in B). The pericycle (phellogen) is localized nearer to the root surface and serves as the meristem of peridermal tissue (see dashed lines in B). The periderm, the outermost cell layers of roots with secondary growth, is suberized. Red and yellow dots in the plasmamembrane of cells in D display influx (red) and efflux (yellow) carriers. In D: ep, epidermis; co, cortex; en, endodermis; pe, pericycle; xp, xylem pole (A – C altered according to Nawrath et al., 2013, D altered according to Andersen et al., 2015)

1.1.2.1 Casparian strip

The Casparian strip appears close to the root tip, basal of the root elongation zone and marks state I of the endodermal differentiation states (fig. 1.1 A and C). The Casparian strip (CS) as defined by Robert Caspary (Caspary, 1865) forms a ring-like structure in the radial and transverse cell walls of the endodermis and exodermis in most land plants. The model organism *Arabidopsis thaliana* does not produce an exodermis and consequently displays CS only in the endodermis. It fills the apoplastic space between endodermal cells, thereby generating an apoplastic diffusion barrier between tissues outside of the endodermis (cortex and epidermis) and the central cylinder with the xylem vessels (Barberon, 2017, fig. 1.1 C). In *A. thaliana*, CS appears to consist predominantly of lignin (Naseer et

al., 2012), whereas in other species both suberin and lignin were found (Schreiber et al., 1999; Zeier and Schreiber, 1997). Lignin is a polymer consisting of covalently linked aromats and is most known for its presence in wooden structures of trees (Boerjan et al., 2003). Several mutants with defective CS elucidated details of its synthesis and its localized deposition (Baxter et al., 2009; Hosmani et al., 2013; Kamiya et al., 2015; Lee et al., 2013; Li et al., 2017; Pfister et al., 2014; Roppolo et al., 2011). Initially, patches of lignin are formed in a linear manner around endodermal cells which then fuse to the ring-like structure of the CS. For the localization of these patches, correct subcellular localization of CS biosynthesis enzymes is necessary. These enzymes are recruited to Casparian strip membrane domains (CSDs), which, in turn, are formed by Casparian strip membrane domain proteins (CASPs). These CSDs are stable transmembrane scaffolds to which the CASPs recruit *ESB1*, a dirigent protein, *RBOHF*, a NADPH oxidase and *PER64*, a peroxidase (Hosmani et al., 2013; Lee et al., 2013). All three proteins can be connected to lignin biosynthesis. In the vicinity of the CSD two kinases are located, the receptor-like kinase *SGN3* (Pfister et al., 2014) and the receptor-like cytoplasmic kinase *SGN1* (Doblas et al., 2017). Both are involved in the signaling pathway for CS formation (Doblas et al., 2017; Nakayama et al., 2017). In case the CS is defect, ectopic lignification and suberization was observed as long as the *SGN3-SGN1* signaling pathway is intact. This compensatory reaction of the plant indicates the necessity of maintaining intact apoplastic barriers. The Casparian Strip machinery is regulated by the transcription factor *MYB36* which is necessary and sufficient for CS formation (Kamiya et al., 2015).

1.1.2.2 Suberin lamella

With the deposition of suberin in the endodermis, the endodermal differentiation state II is reached (fig. 1.1 C). Now the apoplastic space around the endodermal cells contains suberin as well as the CS.

Suberin is a hydrophobic polyester consisting of an aliphatic and an aromatic domain. The aromats, released by dissolving ester bonds, are coumaric and ferulic acid; the aliphatic monomers are long chain fatty acids and their derivatives. A fraction of the aromats seems to contain covalent bonds and is not detectable by treatments dissolving ester bonds, as was shown for potato periderm (Bernards et al., 1995). Additionally, free long chain aliphatics can be extracted from roots with organic solvents (Li et al., 2007b). These may be deposited to serve as waxes or are monomers not yet incorporated into the polymer. Main aliphatic components of suberin are ω-hydroxy fatty acids and α,ω-dicarboxylic acids, whereas primary alcohols and fatty acids are generally present in lower amounts. Occasionally, mid-chain-oxidized or -hydroxylated suberin monomers can be observed (Bernards, 2002). Carbon chain length of the respective monomers can range from 16 to 34 carbons, as has been observed for *A. thaliana* suberin (Franke et al., 2005) but composition can vary between plant species. The aliphatic monomers are interconnected by glycerols, which was determined by incomplete suberin depolymerization (Graça and Santos, 2006). The exact structure of the polymer is not known since only monomers or at most dimers resulting from various depolymerization methods can be identified on the molecular level. Presence of ester linkages was shown with Fourier infrared transform spectroscopy which vanished after depolymerization of suberin (Zeier & Schreiber, 1999). From the available information, several models regarding the 3-dimensional structure of suberin have been

proposed with aliphatic and aromatic domains (Bernards, 2002; Graça & Santos, 2007) and linkage to carbohydrates of the cell wall (Bernards, 2002).

In order to generate monomers of different substances classes and chain lengths, a high number of different enzymes are involved in the biosynthesis of suberin monomers and the formation of the final polymer, several of them still unknown (Li-Beisson et al., 2013). Suberin monomers derive predominantly from a pool of C16 and C18 fatty acids generated in the plastids which are essentially the substrate of all plant lipids (fig. 1.2). In order to elongate the fatty acids, generating the characteristic very long chain fatty acids, the fatty acid elongation (FAE) complex, specifically β-Ketoacyl-CoA synthases *KCS2* and *KCS20* are necessary (Franke et al., 2009; Lee et al., 2009b). Alteration of functional groups and thereby production of fatty acid derivatives needs *FAR1*, *FAR4* and *FAR5* for primary alcohols (Domergue et al., 2010) as well as the hydroxylases *HORST* (*CYP86A1*, Höfer et al., 2008) and *RALPH* (*CYP86B1*, Compagnon et al., 2009) for ω-hydroxy fatty acids. The exact order of most synthesis steps is not completely determined yet and the model might be more flexible in reality than depicted. Presumably, further alteration of ω-hydroxy fatty acids generates α,ω-dicarboxylic acids and α,ω-diols. Acyl chains can be transferred to glycerol by glycerol-3-phosphate acyl transferases (GPATs, Beisson et al., 2007; Yang et al., 2012). The transfer of aliphatic monomers to aromats is conducted by an aliphatic suberin feruloyl transferase (*ASFT*, Molina et al., 2009), fatty alcohol:Caffeoyl-CoA Transferase (*FACT*, Kosma et al., 2012) and further unknown enzymes. Finally, monomers, acylglycerols, alkyl ferulates or polymeric macromolecules are exported from the cell as suberin building blocks into the apoplast. With regard to export mechanisms, only the involvement of ABC transporters has been shown (Yadav et al., 2014). Possibly, lipid transfer proteins as investigated with regard to cutin (DeBono et al., 2009) or exocytosis also play are part in the transport of suberin building blocks to the site of polymerization. In contrast to cutin, the polymer is not deposited on the outside facing site of the primary cell wall but the cell-facing site, between plasmamembrane and primary cell wall (Nawrath et al., 2013). The mechanism responsible for this exact subcellular localization is not known, neither are the polymerizing enzymes. Recently, a peroxidase which is predicted to localize to the apoplast and presumably is involved in covalent linking of suberin-associated aromats has been investigated (Brands, 2014). Visualization of the suberin lamella with electron scanning microscopy reveals a structure with alternating light and dark bands. The electron translucent and electron opaque layers have been ascribed to alternating aromatic and aliphatic domains (Bernards, 2002). Since a suberin mutant which is nearly deficient in the ester-linked aromat ferulic acid still displays the alternating bands in electron microscopy pictures of the root periderm (Molina et al., 2009), further investigation of this structure remains necessary.

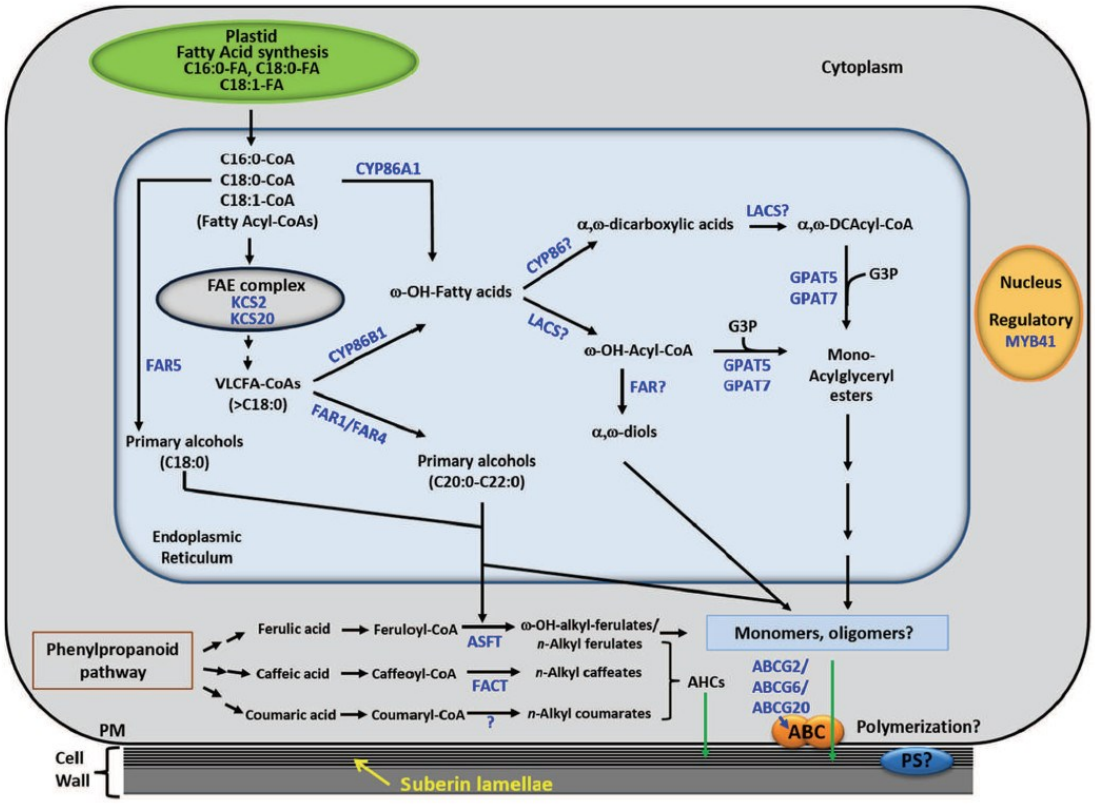

Fig. 1.2 Proposed suberin biosynthesis pathway and subsequent export to the apoplast

Fatty acid (FA) synthesis starts in the plastids, generating acyl chains with carbon chain lengths of 16 and 18 carbons. Those can be imported into the endoplasmatic reticulum (ER) as fatty acyl-CoA. In the ER, acids can be elongated and modified by suberin associated proteins (names in blue are suberin-associated proteins found in *Arabidopsis thaliana*). Fatty acyl elongation is mediated by the FAE complex. *KCS2* and *KCS20* were found to be involved in generation of very long chain fatty acids (VLCFA) with chain lengths above 18. Fatty acids can be hydrolyzed depending on their chain length by *CYP86A1* (*HORST*) and *CYP86B1* (*RALPH*), generating ω-hydroxy fatty acids (ω-OH FA). The same applies to fatty acid reductases *FAR5*, *FAR1* and *FAR4* which produce primary alcohols. Subsequently, α,ω-dicarboxylic acids (α,ω-DCAs) and α,ω-diols are generated. In order to add glycerol to α,ω-DCAs and ω-OH FA, these are activated with Acyl-CoA beforehand and glycerol-3-phosphate acyl transferases (GPATs) then generate monoacylglyceryl esters. Outside of the ER the aromatic components of suberin are produced by *ASFT*, *FACT* and at least one unknown protein. The alkyl hydroxyl cinnamates (AHCs) along with various monomers and monoacylglyceryl esters are transported to the apoplast. ABC transportes *ABCG2*, *ABCG6*, *ABCG20* and possibly other mechanisms are involved. The suberin lamella with characteristic alternating light and dark bands as observed under to electron microscope is deposited onto the plasmamembrane (PM). *MYB41* is a known stress-induced suberin transcription factor. FA, fatty acid; Coenzyme A, CoA; FAE complex, fatty acid elongation complex; KCS, β-ketoacyl-CoA synthase; FAR, fatty acyl-CoA reductase; CYP, cytochrome P450 enzyme; LACS, Long-Chain acyl-CoA Synthetase; *ASFT*, Aliphatic Suberin Feruloyl Transferase; *FACT*, Fatty Alcohol:Caffeoyl-CoA Caffeoyl Transferase, AHC, alkyl hydroxycinnamates; ABC, ATP binding cassette transporter, PS, polyester synthase (Vishwanath et al., 2015).

1.1.3 Effect of Casparian strip and suberin lamella on water and solute uptake into plants

The uptake as well as the retention of water and nutrients is influenced by suberin and the Casparian strip in different ways. Three pathways of water and nutrients uptake are proposed, the apoplastic, the symplastic and the coupled transcellular pathway (fig. 1.1 D, Steudle, 2000). The apoplastic pathway relies on water and solutes passing though the space between the cells, the apoplast, which is filled with a porous network of predominantly cellulose (Peterson & Cholewa, 1998). In the undifferentiated state of the endodermis, this pathway is completely open (fig. 1.1 D). Once the CS fills the apoplastic space between the endodermal cells, the apoplastic pathway is blocked (fig. 1.1 C), as studied with the apoplastic tracer propidium iodide (Naseer et al., 2012). In order to be taken up into the central cylinder, most molecules now have to cross the endodermis by entering the endodermal cells. The symplastic pathway requires solutes and water to be taken up into the cell which is possible at any cell layer, at the earliest by the outermost root hair and epidermis cells. Molecules move towards the central cylinder through the cytoplasmatic continuum as generated by plasmodesmata. These structures connect the cytoplasm of neighboring cells (McLean et al., 1997) and presumably allow molecules to enter the central cylinder uninhibited, regardless of suberin or CS. The plasmodesmata connecting the cortex cells to endodermal cells appear to remain intact through suberin deposition (Ma and Peterson, 2000) but their existence and functionality in the endodermis of *A. thaliana* remains to be investigated. The coupled transcellular pathway combines the apoplastic and the symplastic pathway, as molecules pass partly through the apoplast, are taken up into cells and exit cells again closer to the central cylinder. This pathway relies heavily on ion carriers, aquaporins and their activity as well as their accessibility. Aquaporins are proteins forming channels in plasmamembranes, mainly facilitating water transport (Chaumont et al., 2005). Since suberin is a highly hydrophobic polymer deposited directly onto the plasmamembrane of the endodermis it likely affects uptake of water and nutrients at this cell layer by decreasing transporter accessibility. Therefore the state II of endodermis differentiation with appearance of a suberin lamella in the endodermis might have a predominant effect on the coupled transcellular pathway. *In vivo*, water and nutrients likely switch between pathways and predominance of a particular pathway might be influenced by a couple of different factors, like transpiration.

Impact of root barriers on water and nutrient relations of plants can be investigated with various methods like the uptake of an apoplastic tracer as mentioned before (Naseer et al., 2012) but also by root permeability measurements (Ranathunge and Schreiber, 2011) or analysis of shoot ionomics of relevant mutants (Barberon, 2017). Whole plant water relations depend significantly on plant transpiration which results in a transpiration stream and on root pressure generated by ion accumulation in the root. Increased amounts of suberin in roots were observed to result in a decrease of transpiration rates (Baxter et al., 2009). This ectopic suberization in response to impaired Casparian strips (Hosmani et al., 2013) might result in significantly decreased water uptake in the root and drought-like ABA (abcisic acid) signaling to the shoot, thereby decreasing transpiration. A mutant with wild type suberin amounts but defective Casparian strips displays wild type transpiration rates (Pfister et al., 2014), supporting relations of ectopic suberin and transpiration. All tested mutants impaired in Casparian strip deposition display changes in shoot ionomics (Barberon, 2017). The same applies to a

mutant with strongly decreased suberin amounts and intact Casparian strips. In conclusion, both suberin and the Casparian Strip are necessary for wild type shoot ionomics and likely for upholding of root ion homeostasis. Changes in ion composition might result in impaired ability to generate sufficient root pressure. This was for example observed in a mutant with wild type suberin amounts and impaired Casparian strips as root sap exudation was distinctly decreased (Pfister et al., 2014). Accumulation of Zn^{2+} and K^{+} in the central cylinder of *A. thaliana* wild type root as recently shown (Persson et al., 2016) emphasizes the function of the endodermis as an important barrier protecting against loss of specific ions along a concentration gradient. Ion carriers and aquaporins situated in the plasmamembrane of endodermal cells are probably highly involved in the uptake of the respective molecules. In wild type roots, once the suberin lamella is established only single unsuberized endodermal cells remain, called passage cells (Peterson & Enstone, 1996). These probably facilitate localized water and nutrient uptake into the central cylinder.

Measurement of water and solute permeability of roots with pressure probes or pressure chambers possibly decreases the impact of transporters and transpiration. The roots or root systems are separated from shoots, therefore excluding transpiration as a factor. Still, aquaporins were shown to make up over 80 % of measured root hydraulic conductivity (Tournaire-Roux et al., 2003). When investigating the effect of varying suberin amounts on root hydraulic conductivity (L_{p_r}), lower amounts of suberin seem to result in increased L_{p_r}, whereas ectopic suberin appears to have no effect (Ranathunge and Schreiber, 2011). In case of changes in apoplastic barriers, the proportions of the three pathways involved in water and nutrient uptake might change accordingly as the plant adjusts. The recently revealed plasticity of suberin (Barberon et al., 2016) supports a flexible combination of several mechanisms with which the plant responds to changes in the environment.

1.1.4 Different stresses which induce suberin deposition

Several different biotic and abiotic stresses are known to result in higher amounts of root suberin or additional localized suberin deposition. Among those are drought stress (North & Nobel, 1998; North & Nobel, 1995), salt stress (Barberon et al., 2016; Krishnamurthy et al., 2011, 2009), osmotic stress (Schreiber et al., 1999), water logging conditions (Ranathunge et al., 2011; Shiono et al., 2011) and wounding (Franke et al., 2009; Lulai et al., 1998), as observed in various species.

Salt stress in specific was investigated in relation to suberin multiple times (Barberon et al., 2016; Krishnamurthy et al., 2011, 2009). Plants need to protect against two different components of salt stress. On the one hand there are fast effects, likely caused by osmotic stress and on the other hand the long-term accumulation of salt in the shoot up to toxic levels was observed (Roy et al., 2014). Tolerance of plants to salt stress can be attributed to roughly three different mechanisms: the osmotic tolerance which causes immediate closure of stomata and inhibition of shoot growth, the ion exclusion from the transpiration stream mostly located to the root and, lastly, tissue tolerance. The last mechanism refers to compartmentalization of ions in the shoot at cellular and intracellular level which protects the cellular machinery from toxic ion concentrations. Different species employ different tolerance strategies to different effect. *A. thaliana* is a glaucophyte and highly sensitive to salt (Munns and Tester, 2008). When subjected to NaCl concentrations of above 80 mM it likely will not be able to

complete its life cycle (Volkov et al., 2004). However, the lethal concentration might also depend on the relative humidity and therefore on transpiration rates. The importance of transpiration in stress susceptibility is indicated by a fast decrease of transpiration after NaCl application in *A. thaliana* which was not measured for the closely related halophyte *Eutrema salsugineum* (formely *Thellungiella halophila*, Volkov et al., 2004; Yang et al., 2013). Uptake of NaCl mostly depends on ion transporters (Demidchik et al., 2002; Volkov et al., 2004) and the expression levels of those genes can change depending on salt concentration (Jha et al., 2010). Aquaporin gene expression was also observed to decrease in response to salt stress which limits water uptake and therefore root hydraulic conductivity (Boursiac et al., 2005). This response is rapid, which likely indicates that the plant is reacting to osmotic stress. Furthermore, salt stress causes increased expression of various suberin associated genes, supporting the role suberin has in *A. thaliana* salt tolerance (Domergue et al., 2010; Franke et al., 2009; Lee et al., 2009b; Yadav et al., 2014). Amounts of deposited suberin in *A. thaliana* seedlings are increased within 24 hours after transfer to medium with high salt concentration (Barberon et al., 2016). The function suberin has in salt stress tolerance seem to be two-fold: the fast response indicates a part in osmotic stress resistance but suberin barrier functions also suggest a role in ion exclusion from the transpiration stream by decreasing amount of Na^+ ions that enter the central cylinder.

The correlation of suberin deposition and specifically osmotic stress has been researched less intensively. Experiments were conducted with high concentrations of large molecules like mannitol or polyethylene glycol which are not supposed to enter the plant. They therefore cannot cause toxicity but simulate the osmotic component of drought stress. Osmotic stress did induce expression of suberin associated genes and suberin deposition (Franke et al., 2009; Lee et al., 2009b; Schreiber et al., 1999) but mutants containing lower suberin amounts do not seem to be more susceptible to osmotic stress than the wild type (Beisson et al., 2007). Drought stress resistance on the other hand is increased by high suberin amounts (Baxter et al., 2009; North & Nobel, 1998; North & Nobel, 1995).

1.2 Transcription Factors

Transcription factors are one of the factors regulating gene expression. They are able to influence the gene expression of a specific gene at the transcriptional level by binding to the promoter of the respective gene. Members of one transcription factor (TF) family often bind to specific sequence motifs in the promoter of the target gene. These motifs might also differ slightly or significantly according to TF function. For example, the genes targeted by a TF which was induced by a specific stress might contain a common binding motif in their promoters; the same applies to several genes involved in secondary cell wall synthesis (Tran et al., 2004; Zhong et al., 2010). Transcription factors often exert their function by interaction with multi-protein complexes called co-regulators, which, in turn, can interact directly with polymerases and influence gene expression (Fuda et al., 2009; Lemon and Tjian, 2000). Additionally, several other methods of TFs initiating gene expression are possible.

Complex suberin synthesis and highly localized subcellular deposition in a developmental as well as stress induced manner requires sophisticated control of the suberin machinery.

Transcription factors regulating suberin synthesis and deposition are only partially known until now. In *A. thaliana MYB41* was described as a TF regulating stress-induced suberin deposition whereas developmental deposition appears to be regulated separately (Kosma et al., 2014). Additionally, two transcription factors associated with suberin were detected for seed coat suberin: *MYB9* and *MYB107*, which may be part of a transcriptional feedback loop (Gou et al., 2017; Lashbrooke et al., 2016). Knock-out mutants contain decreased amounts of seed coat suberin but residual suberin remained, indicating additional factors in a possible signaling network. Additionally, regulators of developmental root suberin are still missing since suberin in roots is unaffected in *myb107* and the putative *MYB41* promoter is inactive under control conditions. Additional transcription factors involved in suberin regulation were found in potato (Verdaguer et al., 2016) and apple (Legay et al., 2016). Silencing of the potato *StNAC103* results in increased amounts of suberin and associated waxes in potato tuber skin. Apple *MdMYB93* overexpressed transiently in *Nicotiana benthamiana* leaves causes accumulation of suberin and its precursors. The ortholog of *MdMYB93* is *AtMYB93* which appears to have a role in lateral root emergence (Gibbs et al., 2014; Gibbs and Coates, 2014). The ortholog of *StNAC103* is *ANAC058* which is investigated in this work.

1.2.1 NAC transcription factor gene family

The *NAC* (*NAM*, *ATAF* and *CUC*) gene family constitutes one of the largest plant transcription factor families (Riechmann et al., 2000). The first representative of the gene family was discovered by a mutation in the petunia *NAM* (*NO APICAL MERISTEM)* gene (Souer et al., 1996). The family was defined by Aida and coworkers working on the *cuc1* and *cuc2* mutants (*CUC*, *CUP SHAPED COTYLEDON* and *ATAF*, *ARABIDOPSIS TRANSCRIPTION FACTOR*, Aida et al., 1997). It consists of over 100 genes in *A. thaliana* (Jensen et al., 2010; Olsen et al., 2005a; Ooka et al., 2003) which share the conserved NAM domain in the N-terminal part of the protein, the DNA binding domain (DBD, fig. 1.3). The C-terminal domain serves as the transcription regulatory domain (TRD) and is characterized by a high degree of disorder and nearly no conservation of structures. This structural order of N-terminal DBD and C-terminal TRD can be found in typical NACs, whereas members of the family can also exhibit either N-terminal extensions, a change in the order of DBD and TRD, or two TRD might appear in tandem (fig. 1.3 A).

The NAM domain or DNA binding domain (DBD) itself consists of 5 different subdomains (A – E, fig. 1.3 B). Only domains A, C and D are highly conserved among NAC genes of different species, whereas domains B and E are more diverse (Ooka et al., 2003; Shen et al., 2009). The DNA binding qualities of the DBD were observed (Olsen et al., 2005b) with binding determinants expected in subdomains C and D (Chen et al., 2011; Ernst et al., 2004; Olsen et al., 2005b; Puranik et al., 2012). The DBD adopts a unique tertiary structure with a twisted antiparallel β-sheet which is flanked by α-helices as determined with crystallography (Chen et al., 2011; Ernst et al., 2004; Puranik et al., 2012) and binds DNA with exposed basic residues (Ernst et al., 2004). DBD is also essential for dimerization which is necessary for DNA binding (Olsen et al., 2005b). NACs have been observed to

form both homodimers and heterodimers (Ernst et al., 2004; Olsen et al., 2005b; Xie et al., 2000). Several NAC binding sites (NACBS) in the promoters of target genes are known (Shao et al., 2015). Furthermore, the NAC domain also seems to contain the nuclear localization signal (Ernst et al., 2004; Greve et al., 2003; Ng et al., 2013) and may modulate additional protein binding (Greve et al., 2003; Xie et al., 2002).

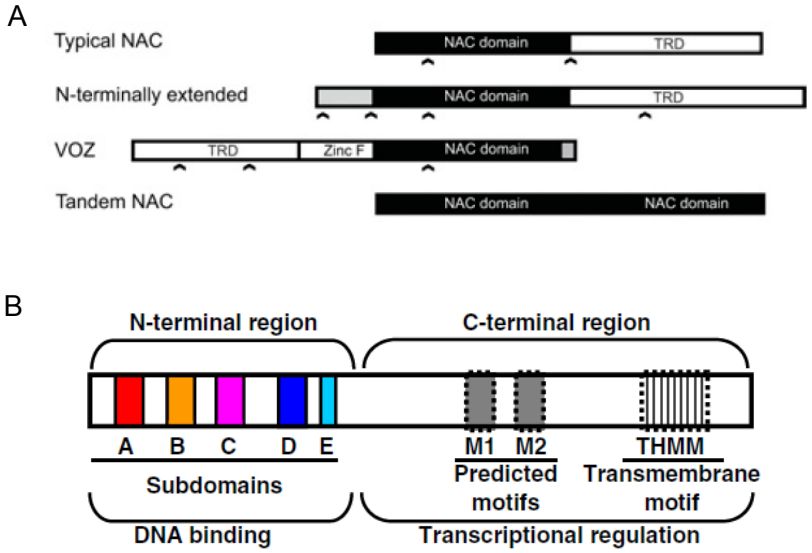

Fig. 1.3 Domain structures of NAC proteins

The NAC gene family is classified according to the highly conserved NAC domain (A, black bar) which is predominantly present in the N-terminal part of the protein (typical NAC) but placement can vary. The NAC domain, responsible for DNA binding has 5 conserved subdomains (B, subdomains A – E). The C-terminal region necessary for transcription regulation (in A, transcription regulatory domain (TRD)) can contain motifs (exemplarily pictured here as M1 and M2) and a transmembrane motif. The status as structures of low conservation is represented by dotted lines. Positions of introns are indicated in A by black arrowheads and the figure is not drawn to scale. Image in A was provided by Jensen and coworkers (Jensen et al., 2010), image in B by Shen and coworkers (Shen et al., 2009).

Tertiary structure of the TRD on the other hand was not determined by crystallography due to intrinsic disorder (ID). ID refers to an absence of a stable tertiary structure and intrinsically disordered protein domains often adapt fluctuating secondary structures (Dyson and Wright, 2005) which allow increased flexibility regarding binding partners and interaction potential. Measurement with size exclusion chromatography suggests an average conformation corresponding to pre-molten globules for several TRDs (O'Shea et al., 2015). Intrinsically disordered proteins can fold upon binding and might contain additional features like molecular recognition features (MoRFs), preformed structural elements and conserved sequence motifs. Structure of the TRD can be variable with, for example, local regions of increased order within the intrinsically disordered sequence. These local regions can correspond to predicted α-helices (O'Shea et al., 2015) or a transmembrane domain (preformed structural features, Shen et al., 2009). MoRFs are short sequences which can fold upon binding (Vacic et al., 2007)

whereas sequence motifs might be characteristic transcription activation motifs, possibly able to bind a transcriptional apparatus (O'Shea et al., 2015). For NACs, conservation of motifs within phylogenetic groups was observed (Jensen et al., 2010; Ooka et al., 2003).

The variability between protein structures and the flexibility of single NACs corresponds to the high diversity of function which was observed for the gene family. They are involved in developmental processes, senescence, formation of secondary cell walls and abiotic stress response. Among the developmental processes are the development of the apical meristem (petunia *NAM*, Souer et al., 1996) and of cotyledons (*CUC1* and *CUC2*, Aida et al., 1997). In case of senescence, several NACs have been observed to be upregulated during leaf senescence (Breeze et al., 2011). *HvNAC005*, *ANAC013* as well as *ANAC046* have been shown to bind *RCD1* (*RADICAL-INDUCED CELL DEATH1*) (Kjaersgaard et al., 2011; O'Shea et al., 2015). Complex transcriptional regulatory networks are hypothesized to control periderm development, suberization and cell death in poplar bark tissues (Rains et al., 2017) implicating a possible connection between suberin and cell death on a regulatory level. Secondary cell walls consist not only of suberin but, depending on the cell type, can also be composed of cellulose, xylan and lignin. The regulatory network of secondary cell wall biosynthesis in fiber and vessel elements containing the latter polymers comprises MYBs and several NACs like VNDs (VASCULAR RELATED NAC DOMAIN) (Ko et al., 2014; Zhong et al., 2010). Stress related NACs can be involved in ABA signaling, salt and drought stress response (Jensen et al., 2010; Nakashima et al., 2007; Tran et al., 2004). Overexpression of the respective NACs can lead to ABA hypersensitivity or increased salt and drought tolerance. Since suberin deposition in response to stress has been connected to ABA signaling and salt stress (Barberon et al., 2016), as well as drought stress (North and Nobel, 1998), NACs are good candidates for regulation of suberin synthesis and deposition. Consequently, a NAC transcription factor has been investigated in detail in this thesis.

1.3 Aims of this work

Apoplastic polyesters have important functions in plants regarding water and nutrient homeostasis. Neither uptake of both water and nutrients into the root, nor their retention under unfavorable conditions has been completely elucidated. Several uptake pathways of water and solutes have been proposed but the extent of each pathway's participation in uptake mechanisms is not known, neither is the exact contribution of suberin and the Casparian strip. Transcription factors might allow alteration of polyesters amounts by influencing expression of all involved proteins. Furthermore, the suberization machinery in all its details is still not entirely resolved. Mutants with altered expression of transcription factors can help reveal downstream and target genes, as these might be subsequently effected.

Several transcription factors are known regulators of suberin but genes involved in the regulation of developmental root suberin are still unknown. As *ANAC058* appears to be co-expressed with various suberin associated genes, the aim of this work is therefore the investigation of its function regarding regulation of suberization. Furthermore, its role in maintaining physiological barriers is of interest. Preliminary results indicate that *ANAC058* expression increases under suberin inducing conditions,

one knock-out mutant showed decreased suberin amounts and overexpression of *ANAC058* in leaves results in increased expression of suberin genes (Frenger, 2014). A reporter construct consisting of the putative *ANAC058* promoter driving the expression of the green fluorescence protein (*GFP*) and the *β-glucuronidase* (*GUS*) gene is intended to reveal cell-specific localization of promoter activity. Expression analysis is supposed to show organ-specific expression. Additional mutants with altered *ANAC058* gene expression as provided by public databases will allow further investigation of the suberin phenotype. For obtaining additional mutants, the RNA interference method can be applied, generating knock-down mutants. The phenotype of overexpression mutants might further reveal *ANAC058* function. All mutants should be investigated with regard to *ANAC058* expression, expression of suberin genes and suberin deposition. The suberin phenotype is intended to be determined with gas chromatography and histological staining with suberin-specific dyes. A physiological impact of observed suberin phenotypes can be determined by subjecting the mutants to environmental stress conditions and observing their subsequent growth.

2 Materials and Methods

2.1 Materials

2.1.1 Chemicals

All used chemicals were of analytical grade quality or higher. Chemicals were obtained from Carl Roth (Karlsruhe, Germany), Thermo Fisher Scientific (Waltham, Massachusetts, USA), Merck (Darmstadt, Germany with Sigma-Aldrich, Munich, Germany), Honywell (Morristown, New Jersey, USA, with Honeywell Riedel-de Haën™ and Honeywell Fluka™, Seelze, Germany), VWR (Radnor, Pennsylvania, USA) and CHEMSOLUTE® (Th. Geyer, Renningen, Germany) if not otherwise indicated. Products for molecular biological applications, including kits, were supplied by Macherey-Nagel (Düren, Germany), Peqlab (Erlangen, Germany), Bio-Rad (Hercules, California, Germany), Invitrogen (Thermo Fisher Scientific, Waltham, Massachusetts, USA), Kapa Biosystems (Wilmington, Massachusetts, USA as part of Roche, Basel, Switzerland), Bio-Budget (Krefeld, Germany) and New England Biolabs (Ipswich, Massachusetts, USA). The vector pBGWFS7 (Karimi et al., 2002) was obtained from VIB vzw (Gent, Belgium) using the website https://gateway.psb.ugent.be/.

Water used in molecular biological experiments, including microbiological applications, media and growth solutions was deionized (H_2O_{deion}) and autoclaved before use. Buffer, various solutions and hydroponical nutrient solutions were prepared with H_2O_{deion} as well. For chemical analytical use, water was of analytical grade quality (H_2O_{HPLC}).

2.1.2 Software

Gene scheme showing the genomic organization of *anac058-1* and *anac058-2* loci (fig. 3.11 A) was generated in Excel. Gene sequence visualization, *in silico* localisation of restriction and primer binding sites, mapping of sequencing results and generation of plasmid maps (fig. 8.15 – 8.24, supp.) was done with Geneious R 6.1.5 (Biomatters Ltd, Aukland, New Zealand). For phylogenetic analyses PhyDe (open source, available at http://www.phyde.de/), MUSCLE (Edgar, 2004) and MrBayes v. 3.1.2 (open source, available at http://mrbayes.sourceforge.net/, (Ronquist and Huelsenbeck, 2003) were used (for details, see 2.1.3). Trees were visualized with TreeGraph2 v. 2.047.206 beta (open source, available at http://treegraph.bioinfweb.info/, Stöver & Müller, 2010). Primers were generated with Primer3 (open source http://primer3.ut.ee, Koressaar and Remm, 2007; Untergasser et al., 2012) and QuantPrime (http://www.quantprime.de, Arvidsson et al., 2008). Amino acid sequence alignment (fig. 8.5 C) was visualized with GeneDoc v. 2.7.000 (open source, available at http://www.nrbsc.org/gfx/genedoc/, Nicholas & Nicholas, 1997).

Procession of data from gas chromatography analyses in case of gas chromatography mass spectrometry (GC MS) analyses was conducted with Enhanced ChemStation, MSD ChemStation v. E.02.00.493 (Agilent Technologies, Santa Clara, USA). Data from GC flame ionization detector analysis (FID) was analyzed with GC ChemStation Rev. B.03.02 [341] (Agilent Technologies, Santa

Clara, USA). Chromatograms were visualized including, in case of GS MS analysis, the molecular fragment patterns and in case of the GC FID analyses the peak integration.

Results from quantitative reverse transcription polymerase chain reaction (qRT-PCR) were processed with StepOne Real-Time PCR Systems, version 2.1 (Applied Biosystems, Foster City, California, USA).

Pictures of fluorescence and accompanying bright field as observed with a fluorescence microscope (Carl Zeiss, Oberkochen, Germany) were obtained with a digital camera (DXM-1200, Nikon, Tokio, Japan) using the software Nikon ACT-1 v. 2-70 (Nikon, Tokio, Japan). Binocular microscope pictures were taken with the EOS 600 D (Canon, Tokyo, Japan) digital camera and the software EOS Utility v 2.10.0.0 (Canon, Tokyo, Japan) with interlinked software Digital Photo Professional v. 3.10.0.0 (Canon, Tokyo, Japan). Confocal microscopy and accompanying bright field pictures were obtained and processed with FluoView FV1000 v. 3.0.1.15 (Olympus, Tokyo, Japan).

Digital images from cameras, microscope and scanners were processed with GNU Image Manipulation Program (GIMP) v. 2.8.10 (open source, available at gimp.org).

Length of main root and root sections were measured with ImageJ version 1.48 (public domain, https://imagej.net).

For data processing of up to three data sets (e. g. genotypes or treatments), Microsoft office 2007 (Microsoft, Redmont, Washington, USA) was used, including spreadsheet analysis and statistic analysis. In case of higher numbers of data sets, data were processed the same way, but statistical analysis was conducted with the program R v.3.1.2 (open source, https://www.r-project.org/) using the graphical interface of RStudio v. 0.98.1091 (open source, R Development Core Team, 2008; RStudio Team, 2015).

2.1.3 *In silico* analysis, phylogenetic analysis and databases

In order to identify NAC binding sites in putative promoters of suberin genes, sequences 3000 bp upstream of transcription initiation site of respective genes were downloaded from the Arabidopsis Information Resource (TAIR) database with the bulk data retrieval tool. Sequences were visualized as alignments in PhyDe and the 1500 base pairs upstream of transcription start were selected for further analysis. Genes used for the analyses can be found in table 8.4, supp.. NAC binding sites were treated as motifs, which are short DNA or protein sequences with specific function. Analysis of motif enrichment (AME, McLeay & Bailey, 2010) and Find Individual Motif Occurrences (FIMO, Grant et al., 2011) analysis were conducted with standard settings at the MEME Suite web portal (http://meme-suite.org/ MEME Suite Version 4.12.0, Bailey et al., 2009).

The AME tool searches for relative enrichment of known or user-provided motifs in a set of given sequences by scanning each sequence and computing an odds-score for each position of each sequence. Per sequence the scores are combined according to the average odds score method. The negative control uses the set of the provided sequences with letters of each sequence shuffled. For

this set the average odds score is calculated in the same way as for the sequences of interest. Finally, the average odds scores for the provided sequences and the shuffled sequences are tested by the statistical Rank sum test for significant differences. Motifs with p-values indicating significant enrichment are reported. The motifs used for this analysis were extracted from the Plant Cistrome Database (http://neomorph.salk.edu, O'Malley et al., 2016) as well as from literature (Olsen et al., 2005b; Tran et al., 2004; Zhong et al., 2010) and were typed in at the web portal (http://meme-suite.org/tools/ame).

The FIMO tool scans a set of sequences, like promoter sequences, for individual matches to the provided motifs. Each motif is turned into a log-likelihood position-specific scoring matrix (PSSM) by assigning each position in the motif a likelihood score. These are often visualized graphically as motif logos in which highly frequent and therefore very likely occurring bases or amino acids are represented by large letters. The FIMO algorithm scans each putative promoter sequence and its reverse complement version with the motif's scoring matrix. The final report entails all sequence positions with significant ($p < 1 * e^{-4}$) log odds scores, meaning all significant matches of the provided motifs in the sequences. The p-value for a specific motif occurrence at a specific position in a sequence represents the probability of a random sequence with the same length matching that position of the searched sequence with the same or a better score. If the p-value is below $1 * e^{-4}$, the probability that the site is a functional motif is significantly higher than the site being a random sequence. The same motifs as for the AME analysis were used in this analysis.

Prediction of protein structure and protein characteristics such as localization of α-helices, β-sheets (with PSIPRED v. 3.0, Bryson et al., 2005; Jones, 1999) and disordered protein structure (with DISOPRED3, Bryson et al., 2005) was conducted with tools provided by the PSIPRED server (http://bioinf.cs.ucl.ac.uk/psipred/ Buchan et al., 2013). PSIPRED uses 4 neural networks that are independently trained to recognize secondary structures from amino acid sequences. DISOPRED uses a combination of a machine learning approach, a neural network and a nearest neighbor classifier. All predictors are trained with known disordered proteins. The machine learning approach is based on evolutionary conserved disordered structures, whereas the neural network and the nearest neighbor classifier use data from the PDB (protein data bank, www.rcsb.org Berman et al., 2000) and DisProd (http://www.disprot.org/ Piovesan et al., 2017) databases. Molecular recognition features (MoRFs) are recognized with the prediction tool provided by the MoRFpred server (http://biomine.cs.vcu.edu/ servers/MoRFpred/ Disfani et al., 2012). The prediction is based on a combination of annotations generated by sequence alignment and a prediction model with associated learning algorithms using a custom designed set of sequence derived features. The features contain information about several amino acid and protein properties associated with MoRFs.

For phylogenetic analysis, the TAIR database BLAST tool was used to extract potential *ANAC058* paralogs from the *Arabidopsis thaliana* genome. The *ANAC058* amino acid sequence was used on the TAIR10 protein dataset and the 57 genes with e-values ≤ e^{-44} were selected. Within this set, surplus sequences of those genes appearing several times were excluded. NAC-like proteins were excluded as well and the final set contained 45 sequences (table 8.5, supp.). Sequences were imported into PhyDE and aligned with MUSCLE as implemented within this program. They were re-aligned with

MUSCLE (15 iterations) in Geneious and gaps outside of the sequences were represented with the "?" symbol. The total alignment consisted of 269 characters of which the C-terminal characters 1-169 including gaps (1-156 amino acids of ANAC058 excluding gaps) were selected. As such, only the C-terminal conserved DNA-binding domain (DBD) was used for phylogenetic analysis. The analysis aims to construct the statistically most likely phylogenetic tree for the submitted alignment using mathematical models like the Markov Chain Monte Carlo-based Bayesian inference. The phylogenetic tree was calculated with the program MrBayes which uses this mathematical model. As the amino acid substitution model, the general time reversible (GTR) model with the command `prset aamodelpr=fixed(gtr)` was selected. 2 000000 generations were run with 4 chains, three of them heated. For the burn-in 25 % of all saved trees were selected. The phylogenetic analysis of the *ANAC058* paralogs including the potato *StNAC103* was conducted the same way except for the generation number which was set to 3 000000.

For motif analysis in the N-terminal transcription regulatory domain of NACs within specific phylogenetic groups, the groups 6 and 7 as labeled in fig. 8.3, supp. were selected. In PhyDe an alignment containing the N-terminal transcription regulatory domain of genes belonging to one phylogenetic group was generated. The complete alignment which was prepared previously for the phylogenetic analysis (fig. 8.3, supp.) was used and the DBD (characters 1-169) was excluded. The TRD remains and TRD of relevant genes was used to construct a new alignment which was degapped before Multiple Em for Motif Elicitation (MEME) analysis. Analysis as conducted with the MEME tool (v. 4.12.0, Bailey & Elkan, 1994) of the MEME Suite web portal (http://meme-suite.org, Bailey et al., 2009) discovers novel, ungapped motifs in sequences of an alignment. The default background model was used, a zero-order model of the input sequences. The probabilistic model which the algorithm employs consists of a two-component finite mixture model. One component describes the motif, one component the background. The relative frequency of motifs is estimated and the model is fitted to the actual sequence data set.

2.1.4 Statistical analysis of data

The testing for significant differences between wild type and mutant or control and non-control conditions was conducted with statistical tests. In case of testing 2 to 3 different data sets (different genotypes or conditions), the student's t-test in Excel was used. The following parameters were selected: two-tailed distribution of values for each data set and equal variance for both sets (homoscedasticity). If more groups had to be tested against each other, an analysis of variance (ANOVA command `aov()`) was conducted with a subsequent TukeyHSD test (command `TukeyHSD()`) with the statistical R program.

Both tests output a probability value (p-value) that indicates the probability with which differences between two or more datasets appear by coincidence. Is the p-value low, coincidence is unlikely and differences were determined as significant. Significant differences were defined as p-values of 0.05 or lower and highly significant differences as p-values of 0.01 and below.

2.2 Plants

2.2.1 Genotypes

Plants used in this work belong to the ecotypes Columbia (Col) and Landsberg (La) of *Arabidopsis thaliana* (L.) Heynh. Several closely related accessions of the Columbia ecotype exist, such as Col-0 or Col-8. For Col-0 and Col-8 plants, no differences in any experiments were observed and both were used as wild type plants. L*er*, the genetic background of one of the mutants used in this work is not a true wild type but a descendant from the Landsberg-1 (La-1) wild type with a mutation in the receptor-like kinase *ERECTA* gene (*er*) (Torii, 1996). The mutation results in a growth phenotype leading to compact plants. As such, due to easy handling of the plants L*er* is now widely used as the genetic background for mutant generation and natural variation analyses. Seeds of insertion lines used in this work were obtained from the Nottingham Arabidopsis Stock Centre (NASC, Nottingham, England) and were propagated from the so obtained seeds. Seeds of the ET11247 line were propagated by Marc Frenger (Frenger, 2014) before they were used in this work. A transposon is inserted into the last exon in this line (fig. 3.11 A) and the mutant is designated *anac058-1*. The SALK line SALKseq084913 has a T-DNA insertion in the promoter of *ANAC058* (fig. 3.11 A) and is referred to as *anac058-2*.

2.2.2 Cultivation

For *Arabidopsis thaliana* plants grown on soil, pots with an edge length of 10 cm x 10 cm were filled with Floradur (Floragard, Oldenburg, Germany) or “Goldhumus Bio Pflanzerde” (Erdenwerke Hülskamp, Bösel, Germany) soil and placed in trays. The pots were irrigated with tap water containing the insecticide Confidor WG70 (Imidacloprid, Bayer CropScience, Langenfeld, Germany) as well as mineral fertilizer (Flory 3 15+10+15 (+2), Euflor, Schermbeck, Germany) (8.1, supp.). Seeds were initially sown in high numbers. They were either thinned out after 1 - 2 weeks of growth, leading to 5 plants per pot or, in case of plant transformation, grown densely until inflorescence development. During the first weeks of seedling development a plastic cover was placed over the pots, ensuring high humidity.

For growth of *A. thaliana* under hydroponic conditions, the commercially available Araponics system (Araponics SA, Lüttich, Belgium) was used. Seeds were stratified for 24 h at 4 °C before they were sown on cigarette filters (Slim Filter Size 6 mm, Gizeh, Gummersbach, Germany) according to a method adapted from Lenz and coworkers (Lenz et al., 2013). Cigarette filters were prepared beforehand by removing the paper sheathing of singular filters and piercing them with split canes, washing them twice in ethanol (tech.) and finally in H_2O_{deion} until ethanol was completely removed. Filters were inserted into the seedholders of the Araponics system and several seeds were placed on each filter surrounding the pierced hole. Before the trays of the Araponics system comes into use, seedlings were grown hydroponically for 2 weeks on the cigarette filters in custom-made 120-plant trays. Nutrient solution was prepared as indicated in 8.1, supp.. Trays were closed with plastic covers, generating high humidity conditions for 1 week. When covers were taken off, surplus seedlings were removed in order to obtain one seedling per seedholder. At 2 weeks seedlings were transferred to 18-

plant trays of the Araponics system, ensuring more growth space per plant. Nutrient solution was exchanged once per week.

In order to grow *A. thaliana* seedlings on Murashige Skoog (MS) medium in plates, seeds were sterilized. Up to 10 mg dry seeds were covered with sterilization solution (see 8.1, supp.) in a 1.5 ml tube. The tube was inverted continuously for 10 min and seeds were washed 3 times with ethanol (tech.) under sterile conditions. Ethanol was completely discarded; seeds were dried for at least 2 h and stored in closed tubes. They were sown under sterile conditions on 1 x MS (MS, for Fluorol Yellow 088 staining) or on 1/2 MS medium (for GUS assays, GFP observation, salt treatment). Seeds were stratified for 1-2 d at 4 °C before transfer to climate chambers.

All plants if not otherwise specified were subjected to long-day conditions with a 16/8 h day/night cycle, including 22/20 °C, average relative humidity of 47/64 % and average light intensity of 116/0 µmol m^{-2} s^{-1}.

2.2.3 Stress treatments

In order to induce salt and osmotic stress as depicted in 3.2.5.1, plants were either grown in the hydroponics system or on ½ MS medium.

Salt stress treatment via growth on ½ MS plates was conducted in two ways, germination on or transfer to high salt medium.

Sterilized seeds of wild type and *anac058* mutants were sown on 50 mM NaCl MS medium and growth was observed for 5 weeks. To investigate growth of different genotypes in detail, a representative time-point (10 d after germination) was chosen at which root length of seedlings was determined by measurement of main root length with ImageJ. In case no single main root was discernible, up to three roots were measured and values were summarized.

Effect of salt on seedlings after transfer to MS medium with 50 mM NaCl was tested by growing seedlings for 3 d on MS medium, then transferring them to NaCl medium. Like for seeds germinated on salt medium, plant growth was observed in total for 5 weeks and genotype-specific seedling growth was investigated in a representative manner for 10 d old seedlings. In case several roots instead of one main root were present, up to 4 roots per plant were measured in length with ImageJ and values were summarized. For seedlings with a single main root, length of the root was determined in the same manner.

For both methods and all plants, means and standard deviations were calculated. The student t-test was conducted for testing significant differences between mutant and respective wild type for each treatment.

Osmotic and salt stress was also applied hydroponically. For this experiment, plants were grown in nutrient solution for 25 d. For stress treatment, plants of all genotypes were transferred to nutrient solution with 50 mM NaCl or 1.7 % PEG 8000, whereas control plants were transferred to new nutrient solution. Water potential (WP4C Dewpoint PotentiaMeter, UMS, Munich, Germany) and osmolality

(Osmomat 030, Gonotec, Berlin, Germany) were measured of freshly prepared solutions. The nutrient solution had a water potential of - 0.09 MPa and an osmolality of 0.007 osmol kg^{-1}. Water potential and osmolality of stress inducing solutions were – 0.36 MPa (NaCl solution) and – 0.49 MPa (PEG solution) as well as 0.1 osmol kg^{-1} (NaCl solution) and 0.3 osmol kg^{-1} (PEG solution), respectively. After 4 d of PEG treatment, plants were harvested and fresh weight was determined. Roots and shoots were separated and excess water was dried off of roots with tissue paper. The material was placed on a scale and after 10 s of adjustment time, values were noted. Plant material was stored on PTFE pieces in petri dishes at 60 °C. Once plant material was fully dried, dry weight was measured.

Plants subjected to salt stress via hydroponics were observed for 2 weeks. After 1 week, osmolality of initial solutions was determined and found to be very similar to values measured at the start of the treatment. Solutions were exchanged after approx. 2 weeks in order to reduce fungal pressure. Freshly prepared solutions were also measured with regard to osmolality and values did no differ strongly from osmolality at all other times. Fresh weight and dry weight was determined after salt treatment the same way as for PEG treated plants.

2.2.4 Measurement of root hydraulic conductivity (L_{p_r})

Sample preparation

Root hydraulic conductivity was measured with semi-automated pressure chambers in the laboratory of Prof. Maurel (INRA institute, Montpellier, France). Plants were cultivated in the institute's growth chamber for three weeks. Seeds were surface sterilized, sown on ½ MS and grown in MS plates for 2 weeks. They were then transferred to hydroponics by fixing up to 22 plants in one polystyrene supported raft so roots are submerged in 8 L nutrient solution (see 8.1, supp.). Plants continued to grow in hydroponics for 10 - 12 d. During growth, plants were subjected to long day conditions with a day/night cycle of 16/8 h, 20 °C, 70 % relative humidity and light intensity of 250 µmol m^{-2} s^{-1}.

L_{p_r} measurements

In order to prepare the samples for measurement, plants were freshly collected from hydroponics and roots were cut off just below the shoot. The root system was immersed into nutrient solution deriving from the hydroponic trays of the respective plants (fig. 2.1 A). Their hypocotyl was gently threaded through a combination of a silicon and metallic seal and sectioned again close to excision site to ensure open xylem vessels. The hypocotyl is sealed in a water and air-tight manner inside the seals using low-viscosity dental paste (President Light, Coltene, Altstätten, Switzerland). The dental paste solidifies and, during the measurements, effectively seals the junction of inside and outside of the pressure chamber against air or liquid flow without affecting the root system. The opening of the root system is connected to a high-accuracy flow meter (Bronkhorst, France) which measures the exuded sap flow (J_v) as µl min^{-1} in an automated manner via a LabVIEW-derived application (LabView, National Instruments, Austin, Texas, USA). Pressure is applied to the chamber and consequently to the root system by a controlled flow of nitrogen gas. The pressure protocol consists of a successive application of a pre-treating pressure of 350 kPa and three different measuring pressures of

approximately 320, 160 and 240 kPa (labeled 1 - 4 in fig. 2.1 B). The pre-treating pressure serves to attain a flow-equilibrium for the individual root. In case the flow doesn't stabilize, the next step in the protocol is forced after 10 min. Measuring pressures are applied for 4 - 7 min. Pressure and flow values are saved for each root system every two seconds. Results are analyzed by an in-house Excel formula selecting pressure and flow values only when flow is stable (fig. 2.1 B, stability test graph). Selection was conducted by excluding unstable flow and pressure values from further analysis. Instances when the system is adjusting to external factors like opening the connection to the flow meter (fig. 2.1 B, labeled 5) or air bubbles (fig. 2.1 B, labeled 6) influence measurements and are eliminated from the final data set.

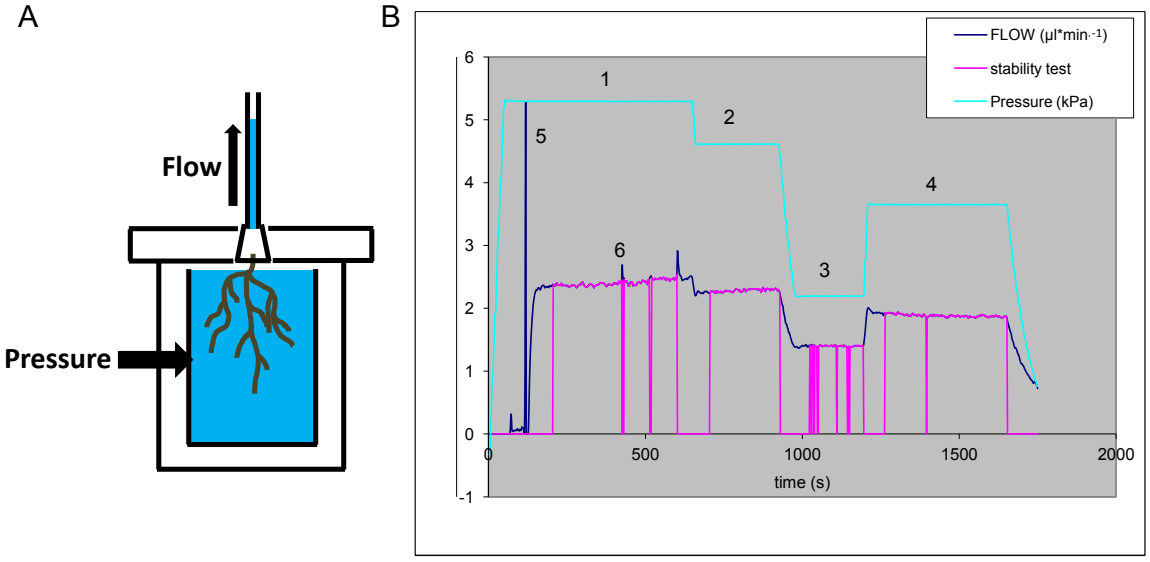

Fig. 2.1 Lp_r measurement details

Model of the pressure chamber (A) as used in the Prof. Maurel's laboratory (INRA, Montpellier, France) is shown. It is depicted a root system submerged in nutrient solution inside the pressure chamber. Pressure is applied to the inside of the chamber by a controlled flow of nitrogen gas. The hypocotyl of the root system is fixed in air-tight seals and the root opening is connected to a flow meter measuring the exudating flow. An example of the measured flow as well as the monitored pressure over time is shown in B. The y-axis displays unit-less numbers since it is used for depiction of flow (µl min^{-1}) and pressure (kPa). The y-axis values correspond to the flow values whereas pressure values were adjusted to be in the range of values measured for flow. The stability test graph marks the selected flow (and corresponding pressure) values according to the sufficient stability of flow values. Four different applied pressures (1 - 4), a spike in flow as the connection between root and flow meter was opened (5) and as an air bubble passes the flow meter (6) are depicted. Image in A was provided by Chloé Champeyroux, based on a model by Yann Boursiac (both from Prof. Maurel's laboratory, INRA, Montpellier, France).

Flow is plotted versus driving pressure, ideally resulting in all data points localized on a trend line representing the linear relationship of flow and pressure. If linearity is not present, the measurement is not taken into further consideration.

Root hydraulic conductivity (Lp_r) was calculated with the following equation (equation 1):

$$Lp_r = \frac{Jv}{DW_r \times P} \quad (1)$$

Lp_r of a single root system was calculated with the slope resulting from plotting sap flow exuded by the excised root system (Jv) against driving pressure (P) which is divided by the dry weight of the respective root system (DW_r) (Javot et al., 2003; Tournaire-Roux et al., 2003).

2.3 Molecular biology methods

2.3.1 Extraction of genomic DNA from plant material

Genomic DNA was extracted from root and shoot material using the peqGOLD plant DNA mini kit (Peqlab, Erlangen, Germany), according the manufacturer instructions. Fresh material was shock frozen in liquid nitrogen, after which it can be stored for indeterminate time at - 80 °C. In order to extract genomic DNA, cell walls are disrupted by grinding frozen material to powder. DNA is separated from cellular debris and subsequently bound to membranes of columns provided by the manufacturer while binding conditions are adjusted. Purified DNA is finally eluted and can be used in further experiments.

2.3.2 Extraction of RNA from plant material

RNA extraction procedure is similar to the way genomic DNA is extracted. In this case the "RNA isolation from plant tissue" protocol of the NucleoSpinR RNA Plant kit (Macherey-Nagel, Düren, Germany) was utilized according to the manufacturer's instructions. Fresh or frozen material stored at - 80 °C was ground in the presence of liquid nitrogen. Immediately after disruption of cell walls, RNases are denatured by adding solutions with large amounts of chaotropic salts and β-mercaptoethanol which dissolves di-sulfide bonds. Conditions are adjusted to bind nucleic acids to the silica membrane of manufacturer provided columns. DNA is digested by addition of rDNase and purified RNA is eluted. For long-term storage RNA was kept at - 80 °C.

2.3.3 Determination of nucleic acid concentration

The concentration in which the nucleic acids were present in solution was measured photometrically. The NanoDropTM 2000c spectral photometer (Peqlab, Erlangen, Germany) was employed for measurements by applying 1 µl of the sample. Concentration of nucleic acid in the sample is calculated specifically for DNA and RNA by selecting the respective extinction coefficient in the program.

In case of expression studies using isolated RNA, similar amounts of total RNA have to be used to compare different samples. Depending on the measured concentrations, samples were diluted with RNase free H_2O_{deion}, until concentrations were approximately the same. Similar concentrations and general RNA quality were confirmed by gel electrophoresis (see 2.3.5) of RNA aliquots. In agarose gels with Ethidium Bromide, 28S rRNA (ribosomal RNA) and 18S rRNA is visualized for samples with sufficient RNA quality. The comparison of band fluorescence intensities of different samples indicates possible RNA concentration differences.

2.3.4 Polymerase Chain Reaction (PCR)

For testing the cDNA quality, semi-quantitative RT-PCR and genotyping of plants and bacteria KAPA2G Fast 2x ReadyMix with Dye (Peqlab, Erlangen, Germany) was used with reaction mix and cycling conditions as depicted in table 2.1. DNA fragments to be used in cloning procedures were amplified with iProof polymerase (Bio-Rad, Hercules, California, USA) as detailed in table 2.2. This polymerase has a 3' - 5' exonuclease activity, thereby allowing proofreading of amplified fragments.

Table 2.1 Protocol for PCR with KAPA2G Fast 2x ReadyMix with Dye

Initital denaturation was conducted for 5 min in case template was genomic DNA and for 3 min for other template DNA. Annealing temperature was approx. T_m (see equation 3, 8.2.2, supp.) of the primer with the lower T_m (either forward or reverse primer) and adjusted as necessary. Extension time was set to 1 s if amplicon length was below 1000 bp. Above 1000 bp, 15 s / 1000 bp were used. Occasionally extension time was adjusted as necessary.

reaction mix	volume [µl]	components
	7.5	2x Ready Mix
	0.75	primer for (10 µM)
	0.75	primer rev (10 µM)
	as needed	DNA
	to 15	H_2O_{deion}

thermo cycler program		temperature [°C]	time	cycles
	initial denaturation	95	template specific	1
	denaturation	95	15 sec	
	annealing	primer specific	10 sec	35
	extension	72	amplicon specific	

Genotyping of bacteria colonies after transformation was conducted with a colony PCR. Bacterial material was taken under sterile conditions from individual colonies by tipping pipette tips gently into the colony, inserting the pipette tip into 10 µl autoclaved H_2O_{deion} and pipetting several times up and down. The shearing forces support opening of cell membranes. Kapa2G polymerase (table 2.1) was

used for amplifying the insert with plasmid-binding primers. In order to ensure opening of cellular membranes of sufficient cells, 1 % Triton X-100 was added to the reaction mix.

For details regarding primer generation, see 8.2.1, supp..

The thermocyclers Primus 96 advanced Thermocycler (MWG-Biotech, Ebersberg, Germany) and Primus Thermocycler (MWG-Biotech, Ebersberg, Germany) were used for all PCRs.

Table 2.2 Protocol for PCR with iProofTM High-Fidelity PCR kit

Annealing temperature was approx. T_m of the primer with the lower T_m (see 8.2.2, supp.) and adjusted as necessary. Extension time was set to 30 s / 1000 bp. (iProofTM High-Fidelity PCR kit, Bio-Rad Laboratories, Inc. Hercules, California, USA)

reaction mix		volume [µl]	components	
		10	5x iProof HF buffer	
		1	dNTP mix (10 mM)	
		2.5	primer for (10 µM)	
		2.5	primer rev (10 µM)	
		0.5	iProof polymerase	
		as needed	DNA	
		to 50	H_2O_{deion}	
thermo cycler program		temperature [°C]	time	cycles
	initial denaturation	95	3 min	1
	denaturation	95	15 sec	
	annealing	primer specific	30 sec	35
	extension	72	amplicon specific	

2.3.4.1 Reverse Transcription (RT)-PCR

cDNA synthesis

Semi-quantitative and quantitative RT-PCR is used to visualize transcript levels of the gene of interest. Before PCR can be conducted, total RNA is transcribed into complementary DNA (cDNA) by use of the Invitrogen SuperScript VILO™ cDNA Synthesis Kit (Invitrogen, Thermo Fisher Scientific, Waltham, Massachusetts, USA) as visualized in table 2.3. The kit provides an enzyme mix including the SuperScript™ III Reverse Transcriptase which generates cDNA in amounts which are linear in relation to RNA concentration. Total RNA is transcribed by use of random primers as provided by the manufacturer.

Table 2.3 cDNA synthesis protocol for the Superscript VILO™ cDNA synthase
Superscript VILO™ cDNA synthase, Thermo Fisher, Thermo Fisher Scientific, Waltham, Massachusetts, USA

reaction mix	components	volume [µl]
	VILO reaction mix	4
	enzyme mix	2
	RNA	as needed
	H_2O_{deion}	to 20
incubation program	temperature [°C]	time
	25	10 min
	42	60 min
	85	5 min
	-20	until further use

Semi-quantitative RT-PCR

From the cDNA, the gene of interest is amplified with gene-specific primers (8.2.3, supp.). The amplicon concentration increases during PCR according to a logarithmic curve. In case of semi-quantitative RT-PCR, PCR is stopped before the end of the logarithmic phase is reached. As a result, amplicon amounts are linear in relation to cDNA amounts and therefore to RNA amounts. As a result, PCR products display transcript abundance of a particular gene in specific plant organs or under defined environmental conditions. Amplicon amounts are visualized by fluorescence intensity via Ethidium Bromide after gel electrophoresis (see 2.3.5).

Quantitative RT-PCR

Quantitative RT-PCR (qRT-PCR) relies on monitoring of amplicon amounts during all times of real time PCR. For the polymerase reaction, the EvaGreen® QPCR-Mix II (ROX) (my-budget, Bio-Budget Technologies, Krefeld, Germany) was used (see table 2.4). The mix contains the EvaGreen dye and an internal reference dye (glycine conjugate of 5-carboxy-X-rhodamine, succinimidyl ester (ROX)). EvaGreen binds to the DNA, forming a fluorescing dye-DNA complex. ROX as the internal reference dye on the other hand ensures that different fluorescence signals don't derive from different reaction mix volumes. Samples were readied in 48 well plates (MicroAmpTM Fast Optical 48 Well Reaction Plate, 0.1 ml, Applied Biosystems, Thermo Fisher Scientific Waltham, Massachusetts, USA) and well plates were covered with a plastic film (MicroAmpTM 48 Well Optical Adhesive Film, Applied Biosystems, Thermo Fisher Scientific, Waltham, Massachusetts, USA) which ensures airtight covering of wells. Fluorescence intensity data were collected throughout the PCR process (table 2.4) for each sample individually by the StepOne™ Real-Time PCR System (Applied Biosystems, Thermo Fisher Scientific, Waltham, Massachusetts, USA).

Table 2.4 Protocol for PCR with 5x QPCR Mix EvaGreen®

5x QPCR Mix EvaGreen® my-budget, Bio-Budget Technologies, Krefeld, Germany

reaction mix	volume [µl]	components
	4	5x Eva Green
	0.1	primer for (50 µM)
	0.1	primer rev (50 µM)
	2	DNA (2.5 - 5 ng/µl)
	to 20	H_2O_{deion}

thermo cycler program		temperature [°C]	time	cycles
	initial denaturation	95	10 min	1 (holding stage)
	denaturation	95	15 s	40 (cycling stage)
	elongation	60	1 min	
	denaturation	95	15 s	1 (melt curve stage)
	elongation	10	1 min	
	temperature gradient	60 - 95	0.3 °C / min	
	final denaturation	95	15 s	

For data analysis the comparative C_T method (ΔΔ C_T method with C_T for cycle threshold) was employed in order to determine the relative target quantity in samples. This method uses the cycle number at which fluorescence crosses a set threshold (C_T) in the amplification plot. The threshold is set in the exponential phase of the amplification curve, as automatically calculated by the StepOne™ Software (Applied Biosystems, Thermo Fisher Scientific, Waltham, Massachusetts, USA) depending on the baseline and the amplification curve. C_T values are given for each well of the 48 well plates. For each sample, three wells are prepared as technical replicates. A housekeeping gene, for example expression of GAPDH is monitored for each investigated genotype or condition as well as for the control.

Data were interpreted according to the manufacturer's instructions with the ΔΔ C_T method, employing the following equation (equation 2):

$$fold\ difference\ in\ expression = 2^{-\Delta\Delta C_T} \qquad (2)$$

Mean C_T and standard deviation was calculated for each sample from the three technical replicates. Mean C_T of the endogenous control was subtracted from mean sample C_T which results in Δ C_T. From Δ C_T of samples of interest (investigated conditions or mutants), Δ C_T of the control (control conditions or wild type) are subtracted for each gene, which gives ΔΔ C_T values. In order to calculate the -fold expression of genes compared to control (fold difference in expression), equation 2 is employed.

2.3.4.2 Organ specific expression analysis

Gene expression in plant organs was investigated in plants grown under different conditions. Leaf and whole root systems were collected from plants cultivated for 4 weeks in hydroponics (2.2.2). Investigation of gene expression specifically in different sections of the root system (3.1.2) was conducted with 5 weeks old plants grown on soil in order to obtain sufficient root material for the analysis. Root systems were quickly cleaned from soil particles under running tap water and arranged as shown in figure 2.2. As indicated by a white line in the same figure, basal and apical root parts were separated with a razor blade. The basal part entailed thickened roots which are subjected to secondary root growth. The apical section consisted of the remaining root system of fine roots. Subsequently, samples were quickly frozen in liquid nitrogen and further prepared as explained in 2.3.2 - 2.3.4.1.

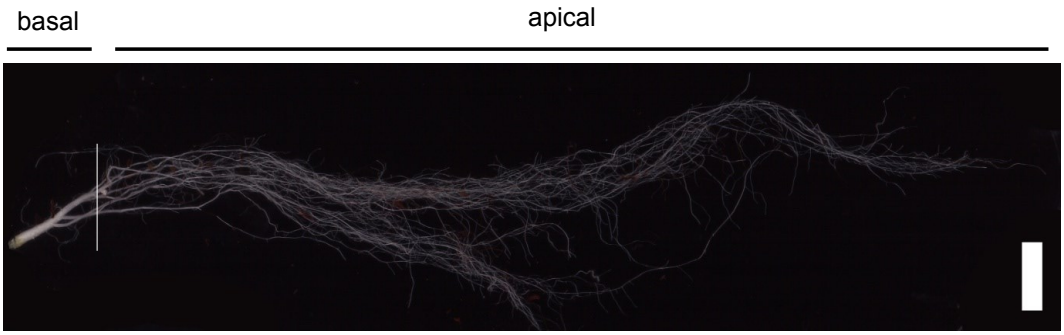

Fig. 2.2 Sample preparation for organ-specific expression analysis
Root system was separated along the white line into a basal section with mainly peridermal suberin and an apical section consisting of fine roots. The scale bar represents 1 cm.

2.3.4.3 Identification of T-DNA insertion and enhancer trap lines

T-DNA and enhancer trap lines both rely on insertion of foreign DNA into the gene of interest and thereby disrupting the native sequence. Genotyping by competitive PCR allows identification of plants either homozygous for the insertion, of wild type plants or heterozygous plants. A set of three primers was used, two of them binding in the gene and one primer binding in the T-DNA or in the enhancer trap (ET) transposable Ds element (Sundaresan et al., 1995). Looking at the gene-binding primers, the forward primer binds upstream of the insertion site, the reverse primer downstream and together they allow the amplification of a gene segment in the wild type. In the mutant, the long foreign DNA between the primers increases their distance to each other which results in an amplicon too large to amplify with standard PCR conditions. The third primer which binds in the foreign DNA is a reverse primer. It allows amplification of a fragment together with the forward primer binding in the gene. The resulting amplicon differs in length from the wild type amplicon, allowing the distinction of wild type and mutant. In case of heterozygous plants, both amplicons are generated.

2.3.5 Gel electrophoresis

DNA amplified by PCR, plasmid fragments generated by restriction endonucleases as well as isolated RNA were visualized in a size dependent manner by gel electrophoresis in the presence of Ethidium Bromide. The gels consist of approx. 0.05 % Ethidium Bromide and agarose in TAE buffer. The agarose polymerizes after boiling into a uniform three-dimensional matrix. Nucleic acid samples are loaded onto the gel with loading dye which was either present in the polymerase reaction mix (Kapa2G) or supplied as aliquots by Carl Roth (supplied with 100 bp DNA-ladder extended, Carl Roth, Karlsruhe, Germany) and added to the final PCR product as needed. DNA is pulled through the pores of the agarose matrix by applying a positive charge to the opposite site of the gel and fragments are retained in a length-dependent manner. Absolute fragment length is evaluated by applying a DNA fragment size marker (100 bp DNA-ladder extended, Carl Roth, Karlsruhe) with the samples and treating both the same.

2.4 Microbiological methods

2.4.1 Transformation of chemically competent *Escherichia coli* cells

In order to amplify plasmid amounts and use generated constructs for further cloning steps, plasmids were introduced into *E. coli* by heat shock transformation. NEB ® 5-alpha Competent *E. coli* (High Efficiency) (NEB, Ipswich, Massachusetts, USA) were employed as chemically competent *E. coli* cells. 50 µl of the cells were thawed on ice and carefully mixed with 10 ng of the plasmid or 2 µl of the Gateway® reaction mix (BP or LR reaction, see 2.5.1 and 2.5.2). Cells with foreign DNA were incubated on ice for 30 min, subjected to a heat shock for 30 s at 42 °C in a water bath and placed for 5 min back on ice. 950 µl SOC medium (supplied with NEB ® 5-alpha Competent *E. coli* (High Efficiency), NEB, Ipswich, Massachusetts, USA) was added afterwards and cells were incubated at 37 °C and 220 rpm for 1 h. Bacteria were plated on LB plates with appropriate antibiotics (50 µg mL^{-1} Zeocin, 50 µg mL^{-1} Kanamycin or 100 µg mL^{-1} Spectinomycin) and were incubated over night at 37 °C. Accordingly, selection with antibiotics allows survival of transformed bacteria with respective antibiotics resistance genes.

2.4.2 Transformation of chemically competent *Agrobacterium tumefaciens* cells

A. tumefaciens strain GV3101::pMP90 was transformed with plasmids via heat shock transformation similar to *E. coli*. 200 µl chemically competent cells were thawed on ice, were carefully mixed with 1 µg plasmid, kept in ice for 5 min, in liquid nitrogen for 5 min and were heat-shocked for 5 min at 37 °C. Afterwards, 1 mL LB medium was added immediately to the cells and the suspension was incubated at 28 °C at 300 rpm for 3 h. After plating the cells on LB with appropriate antibiotics (10 µg mL^{-1} Rifampicin and 50 µg mL^{-1} Kanamycin or 100 µg mL^{-1} Spectinomycin), plates were incubated for 4 d at 28 °C. Accordingly, only successfully transformed *A. tumefaciens* cells, resistant to the antibiotics, were able to grow.

2.4.3 Extraction, restriction and sequencing of plasmid DNA

In order to investigate the genotype after transformation of *E. coli*, plasmids were isolated using the "Isolation of low-copy plasmids" protocol from the NucleoSpin® Plasmid kit (Machery-Nagel, Düren, Germany). Bacteria cells are opened with alkaline lyses, denaturing genomic and plasmid DNA in the process. Conditions are adjusted to allow re-annealing of single stranded plasmid DNA and binding the plasmids to the membrane of the columns. Finally, the remaining cellular debris and genomic DNA are separated by centrifugation. Subsequently, plasmid DNA is eluted and used for further experiments.

To get an estimation of the plasmid sequence after cloning, isolated plasmids were digested with restriction endonucleases according to the manufacturer's instruction for the respective enzyme. The enzymes break the double stranded DNA at specific recognition sequences, generating characteristic DNA fragments that can be visualized by gel electrophoresis (2.3.5) in presence of Ethidium Bromide. Specific restriction enzymes, provided by NEB, were selected according to the plasmid sequence, generating usually two or more fragments per plasmid. In order to confirm correct sequence of the insert cloned into the respective vector, insert was sequenced with plasmid specific primers (8.2.3, supp). Samples were prepared for sequencing according to the instructions of the sequencing service and sequenced by Eurofins Genomics GmbH (Ebersberg, Germany). Genotyping of *A. tumefaciens* colonies was restricted to colony PCR (2.3.4).

2.4.4 Long-term storage of transformed bacteria

Glycerol stocks were generated for *E. coli* and *A. tumefaciens*. A glycerol:H_2O_{deion} (1:1 v/v) solution was sterilized by autoclaving. 30 % glycerol:H_2O_{deion} solution was mixed carefully with 70 % overnight culture in 2 ml tubes, resulting in 15 % glycerol per glycerol stock. The overnight culture was generated beforehand by inoculation of 5 mL LB medium with respective antibiotics and incubation at the optimal growth temperatures of *E. coli* (37°C) or *A. tumefaciens* (28 °C) over night at 170 rpm. The glycerol stock was stored at - 80 °C until further use.

2.5 Generation of transgenic *A. thaliana*

For generation of transgenic *A. thaliana*, vectors with T-DNA are necessary which allow transfer of specific DNA, the generated construct, into the plant germline via use of *A. tumefaciens*.

For generating these vectors and finally transgenic *A. thaliana*, the Gateway® Technology System (Invitrogen, Thermo Fisher Scientific, Waltham, Massachusetts, USA) was used. With a two-step system, it allows cloning of an insert into an empty vector, generating an entry clone (BP reaction). The insert then can be transferred to various destination vectors (LR reaction), resulting in an expression clone that can transform plants.

2.5.1 Cloning an entry clone with the Gateway® system

The Gateway® technology uses the recombinant system employed by a bacteriophage, phage lambda, when infecting their host. It aims to integrate its DNA into the *E. coli* genome, to replicate using the bacterial cell machinery and finally to lyse the bacterial cell, releasing the viral progeny. This life cycle of bacteriophages is called lytic. The second possible life cycle, the lysogenic cycle, occasionally also ensues under specific conditions. The lysogenic cycle allows integration of viral DNA into the bacterial genome without any further actions regarding virus propagation. The recombination system facilitates the integration of the phage's DNA into the *E. coli* genome and the switch between lytic and lysogenic life cycle. This means in specific, the system needs specific attachment sites (att sites) with homologous core regions in host and phage DNA as well as viral and bacterial recombination proteins. These proteins are necessary for bringing target sites together, cleaving them and ligating DNA in novel form. Two sets of proteins with essentially the same function exist and are employed depending on whether the virus uses the lytic or lysogenic pathway.

The BP reaction uses the enzymes catalyzing the lysogenic pathway which bind to the attachment B (attB) sites, originally on the *E. coli* DNA and the attachment P (attP) sites, originally on the lambda genome. The Gateway® system uses these attachment sites in order to insert PCR amplified products of a sequence of interest (SOI) into donor vectors (table 2.5, fig. 2.3). These empty donor vectors, among them the pDONR/Zeo (fig. 8.15, supp.), contain a *ccd*B gene at the site of SOI insertion, surrounded by attP sites. The *ccd*B protein interferes with the function of the *E. coli* DNA gyrase which inhibits growth of most *E. coli* strains. When amplifying the SOI by PCR using the iProof polymerase (table 2.2) the primers add the attB sites to the 5' and 3' ends of the SOI. The PCR product is visualized via gel electrophoresis. DNA is isolated from the agarose gel by cutting out the band and purifying the DNA using the gel extraction protocol of the PCR cleanup and gel extraction kit (Macherey Nagel, Düren, Germany).

Table 2.5 Gateway BP reaction mix for the generation of an entry clone

BP reaction mix	15 - 150 ng	PCR product with attB sites
	150 ng	Donor vector
	to 8 µl	TE buffer
	2 µl	BP enzyme mix (Gateway®)

The BP reaction (table 2.5) causes exchange of the *ccd*B gene for SOI via recombination due to application of the BP Clonase™ enzyme mix. Consequently, the product of the reaction which is transformed into a *ccd*B-sensitive strain (NEB ® 5-alpha Competent E. coli (High Efficiency), NEB, Ipswich, Massachusetts, USA) does not cause cell death. Therefore, all surviving *E. coli* cells contain the correct construct or are not transformed. In order to distinguish between transformed and untransformed cells, antibiotic resistance genes in the pDONR/Zeo vector are used. Transformed cells are grown on medium with respective antibiotics and surviving cells contain the BP reaction result. The

E. coli colonies grown on the selective medium were tested for positivity regarding the BP reaction product by colony PCR (2.3.4) with plasmid-specific primers (8.2.3, supp.). The clone resulting from donor vector and SOI is called entry clone (fig. 2.3). The recombination of the attB and attP sites generates attL sites which frame the SOI in the entry clone. Positive colonies were propagated over night; plasmids were isolated and sequenced as described in 2.4.3. Glycerol stocks were generated of positive clones (2.4.4).

Fig. 2.3 Schematic drawing of the gateway BP reaction to generate the entry clone

The PCR product with attB sites is transferred by the BP reaction enzyme mix (BP ClonaseTM II) into the donor vector, resulting in an entry clone. Due to the recombination reaction, the suicide gene *ccd*B (gyrase inhibitor) is exchanged for the sequence of interest (gene) and ends up in the by-product. In the process, the attachment sites (att-sites) are recombined from attB and attP to attL and attR.

2.5.2 Cloning an expression clone with the Gateway® system

With the LR reaction the SOI can be transferred to a destination vector which allows the transformation of plants. Since most destination vectors contain attR sites necessary for the LR reaction, the SOI can be transferred into various destination vectors once it is part of the entry clone. The LR reaction uses the LR Clonase™ enzyme mix (table 2.6) containing proteins originally catalyzing the lytic pathway of a bacteriophage. The LR Clonase™ enzyme mix works essentially the same way as the BP Clonase™ enzyme mix.

Table 2.6 Gateway LR reaction mix for the generation of an expression clone

LR reaction mix	10 fmol	Entry clone
	20 fmol	Destination vector
	to 8 µl	TE buffer
	2 µl	LR Clonase™ II enzyme mix (Gateway®)

With the LR reaction the *ccd*B gene, framed by attL sites in the destination vector, is exchanged for the SOI (fig. 2.4). The enzymes recognize and bind to the attL sites of the destination vector and the attR sites of the entry clone, strands are exchanged in the core region and ligated. The recombined product consists of the SOI framed by attB sites as part of an expression clone. The LR reaction product is transformed into *E. coli* and positive clones are selected via viability by absence of the *ccd*B gene and antibiotics resistance for presence of the correct construct. Positive colonies were confirmed by colony PCR (2.3.4) with expression clone specific primers. Positive clones are propagated,

plasmids isolated and transformed into *A. tumefaciens* (2.4.2). Glycerol stocks are generated of positive clones according to specification in 2.4.4.

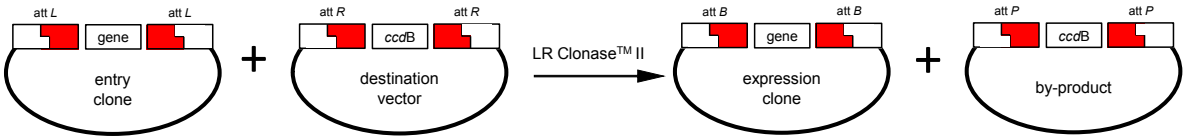

Fig. 2.4 Schematic drawing of the gateway LR reaction to generate the expression clone
The sequence of interest (gene) with attL sites is transferred by the LR reaction enzyme mix (LR Clonase™ II) into the destination vector, resulting in an expression clone. Due to the recombination reaction, the suicide gene *ccd*B (gyrase inhibitor) is exchanged for the sequence of interest and ends up in the by-product. In the process, the attachment sites (att-sites) are recombined from attL and attR to attB and attP.

2.5.3 Generation of the artificial microRNA interference construct

The method of using artificial microRNAs (amiRNAs) for the knock-down of gene expression relies on the plant's own RNA interference machinery which negatively regulates expression of certain genes (Bartel, 2004). *In planta*, miRNA are short single stranded RNAs (19 - 24 nt) that are nearly or perfectly complementary to their target. These RNAs derive from a precursor which is a longer single-stranded RNA with characteristic fold-back structures (fig. 2.5). RNases of the Dicer family process these precursors by cleaving at specific sites and generate short double-stranded RNAs (fig. 2.5 D). While still being bound to the Dicer, other RNA binding proteins interact with the dicer-RNA complex and the RNA is transferred to the RNA-induced silencing complex (RISC). During this transfer the RNA is activated by generating the single-stranded miRNA. It can now bind to the RNA of the target gene. Artificial miRNAs (amiRNAs) are 21 bp long single-stranded RNAs not naturally occurring in plants, intended to silence specific target genes.

The amiRNAi construct was generated according to Ossowski et al., 2008. When inquiring *in silico* for potential amiRNAi sequences with the Designer tool of the WMD3 - Web MicroRNA Designer web portal (http://wmd3.weigelworld.org), the website supplies several short sequences of 21 bp, selected for the gene of interest (GOI) sequence. These sequences are selected according to their predicted success in silencing the provided gene of interest. Selection criteria for amiRNA sequence generation include specificity to the GOI, therefore avoiding silencing of other genes. Additionally, mismatches to the GOI sequence at specific positions of the amiRNA sequence and perfectly matching nucleotides at others are incorporated into the provided amiRNA sequence. Further criteria are the GOI sequence position that is targeted by the amiRNA and hybridization energy for hybridization of amiRNA and the target sequence. These criteria are inferred from existing microRNA and their experimentally proven interaction with their target. Once the amiRNA sequence is selected, it has to be inserted into a well-characterized hairpin portion of an endogenous miRNA transcript which serves as the precursor for the amiRNA. In case of the WMD3 method, the *Arabidopsis thaliana* MIR319a (ath-MIR319a, fig. 2.5 F) provides the microRNA 3D structure that is recognized by Dicers. Since Dicer cleavage sites are well known for this microRNA, specific targeting of a GOI is possible. For generating *ANAC058*

amiRNA lines, the original miRNA (pink in fig. 2.5 F) is exchanged for the amiRNA targeting the GOI, in this case *ANAC058*. The instructions for generating the amiRNA construct with the WMD3 method specify cloning via overlapping PCR. The respective primers can be obtained by the Oligo tool on the WMD3 web portal (in fig. 2.5 A, primers as arrows are labled A, B, I - IV) and template RS300 vector can be obtained from Prof. Detlef Weigel (Max-Plank Institute, Tübingen, Germany). Procedure was changed in this case from overlapping PCR to *in silico* cloning of the amiRNAi construct and subsequent synthesizing of the construct in an entry vector (Invitrogen, Thermo Fisher Scientific, Waltham, Massachusetts, USA). The amiRNA construct was finally cloned behind the 35S promoter with the LR reaction (2.5.2).

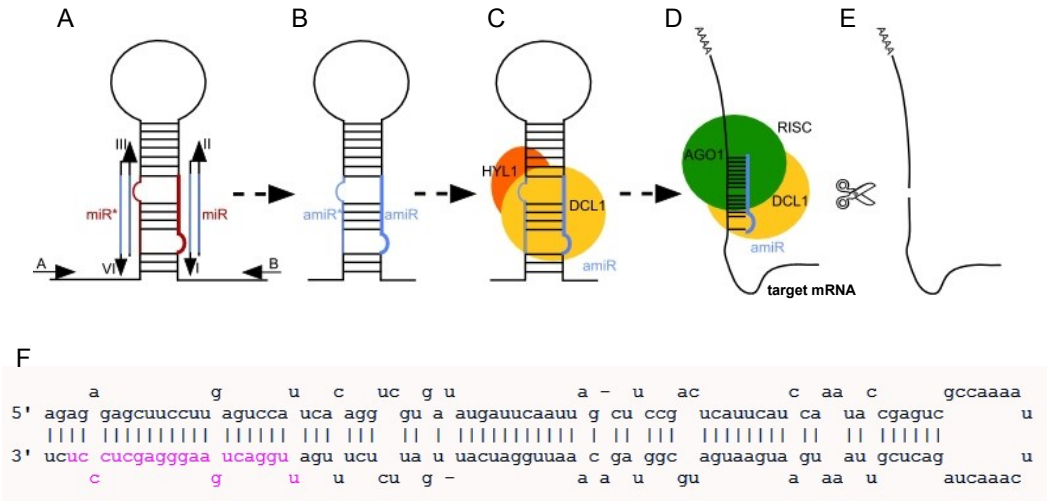

Fig. 2.5 Schematic drawing of the amiRNA cloning and *in planta* gene expression knock-down
The hair-pin structure in A represents the *A. thaliana* MIR319a (ath-MIR319a) microRNA precursor (sequence in F). Four primers (A, B, I - IV in A) allow cloning of amiRNA sequence (signified by blue lines in B and C, labeled amiR) into the endogenous precursor, replacing the sequence regulating gene expression. Once plants are transformed with the construct, the generated sequence forms the hair-pin structure in B which is recognized by an endonuclease complex of DCL1 and HYL1 (C). The active amiRNA sequence is cleaved from the precursor and transferred as a single strand to the RISC (D) which allows recognition of the target mRNA. The target RNA is cleaved subsequently (E) and cleavage products are often degraded. As a result, expression of the target gene is down regulated. Image (A - E) obtained from WMD3 web portal http://wmd3.weigelworld.org last accessed 10. 2017), ath-MIR319a stem loop structure was obtained from the miRBase web portal (http://www.mirbase.org/, Griffiths-Jones, 2004, last accessed 10. 2017).

2.5.4 Transformation of *A. thaliana*

A. thaliana is transformed via the floral dip method introduced by Clough and Bent, 1998 using *A. tumefaciens* as the transforming bacterium. The floral dip method is conducted by immersing inflorescences of plants in an *A. tumefaciens* suspension.

Beforehand, *A. thaliana* plants were grown densely on soil until inflorescence emergence. If necessary, few days before floral dip siliques were cut off ensuring development of new unopened flowers. For the suspension, the *A. tumefaciens* strain GV3101::pMP90 was grown first to high density in pre-culture and main-culture. For the pre-culture, 50 mL LB liquid medium with respective antibiotics

was inoculated with *A. tumefaciens* cells which were positive for the construct. The pre-culture was incubated at 28 °C over night in Shikane flasks at 170 rpm and was used to inoculate the main-culture. For the main-culture, 300 mL LB medium and antibiotics were prepared and after inoculation, the culture was split into two cultures in separate Shikane flasks, each incubated at 28 °C over night at 170 rpm.

The main culture was split into aliquots and centrifuged for 15 min at 5000 rpm. The resulting supernatant was discarded and pellets were resuspended in 200 mL inoculation medium (8.1, supp.).

The *Arabidopsis* plants were dipped by submerging inflorescences into inoculation medium with *A. tumefaciens* two times for 10 s. Subsequently they were kept lying horizontally, completely covered with plastic sheets on all sides. Covered plants were kept in trays in the climate chamber for 2 - 3 d. When removing the cover, plants were re-erected and watered. Inflorescences were covered with paper bags and cut off when seeds were mature.

2.5.5 Selection of transformed *A. thaliana* plants for positive transformants

Selection with Hygromycin

After transformation of *A. thaliana* plants with expression vectors which contain a Hygromycin resistance gene (fig. 8.22, fig. 8.23, supp.), plants of the T1 generation were selected on MS medium with 25 µg mL^{-1} Hygromycin. Approximately 10 mg seeds were sterilized in 1.5 ml tubes according to the protocol in 2.2.2 and dispersed in rectangular petri dishes on the selection medium. After approximately 1.5 weeks, differences in growth of plants negative or positive for the construct were visible. Potentially positive seedlings were transferred under sterile conditions to MS without antibiotics and finally to soil once seedlings were deemed large enough. All plants were genotyped to ensure elimination of false positives with primers specific to the respective construct plants were transformed with (8.2.3, supp.).

Selection with BASTA

Plants transformed with constructs allowing plant selection via BASTA (fig. 8.24, supp.) were cultivated on soil. Even dispersion of plants was achieved by mixing seeds with 0.1 % agar solution at room temperature and pipetting seeds in this solution onto the soil surface. After 2 weeks of growth, plants were treated with a 0.1 % BASTA solution (v/v, in tap water, Bayer, Munich, Germany). The active ingredient is glufosinate-ammonium which is present in the plant applied solution with a concentration of 0.2 g L^{-1}. BASTA treatment was repeated after 2 d and plant health was documented another 3 d later (fig. 2.6). Surviving plants were genotyped for the respective construct before further use. The BASTA treatment effectively killed wild type plants whereas transformed plants containing a construct with the BASTA resistance gene appeared unaffected (fig. 2.6).

Fig. 2.6 BASTA treated plants of the T1 generation transformed with the *Prom$_{ANAC058}$::GFP-GUS* construct and wild type

2 weeks old plants, progeny from *A. thaliana* plants transformed by floral dip with a construct containing the BASTA resistance gene (fig. 8.24, supp.) were treated with a 0.1 % BASTA solution. Wild type plants grown and treated the same way served as the negative control. Treatment was repeated 2 d later and obvious plant health effects were documented 3 d after the second treatment.

2.6 Chemical analysis

All glass wares used in analytical investigation were cleaned prior to use with chloroform and all solvents were of analytical purity. Any non-glass material like lids and septa are lined with polytetrafluoroethylene (PTFE) which was also throughoutly rinsed with chloroform before use.

2.6.1 Suberin sample preparation

Root samples were collected after plant growth for 4-5 weeks as root system sections or whole root systems. In order to get rid of the primary cell wall, roots were incubated in enzyme solution containing cellulase and pectinase (8.1, supp.). To ensure the solution reaches all cells of the root, samples were vacuum infiltrated using a vacuum pump (Vacuubrand GmBH + CO, Wertheim, Germany). Solution was exchanged two times and replaced with borax solution (8.1, supp.). This solution has a more alkaline pH compared to the enzyme solution, causing different molecules to dissolve. As a result, both molecules soluble in acidic and alkaline environment are extracted. Borax solution was exchanged once and then changed to chloroform:methanol (1:1) solution for extraction of free lipids. The extraction solution itself was exchanged twice. In case cell wall digestion was skipped (all experiments with apical root sections, fig. 3.13, fig. 3.24), root material was submerged directly after

harvest in lipid extraction solution. Root material in all solutions was kept on a rotary shaker during extraction of various compounds. After free lipid extraction, root material was dried on chloroform-cleaned polytetrafluorethylene (PTFE) sheets and stored on silica gel in an exsiccator. Dry weight of root samples was measured with a micro balance (MC21S, Sartorius, Göttingen, Germany).

2.6.2 Transesterification with BF_3:methanol

Up to 10 mg root material was cut into pieces in glass vials and covered with 1 ml BF_3:methanol solution (approx. 10 % (1.3 mol L^{-1}) boron trifluoride-methanol solution, Sigma-Aldrich, Munich, Germany). Transesterification of esters present in root material proceeded at 70 °C for 16 h. Afterwards samples were cooled to room temperature. In order to be able to relate measured monomer amounts to root dry weight, an internal standard is needed. To each sample 10 µg of C32 alkane was therefore directly added. Transesterification reaction was stopped by adding the BF_3:methanol solution to saturated $NaHCO_3$ solution and vials were mixed for throughoutly for 10 s, as was also done for all subsequent steps when adding solutions. Most lipophilic compounds were extracted by adding once 2 ml chloroform and twice 1 ml chloroform. Each time, the lower chloroform phase containing the suberin monomers is transferred to a new vial. Subsequent extraction of polar compounds was achieved by adding three times H_2O_{HPLC} and discarding the aqueous phase. Remaining H_2O_{HPLC} was bound by adding anhydrous $NaSO_4$ as necessary. Solute concentration was increased by evaporation of solvent in new vials under a steady stream of nitrogen gas to approximately 100 µl.

2.6.3 Wax sample preparation

Leaf wax was extracted from leaves of 4 weeks old, β-estradiol treated TRANSPLANTA lines *TPT_3.18400.1D* (*TPT.D*) and *TPT_3.18400.1G* (*TPT.G*) (Coego et al., 2014) 2 weeks after treatment. Whole rosettes were dipped in 50 mL chloroform for 10 s in beakers. For plants of each genotype the same beaker was used which was cleaned with chloroform in between sample preparations. After dipping, leaf material was transferred to extraction solution (chloroform:methanol 1:1) to allow eventual further analysis of cutin by extracting all free lipids. For analysis of wax, an internal standard is necessary which was added as 10 µg C24 alkane to the 50 mL chloroform wax solution. An aliquot of 20 mL was filled into vials and solvent was evaporated to approximately 100 µL. The remaining 100 µL chloroform with wax monomers were transferred to Reacti-vials. The leaf material was dried on PTFE sheets in petri dishes and stored until use on silica gel in exsiccators. In order to relate leaf dry weight to leaf surface exemplarily, 5 leafs of all used genotypes were dipped in chloroform, leaves were scanned and leaf material dried afterwards. Surface and dry weight relation was linear (not shown), justifying using dry weight for data analysis.

2.6.4 GC-MS and GC-FID analysis

Monomers have to be volatile for gas chromatography. This is achieved by derivatization with bis(trimethylsilyl)trifluoroacetamide (BSTFA, Sigma-Aldrich, Munich, Germany). BSTFA masks the

polar groups of molecules by converting groups such as carboxyl- and hydroxyl-groups into the corresponding trimethylsilyl esters and ethers. To every sample 20 µl BSTFA and pyridine each were added and samples were kept subsequently for 40 min at 70 °C.

1 µl of each sample is injected onto a DB-1 capillary column (30m ± 0.32mm; 0.1 µm poly(dimethylsiloxane) coating; Agilent J&W Scientific, Santa Clara, California, USA) and carried along by carrier gas with a flow rate of 2 mL min^{-1}. In case of mass spectrometry (MS 5973N Mass Selective Detector, Agilent Technologies, Santa Clara, USA) coupled to gas chromatography (GC), carrier gas is helium. For GC-FID (GC – flame ionization detector) analysis, carrier gas is hydrogen. The GC (GC 6890N, Agilent Technologies, Santa Clara, USA) was conducted with temperature programs specific to the expected monomer composition of a sample, ensuring that monomers are separated clearly according to their molecular characteristics. Among these characteristics are molecule size and polarity, which changes the retention of a specific molecule in the column. The column coating serves as the stationary phase. As a result, retention time of a monomer at the specific temperature program is specific to the molecule.

Monomers are identified by MS according to their specific fragmentation pattern. Fragmentation is achieved by ionization of molecules. The resulting fragments are separated in the quadrupole according to their mass to charge ratio. Fragments at their retention time are detected, resulting is a chromatogram with all detected monomers as peaks and fragmentation patterns for each monomer. Using a fragmentation library generated in the Ecophysiology laboratory (University of Bonn, Germany), peaks are related to identified monomers. GC-FID allows nearly exact quantification of monomer amounts by the peak area. FID uses combustion to generate ions from molecules relative to their atom number. The charged particles generate an electric current which is proportional to the rate of ionization and thereby to atom number. The peak area was converted into µg using the amount of the internal standard and related to root or leaf dry weight.

Table 2.7 Temperature programs for GC analyses of suberin, wax and the acid standard

	change	final	hold
suberin	injection	50 °C	2 min
	10 °C / min	150 °C	1 min
	3 °C / min	310 °C	25 min
wax	injection	50 °C	2 min
	40 °C / min	280 °C	2 min
	3 °C / min	310 °C	30 min
acid standard	injection	50 °C	2 min
	40 °C / min	200 °C	1 min
	3 °C / min	300 °C	15 min

Column quality decreases with GC analyses due to very polar and very large molecules accumulating at the injection site of the column. Column quality was tested using an acid standard solution containing equal amounts of an C24 alkane and three acids, C29, C30 and C31 acid in chloroform. It

was analyzed with gas chromatography with the temperature program in table 2.7. Monomer peak shapes were evaluated with regard to symmetry and a quality factor from measured alkane peak area per C31 acid peak area was calculated. If the factor is above 1.3, polar compounds are distinctly more retained on the column and column maintenance was conducted. For maintenance, the column at the injector site was shortened, followed by heating of the column to 310 °C.

2.7 Histology

2.7.1 GUS assay

The GUS assay reveals the cells in which a specific promoter is active, provided plants contain the *β-glucuronidase* (*GUS*) gene behind the promoter of interest.

Testing promoter activity in seedlings, plants with the $Prom_{ANAC058}$*::GFP-GUS* construct (fig. 8.24, supp. Karimi et al., 2002) were grown on MS plates with 1/2 MS and 0.65 - 0.8 % agar. After stratification at 4 °C plates were transferred to a climate chamber with standard climate conditions (see 2.2.2) where seedlings grew vertically for 5 d. Seedlings were submerged in staining solution containing X-Gluc (cyclohexylammonium salt) (8.1, supp.) in 24 well plates. Uptake of solution into all cells is ensured by vacuum infiltration using a vacuum pump (Vacuubrand GmBH + CO, Wertheim, Germany). Seedlings were incubated in staining solution at 37 °C over night or, in case of ABA treated seedling (fig. 3.7), for 7 h. The GUS protein hydrolyzes the X-Gluc substrate which produces an indoxyl derivative. Once this derivative undergoes on oxidative dimerization, a blue, insoluble dye is produced. Since tissue structure remains intact, GUS protein and therefore blue color is localized to cells where the putative *ANAC058* promoter is active. Thus, the reporter construct allows tracking of promoter activity. In order to stop the reaction, samples were washed several times in 100 % ethanol until chlorophyll was absent. For storage of seedlings fixation solution (8.1, supp.) was employed which preserves tissue and cellular structures. Plants were observed under and pictures were taken with an Axioplan microscope (Carl Zeiss, Oberkochen, Germany) connected to the digital camera DXM-1200 (Nikon, Tokyo, Japan). Contrast in picture of 3 weeks old plant roots (fig. 3.5) was increased post-experiment to increase visibility of blue staining.

Using the GUS assay to reveal promoter activity in response to wounding can show changes in staining intensity close to wounding sites. $Prom_{ANAC058}$*::GFP-GUS* plants were grown on soil for 5 weeks. Before conducting the GUS assay, leaves were pierced at several time points on one half of the leaf with steel forceps, generating several small wounding sites. When leaves were collected, wounding dated back 2 h, 6 h, 3 d and 7 d. Leaves were submerged in the X-Gluc solution in 50 ml falcons, vacuum infiltrated and incubated at 37 °C over night. For stopping the reaction, X-Gluc solution was exchanged for 100 % ethanol which was changed until chlorophyll was extracted fully. During washing of samples, falcons were moved gently on a roller mixer. Finally, leaves were observed under the stereomicroscope SZ61 with a binocular observation tube (Olympus SZ61,

Olympus, Tokyo, Japan) and pictures were obtained with the digital camera Canon EOS600D (Canon, Tokyo, Japan) and the program EOS Utility v. 2.10 (Canon, Tokyo, Japan).

2.7.2 GFP fluorescence observation

Plants with the *Prom$_{ANAC058}$::GFP-GUS* construct (fig. 8.24, supp., (Karimi et al., 2002)) allow observation of promoter activity via green fluorescent protein (GFP) localization. Seedlings were grown for 5 d on 1/2 MS and 0.8 % agar in petri dishes. Fluorescence was investigated and documented with the Olympus FluoView™ FV1000 laser scanning confocal microscope and the FluoView™ FV1000 v. 3.0.1.15 software in Plant Cell Biology laboratory (University of Bonn, Germany). Confocal microscopy allows the focus of light on a single point in a sample whereas conventional fluorescence microscopy uses emitted light from all tissue layers which are penetrated by exciting wave lengths. With conventional fluorescence observation, tissues on the inside of the sample are more difficult to observe since illuminating light might not reach that far, emitted light is absorbed on its way out of the sample or obscured by light signals of surrounding tissue. In confocal microscopy, bundled light of high intensity (laser light) is focused on one specific localization in the sample and moves through the sample as determined using the respective computer program. Emitted light on the way to the detector passes a pinhole aperture, eliminating reflection from out-of-focus regions and the final picture is constructed digitally. In this case, GFP was excited at 488 nm with an argon ion laser and emission signals were collected in a wavelength span from 500 nm to 600 nm. Due to absence of colors for recorded light intensities, green color was assigned to GFP fluorescence by the FluoView™ program. Roots were investigated in the XY plane, as well as the Z plane. The resulting image stacks comprise layers of several two-dimensional images. For images used in this work, several images in the Z plane were selected and an overlay was generated, called Z-stack.

2.7.3 Fluorol Yellow 088 staining and observation

Suberin deposition in seedlings was investigated with the lipophilic dye Fluorol Yellow 088 (Brundrett et al., 1991). Plants grew for 6 d on MS medium and staining was conducted as published by Naseer et al., 2012 and Pfister et al., 2014. Seedlings were incubated in Fluorol Yellow 088 solution (0.01 % w/v, in lactic acid) at 70 °C for 30 min. Subsequent rinsing was conducted with H_2O twice for 5 min each. Aniline Blue (0.5 % w/v, in H_2O_{deion}) counter-stains plant material by incubation of the material in the solution for 30 min at room temperature in the dark. Seedlings were washed in H_2O until water stayed clear and kept in the dark until microscopy investigations. Observation of samples proceeded with an Axioplan microscope (Carl Zeiss, Oberkochen, Germany), employing bright field settings and a standard GFP filter. Each section of the root from root tip to root-shoot junction was documented with both settings via digital camera (DXM-1200, Nikon, Tokyo, Japan). Fluorescence was imaged as green and changed afterwards to yellow with the software GIMP (gimp.org). Overlay of fluorescence and bright field images was generated with ImageJ (https://imagej.net). Color intensity of depicted fluorescence was increased for overlay images to allow better visibility of suberin. Investigation of stained suberin along the root, separated into sections of no suberin, continuous and patchy suberin (fig. 2.7 B, Naseer et al., 2012; Pfister et al., 2014) was conducted with ImageJ,

measuring the length of each section. In each image the length of the root as imaged with bright field, objective x10, was measured. By an image overlay of the bright field and fluorescence images, section starts and ends were determined. Values for each section were summarized for one root, giving the total root length.

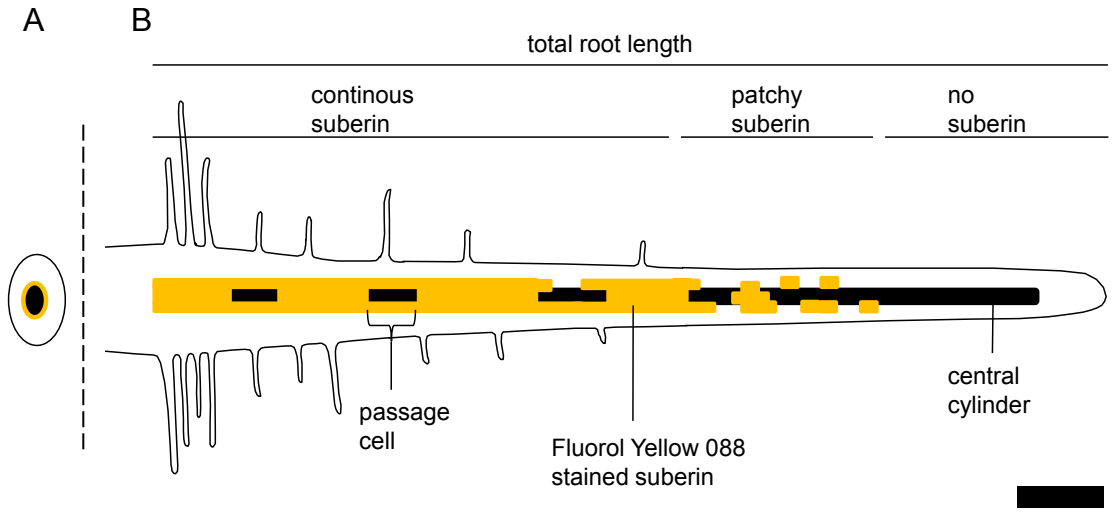

Fig. 2.7 Seedling root model with Fluorol Yellow 088 stained suberin

The pattern of endodermal suberin deposition (colored yellow) is sectioned along the root into continuous suberin, patchy suberin and no suberin (B). A cross section of the continuous suberin section (A) shows suberin localization surrounding the central cylinder (colored black), simplified for suberin being deposited onto endodermal cell plasma membranes. As the enodermal cell layer surrounds the central cylinder, the same applies to suberin. Continuous suberin contains single unsuberized cells, the passage cells. The scale displays approximately 1 mm, derived from mean total root length of all measured roots.

3 Results

3.1 Protein and expression analysis

3.1.1 *In silico* co-expression analysis

Several expression studies implicate *ANAC058* as one of the possible regulators of suberin in different species. Studies are based on analysis of tissue containing suberin, such as russeting apple skin (Legay et al., 2015), cork of the cork oak (Soler et al., 2007; Soler et al., 2008) and stressed rice roots (Shunsaku Nishiuchi and Mikio Nakazono, Nagoya University, Japan, personal communication). *ANAC058* orthologs are upregulated in those tissues along with suberin-associated genes, which are involved in suberin polyester synthesis and assembly. Additionally, the ortholog of *ANAC058* in potato negatively regulates suberin deposition (Verdaguer et al., 2016). A co-expression analysis using several known suberin genes (Beisson et al., 2007; Compagnon et al., 2009; Domergue et al., 2010) as bait confirmed *ANAC058* as a promising candidate gene likely involved in regulation of suberin formation (fig. 3.1).

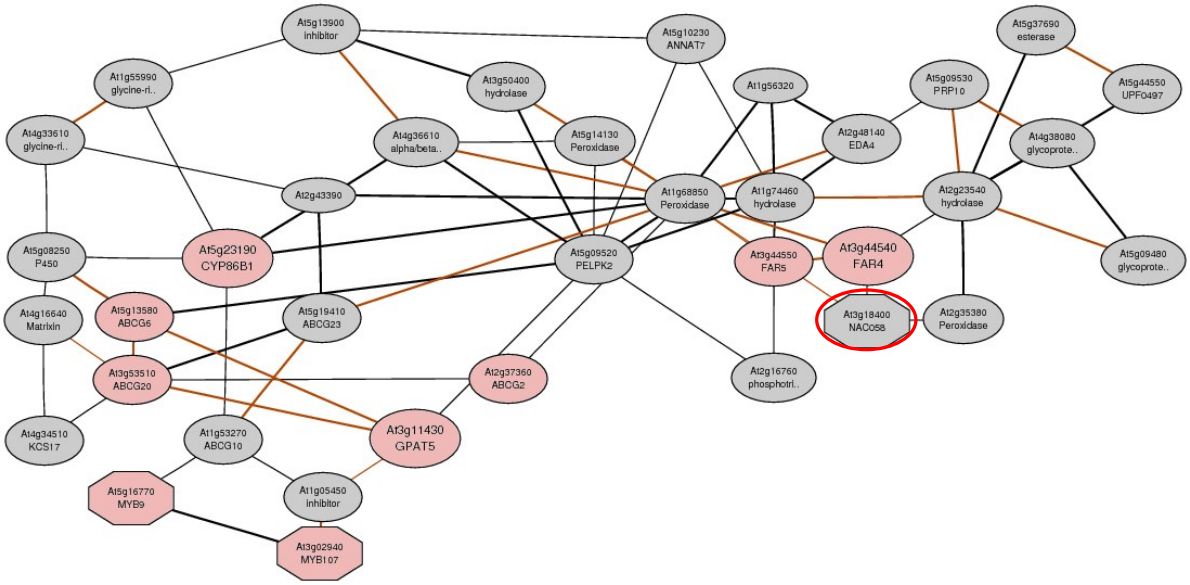

Fig. 3.1 Network of genes co-expressed with *RALPH/CYP86B1*, *GPAT5* and *FAR4*
Network was generated with the NetworkDrawer tool of the ATTED-II database ver. 8.0 (http://atted.jp, Aoki et al. 2016), last accessed 04. 01. 2016, modified. Genes involved in suberin synthesis and deposition have a red background (*RALPH/CYP86B1* (Compagnon et al., 2009), *GPAT5* (Beisson et al., 2007), *FAR4* and *FAR5* (Domergue et al., 2010), *ABCG2*, *ABCG6* and *ABCG20* (Yadav et al. 2014) as well as *MYB9* and *MYB107* (Lashbrooke et al., 2016)). Blue background indicates unpublished genes or their known function is not clearly related to suberin. The *ANAC058* gene is encircled in red. The genes with annotations are listed in table 8.1, supp..

The co-expression network shows *ANAC058* in direct proximity of two FARs involved in suberin synthesis (Domergue et al., 2010) and a unpublished peroxidase. Several other suberin genes, highlighted with a red background, also show up in the network - the three ABCG transporters involved

in suberin deposition (Yadav et al., 2014) and two MYB transcription factors required for normal seed coat suberin assembly (Lashbrooke et al., 2016).

Additionally to the co-expression data, the expression pattern of *ANAC058* inferred from databases (Cell Type Specific Arabidopsis eFP Browser (Mustroph et al., 2009) and AtGenExpress Visualization Tool AVT (Schmid et al., 2005)) also indicates an involvement in suberization (fig. 8.1, supp. and table 8.2, supp.). Its expression pattern is very similar to the expression of suberin genes like *GPAT5* (Beisson et al., 2007) since expression of both genes seems to be localized to the endodermis of roots.

3.1.2 Organ-specific expression of *ANAC058*

Semi-quantitative RT-PCR amplifying *ANAC058* cDNA generated from root and leaf RNA yielded the same result (fig. 3.2) as indicated by databases (fig. 8.1, supp.). In plants grown hydroponically for 4 weeks, *ANAC058* is expressed in roots, whereas in leaves its RNA is absent (fig. 3.2, A). Additionally, plants were grown on soil for 5 weeks in order to investigate apical and basal root sections. Upon sample collection, the root system was separated into a basal section including the hypocotyl and thickened roots (fig. 3.2, root, labeled b) and an apical section comprised of the fine roots of the remaining root system (fig. 3.2 root, labeled a) (for sample preparation details, see fig. 2.2). Both sections reveal a similar expression of *ANAC058* in two individual plants, with slightly stronger expression in the basal section.

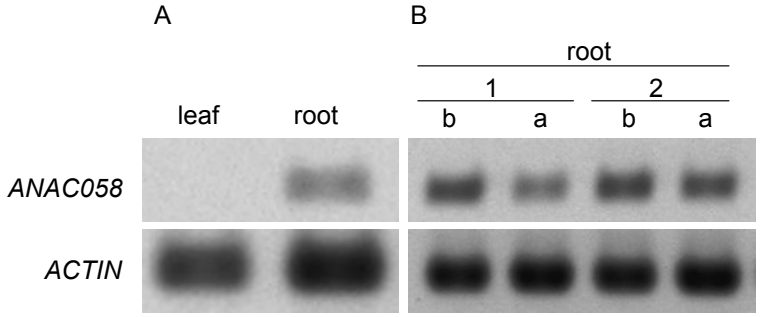

Fig. 3.2 Organ-specific expression of *ANAC058* and *ACTIN* in 4 weeks old hydroponically-grown (A) and 5 weeks old soil-grown (B) plants

For A, a leaf and the whole root system (root) was harvested, for B the root system of two plants (1 and 2) was separated into a basal part including hypocotyl and thickened roots (b) and the apical section consisting of the remaining root system (a) (for details, see fig. 2.2). *ACTIN* served as the control.

3.1.3 Activity of the putative *ANAC058* promoter

In order to test the activity of the putative *ANAC058* promoter regarding root tissue-specificity and in response to treatments, a promoter reporter construct was generated. It contains the putative promoter of *ANAC058* upstream of the *green fluorescence protein* gene (*GFP*) and the *β-glucuronidase* gene (*GUS*) (fig. 8.24, supp.). This construct was used to stably transform wild type

plants (genotyping of transformants in fig. 8.14, supp.). To test the promoter activity, *Prom$_{ANAC058}$::GFP-GUS* seedlings were grown on 1/2 MS plates for 5 d.

Seedlings were submerged in X-Gluc (cyclohexylammonium salt) staining solution (8.1, supp.) which turns blue in the presence of the GUS protein activity. Putative *ANAC058* promoter activity was detected in the root but not in the shoot (fig. 3.3 A). Specifically, it is active in the endodermis and causes GUS activity as well as GFP fluorescence in a specific pattern. According to this pattern, promoter activity changes along the root from root tip towards root-shoot junction, also known as the root base (fig. 3.3 F - K). No activity was found at the root meristem, whereas single blue and fluorescing endodermal cells (patchy) appeared later, finally leading to a fully stained and fluorescing endodermis. This activity is similar to the pattern of suberin deposition (see model in fig. 2.7) which was published for example by Naseer and colleagues in 2012. Similar promoter activity was observed in the same study for several suberin-associated genes.

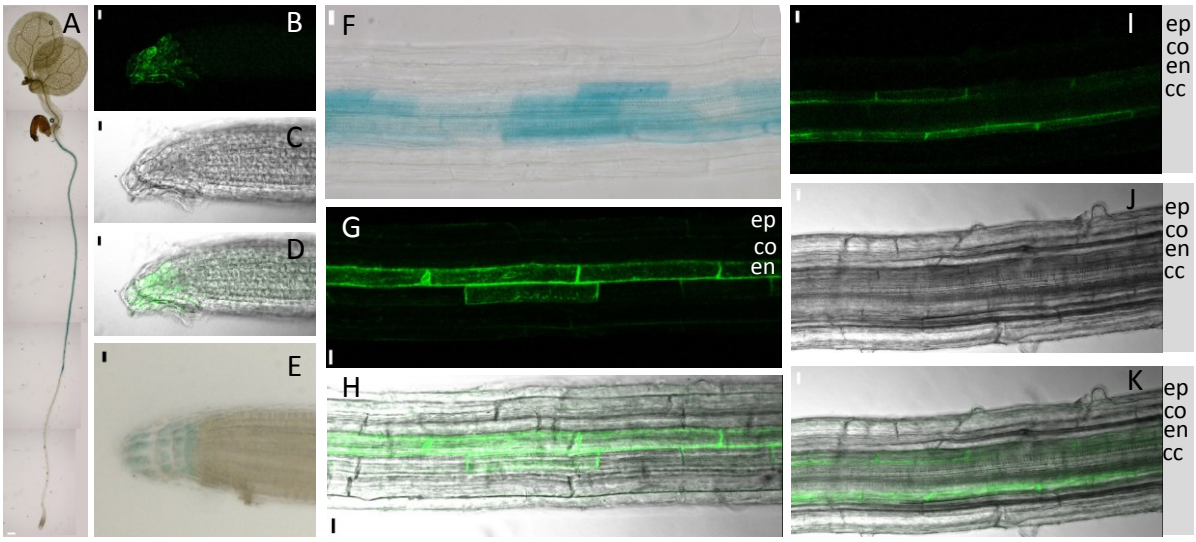

Fig. 3.3 Putative *ANAC058* promoter activity in roots of *Prom$_{ANAC058}$::GFP-GUS* plants

GUS activity and GFP fluorescence was detected in roots of 5 d old seedlings (A), specifically in the root cap cells (B - E, fig. 3.4 C) and the endodermis (F - K). Promoter activity via GPF fluorescence was investigated using confocal microscopy. Pictures were taken with bright field (C, J) employing a standard GFP filter (B, G, I). Depicted are Z-stacks of 6 - 7 individual pictures (G - K). Overlays of bright field and GFP fluorescence pictures were generated with FluoView program (D, H, K). Scale bars represent 200 µm (A) and 10 µm (B - K). ep epidermis, co cortex, en endodermis, cc central cylinder

Accordingly, no staining or fluorescence is visible in the meristematic zone and the only GUS staining and GFP fluorescence in the root tip was observed in root cap cells (fig. 3.3 A - E). GUS activity and GFP fluorescence starts being visible in single endodermal cells (fig. 3.3 F - H) in the differentiation zone. Measuring the distance from the root tip to the first stained cell shows that promoter activity starts at approx. 20 % of the whole root length (19.74 ± 5.22 %, fig. 8.2, supp.). The putative promoter of the suberin biosynthesis gene *HORST* in *Prom$_{HORST}$::GUS* (Höfer et al., 2008) becomes active at a very similar distance from the root tip (fig. 3.4 H and fig. 8.2, supp.). The distance corresponds well to the start of suberin deposition (fig. 8.2, supp.). Closer to the root base all endodermis cells with only

few exceptions show staining (fig. 3.3 A, fig. 3.4 F) and fluorescence (Fig. 3.3 I - K). No staining or fluorescence is observed in the outermost cell layer, the epidermis (fig. 3.3 F, G and I, labeled ep) or the cell layer below, the cortex (fig. 3.3 F, G and I, labeled co). Neither was GFP detected in the central cylinder (fig. 3.3, I - K, labeled cc). Single cells without staining in an otherwise fully stained endodermis (not depicted) indicate passage cells. Those cells are unsuberized and are suspected to allow passage of ions and water into the central cylinder (Peterson and Enstone, 1996).

While the root of *Prom$_{ANAC058}$::GFP-GUS* plants in fig. 3.3 A and fig. 3.4 F shows continuous GUS staining until root-shoot junction, roots that are developmentally slightly older indicate that promoter activity in the endodermis decreases again towards the root base (fig. 3.4 H, labeled A). At the root base, on the other hand, staining intensity was often observed to increase again. It appears in sub-epidermal root cells (fig. 3.4 D and F), observed in three of four independent transformed lines. Blue staining in the endodermis and root cap cells was observed in all four independent transformed lines.

Specific promoter activity of the putative *ANAC058* promoter was also observed during lateral root development. In root sections in which the promoter is already strongly active, no additional promoter induction was present in cells surrounding the lateral root base (fig. 3.4 A). If promoter activity on the other hand is weak at the site of lateral root development, the activity increases in endodermal cells of the main root in the vicinity (fig. 3.4 B and C). In later developmental stages of the lateral root, cells at its root base which seem to be morphologically part of the lateral root but in contact with the main root epidermis occasionally also show staining (fig. 3.4 B and C). In case the emergence of the lateral root disrupts cells of the epidermal cell layer the promoter is activated locally in those epidermal cells (fig. 3.4 A).

Additionally, the putative *ANAC058* promoter becomes active in the root tip of lateral roots at a certain developmental stage. Only when the meristematic and elongation zone are distinct in lateral roots, was promoter activity observed in the root tip (fig. 3.4 C). This staining seems to be localized to the root cap cells in the same manner as for the main root (fig. 3.3 B - E). The activity of the promoter was also observed occasionally in the radicle of mature embryos, extracted from green seeds. Whereas promoter activity in lateral roots seemed to be localized to single root cap cells, localization of activity in the embryo was less certain. Staining was observed in root cap cells but might also be present in other cell types in the radicle (fig. 3.4 E).

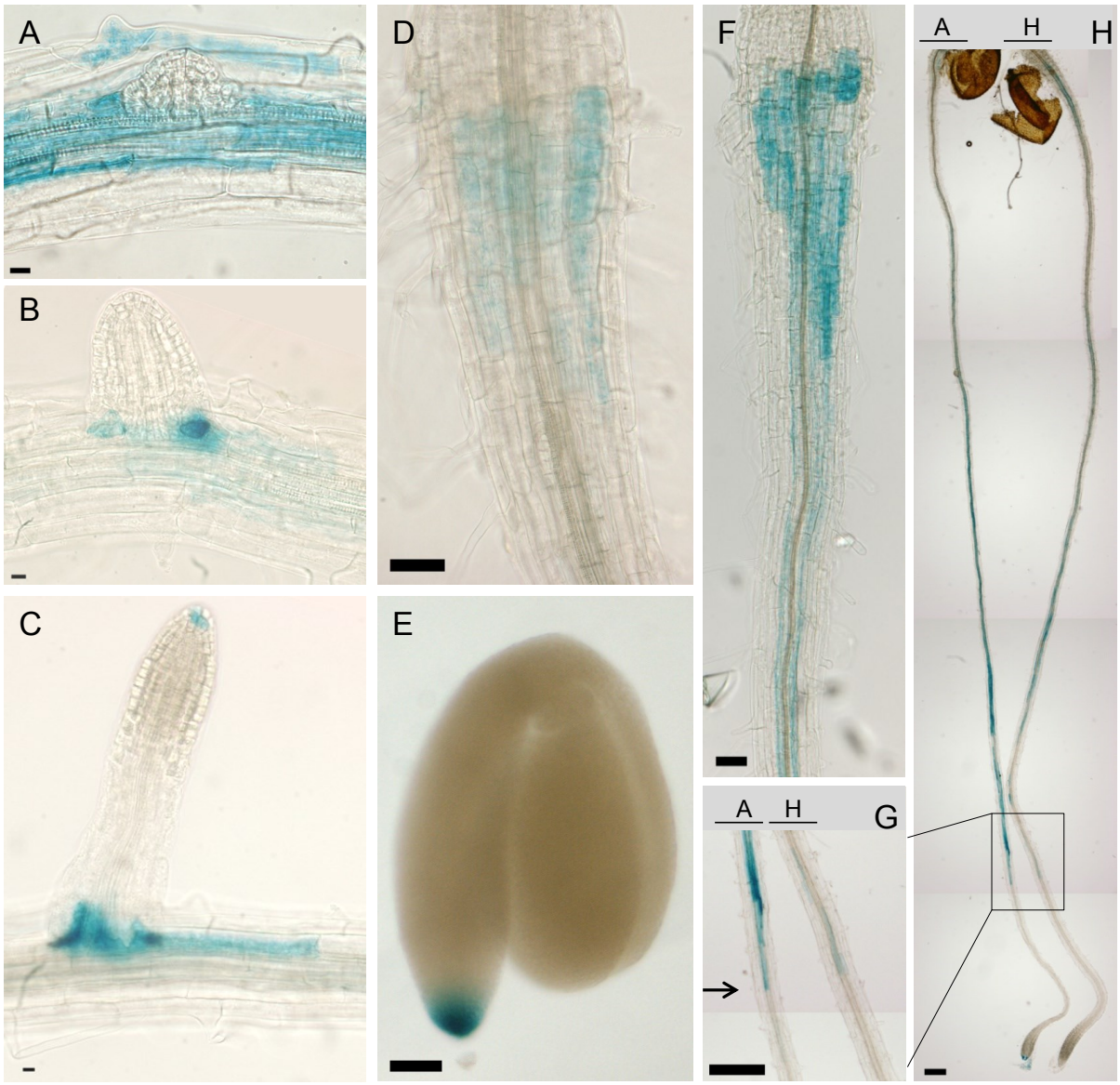

Fig. 3.4 GUS activity during lateral root emergence, in root base and embryo of *Prom$_{ANAC058}$::GFP-GUS* plants and in roots of *Prom$_{HORST}$::GUS* plants

During lateral root development in *Prom$_{ANAC058}$::GFP-GUS* plants, the promoter is active in adjacent endodermal cells of the main root, the basal-most endodermal cells of the developing lateral root and occasionally in main-root epidermal cells at the site of lateral root emergence (A - C). At the main root base, GUS activity was detected in sub-epidermal cell in roots (D). In mature embryos extracted from green seeds, promoter activity was occasionally observed in the root tip (E). The distance from root tip to the start of GUS activity was the same for *Prom$_{ANAC058}$::GFP-GUS* (G and H, seedling labeled A) and *Prom$_{HORST}$::GUS* (G and H, seedling labeled H). G shows the root section encircled in H in higher magnification, the arrow marks the first stained cells. Scale bars represent 200 µm (G, H), 50 µm (D, E, F) and 10 µm (A - C).

In *Prom$_{ANAC058}$::GFP-GUS* plants grown for 3 weeks on 1/2 MS, activity of the putative *ANAC058* promoter was clearly present in young sections of the main root as well as in young parts of lateral roots (fig. 3.5, black arrows). Close to the root tip of main root or side roots, GUS staining was absent. Staining in root cap cells was detected in main and side roots using a higher magnification than in fig. 3.5 (not shown). Promoter activity at the age of 3 weeks was investigated for 1 transgenic line.

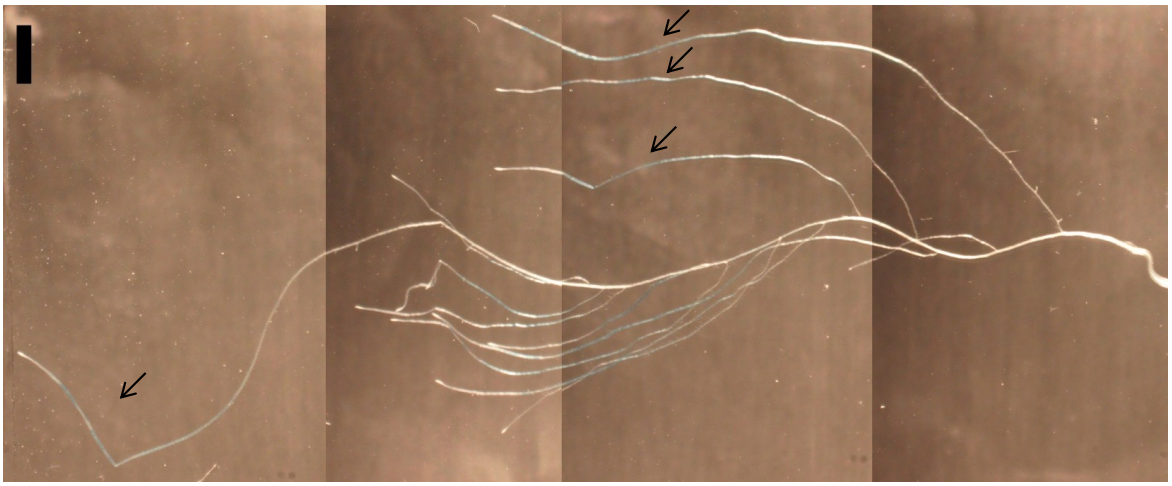

Fig. 3.5 Putative *ANAC058* promoter activity in 3 weeks old *Prom$_{ANAC058}$::GFP-GUS* plants

The putative *ANAC058* promoter is active in young root sections (black arrows) of plants grown on 1/2 MS plates. Promoter activity was visualized via GUS activity and observed under the binocular microscope. The scale bar represents 2 mm.

3.1.3.1 Induction of putative *ANAC058* promoter activity by wounding

Suberin-associated genes are known to respond to environmental stress with increased expression (Domergue et al., 2010; Franke et al., 2009). The *ANAC058* promoter is induced in leaves by wounding after 3 d and 7 d (fig. 3.6 C and D, G and H) and shortly after wounding in seeds (fig. 3.6 I, black arrow). Wounding of leaves for 3 h and 6 h did not result in GUS staining (fig. 3.6 A and B, E and F) and promoter activity in 3 d and 7 d wounded leaves is restricted to wounding sites.

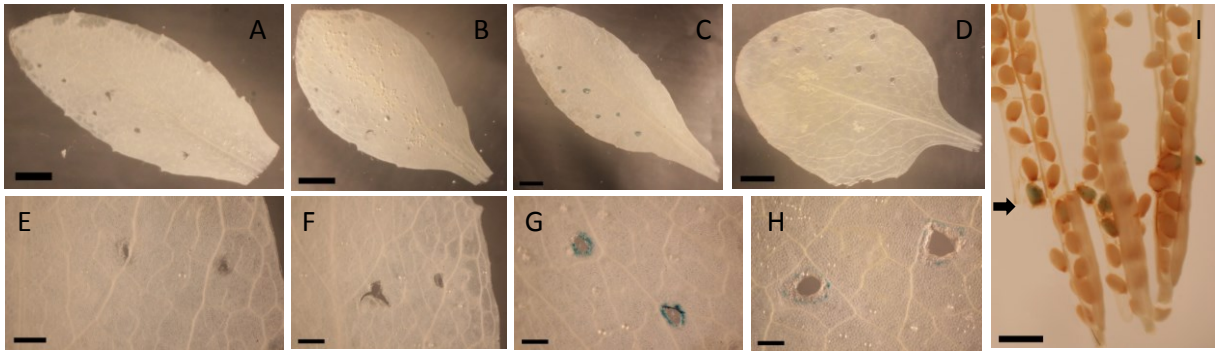

Fig. 3.6 Putative *ANAC058* promoter activity in wounded leaves and seeds of *Prom$_{ANAC058}$::GFP-GUS* plants

Leaves were pierced with forceps and tested for GUS activity 3 h (A and E), 6 h (B and F), 3 d (C and G) and 7 d (D and H) after wounding. Seeds show GUS activity in seed coats at sites where siliques were opened with a cut perpendicular to silique length (I). Localization of incision is marked with an arrow. Scale bars signify 5 mm (A - D), 0.5 mm (E - H) and 1 mm (I).

Seeds not in the vicinity of the silique incision site were absent of GUS activity as well (fig. 3.6 I), as was also observed for intact seeds at various developmental stages (data not shown). When

separating seed coats from embryos, wounding response was observed in both, not necessarily together (data not shown). In order to cause the wounding response, leaves were pierced with a forceps to generated small holes and siliques were cut perpendicular to their lengths shortly before covering them with X-Gluc solution. Wounding response was observed in four of four investigated transgenic lines.

3.1.3.2 Induction of putative *ANAC058* promoter activity by ABA application

Abscisic acid (ABA), a known mediator of stress signals has been shown to induce several genes related to suberin assembly (Barberon et al., 2016; Boher et al., 2013; Yadav et al., 2014).The same applying to *ANAC058* is possible, supported by high sensitivity of *ANAC058* overexpressing plants to ABA (Coego et al., 2014).

Accordingly, testing for ABA susceptibility of *ANAC058* by transferring *Prom$_{ANAC058}$::GFP-GUS* seedlings to MS medium with 1 µM and 30 µM ABA resulted in promoter activity closer to the root tip in ABA treated plants in comparison to mock-treated plants (fig. 3.7). Distance from the root tip at which putative promoter activity decreases again in basal root sections varied in ABA-treated seedlings around the distance observed in the control. Staining intensity also did not seem to differ significantly. The effect was observed in two of two independent transformed lines and appeared to be the same for both ABA concentrations.

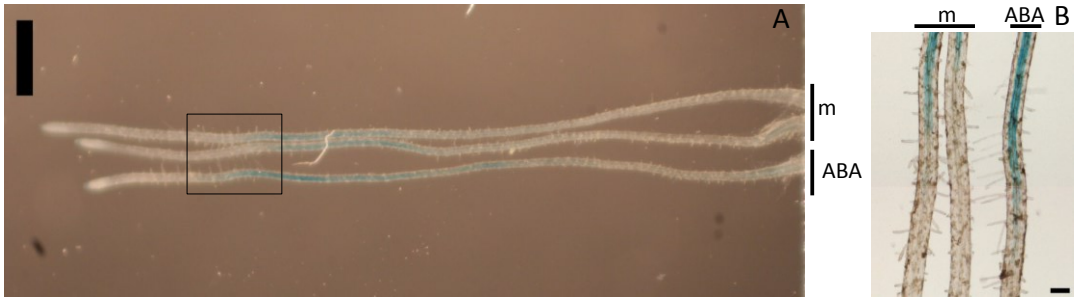

Fig. 3.7 Promoter activity in *Prom$_{ANAC058}$::GFP-GUS* seedlings exposed to ABA
3 d old seedlings were transferred to 1/2 MS with 1 µM and 30 µM ABA, mock-treated seedlings were transferred to ½ MS without ABA (seedlings labeled m). Incubation in X-Gluc solution started 13 h after transfer to ABA. Depicted are representative seedlings for 1 µM and 30 µM ABA treatment (seedling labeled ABA) since both treatments had the same effect. Overview (A) was taken with a binocular microscope; detailed picture (B) of encircled area in A was generated with bright field microscopy. Scale bars signify 1 mm (A) and 0.1 mm (B).

3.1.4 NAC binding sites in suberin gene promoters

As was shown in 3.1.3, the putative *ANAC058* promoter is active in tissues where suberin is known to be deposited and *ANAC058* is co-expressed with genes involved in suberin synthesis and deposition (fig. 3.1). If the *ANAC058* protein binds directly to the promoter of these genes, detection of NAC binding sites (NACBS) in promoters of suberin-associated genes should be possible. Accordingly, the

relative enrichment of NACBS (fig. 3.8 C) was tested for promoter sequences in all suberin genes published to date. For promoter sequences, 1500 bp upstream of transcription start were selected and enrichment was tested with the Analysis of Motif Enrichment (AME, McLeay & Bailey, 2010) tool against the shuffled version of the same sequences. No significant relative enrichment of NACBS motifs was detected (data not shown).

In case NAC binding sites (fig. 3.8 C) might be present in some but not all suberin gene promoters, the same putative promoter sequences as used for the AME analysis were scanned for the relevant motifs with the 'Find Individual Motif Occurrences' (FIMO, Grant et al., 2011) tool. NACBS were found in putative promoter sequences of *FAR1*, *FAR5*, *ABCG20*, *GPAT5* and *GPAT7* as well as *RALPH* and *HORST* (fig. 3.8 A).

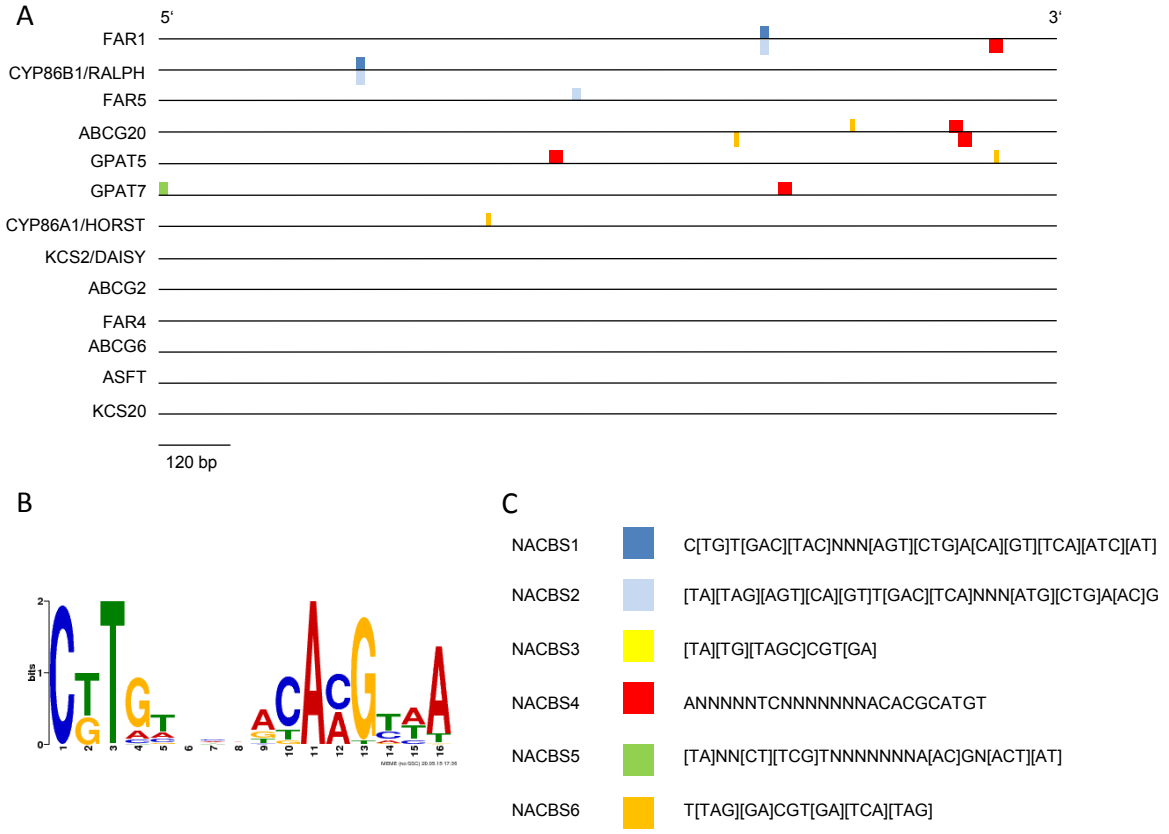

Fig. 3.8 NACBS in promoters of suberin genes

Published NACBS sequences NASBS1 (B) and NACBS2 (O'Malley et al., 2016), downloaded from Plant Cistrome Database http://neomorph.salk.edu as the binding site detected for *ANAC058*, last accessed 13. 06. 17), NACBS3 (Olsen et al., 2005b), NACBS4 (Tran et al., 2004), NACBS5 (Zhong et al., 2010) and NACBS6 (Olsen et al., 2005b) (C) were used for identifying NACBS in promoters of published suberin genes (Beisson et al., 2007; Compagnon et al., 2009; Domergue et al., 2010; Franke et al., 2009; Höfer et al., 2008; Molina et al., 2009; Yadav et al., 2014; Yang et al., 2012). NACBS were found in promoters with the FIMO tool (last accessed 30. 09. 2017) of the MEME Suite web portal (http://meme-suite.org/). Results of the FIMO analysis including exact NACBS location and p-values are available in table 8.3, supp., list of suberin genes in table 8.4, supp..

The most prominent motif is NACBS4 which occurs in 4 of the tested 13 sequences 5 times. NACBS1 (fig. 3.8 B) and NACBS2, which are the same motifs, only reverse complement versions of each other occur together 5 times, NACBS6 4 times and NACBS5 1 time. The motif NACBS3 was not found at all. The promoters of *DAISY*, *ABSG2* and *ABCG6*, *FAR4*, *ASFT* and *KCS20* do not appear to contain any known NAC binding site. The core NACBS sequence was determined as CGT[GA] (Olsen et al., 2005b) which is present in NACBS1, NACBS2, NABS3 and NACBS6. In NACBS1 (fig. 3.8 B) and NACBS2 the core sequence can be found twice – once forward, once reverse which results in a palindromic sequence (C[GT]TG and CA[CA]G and their respective complementary sequences on the other strand G[CA]AC and GT[GT]C).

3.1.5 *In silico* ANAC058 protein structure and domain analyses

In order to investigate the possible ANAC058 protein function in detail, protein structure analyses were conducted. Whereas the DNA binding domain (DBD) in the N-terminal half of the protein is highly conserved within the NAC family (Ooka et al., 2003), the transcriptional regulatory domain (TRD) is often intrinsically disordered (O'Shea et al., 2015).

Testing for the intrinsic disorder (ID) in ANAC058 revealed a completely disordered C-terminal TRD with one predicted α-helix and several molecular recognition features (MoRFs). One MoRF is present in the TRD towards the N-terminus (approx. 160 aa downstream from translation start) and at the very C-terminus (approx. 300 aa downstream from translation start), implicating these amino acids stretches to be of specific importance for the function of the protein. Protein binding, on the other hand, is not predicted with sufficient confidence for any position of the amino acid sequence. The DBD shows a predicted secondary structure similar to the protein structure of ANAC019 which was determined by crystallography (Ernst et al., 2004) (fig. 3.9, below graph). α-helices are localized more to the N-terminus while β-sheets make up the majority of the C-terminal part of the DBD.

Occasionally, NAC activity can be related to motifs specific to phylogenetic groups within the gene family (Kjaersgaard et al., 2011; O'Shea et al., 2015). These motifs can be found by Multiple EM of Motif Elicitation (MEME, Bailey & Elkan, 1994) analysis conducted with the TRDs of NACs belonging to one phylogenetic group. A phylogenetic analysis based on the DBD of NACS revealed ANAC058 to belong to a phylogenetic group called the NAM group in literature (Ooka et al., 2003) and group 7 in the generated phylogenetic tree (fig. 8.3, supp.). MEME analysis was conducted with TRDs of NACs belonging to group 7 and several motifs common within this group were identified (fig. 8.4, supp.). Motif LPPL[MIT]DPS[PF] (sequence contains only amino acids with highest relative frequency at the given position, see fig. 8.4, supp., motif 4 for the complete motif) is the only motif present in *ANAC058* TRD. It consists of ANAC058 amino acids 269 to 277. The amino acids of the motif are close to, but not identical with the amino acids predicted to form an α-helix (amino acids 255 – 261, fig. 3.9). No motif was found at the C-terminus where a MoRF is located.

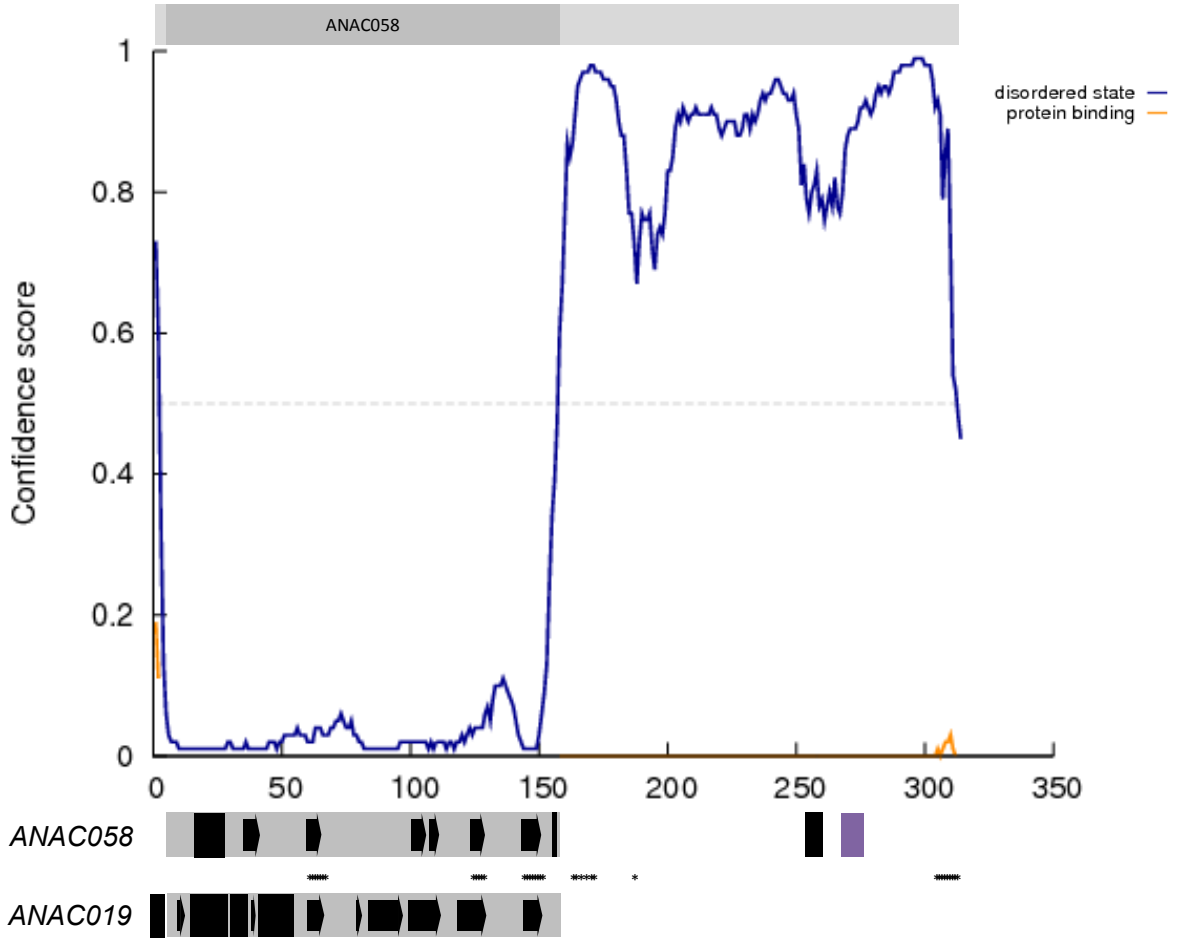

Fig. 3.9 Predicted structural features of ANAC058

Intrinsic disorder of the protein structure was predicted for the very N-terminal end and for the C-terminal domain of the protein by DISOPRED (Bryson et al., 2005) as shown by the graph. The x-axis displays the disorder confidence score, the y-axis the amino acid position. The length of the DBD is represented by the dark gray bar above and below the graph. The complete protein length is signified by the light gray bar above the graph. Beneath the graph, the secondary structure of *ANAC058* with β-sheets (arrows) and α-helices (black bars) as predicted by PSIPRED (Bryson et al., 2005) is depicted. Motif (violet bar) as predicted with MEME (see fig. 8.4, supp.) is shown. Predicted MoRFs (MoRFpred, Disfani et al., 2012) are represented by asterisks. The experimentally determined secondary structure of the DBD of ANAC019 (Ernst et al., 2004) is depicted beneath the predicted ANAC058 structure in the same manner.

3.2 Analysis of *ANAC058* knock-out and knock-down mutants

In order to elucidate the function of *ANAC058*, mutants with depleted or decreased gene expression are of importance. Changes of gene expression can lead to phenotypic effects, indicating the role of *ANAC058* in plant development.

3.2.1 Selection and generation of knock-out and knock-down lines

Databases were used in order to obtain *Arabidopsis thaliana* lines with depleted or decreased expression of *ANAC058*. According to the Salk Institute Genomic Analysis Laboratory (SIGnAL,

fig. 3.10 A - C) and the Arabidopsis Information Resource (tair, fig. 3.10 D) only few lines with insertions inside the coding sequence of the gene in question were found.

While T-DNA insertions in the genomic area surrounding *ANAC058* are frequent (fig. 3.10 A and B), only two lines were annotated with insertions inside the coding sequence of *ANAC058* by the SALK institute (fig. 3.10 C, labeled 1 and 2).

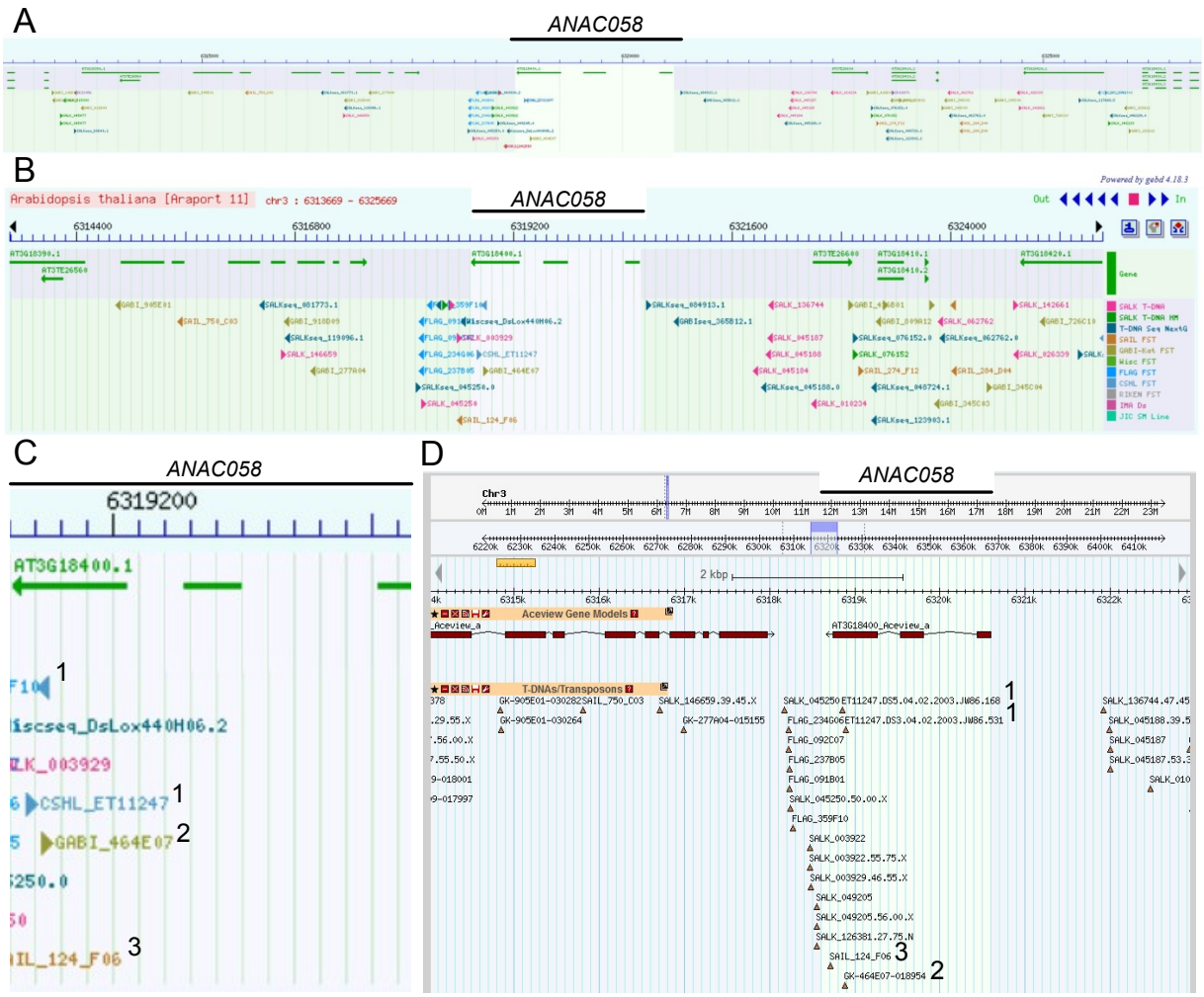

Fig. 3.10 T-DNA insertion frequency in *ANAC058* and surrounding genomic regions
Depicted is an overview of the genomic area surrounding *ANAC058* and the T-DNA insertion lines (triangles) within (A - D). Overview of genomic area (A), a more detailed depiction (B) and the *ANAC058* segment alone (C) indicate three T-DNA insertion lines located within or close to *ANAC058* (lines labeled 1 - 3) as available by the SIGnAL SALK institute T-DNA Express database (Alonso et al., 2003). The database Generic Genome Browser (GBrowse) tool of Arabidopsis Information Resource (tair) indicates the same three T-DNA insertion lines to be located within *ANAC058* (D).

One of those is the CSHL_ET11247 line (fig. 3.10 C and D, annotated with "1") with an insertion at the end of the last exon. It was partially investigated by Marc Frenger in 2014 (Frenger, 2014). It is subsequently referred to as *anac058-1* and its background ecotype is Landsberg *erecta* (L*er*). Its transcript is completely absent when tested by semi-quantitative and quantitative RT-PCR (qRT-PCR) (fig. 3.11 D and E) and the protein is slightly shorter (fig. 8.5, supp.). The other annotated line is

GABI_465E07 (fig. 3.10 C and D, annotated with "2"). Upon further investigation, this line did not contain the insertion at the expected location but further downstream (not shown), outside of the coding sequence. It therefore did not show altered transcript levels (Frenger, 2014). Another line, SAIL_124_F06 suggested an insertion in the last exon according to GBrowse as well (fig. 3.10 D, annotated with "3") but was mapped outside the gene by SIGnAL (fig. 3.10 C, annotated with "3"). Alignment of the sequencing result for this line provided by the distributing institute also showed location outside the gene (not shown).

The absence of a second knock-out line necessitated investigation and generation of knock-down lines. Two lines with insertion in the promoter of *ANAC058* were annotated in the database. Accordingly, the line SALKseq084913 (fig. 3.11 A) was obtained, genotyped (fig. 3.11 C, background ecotype is Columbia) and tested for altered expression. The expression profile showed strongly decreased amounts of transcript and the line therefore served as a strong knock-down line, subsequently labeled *anac058-2* (fig. 3.11 D and E). Whereas expression of *ANAC058* visualized with semi-quantitative RT-PCR was not visible, qRT-PCR showed a small amount of remaining transcript.

Artificial microRNA interference (amiRNAi) lines were generated as described in 2.5.3. The resulting expression clone vector is depicted in supplemental figure 8.22 and plants were transformed (2.5.4 - 2.5.5). Genotyping of plants potentially positive for the amiRNAi construct revealed line 1 to be negative and lines 2 - 4 to be positive (fig. 8.14 A, supp.). *35S::ANAC058 amiRNAi-3* and *-4* were subsequently labeled *anac058-3 (amiRNAi)* and *anac058-4 (amiRNAi)*, respectively.

The *anac058-3 (amiRNAi)* and *anac058-4 (amiRNAi)* lines showed lower amounts of expression in the apical sections of roots compared to the wild type (fig. 3.11 D). Specifically in *anac058-3 (amiRNAi)* roots, about half of the wild type transcript amount remained as shown by qRT-PCR (fig. 3.11 E).

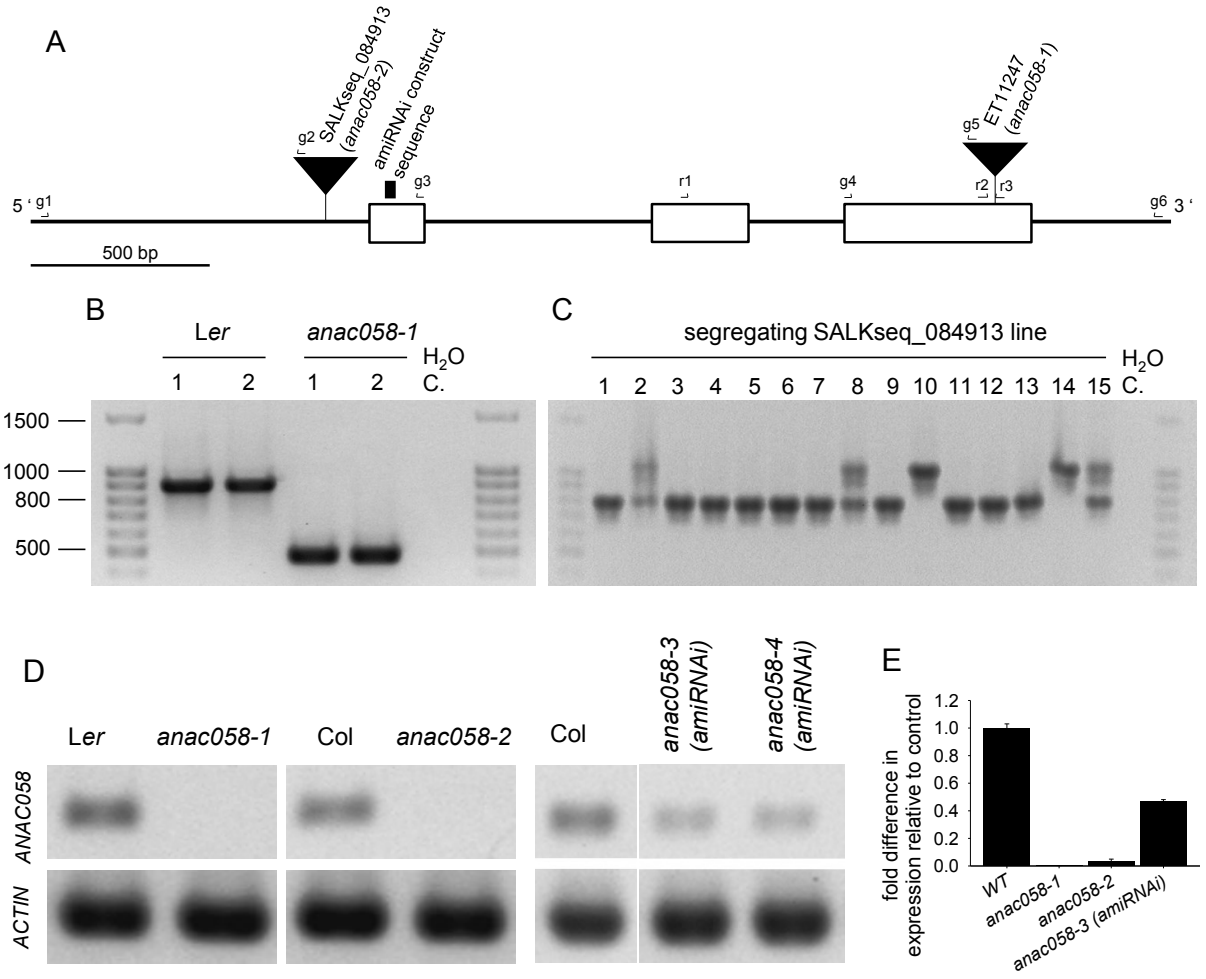

Fig. 3.11 Genotyping and expression analysis of *anac058* lines

The ANAC058 gene locus is depicted (A), including insertion site of T-DNA (black triangle, not to scale) for the respective *anac058* insertion line and the amiRNA construct sequence used to generate *anac058 (amiRNAi)* plants. The DNA sequence including the putative promoter is represented by a black line, the exons by white boxes. Primers for genotyping (g1-6) and qRT-PCR as well as RT-PCR (r1-3) are included. For genotyping of *anac058-1* (ET11247, B) and *anac058-2* (SALKseq_084913, C) primers g4-g6 and g1-g3 were used, respectively. For genotyping of *anac058 (amiRNAi)* lines see fig. 8.14, supp. Semi-quantitative RT-PCR primers r1 and r3 were used, for quantitative RT-PCR (qRT-PCR) primers r2 and r3 were employed.

Semi-quantitative RT-PCR (D) and qRT-PCR (E) analysis of *ANAC058* transcription in wild type and mutant (*anac058-1*, *anac058-2, anac058-3 (amiRNAi) and anac058-4 (amiRNAi)*) lines is depicted. The samples were root tips (apical 6 cm for *anac058-1* and *anac058-2*, apical 3 cm for *anac058 (amiRNAi)* lines) of hydroponically grown plants (5 weeks old for *anac058-1* and *anac058-2*, 4 weeks old for *anac058 (amiRNAi)* lines). Analysis shows decreased or diminished *ANAC058* expression in the mutants. *ACTIN* was used as the control for the semi-quantitative PCR, *GAPDH* for qRT-PCR. Wild type expression of qRT-PCR was set to 1 and mutant expression values were calculated as –fold expression of WT. Pictured are the means and standard deviations of three technical replicates.

3.2.2 Analytical investigation of suberin in *anac058* mutants

ANAC058 shows several indications of being involved in suberin synthesis, among them close linkage to suberin genes in co-expression networks (fig. 3.1), endodermis-specific expression patterns *in silico* (fig. 8.1, supp.) and promoter activity (see 3.1.3) resembling that of known suberin genes. Suberin investigation of the whole root systems of *anac058* mutants by gas chromatography according to the method described in 2.6 was conducted subsequently. However, it did not show consistent effects on suberin amounts or composition for either mutant line (fig. 3.12). Since mutant lines differed in their ecotype background, individual analyses were conducted, either together with L*er* or the Columbia (Col) ecotype. Both mutants and wild type ecotypes were grown and harvested together at the same time.

Identified suberin components belong to the substance groups of fatty acids, primary alcohols, ω-hydroxy fatty acids and α,ω-dicarboxylic acids with carbon chain lengths ranging from C18 to C24 (fig. 3.12). Main components of suberin are ω-hydroxy fatty acids and α,ω-dicarboxylic acids, with ω-hydroxy fatty acids making up 44 % of all found aliphatic components in L*er* and 51 % in Col. α,ω-dicarboxylic acids account for 25 % in L*er* and 26 % in Col.

No significant differences are visible for suberin constituents in either line, except for C22 and C24 fatty acids as well as for the C24 α,ω-dicarboxylic acid which are significantly increased in *anac058-2*. Non-significant differences include most components present in slightly higher amounts in *anac058-2* like C18:1 ω-hydroxy fatty acid. The amount of aliphatic suberin is, consequently, in *anac058-2* slightly higher with 34.91 ± 6.53 µg mg^{-1} than in the wild type (30.79 ± 3.46 µg mg^{-1}). In *anac058-1* most suberin components are present in slightly lower amounts compared to the corresponding wild type which results in slightly lower aliphatic suberin amounts (16.69 ± 2.25 µg mg^{-1}) than in the wild type (19.44 ± 4.37 µg mg^{-1}). A consistent effect on root suberization in whole root systems of soil grown plants due to of the knock-down and knock-out of the *ANAC058* gene expression cannot be shown.

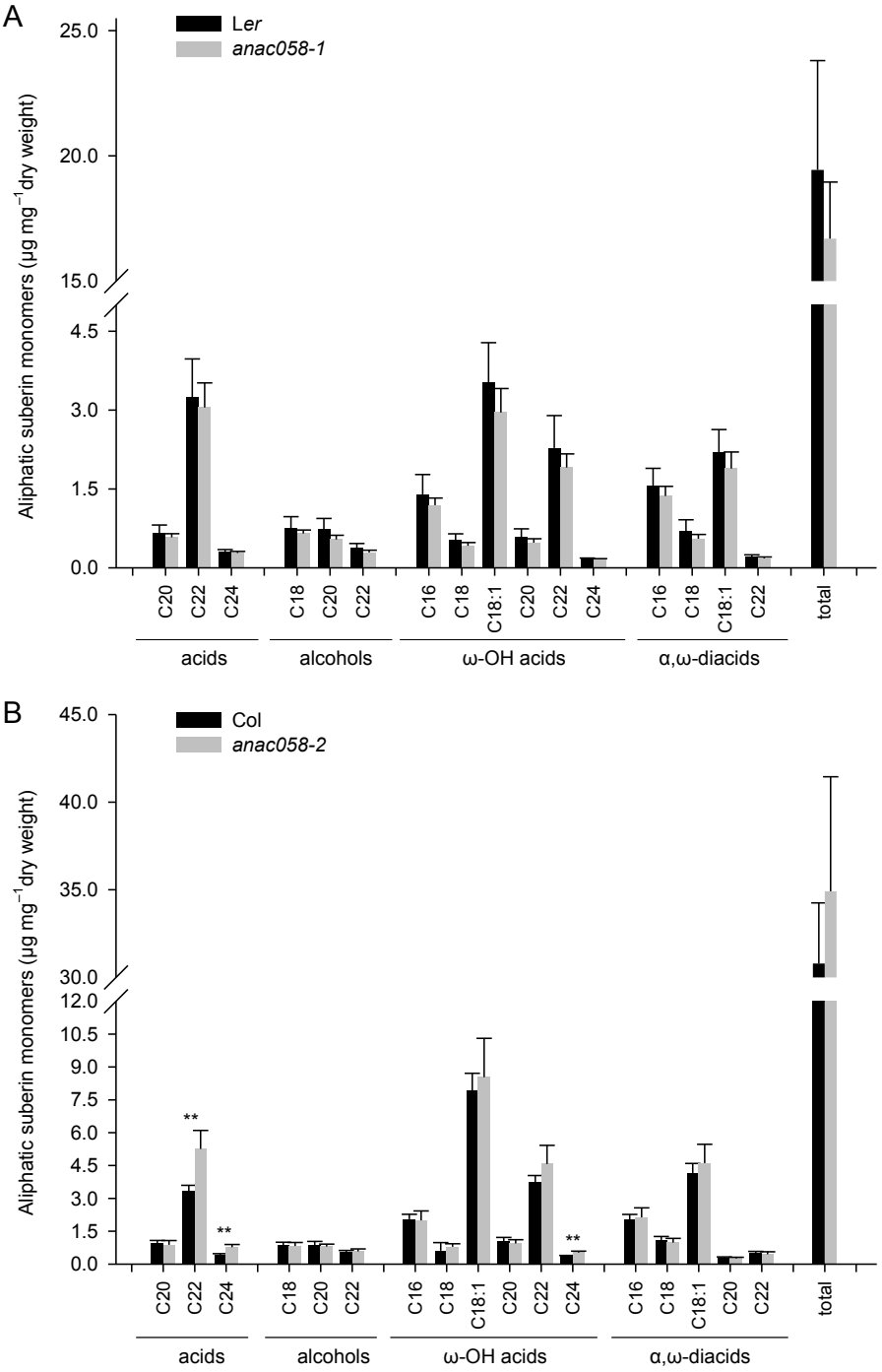

Fig. 3.12 Root suberin composition in *anac058-1* (A) and *anac058-2* (B) mutants and corresponding wild type

Whole root systems of 5 weeks old, soil-grown plants were investigated. Depicted are amounts of aliphatic suberin monomers in µg per mg root dry weight sorted according to substance classes and carbon chain length (fatty acids (acids), primary alcohols (alcohols), ω-hydroxy fatty acids (ω-OH acids) and α,ω-dicarboxylic acids (α,ω-diacids)). Mean values and standard deviations represented by error bars were calculated from 4 independent samples of mutant and wild type each. For related suberin monomer amounts, see table 8.8 and table 8.9, supp.. Significant differences are represented by one ($p \leq 0.05$) or two ($p \leq 0.01$) asterisks as determined by a two-tailed student t-test.

Analyzing the apical root section of hydroponically grown plants yielded a different result on the other hand (fig. 3.13). Plants were grown for 5 weeks hydroponically and apical parts of the root system, 7 cm and 6.5 cm for *anac058-1* and *anac058-2* respectively, were collected for suberin analysis. The root samples, not treated with cell wall degrading enzymes before analysis reveal less aliphatic suberin per root dry weight (3.96 ± 0.92 µg mg^{-1} for L*er* and 3.04 ± 0.37 µg mg^{-1} for Col) than samples in figure 3.12. Composition of suberin is the same. Accordingly, identified monomers belong to the substance classes of fatty acids, primary alcohols, ω-hydroxy fatty acids and α,ω-dicarboxylic acid and their carbon chain lengths range from C18 to C24.

In case of *anac058-1*, a consistent, though not significant, decrease is visible for all detected suberin monomers. Just the C18 and C24 ω-hydroxy fatty acid amounts are very similar to wild type values. The effect on suberin in apical sections of root systems resembles that on suberization of whole root systems but is more pronounced. The amount of total aliphatic suberin in *anac058-1* is 15.36 % lower than in the corresponding wild type.

A much clearer picture is generated by the analytical investigation of suberin in apical root sections of *anac058-2* plants. Grown under the same conditions as *anac058-1* mutants, the apical section of roots in *anac058-2* contained in total 34.78 % less aliphatic suberin than the wild type. A significant decrease in amounts is visible for almost every monomer. This effect can especially be seen for the major suberin components C18:1 ω-hydroxy fatty acid and C18:1 α,ω-dicarboxylic acid, which are reduced in their amounts by 55 % and 36 %, respectively.

The suberin phenotype in apical root sections of *anac058* mutants was observed for both alleles in two separate experiments.

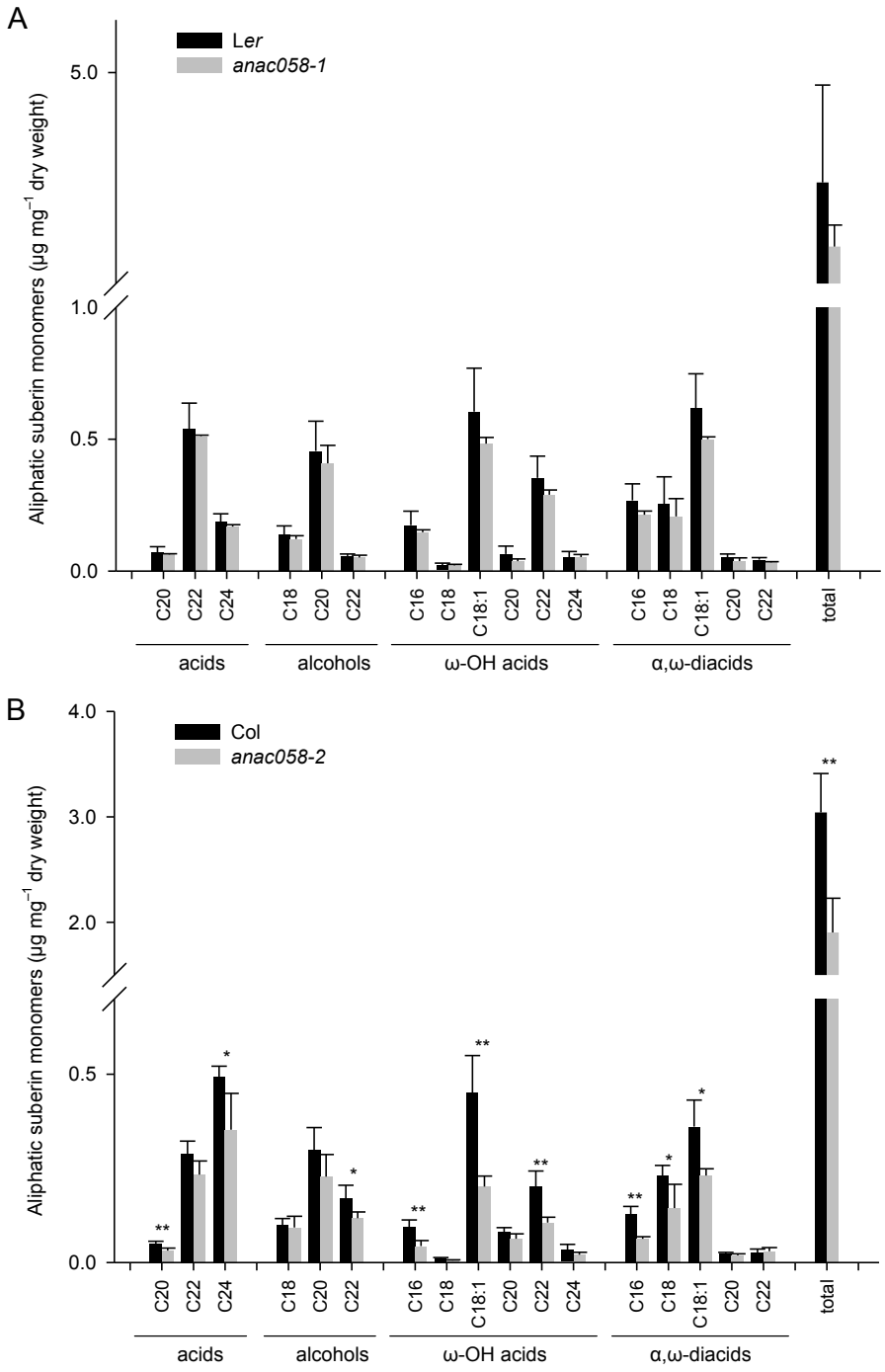

Fig. 3.13 Root suberin composition in apical root sections of *anac058-1* (A) and *anac058-2* (B) mutants in comparison to the corresponding wild type

Apical root sections (*anac058-1*: apical 7 cm (A), *anac058-2*: apical 6.5 cm (B)) of 5 weeks old, hydroponically grown plants were analyzed. Depicted are amounts of aliphatic suberin monomers in µg per mg root dry weight sorted according to substance classes and carbon chain length (fatty acids (acids), primary alcohols (alcohols), ω-hydroxy fatty acids (ω-OH acids) and α,ω-dicarboxylic acids (α,ω-diacids)). Mean values and standard deviations represented by error bars were calculated from 4 independent samples of mutant and wild type each. For related suberin monomer amounts, see table 8.10 and table 8.11, supp.. Significant differences are represented by one ($p \leq 0.05$) or two ($p \leq 0.01$) asterisks as determined by two-tailed student t-test.

3.2.3 Histological investigation of suberin in *anac058* mutants

The results from the suberin analysis using gas chromatography (fig. 3.13) and the presence of promoter activity in apical root sections (fig. 3.5) suggested *ANAC058* knock-out and knock-down mainly effects seedling roots and young root sections. Staining of suberin with the lipophilic dye Fluorol Yellow 088 visualizes presence of suberin in single young seedlings with regard to tissue- and development-specific localization.

Accordingly, 6 d old seedlings grown on MS agar were stained with Fluorol Yellow 088 and a clear effect was discovered in *anac058* mutants (fig. 3.14, for the method, see 2.7.3).

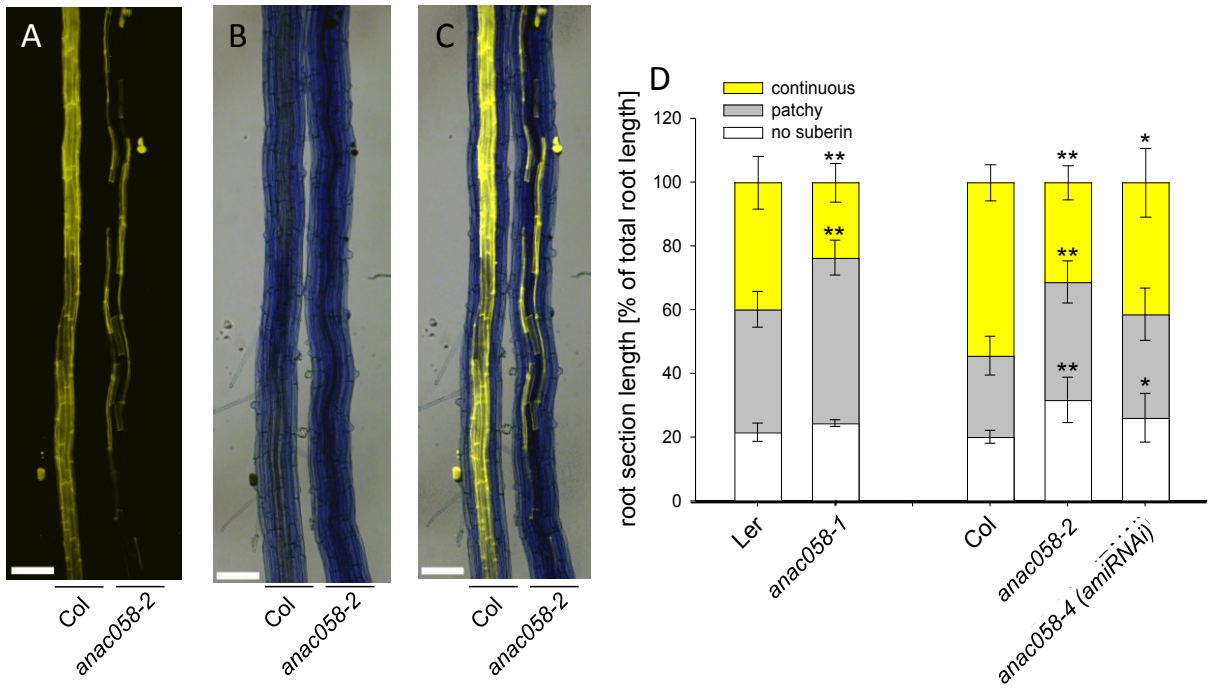

Fig. 3.14 Suberin deposition in *anac058* and wild type seedlings stained with Fluorol Yellow 088
Suberin was stained with Fluorol Yellow 088 in 6 d old seedlings grown on MS plates. Depicted are representative pictures showing Col and *anac058-2* roots of the same length at a position where the endodermis is fully suberized (continuous) in the wild type but in *anac058-2* suberin appears still in a patchy manner (A). Fluorescence was observed with a fluorescence microscope employing a standard GFP filter, bright field pictures of the same root section was taken (B) and an overlay of both pictures was generated in ImageJ (C). Measuring the length of root sections with different suberization states (no suberin, patchy, continuous, for a model, see fig. 2.7) allows the calculation of root section length as percentage of total root length (D). Mean values and standard deviation represented by error bars were calculated from 5 (L*er* and *anac058-1*), 6 (*anac058-2*), 7 (Col) or 10 (*anac058-4 (amiRNAi)*) independent seedlings. Col values corresponding to *anac058-4 (amiRNAi)* are not included in D since they are very similar to the depicted Col values (see table 8.17, supp). Significant differences are represented by one ($p \leq 0.05$) or two ($p \leq 0.01$) asterisks as determined by student t-test. For all values, see table 8.15 - 8.17, supp., for representative pictures of *anac058-1*, *anac058-4 (amiRNAi)* and respective wild types see fig. 8.6, supp..

Comparing mutants with depleted (*anac058-1*) and decreased (*anac058-2* and *anac058-4 (amiRNAi)*) *ANAC058* expression (fig. 3.11 D and E) to their respective wild types revealed delayed suberization

along the root in the mutants (fig. 3.14). The length of the root section without any suberin, with patchy suberin where only single cells are suberized (fig. 3.14 A and C*, anac058-2* root) and with continuous suberin was measured (fig. 3.14 A and C, WT root). In case of continuous suberin, all cells of the endodermis are showing Fluorol Yellow 088 staining with the exception of single cells. These unsuberized cells in a fully suberized endodermis are passage cells and allow controlled uptake of water and nutrients (Peterson and Enstone, 1996). In the wild type L*er*, 21.55 % of the total root length showed no suberin (fig. 3.14, no suberin), 38.53 % showed patchy staining and 39.92 % a continuously suberized endodermis. In *anac058-1*, a delay in suberin deposition resulted in significantly less continuous suberin (23.7 % of total root length). The proportion of the root without suberin and with patchy suberin is therefore increased. Col compared to L*er* has more continuous suberin (54.44 % of total root length) but a lower percentage of the root is unsuberized or shows patchy suberin. In the case of *anac058-2* compared to Col, the suberin deposition delay is even more pronounced. The mutant has significantly less endodermis with continuous suberin (31.33 % of total root length) compared to the WT (54.44 % of total root length). The *amiRNAi line anac058-4* (amiRNAi) displays an intermediate phenotype as the proportion of the root with continuous suberin is significantly lower with 41.47 % of total root length compared to Col (54.44 % of total root length). The delay in suberization was observed for *anac058-2* in three and for *anac058-1* in two separate experiments.

3.2.4 Expression analysis of suberin genes in *anac058* mutants

In *anac058* mutant lines, a decrease in expression of the *ANAC058* gene resulted in lower amounts of suberin as shown in 3.2.2 and 3.2.3. Since *ANAC058* is a transcription factor, expression of suberin-associated genes can be expected to decrease accordingly. Expression of three genes involved in suberin synthesis, *RALPH*, *GPAT5* and *HORST*, was tested with qRT-PCR in the apical section of root systems for the knock-out line *anac058-1* as well as the knock-down lines *anac058-2* and *anac058-3 (amiRNAi).* Plants were grown hydroponically for 4-5 weeks before sample collection. *ANAC058* expression is non-existent in *anac058-1*, strongly decreased in *anac058-2* to 0.03 times the wild type expression and in the RNAi lines *anac058-3 (amiRNAi)* the expression is 0.5 fold that of the wild type (fig. 3.15).

All three suberin synthesis genes revealed lower expression in both lines except for *GPAT5* in *anac058-1*. In *anac058-1 RALPH* and *HORST* expression is decreased to 0.6 – 0.8 -fold the wild type expression level. In *anac058-2*, expression of *RALPH* and *HORST* is decreased by half compared to the wild type (0.54 ± 0.05 and 0.47 ± 0.02 respectively), whereas *GPAT5* expression is lower only by 0.73-fold the wild type expression. The amiRNAi line *anac058-3 (amiRNAi)* contains half the amount of *ANAC058* transcript compared to wild type and expression of *RALPH* and *GPAT5* is lower by the same margin. For *anac058-1* and *anac058-2* the expression of *RBOHF* was measured as well in order to clarify whether the knock-out and knock-down of *ANAC058* expression has an effect on genes involved in Casparian strip (CS) formation. *RBOHF* has been shown to be necessary for the correct formation of CS by Lee and coworkers (Lee et al., 2013). Since CSs are located to the endodermis as well as suberin, the endodermal-specific expression of *ANAC058* could indicate involvement in

regulation of the CS formation as well as suberin. The knock-out and knock-down of *ANAC058* has no decreasing effect on *RBOHF* expression, as expression is slightly increased in *anac058-1* and *anac058-2*.

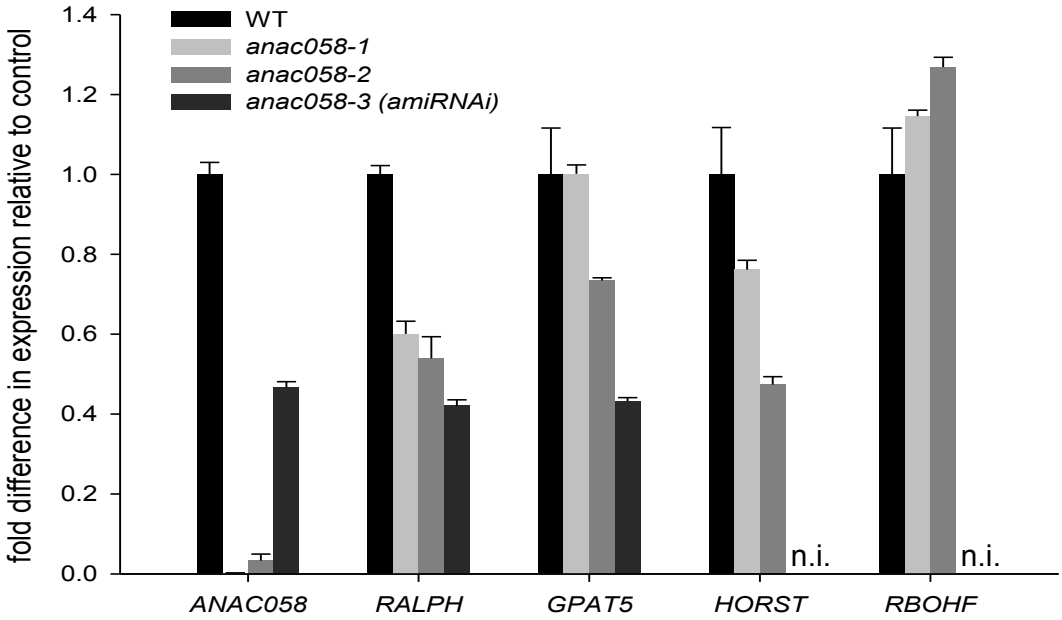

Fig. 3.15 Suberin gene expression in apical root sections of *anac058* mutants

Gene expression was measured in hydroponically-grown plants (*anac058-1*, *anac058-2* and respective wild type grown for 5 weeks, *anac058-3 (amiRNAi)* and respective wild type grown for 4 weeks) and apical 6 cm (*anac058-2* and respective wild type), 4 cm (*anac058-1* and respective wild type and 3 cm (*anac058-3 (amiRNAi)* and respective wild type) were collected. All wild type values were set to one and only wild type values corresponding to *anac058-2* are depicted. The expression values for *anac058* mutants are the -fold expression of their respective wild type expression. *GAPDH* was used as the endogenous control. For all values, see table 8.6, supp.. Depicted are the means of three technical replicates. n. i.: not investigated

3.2.5 Physiological effect of decreased suberin amounts in *anac058* mutants

Changes in root suberin may have a physiological effect on the root's barrier function which in turn can change the root physiology. In order to investigate the impact of a mutation in *ANAC058* and consequently decreased suberin amounts, root hydraulic conductivity was measured as well as the susceptibility to salt and osmotic stress.

3.2.5.1 Susceptibility of *anac058* mutants to salt and osmotic stress

Possible effects of lower suberin amounts in *anac058* on stress susceptibility were tested by applying salt stress. The plants were grown on ½ MS plates with 50 mM NaCl by letting them germinate on as well as transferring 3 d old seedlings to this high salt medium. Root growth was measured as main root length.

Germination on control medium and 50 mM NaCl MS medium yielded no significant differences between mutants and their respective wild types as suggested by figure 3.16. Plant growth was observed over 5 weeks in total without any visible effect of the NaCl treatment. Representative seedlings of 10 d age were selected for in-depth analysis of salt-treatment effect. The measurement of root length shows that seedlings of all genotypes are affected by NaCl, causing increased root growth compared to seedlings growing on control medium (fig. 8.7, supp.). This effect is predominantly observed for Col and *anac058-2*. The measurement also confirms same root growth of wild type and mutants. Additionally, occasional growth arrest shortly after germination was observed under NaCl conditions. This effect does not differ between wild type and mutant plants (not shown) and is therefore not influenced by a mutation in *ANAC058*.

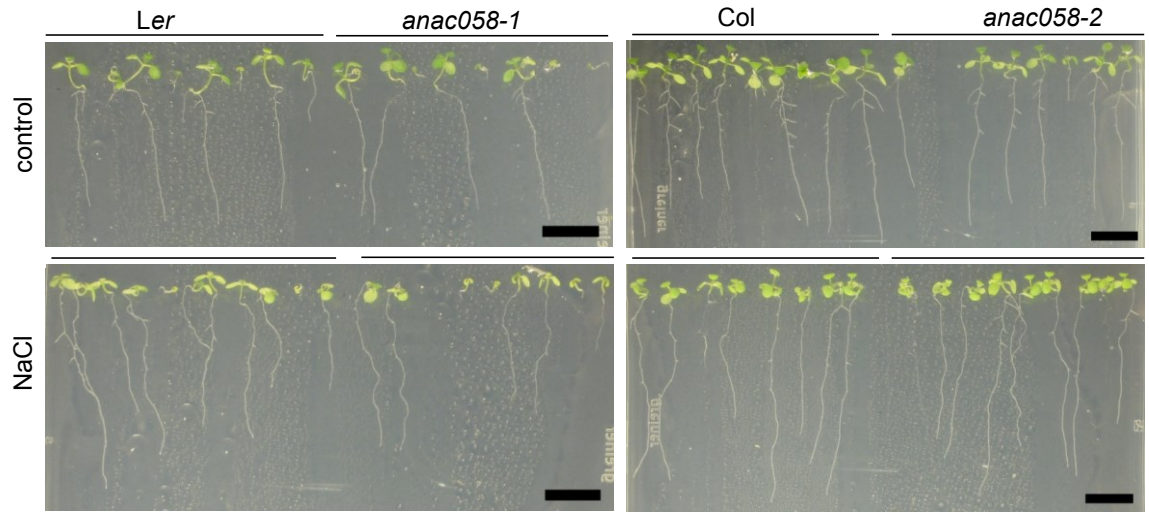

Fig. 3.16 Germination of *anac058* mutants and corresponding wild type on 50 mM NaCl and control medium

Representative picture of plants observed in total over 5 weeks, here seedlings grown for 10 d on 1/2 MS and 1/2 MS supplemented with 50 mM NaCl are depicted. For root length measurements, see fig. 8.7, and table 8.20, supp.. Scale bars represent 1 cm.

In order to exclude potential early effects of NaCl as well as prior adjustment of plants to high salt concentration, seedlings were grown for 3 d on MS medium and transferred to MS with 50 mM NaCl. Seedling growth was observed over 5 weeks in total but no significant differences between wild type and mutants due to salt treatment were observed (fig. 3.17). For representative in-depth analysis, 10 d old seedlings, grown for 3 d on MS and 7 d on NaCl medium were selected. Root growth differed between individual seedlings considerably, especially in case of *anac058-1* and its respective wild type. Significant differences between mutant lines and their wild type were not observed, as shown by their similar root length (fig. 3.17). L*er* seedlings had a root length of 3.9 ± 1.54 cm, *anac058-1* seedlings of 3.63 ± 1.2 cm (fig. 3.17 B). Comparing Col and *anac058-2* root length with respective 4.68 ± 0.75 cm and 4.42 ± 0.69 cm revealed only slightly shorter roots for the mutant. To measure only root growth on NaCl medium, the distance from the root tip until the dot marking the position of the root tip directly after transfer to NaCl medium was quantified. After 7 d growth on NaCl medium, same

trends as for total root length were observed. The slight differences were not significant and differences between ecotypes were larger than between mutant and respective wild type. Generally, a very slight trend toward shorter roots in the mutant appeared which, on the other hand, was not observed for seedlings germinating on NaCl medium (fig. 3.16 and fig. 8.7, supp.).

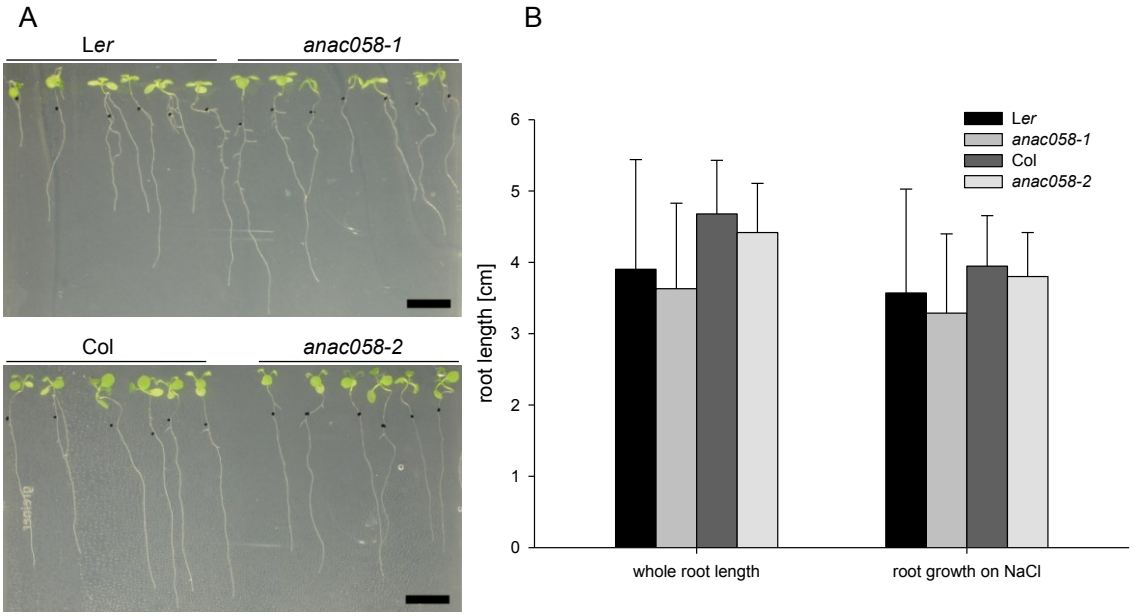

Fig. 3.17 Growth of *anac058* seedlings on 50 mM NaCl in comparison to the corresponding wild type
Of seedlings observed in total for 5 weeks, representative pictures of seedlings transferred after 3 d growth on 1/2 MS and grown for 7 d on 1/2 MS with 50 mM NaCl were selected (A). Root tip position directly after the transfer to NaCl medium was marked by a black dot and total root length of the main root as well as main root length grown only on NaCl medium (dot to root tip) was measured (B). Mean values and standard deviation represented by error bars were calculated from 23 (Col), 24 *(anac058-2*), 16 (L*er*) and 14 (*anac058-1*) independent seedlings. Significant differences are represented by one ($p \leq 0.05$) or two ($p \leq 0.01$) asterisks as determined by student t-test. For related values see table 8.21, supp.. Scale bars represent 1 cm.

In contrast to the results from seedlings growing on 50 mM NaCl MS plates, long term salt treatment of *anac058* mutants and wild types with 50 mM NaCl by growing them in hydroponics had a different effect (fig. 3.18).

anac058-1, *anac058-2* and wild type plants were transferred to hydroponic solution with 50 mM NaCl for salt treatment and control plants were transferred to new hydroponic solution without changed salt concentrations. Water potential of respective solutions was measured and – 0.09 MPa was detected for the control solution, whereas water potential in the NaCl solution was distinctly lower (- 0.36 MPa). All genotypes were affected by the salt treatment with leave margins showing necrotic spots (fig. 3.18 B). Additionally, fresh weight and dry weight of plants subjected to 50 mM NaCl is lower than for control plants (fig. 3.18 C and fig. 8.8, supp.).

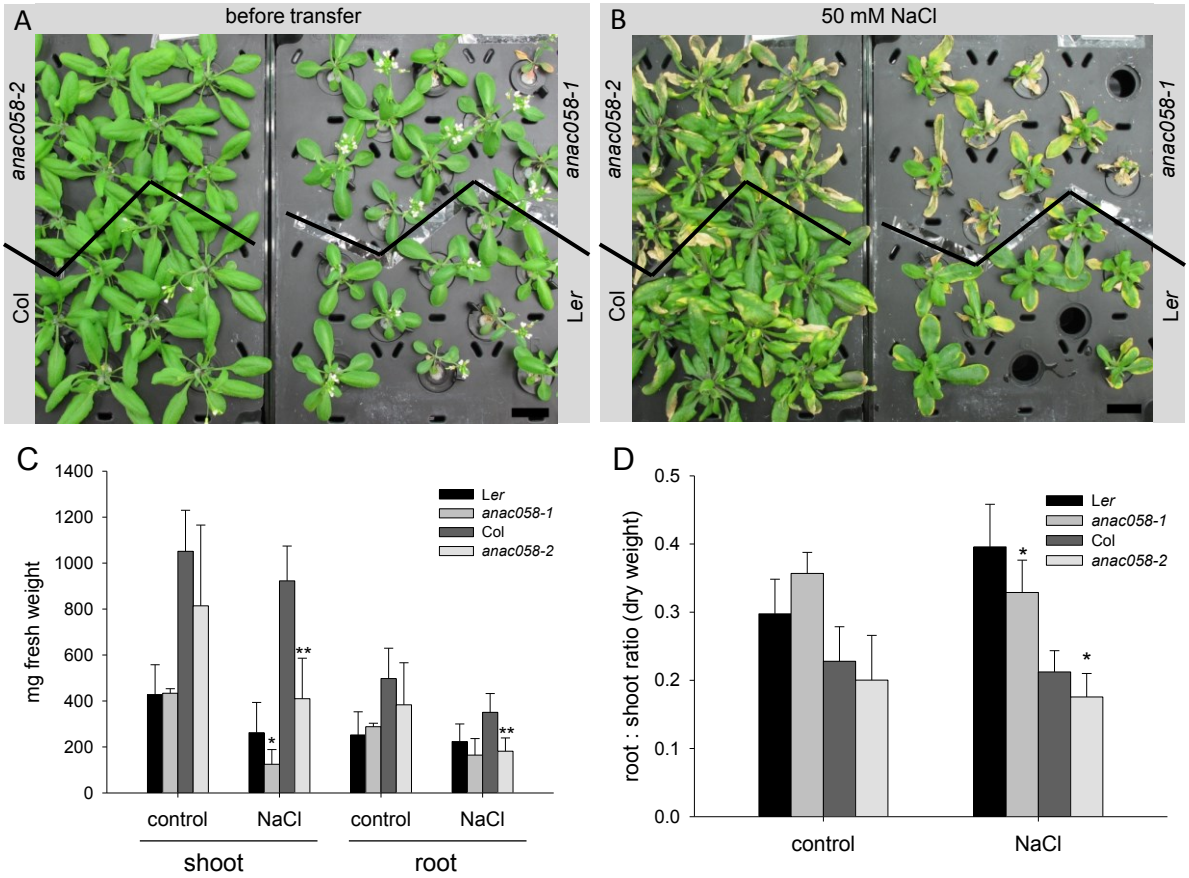

Fig. 3.18 Growth of *anac058* mutants and wild type in 50 mM NaCl and control solution

Plants were grown for 25 d in hydroponics (A) and were transferred to new hydroponics solution (control) or hydroponics solution supplemented with 50 mM NaCl. Plant health was investigated after 2 weeks of NaCl treatment (B - D). Root and shoot fresh weight (C) and dry weight (fig. 8.8 A, supp.) were measured and root:shoot ratio was calculated from fresh weight (fig. 8.8 B, supp.) and dry weight (D). The ratio fresh weight:dry weight is depicted in fig. 8.8 C, supp. Mean values and standard deviations represented by error bars were calculated from 5 (Col), 4 (*anac058-2*), 6 (L*er*) and 3 (*anac058-1*) independent seedlings for control conditions and from 7 (Col), 9 (*anac058-2*), 7 (L*er*) and 8 (*anac058-1*) independent seedlings for salt conditions. Significant differences are represented by one ($p \leq 0.05$) or two ($p \leq 0.01$) asterisks as determined by student t-test. All related values are present in table 8.22, supp.. Scale bars represent 2 cm.

Mutants seemed more susceptible to 2 weeks of salt treatment than control plants. As a consequence, they generated significantly less biomass (fig. 8.8, supp.). Plant health deterioration is visible (fig. 3.18 B) since the shoots of the mutants show more necrosis than the respective wild type. *anac058* fresh weight is significantly reduced for the shoot as well as root under high salt conditions. The only exceptions are *anac058-1* roots for which fresh weight is decreased but insignificantly. Dry weight is lower as well for mutants compared to the respective wild type but only significantly in case of *anac058-2* (fig. 8.8, supp.). The fresh weight:dry weight ratio indicates the impact of salt stress on water content and biomass. The ratio generally decreases for the mutants (fig. 8.8, supp.), indicating that water content decreases in mutants more than biomass. The root:shoot ratio derived from dry weight values is significantly lower in *anac058-1* and *ana058-2* with 0.33 ± 0.05 mg and 0.18 ± 0.03 mg, respectively, compared to their wild types with 0.4 ± 0.06 mg (L*er*) and 0.21 ± 0.03 mg

(Col). Since biomass of root and shoot decreases, the lower ratio indicates that roots are more strongly affected than shoots in mutants compared to the respective wild types. Occasionally, differences were observed between wild type and *anac058-2* already under control conditions (fig. 8.8, supp.) although effects were stronger after salt stress treatment. Additionally, differences between the wild types which belong to disparate ecotypes were observed in reaction to salt stress. For Col, root:shoot ratio decreases whereas for L*er* the ratio increases with regard to dry weight (fig. 3.18) and fresh weight (fig. 8.8, supp.). Consequently, Col roots are more affected by salt stress, whereas for L*er* a strong effect on shoots is observed.

In order to generate osmotic stress, *anac058-1*, *anac058-2* and wild types were transferred to a nutrient solution with 1.73 % PEG, whereas control plants were transferred to a new hydroponic control solution.

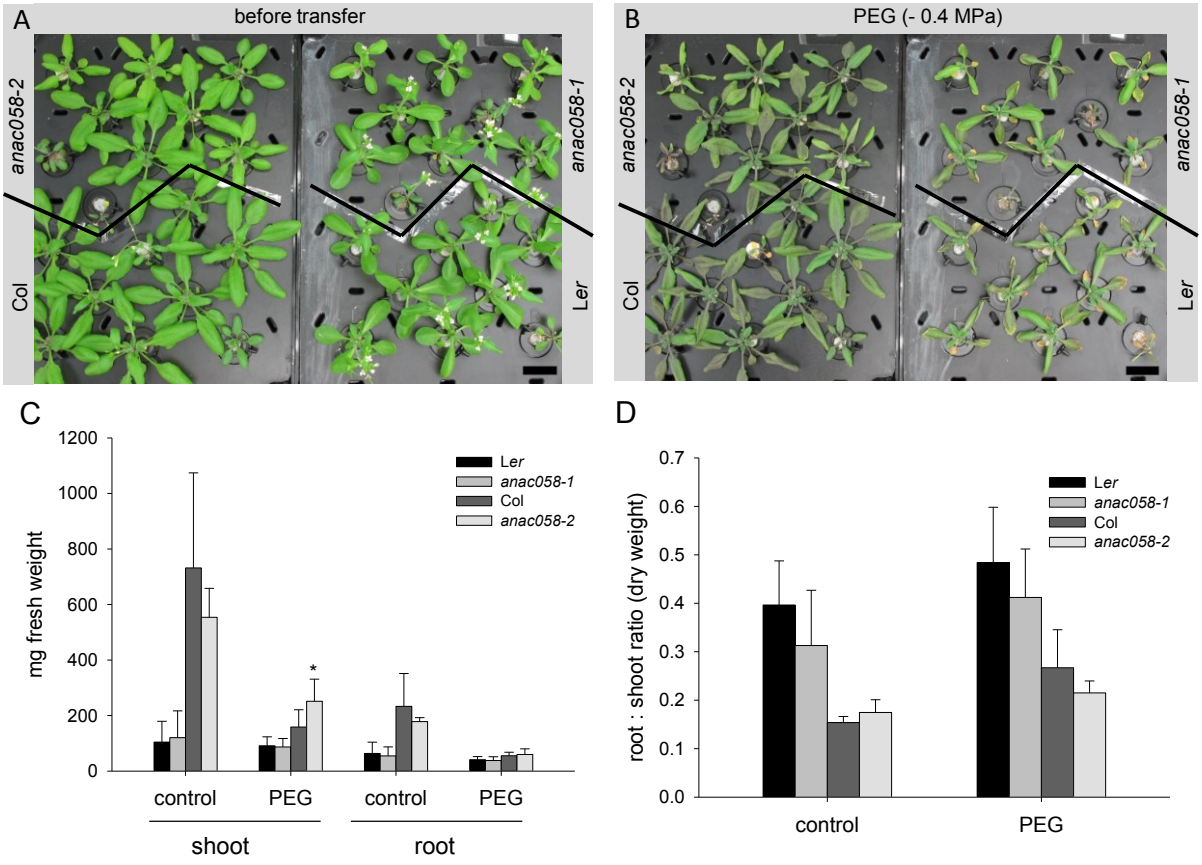

Fig. 3.19 Growth of *anac058* mutants and wild type in 1.73 % PEG and control solution

Plants were grown for 25 d in hydroponics (A) and were transferred to new hydroponics solution (control) or hydroponics solution supplemented with 1.73 % PEG (173 g/l H_20, water potential Δ - 0.4 MPa). Plant health was investigated after 4 d of PEG treatment (B - D). Root and shoot fresh weight (C) and dry weight (fig. 8.9 A, supp.) was measured and root:shoot ratio was calculated from fresh weight (fig. 8.9 B, supp.) and dry weight (D). The ratio fresh weight:dry weight is depicted in fig. 8.9 C, supp.. Mean values and standard deviations represented by error bars were calculated from 3 (Col, *anac058-2*, L*er*, *anac058-1*) independent seedlings for control conditions and from 6 (Col), 7 (*anac058-2* and L*er*) and 8 (*anac058-1*) independent seedlings for PEG conditions. Significant differences are represented by one ($p \leq 0.05$) or two ($p \leq 0.01$) asterisks as determined by student t-test. All related values are present in table 8.23, supp.. Scale bars represent 2 cm.

4 d of PEG treatment affected health of all genotypes in a severe manner (fig. 3.19 B). 1.73 % PEG changed the water potential of the hydroponics solution to - 0.49 MPa compared to - 0.09 MPa of the control nutrient solution as measured with a potentiometer. This change in water potential resulted in plant health deterioration visible as curling and red coloration of leaves. Specifically L*er* and *anac058-1* also displayed necrosis at the leaf margins, indicating the L*er* ecotype to be more severely affected. When measuring root and shoot biomass, dry weight and fresh weight for plants subjected to PEG treatment was lower than for control plants. No significant differences between mutants and respective wild types appeared except for the shoot fresh weight amounts of *anac058-2.* Those were significantly increased compared to Col. This effect was not observed in the other mutant line or for root fresh weight and was therefore deemed unrelated to suberin amounts. The root:shoot ratio increased for all genotypes upon PEG treatment and was slightly lower in mutants than in the wild type but significant differences were absent.

3.2.5.2 Root hydraulic conductivity of *anac058* mutants

To investigate root barrier properties of *anac058* plants, root hydraulic conductivity was measured (fig. 3.20). Whole root systems of 3 weeks old, hydroponically grown plants were excised and inserted into a pressure chamber as described in 2.2.4. Pressure was applied and root hydraulic conductivity L_{p_r} was calculated with the slope from exuded sap flow and applied pressure per root dry weight.

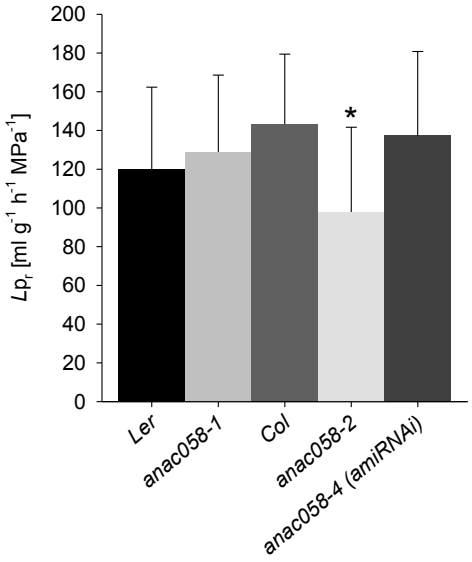

Fig. 3.20 Root hydraulic conductivity L_{p_r} of *anac058* mutants in comparison to the wild type
Seedlings were grown for 10 d on 1/2 MS plates, transferred to hydroponics and measured at the developmental stage of 3 weeks. L_{p_r} is calculated from root sap flow (ml h^{-1}) per applied pressure (MPa) related to root dry weight (g) (for details, see 2.2.4). Mean values and standard deviations represented by error bars were calculated from 20 (L*er*), 21 (*anac058-1*), 19 (Col and *anac058-4 (amiRNAi)*) and 18 (*anac058-2*) independent plants. Significant differences are represented by one ($p \leq 0.05$) or two ($p \leq 0.01$) asterisks as determined by Tukey test. All related values are present in table 8.24, supp..

The ecotypes Col and L*er* differed in their Lp_r values with 143.22 ml g^{-1} h^{-1} MPa^{-1} (± 36.23) and 119.65 ml g^{-1} h^{-1} MPa^{-1} (± 42.71), respectively. Root hydraulic conductivity in *anac058* mutants, on the other hand did not differ consistently from the wild type. Whereas L*er* and *anac058-1* have very similar Lp_r, it is significantly decreased in *anac058-2* (97.9 ± 43.75) compared to Col. The line *anac058-4 (amiRNAi)* did not show a significant effect but Lp_r is tendentially lower.

3.3 Overexpression of *ANAC058*

3.3.1 Tissue-specific overexpression of *ANAC058* in $Prom_{RALPH}$::*ANAC058* plants

As shown in 3.2, decrease in *ANAC058* expression co-exists with lower expression of suberin synthesis genes and reduced amounts of suberin. Overexpression of *ANAC058* therefore was suspected to result in increased expression of suberin genes and suberin amounts. Constitutive overexpression lines generated by Marc Frenger (Frenger, 2014) with the *ANAC058* expression driven by the constitutive 35S promoter showed strong overexpression of *ANAC058* in leaves and, accordingly, *RALPH*, *GPAT5* and *HORST* expression is also increased. Suberin amounts in roots of *35S::ANAC058* plants, quantified by gas chromatography analysis, on the other hand remained the same. Constitutive overexpression in all tissues and developmental stages might result in silencing of expression in specific organs as the plant may need to protect itself against damaging effects of overexpression. In order to avoid this effect, a tissue-specific overexpression line was generated with *ANAC058* CDS cloned behind the putative *RALPH* promoter. This promoter has been shown to be active in the endodermis of primary roots and the *RALPH* gene itself is necessary for generation of wild type suberin (Compagnon et al., 2009).

The $Prom_{RALPH}$::*ANAC058* construct (fig. 8.23, supp.) was generated by Marc Frenger (Frenger, 2014) as described in 2.5 with the Gateway system. The vector was transformed into *Agrobacterium tumefaciens* and wild type plants transformation followed as mentioned in 2.5.4. Selection for positive transformed T1 plants followed as described in 2.5.5. Three independent transformed lines were found (fig. 8.14, supp.).

3.3.1.1 Expression of *ANAC058* and suberin genes in roots of $Prom_{RALPH}$::*ANAC058* plants

After confirming the correct genotype, expression levels of the *ANAC058* gene were tested in the tissue-specific overexpression lines compared to the wild type by reverse transcription PCR. Expression in whole root systems of two individual plants per $Prom_{RALPH}$::*ANAC058* transformed line (fig. 3.21, labeled 1 and 2 each) and three wild type plants (fig. 3.21, labeled 1-3) were tested.

Slight overexpression of *ANAC058* was detected in $Prom_{RALPH}$::*ANAC058 lines-17* and *-20* but not in line $Prom_{RALPH}$::*ANAC058-18*. Expression of *GPAT5* and *RALPH* was tested as well since both genes have been shown to be overexpressed in leaves of *35S::ANAC058* plants (Frenger, 2014). The

expression pattern of both genes did not fit to the *ANAC058* expression pattern and expression is not distinctly increased in the lines overexpressing *ANAC058*.

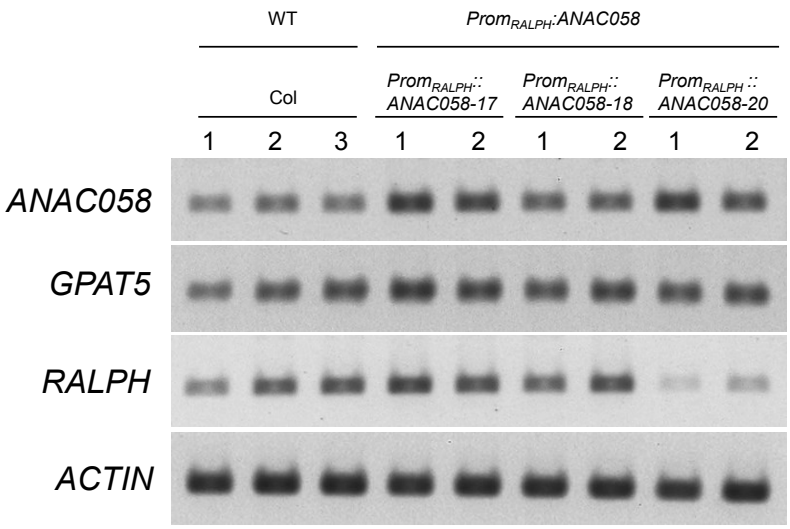

Fig. 3. 21 Expression of *ANAC058* and suberin genes in roots of *Prom$_{RALPH}$::ANAC058* and wild type
Whole root systems of hydroponically-grown 5 weeks old plants were collected. Three Col plants were investigated (1 - 3) and 2 plants of each *Prom$_{RALPH}$::ANAC058* line (labeled 1 and 2). *ACTIN* was used as the control.

3.3.1.2 Histological investigation of suberin in *Prom$_{RALPH}$::ANAC058* plants

In order to reveal whether suberin amounts are affected in plants overexpressing *ANAC058* in a tissue-specific manner, seedlings of two of the transformed lines were stained with Fluorol Yellow 088. Instead of higher amounts of suberin, as expected for *ANAC058* overexpressing mutants, suberin deposition seems to be slightly delayed (fig. 3.22 A and C).

When measuring the distance from the root tip until first fluorescence signal, this distance is larger in the overexpressing lines than in the wild type. Since the lines are still segregating, wild type suberin deposition was seen in several seedlings of both lines which accounts for the high variability of the measured values (fig. 3.22 D). Nevertheless, the delay of suberin deposition in *Prom$_{RALPH}$::ANAC058-17* is highly significant regarding patchy suberin start and significant regarding the start of continuous suberin. Suberin deposition was first observed in the wild type at 41 % of total root length, in *Prom$_{RALPH}$::ANAC058-17* first staining appeared delayed at 58 % and in *Prom$_{RALPH}$::ANAC058-20* at 51 %. While the percentage with patchy suberin in the overexpressing lines is only slightly lower, the decrease in the root proportion with continuous suberin is distinctive.

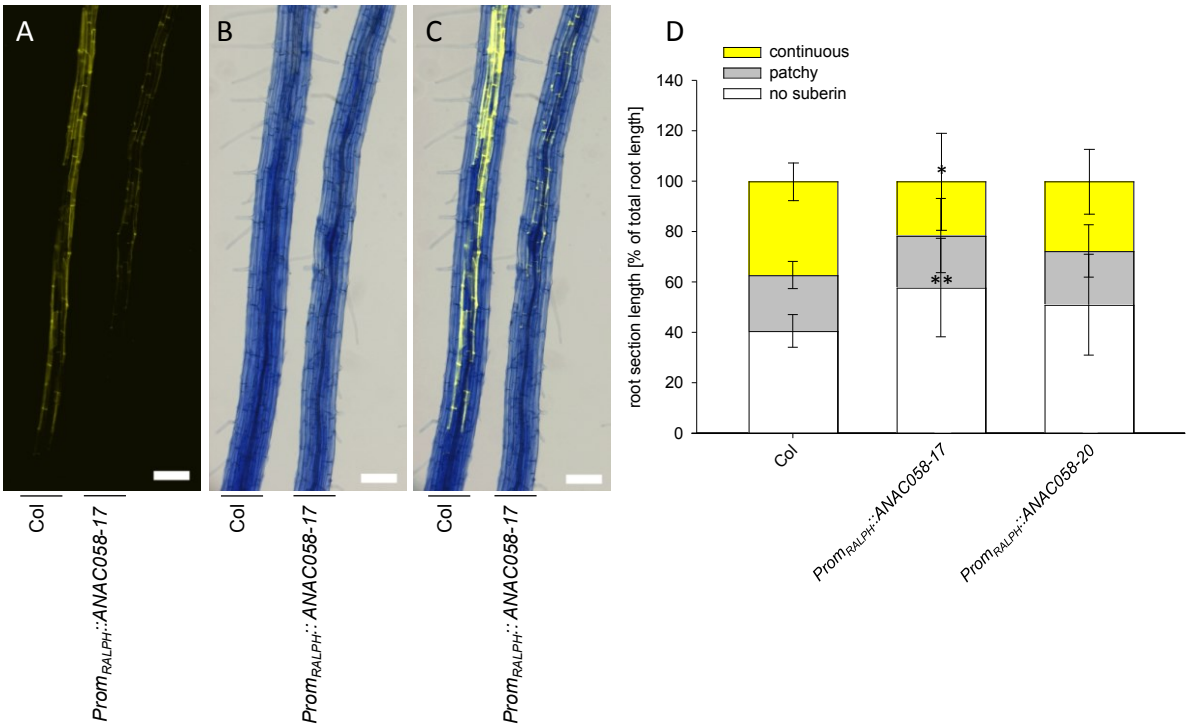

Fig. 3.22 Suberin deposition in *Prom$_{RALPH}$::ANAC058* seedlings stained with Fluorol Yellow 088 in comparison to the wild type

Suberin was stained with Fluorol Yellow 088 in 6 d old seedlings grown on MS plates. Depicted are representative pictures showing Col and *Prom$_{RALPH}$::ANAC058* of the same root length at a position where the endodermis is fully suberized (continuous) closer to the root tip in the wild type than in *Prom$_{RALPH}$::ANAC058* (A). Fluorescence was observed with a fluorescence microscope employing a standard GFP filter, bright field pictures of the same root section were taken (B) and an overlay of both pictures was generated in ImageJ (C). Measuring the length of root sections with different suberization states (no suberin, patchy, continuous, for a model, see fig. 2.7) allows the calculation of root section length as percentage of total root length (D). Mean values and standard deviations represented by error bars were calculated from 9 (*Prom$_{RALPH}$::ANAC058-20*), 10 (*Prom$_{RALPH}$::ANAC058-17*) or 19 (Col) independent seedlings. Significant differences are represented by one ($p \leq 0.05$) or two ($p \leq 0.01$) asterisks as determined by student t-test, placed directly above the bar. For all values, see table 8.18.

3.3.2 Induced overexpression of *ANAC058* in TRANSPLANTA (TPT) lines

Constitutive overexpression of *ANAC058* and even overexpression controlled by the *RALPH* promoter might cause negative side effects during plant development. Signaling pathways regulating the expression of several genes in a developmental and stress related manner are often complex and might include feed-forward and feedback loops. Therefore, long term overexpression of a gene central in such a pathway might not show effects in the plants whereas short term overexpression might yield different results. Accordingly, TRANSPLANTA lines (Coego et al., 2014) were obtained. These lines contain a construct that allows the overexpression of *ANAC058* by applying β-estradiol to the plant via growth medium or by spraying the hormone onto the plant surface.

3.3.2.1 Expression of *ANAC058* in induced *TPT.D* and *TPT.G* plants

In the two TRANSPLANTA lines *TPT_3.18400.1D* and *TPT_3.18400.1G* (subsequently referred to as *TPT.D* and *TPT.G*, respectively), overexpression was induced in 3 weeks old plants grown in hydroponics by transferring plants to nutrient solution with β-estradiol. Medium for mock treatment was supplemented with the solvent used for β-estradiol stock solution in the same amount as β-estradiol medium. Apical root sections were harvested at the age of 4 weeks, after 1 week of β-estradiol induced overexpression. The expression level of *ANAC058* was tested by semi-quantitative RT-PCR.

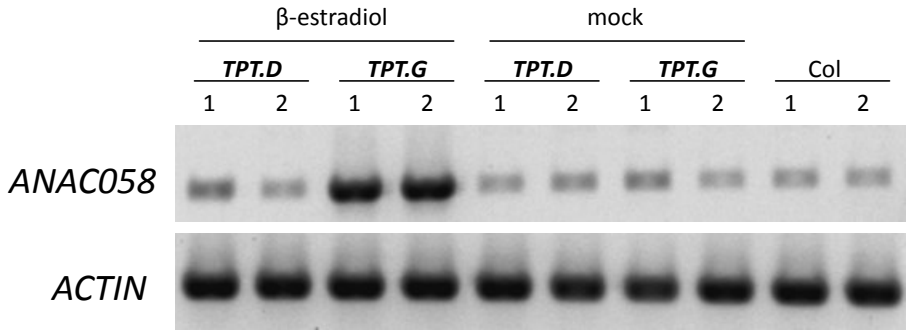

Fig. 3.23 Expression of *ANAC058* in roots of induced *TPT.D* and *TPT.G* plants
Apical root sections (apical 6 cm) of 4 weeks old, hydroponically grown plants (2 plants for each genotype labeled 1 and 2), were investigated. Plants were either treated with a 10 µM β-estradiol solution or a mock solution for 8 d before harvest. *ACTIN* was used as the control.

For two investigated plants of the line *TPT.G*, strong overexpression of *ANAC058* was visible after addition of β-estradiol (fig. 3.23). However, *TPT.D* showed slight overexpression in plant 1 and no effect on the second plant. As a result, further research was concentrated on *TPT.G*.

3.3.2.2 Chemical analysis of root suberin in induced *TPT.G* plants

Since lower expression of *ANAC058* leads to decreased amounts of suberin in apical sections of root systems (3.2.2), the reverse might occur in plants that overexpress *ANAC058*. Analyzing suberin amounts in the 4 weeks old plants of the *TPT.G* line after 1 week of β-estradiol treatment reveals no change in suberin compared with control plants (fig. 3.24). Apical root sections were collected and analyzed without applying cell wall digesting enzymes beforehand. Total aliphatic amounts per root dry weight of Col (1.37 ± 0.54 µg mg^{-1}) are similar to amounts found in 3.2.2 for Col. Suberin composition is also comparable to monomers found in 3.2.2 belonging to the substance classes fatty acids, alcohols, ω-hydroxy fatty acids and α,ω-dicarboxylic acids with carbon chain lengths ranging from C18 to C24.

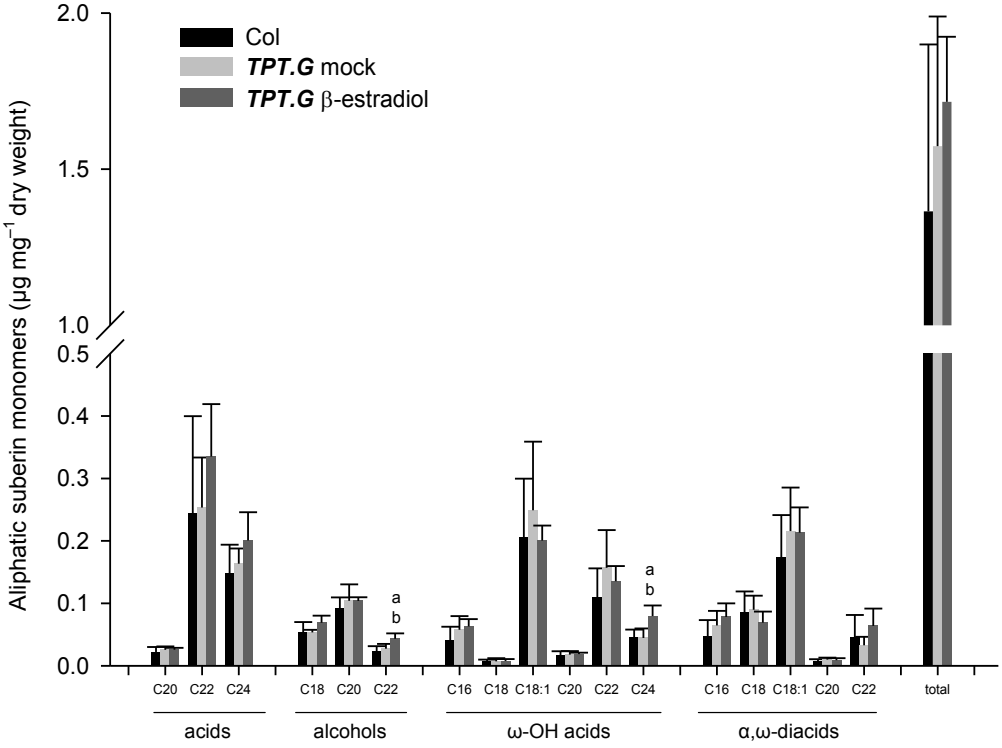

Fig. 3. 24 Root suberin composition in apical root sections of induced *TPT.G* and control plants

Apical root sections (apical 6 cm) of 4 weeks old, hydroponically grown plants were analyzed. Plants were either treated with a 10 µM β-estradiol or a mock solution for 8 d before harvest. Depicted are amounts of aliphatic suberin monomers in µg per mg root dry weight sorted according to substance classes and carbon chain length. Mean values and standard deviations represented by error bars were calculated from 4 samples (Col and *TPT.G* mock) or 3 independent samples (*TPT.G* β-estradiol). Fatty acids (acids), primary alcohols (alcohols), ω-hydroxy fatty acids (ω-OH acids) and α,ω-dicaorboxylic acids (α,ω-diacids) were found. Significant differences between Col and *TPT.G* β-estradiol are represented by the letter a, between *TPT.G* mock and *TPT.G* β-estradiol by the letter b with one ($p \leq 0.05$) or two ($p \leq 0.01$) respective letters as determined by student t-test. For related suberin monomer amounts, see table 8.12, supp..

Total aliphatic amounts are slightly higher in *TPT.G* mock treated and *TPT.G* β-estradiol treated, although these differences are not significant. The only significant changes in the TRANSPLANTA line with induced *ANAC058* overexpression are higher amounts of C22 alcohol and C24 ω-hydroxy fatty acids compared to the wild type and the mock treated *TPT.G* line. Tendentially, suberin amounts are slightly higher in the induced TRANSPLANTA line but potential effects might be too small to visualize by gas chromatography analysis.

3.3.2.3 Histological investigation of suberin in induced *TPT.G* plants

Changes in suberin amounts caused by different *ANAC058* expression levels were often more distinct when investigated with Fluorol Yellow 088 staining than with gas chromatography. Therefore, induction of *ANAC058* by β-estradiol application to TRANSPLANTA line *TPT.G* was investigated in seedlings with regard to suberin effects with Fluorol Yellow 088 staining.

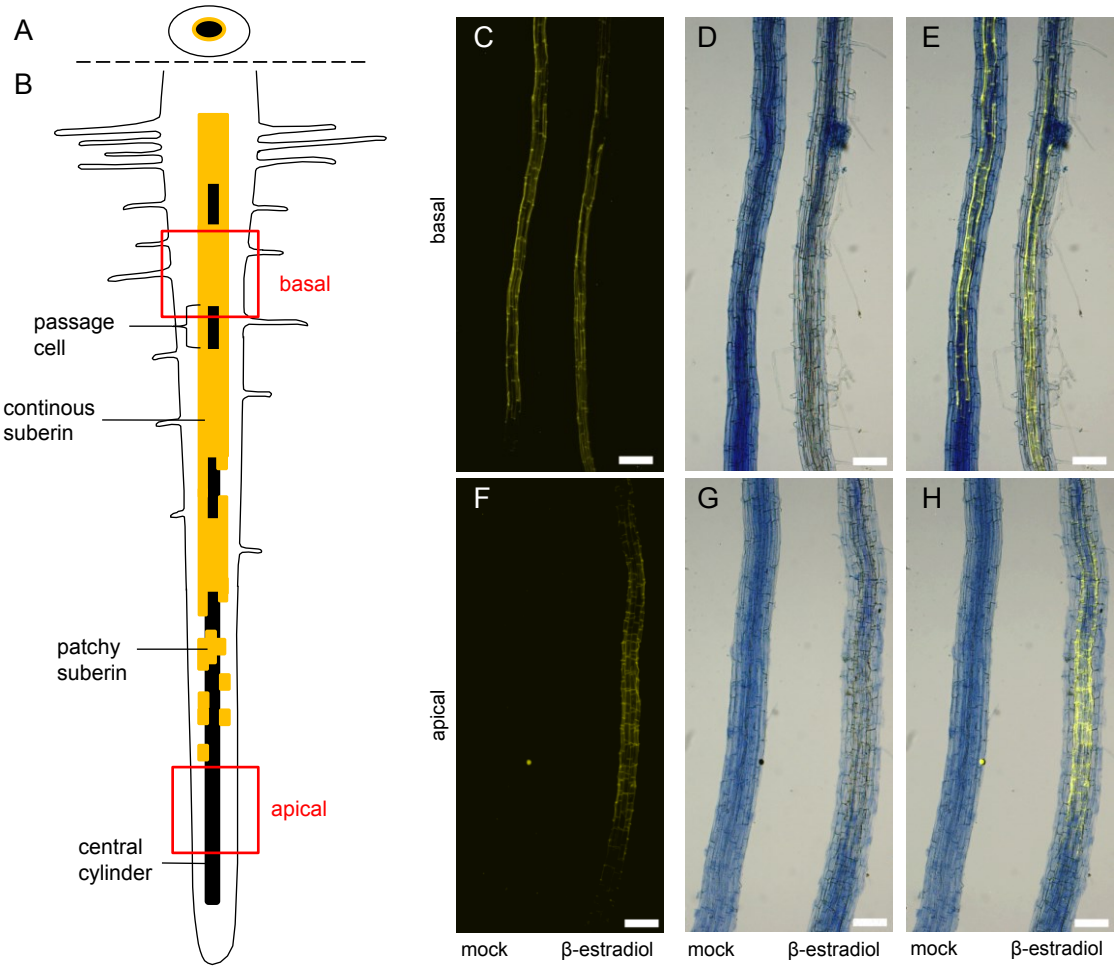

Fig. 3.25 Suberin deposition in induced *TPT.G* and control seedlings stained with Fluorol Yellow 088

Suberin was stained with Fluorol Yellow 088 in 6 d old seedlings grown for 4 d on MS plates and transferred to MS supplemented with 10 µM β-estradiol or mock solution. Depicted are representative pictures showing *TPT.G* seedlings of the same root length, either mock or β-estradiol treated. Selection shows the apical part 1.4 - 2.8 mm from the root tip (F - H) and the basal part 5.5 - 6.9 mm from the root tip (C - E). Respective positions are indicated in the root model showing endodermal suberin deposition in seedlings via a view onto the endodermis (B). A cross sectional view of the root (A) indicates continuous suberin deposition around the central cylinder. Fluorescence was observed with a fluorescence microscope employing a standard GFP filter (C and F), bright field pictures of the same root section were taken (D and G) and an overlay of both pictures was generated in ImageJ (E and H). For an overview of suberin deposition along the root in induced *TPT.G* seedlings, see fig. 8.12, supp.. For root section measurements, see fig. 3.26. Scale bars represent 100 µM.

Induction of *TPT.G* seedlings was conducted by transferring them to MS medium supplemented with β-estradiol and suberin was investigated after 2 d. Medium for mock treatment was supplemented with the solvent used for β-estradiol stock solution in the same amount as β-estradiol medium. Induction of *ANAC058* expression by applying β-estradiol to seedlings via MS medium was observed beforehand (fig. 8.11, supp.).

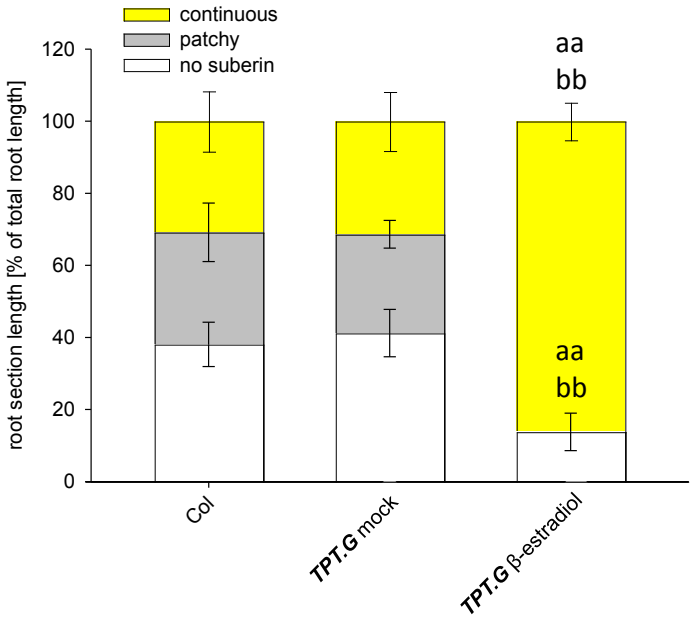

Fig. 3.26 Measured suberin deposition in induced *TPT.G* and control seedlings stained with Fluorol Yellow 088

Suberin was stained with Fluorol Yellow 088 in 6 d old seedlings grown for 4 d on MS plates and transferred to MS supplemented with 10 µM β-estradiol or mock solution (for representative seedling pictures, see fig. 3.25). Measuring the length of root sections with different suberization states allows the calculation of root section length as percentage of total root length. Mean values and standard deviation represented by error bars were calculated from 3 (Col), 11 (*TPT.G* mock) or 12 (*TPT.G* β-estradiol) independent seedlings. Values from mock and β-estradiol treated Col seedling were combined since treatments caused no differences. Significant differences between Col and *TPT.G* β-estradiol are represented by the letter a, between *TPT.G* mock and *TPT.G* β-estradiol by the letter b with one ($p \leq 0.05$) or two ($p \leq 0.01$) respective letters as determined by student t-test. For all values, see table 8.19.

The result was a clear suberin effect in *TPT.G* seedlings treated with β-estradiol while neither mock treated *TPT.G* seedlings nor WT seedlings treated with mock or β-estradiol solution showed any effects. Suberin deposition in induced *TPT.G* lines started much closer to the root tip compared to non-induced and wild type plants (fig. 3.25 F and H). Accordingly, the root section without suberin in induced *TPT.G* seedlings was significantly shorter with 14 % of total root length compared to the 41 % in *TPT.G* mock treated seedlings (fig. 3.26). Towards the root base, staining differed less between the β-estradiol treated seedlings and plants with wild type *ANAC058* expression as staining intensity varied around the wild type level. The newly developed section of the root of induced *TPT.G* seedlings sported slightly shorter and rounder cells, which was not observed for *TPT.G* mock treated seedlings.

3.3.2.4 Analysis of gene expression in roots of induced *TPT.G* plants

ANAC058 overexpression in leaves leads to increased expression of typical suberin genes, as shown by Marc Frenger (Frenger, 2014). In roots, the overexpression controlled by the *RALPH* promoter however did not have a strong effect on *ANAC058* nor on suberin gene expression as shown in 3.3.1. Investigating other ways of overexpressing *ANAC058* in roots, it was induced by β-estradiol

application in the *TPT.G* line. This induction caused earlier deposition of suberin very close to the root tip (3.3.2.3). Accordingly, when testing the expression level, *ANAC058* is strongly overexpressed in roots of induced plants with 170 times stronger expression compared to mock treated roots (fig. 3.27). Expression of suberin genes is also higher in the induced line. Genes involved in suberin synthesis, *RALPH*, *GPAT5*, *HORST*, a suberin component transporter, *ABCG6* and a proposed suberin transcription factor, *ANAC038* (Frenger, 2014) all show increased expression with 2.3 - 3.0 times the expression level in control plants. Genes shown to be involved in Casparian strip formation (*RBOHF*, *ESB1* and *PER64*) are also higher expressed in the induced plants though lower than the suberin genes with 1.7 - 2.2 times the expression in mock treated plants.

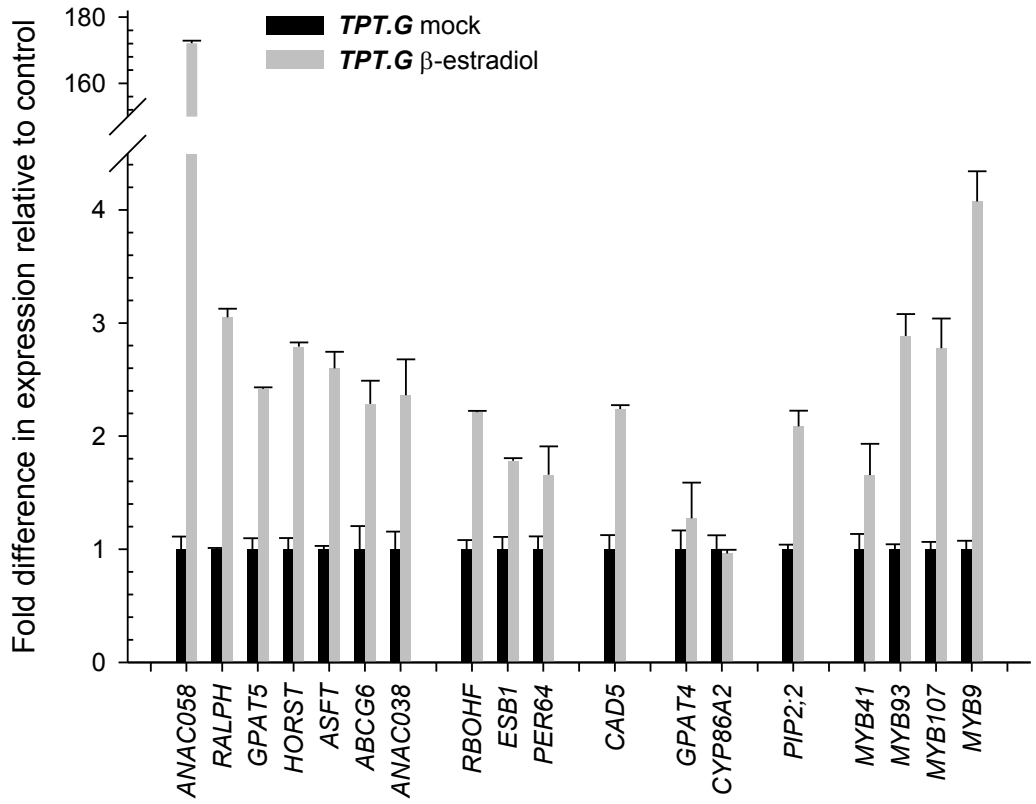

Fig. 3.27 Expression of suberin, Casparian strip, lignin, cutin, aquaporin and various MYB genes in induced *TPT.G* and control plants

Apical root sections (apical 6 cm) of 4 weeks old, hydroponically grown plants were investigated. Plants were either treated with a 10 µM β-estradiol solution or a mock solution for 8 d before harvest. *GAPDH* was used as endogenous control and results were normalized to the expression in *ANAC058.TPT.G* mock which was set to 1. Pictured are the means and standard deviations of three technical replicates. For related values see table 8.7, supp..

The one tested lignin gene, *CAD5*, is 2.2-fold higher expressed than in the non-induced plant, similar to suberin gene and *RBOHF* expression levels. Cutin associated genes like *GPAT4* and *CYP86A2* on the other hand are not induced when *ANAC058* is overexpressed. *PIP2;2* is the gene of an aquaporin protein and is expressed 2.1 times higher in plants with *ANAC058* overexpression. Several MYB

transcription factors with no clear role in developmental root suberin regulation were also investigated. *MYB41*, a transcription factor regulating stress-induced suberin deposition (Kosma et al., 2014) is 1.7 times stronger expressed than in the control. Its expression is therefore slightly induced in case of *ANAC058* overexpression. The expression of *MYB9* and *MYB107* which were shown to be involved in seed coat suberin regulation (Lashbrooke et al., 2016) are 4.1 and 2.8 times higher expressed, respectively. *MYB93*, a transcription factor associated with lateral root emergence (Gibbs et al., 2014; Gibbs and Coates, 2014) is 2.9 times higher expressed.

3.3.2.5 Analysis of *ANAC058* expression and wax composition in leaves of induced *TPT.D* and *TPT.G* plants

Induction of *ANAC058* overexpression is not only possible by β-estradiol application to the roots but also by spraying the hormone onto the leaves. This method was deployed by Sanu Shrestha (Shrestha, 2016). When testing the *ANAC058* expression in leaves of 3 different plants of 3 genotypes (Col, *TPT.D* and *TPT.G*) treated with β-estradiol, no *ANAC058* expression is visible in leaves of the wild type (fig. 3.28). The TRANSPLANTA lines *TPT.G* and *TPT.D*, when treated with β-estradiol, show induced expression of *ANAC058* in both lines. Overexpression is again stronger in *TPT.G* than in *TPT.D*.

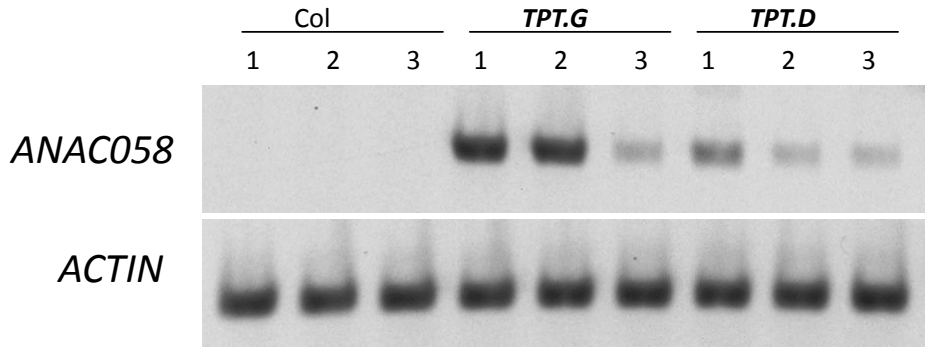

Fig. 3.28 *ANAC058* expression in leaves of induced *TPT.G* and control plants
Plants were treated with 10 µM β-estradiol 24 h prior to harvest by application to the leaf surface to 4 weeks old, soil grown plants. Experiment conducted by and picture courtesy of Sanu Shrestha (Shrestha, 2016). *ACTIN* was used as the endogenous control.

Increased expression of suberin genes was observed in leaves when *ANAC058* is overexpressed (Frenger, 2014) as well as when treating seedlings on MS plates with β-estradiol (fig. 8.11, supp.). Therefore, the incorporation of suberin monomers in leave cutin or wax was a possibility. Li and coworkers (Li et al., 2007a) were able to show that overexpression of suberin-associated genes *GPAT5* and *HORST/CYP86A1* resulted in accumulation of monomers typical for suberin in leaf wax. Subsequently, the wax of leaves to which β-estradiol was applied 2 weeks earlier was analyzed by gas chromatography. Typical *A. thaliana* leaf wax consisting of acids, primary and secondary alcohols, aldehydes, and alkanes was detected in all samples but no new monomers were found in the plants treated with β-estradiol (fig. 3.29). Some significant differences between samples were observed but

no consistent changes in monomer amount related to suberin biosynthesis. C32 aldehyde in induced *TPT.D* and in mock treated *TPT.G* as well as the C34 aldehyde in both TRANSPLANTA lines, induced plants and not induced, were present in significantly higher amounts compared to the wild type. C31 and C33 alkane amounts were significantly lower in *TPT.D*, β-estradiol treated, compared to *TPT.D* mock treated. Total wax amounts of the wild type with 2 µg per mg leaf dry weight (2 ± 0.477 µg mg^{-1}) were lower than for *TPT.D* mock treated (2.283 ± 0.141 µg mg^{-1}) and higher than for *TPT.D* induced (1.807 ± 0.330 µg mg^{-1}), *TPT.G* mock treated (1.974 ± 0.265 µg mg^{-1}) and *TPT.G* induced (1.879 ± 0.290 µg mg^{-1}) plants.

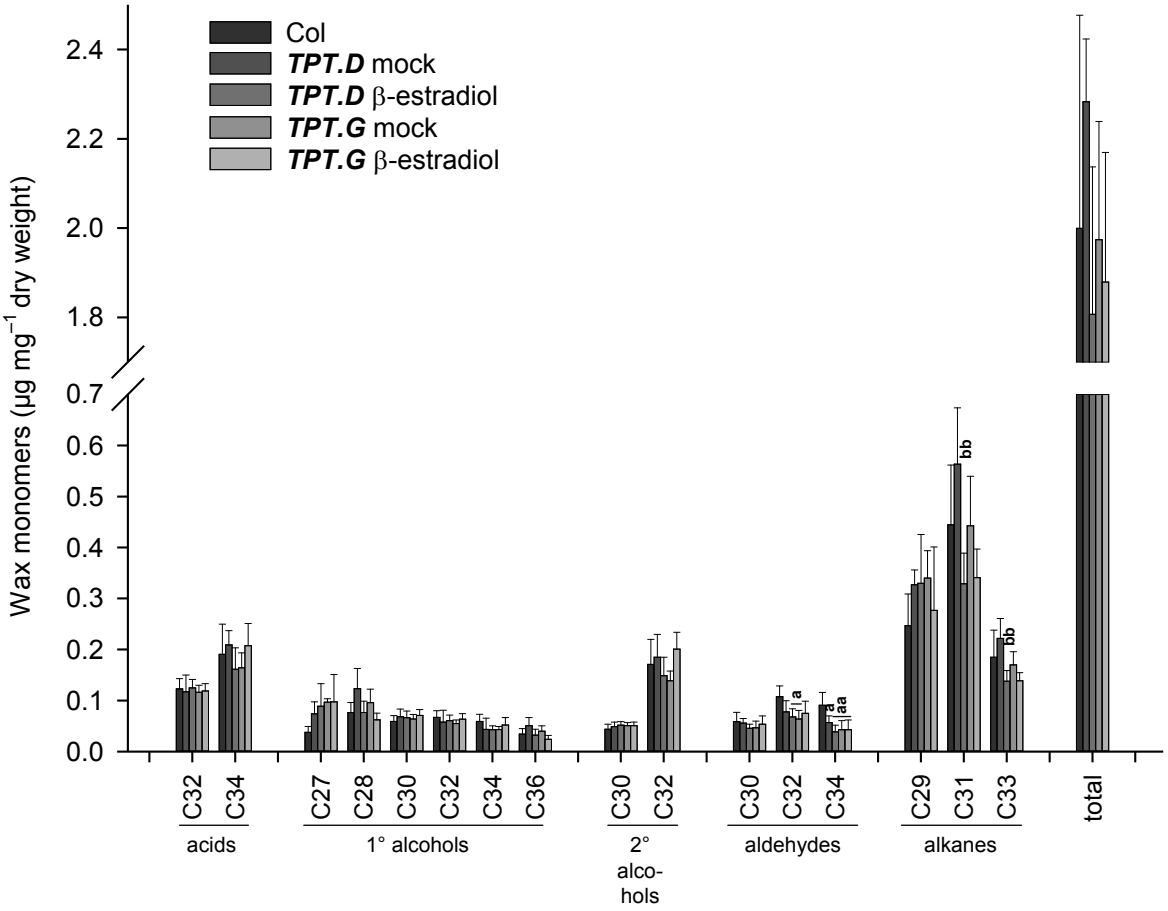

Fig. 3.29 Leaf wax composition of induced *TPT.D, TPT.G* and control plants

5 replicates for each genotype and treatment of 6 weeks old soil grown plants were analyzed 2 weeks after induction with 10 µM β-estradiol. Depicted are amounts of wax monomers in µg per mg leaf dry weight sorted according to substance classes and carbon chain length (fatty acids (acids), primary alcohols (1° alcohols) and secondary alcohols (2° alcohols)). Mean values and standard deviation represented by error bars were calculated from 5 independent samples each. Significant differences are represented by one ($p \leq 0.05$) and two ($p \leq 0.01$) letters as determined by ANOVA Tukey test. The letter a stands for significantly different to Col, the letter b for significant differences between *TPT.D* mock and *TPT.D* β-estradiol, the letter c for significant differences between *TPT.G* mock and *TPT.G* β-estradiol. For related wax monomer amounts, see table 8.13, supp..

4 Discussion

Suberin is an apoplastic barrier that can prevent uncontrolled water and nutrient movement. As such, suberin is an important factor in resistance towards abiotic stress. The true extent and the exact role suberin has in that regard is still not fully elucidated, although a lot of process has been made in recent years. Additional to an involvement in water and nutrient stress, suberin also has a function in response to various other abiotic and biotic stresses as well as an essential part in plant development. The exceedingly versatile polymer is deposited in response to wounding as well as developmentally in roots and seed coats. Regulation of suberin is still not entirely elucidated. Recently, several advances have been made by identifying transcription factors involved in suberin synthesis and deposition, starting with *MYB41* (Kosma et al., 2014). Complete understanding of the regulatory process might allow adjustment of plant stress resistance with potentially increased yield or survival rates. Especially in regions subjected to harsh climate conditions, possibly caused by climate change, this might be of interest.

4.1 Identification of *ANAC058* as a suberin involved transcription factor candidate

In order to find a candidate for a suberin-involved transcription factor, a co-expression analysis with known suberin genes was conducted. The suberin biosynthesis genes *GPAT5* (Beisson et al., 2007), *RALPH/CYP86B1* (Compagnon et al., 2009) and *FAR4* (Domergue et al., 2010) were used as bait. The final network included several suberin-associated genes (fig. 3.1), for example an ABC transporter which is involved in the export of suberin components from the cell to the apoplast (Yadav et al., 2014). The transcription factors co-expressed with suberin genes are *MYB9*, *MYB107* and *ANAC058* (*NAC058* in fig. 3.1). Recently, *MYB9* and *MYB107* have been shown to be involved in seed coat suberin (Gou et al., 2017; Lashbrooke et al., 2016). *ANAC058* on the other hand was investigated in this work.

Additional support for *ANAC058* as a good candidate for suberin regulation can be found in literature. Several large scale expression analyses using suberized tissue of various species identified upregulated transcription factors orthologous to *ANAC058*. These orthologs are upregulated in cork (Soler et al., 2007; Soler et al., 2008), russeted apple skin (Legay et al., 2015) and in rice under waterlogging stress (Shunsaku Nishiuchi and Mikio Nakazono, Nagoya University, Japan, personal communication) compared to control tissue or condition. The same applies to the co-expression analysis using *Arabidopsis thaliana*, apple, tomato, rice and grape vine tissue that contains suberin or where suberin is induced (Lashbrooke et al., 2016). The potato *StNAC103*, orthologous to *ANAC058*, was investigated specifically and deemed a negative regulator of suberin synthesis and deposition (Verdaguer et al., 2016).

The remaining genes co-expressed with the designated suberin-associated genes in fig. 3.1 are mostly not published at the present time. The peroxidase At1g68850 was shown to be involved in suberin polyester generation with a proposed function in the polymerization of the aromatic domain (Brands, 2014). In knock-out mutants of the gene, suberin deposition is delayed. *KCS17* (At4g34510)

is mainly expressed in flowers and siliques (Joubès et al., 2008) but was also shown to be involved in seed coat suberin synthesis (Nosbüsch, 2009). A possible involvement in root suberin might be a contribution to sealing the endodermis around the site of lateral root emergence since the putative *KCS17* promoter activity is active at this localization (Nosbüsch, 2009).

Three of the genes depicted in the co-expression network are putative lipid transfer proteins (At5g13900, At248140 and At1g05450, see also table 8.1). LTPs (lipid transfer proteins) have been associated with apoplastic polyester formation (DeBono et al., 2009; Lee et al., 2009a) but involvement in suberin formation has not been shown yet. A member of the LTP family also appears in a multi-species co-expression network of suberin genes (Lashbrooke et al., 2016). In a similar manner, GDSL-motif esterases/acyltransferase/lipases have been suspected of involvement in suberin synthesis (Li-Beisson et al., 2013). For one member of the gene family, knock-out of the gene resulted in increased root suberin amounts (Frenger, 2014) and another member appears in the aforementioned co-expression analysis (Lashbrooke et al., 2016). Several GDSL-motif esterases were also shown to be involved in the synthesis of the leaf polyester cutin (Yeats et al., 2014, 2012). It is possible that members of the gene family also play a role in suberin assembly. Members of both the LTP gene family and the GDSL-motif esterases/lipases are upregulated when overexpressing suberin associated transcription factors (Cominelli et al., 2008; Legay et al., 2016), emphasizing a possible role in suberin formation.

The co-expression network additionally includes a CASP-like protein (At5g44550), a member of the CASPARIAN STRIP MEMBRANE DOMAIN gene family. *CASP1* and *CASP3* are essential for the correct formation of the Casparian strip, another apoplastic polymer localized in the endodermis (Hosmani et al., 2013; Roppolo et al., 2011). CASPL (CASP-like) proteins are suspected of similar functions as CASPs, possibly recruiting cell wall modifying enzymes (Roppolo et al., 2014). The remaining genes in the co-expression network do not have functions that can be directly related to possible roles in suberin synthesis or assembly but the high number of proven and possible suberin-associated genes suggests a substantial role for the transcription factor *ANAC058* in suberin regulation.

4.2 Localization of *ANAC058* expression and activity of the putative *ANAC058* promoter

4.2.1 *ANAC058* is expressed during plant development in roots but not in leaves

Suberin-associated genes are usually expressed in specific plant organs and tissues since suberin deposition is distinctly localized. In order to verify *ANAC058* as the suberin TF candidate, gene expression was measured in roots and leaves. *ANAC058* expression was absent in leaves but measured in roots (fig. 3.2). This is an expression pattern that was also observed for other suberin associated genes like *GPAT5* (Beisson et al., 2007). Investigating different sections of the root system separately can give an indication about whether a gene is predominantly expressed in young apical parts of the root system or periderm-containing basal parts. According to figure 3.2, expression of

ANAC058 is similar in both sections of the root system of 5 weeks old soil grown plants with a propensity towards higher expression in the basal section. Since the basal sections contained mostly root material in the stages of secondary growth (see also fig. 2.2 for sample preparation), *ANAC058* expression might be involved with peridermal suberin synthesis and deposition which was further investigated with a promoter reporter construct in 4.2.1.2.

4.2.1.1 The putative promoter of *ANAC058* is active in the root endodermis

Tissue-specific and developmental expression patterns of *ANAC058* were investigated in detail since suberin deposition is tightly regulated with regard to tissue, developmental and stress specific deposition. *In silico* expression patterns as provided by the ATTED-II database (Mustroph et al., 2009) indicated strong expression in the endodermis of roots and no expression in other investigated root cell layers (fig. 8.1, supp.). Employing the promoter activity reporter construct $Prom_{ANAC058}$*::GFP-GUS*, activity of the putative *ANAC058* promoter was localized in the endodermis in roots and was absent in above-ground tissue (fig. 3.3). The pattern of GUS stained endodermal cells along the root is typical for suberin-associated genes. It starts with absent staining at the root tip, develops into single stained endodermal cells (patchy) and finally displays a fully stained endodermis with further distance from the root tip. The pattern was observed for *RALPH*, *DAISY*, *FAR1*, *HORST* and *GPAT5* (Beisson et al., 2007; Naseer et al., 2012) and applies also to suberin deposition (see model in fig. 2.7). Measuring the distance from root tip until the start of promoter activity for the putative *ANAC058* and *HORST* promoters correlated strongly with distance from root tip until the start of suberin deposition (fig. 8.2, supp.). Since deposition of suberin starts at a determined developmental stage in roots, this correlation indicates that *ANAC058* is likely involved in developmental regulation of root suberin synthesis and possibly deposition. Promoter activity in 2 weeks old plants (fig. 3.5) shows most activity in apical root sections and a decrease of activity towards the root-shoot junction. This indicates that *ANAC058* mostly regulates developmental root suberin in early developmental stages of the root. Investigation of GFP fluorescence with a confocal laser scanning microscope in young roots reveals promoter activity only in the endodermis and its absence in all other root cell layers. Promoter activity at the root base was not investigated with GFP fluorescence (see 4.2.1.2). Another polymer present in the endodermis is the Casparian strip, consequently promoters of Casparian strip genes are also active in this cell layer. Differently from suberin gene promoters, promoter activity of Casparian strip genes starts very close to the root tip (Naseer et al., 2012). This does not apply to the putative *ANAC058* promoter. Co-expressed genes, as well as promoter activity, strongly indicate that *ANAC058* is not involved in Casparian strip formation.

4.2.1.2 Activity of the putative *ANAC058* promoter is found in the root cap and the root base

Additional to the endodermal promoter activity, activity was also observed in root cap cells of main and lateral roots, occasionally at the root tip of embryos, at the root base of developing lateral roots and often at the root base of the main root, very close to the root-shoot junction.

Activity of the putative *ANAC058* promoter at the root base of the main root is localized to sub-epidermal cell layers (fig. 3.4). The activity can be nicely correlated with peridermal suberin

deposition. Periderm in *Arabidopsis* roots develops as part of secondary root growth where the vascular tissue, phloem and xylem, expand. The surrounding outermost cell layers consist of non-vascular tissue. This tissue includes periderm that serves as the root-environment interface. It contains suberin and can be detected with suberin specific dyes (Höfer et al., 2008; Ranathunge and Schreiber, 2011). The details of the developmental process producing root periderm are, specifically in *A. thaliana*, still not elucidated. With regard to periderm development in potato tubers, peridermal tissue is produced by the phellogen, a meristematic cell layer beneath the periderm (Lulai and Freeman, 2001; Sabba and Lulai, 2002). Secondary root growth in the investigated 5 d old seedlings, even in the basal-most root section, is not far advanced (Nieminen et al., 2015). Accordingly, peridermal suberin was not observed in 5 d or 11 d old plants after staining with Fluorol Yellow 088 (data not shown), whereas endodermal suberin was clearly visible (fig. 3.14). Still, *ANAC058* might control the preparation of suberin deposition in outer cell layers which may serve as a predecessor to the peridermal cells. Additionally, respective suberin amounts which at one point may form the peridermal suberin might be below histological detection limits at this developmental stage of roots. A similar promoter activity pattern was not investigated or observed for most other suberin associated genes. In 5 d old $Prom_{HORST}$*::GUS* seedlings, promoter activity was exclusively restricted to the endodermis (fig. 3.4). On the other hand, putative promoters of *GPAT5*, *ABCG2* and *ABCG6* at various developmental stages show strong staining at the root base (Beisson et al., 2007; Yadav et al., 2014). It is possible that *ANAC058* regulates only a subset of suberin associated genes with regard to peridermal suberin. In order to elucidate this process further, investigation of promoter reporter construct lines of various suberin associated genes at different developmental stages would be of interest.

Besides basal localization of activity, the putative *ANAC058* promoter is also active in root cap cells. The root cap consists of columella cells which are localized apically from the meristem at the very tip of the root and of lateral root cap cells which flank the columella and the meristem as the outermost cell layer. Lateral root cap cells are still present at the beginning of the elongation zone but are entering programmed cell death and are sloughed off at that developmental stage (Fendrych et al., 2014). GUS activity in $Prom_{ANAC058}$*::GFP-GUS* seedlings was only seldom observed in lateral cap cells situated at the elongation zone but frequently in apically located root cap cells. Since *ANAC058* shows strong indication that it is involved in apoplastic polyester formation in the endodermis, a similar function might apply to the root cap. The cells at the root tip are necessary for protecting the sensitive root meristem for which a layer consisting of a polymer with suberin-like composition would be useful. Expression of cuticle associated genes has been observed at root caps (Bird et al., 2007; Jakobson et al., 2016; Kurdyukov, 2006) and a cuticle-like layer was observed covering the outermost cell wall of root cap cells (Berhin et al., 2017). Since NACs need to dimerize in order to bind to DNA, different dimerization partners forming various heterodimers may confer separate specificity to suberin or cutin target genes. It is tempting to speculate that *ANAC058* is a root-specific transcription factor involved in endodermal suberin, periderm and root cap cuticle generation, playing a versatile role regulating polymers of the root-environment and root-tissue interface.

Activity of the *ANAC058* putative promoter was observed in root tips of lateral roots and occasionally of mature dormant embryos as well. Since root tip staining appeared in lateral roots once meristematic and elongation zones are distinct, the putative *ANAC058* promoter seems to become active in the root cap after the root reaches a certain developmental stage. Activity of the promoter during embryo development was not investigated in detail but seemed to be completely absent during developmental stages earlier than the mature embryo stage. This indicates a similar specificity to mature root developmental stages as for the seedling main and lateral root. Promoter activity in the embryo was not definitely identified as root cap localized and may also be localized to the meristem. However, the root cap localization is likely due to similar activity patterns in main and side roots of seedlings. Lateral roots and embryos are covered by polyesters in early developmental stages (Li et al., 2017; Szczuka & Szczuka, 2003) and *ANAC058* might be involved in providing protective layers at root tips during further development. The function of *ANAC058* in embryos related to root meristem development is another possible function. As mentioned earlier, different dimerization partners of *ANAC058* might also allow targeting of genes that are not associated with polyesters, which would lead to regulation of other processes. Further experiments investigating GFP fluorescence of the $Prom_{ANAC058}$*:GFP-GUS* construct with confocal microscopy might elucidate the role *ANAC058* has in root tip development. Investigation of the embryo cuticle and the root cap cuticle with specific dyes in *anac058* knock-out and knock-down mutants may elucidate whether *ANAC058* is involved in their regulation. Determination of the target genes with a chromatin immunoprecipitation (ChIP) assay may help to identify target gene specificity. With this assay, promoter fragments which are bound by the TF are isolated, amplified and identified. If *ANAC058* is then determined to bind to promoters of suberin and cutin genes which are expressed the root cap, its involvement in regulation of suberin as well as root cap cuticle can be deemed likely.

Activity of the putative promoter of *ANAC058* was also observed at the root base of lateral roots and specifically in the surrounding endodermal cells of the main root. During branching of roots, lateral roots have to break through the endodermis of the main root. In the process, this would generate an opening in the apoplastic diffusion barrier due to disruption of Casparian strips. Li and coworkers observed suberin deposition at lateral root emergence sites (LRES) which closes the apoplastic pathway (Li et al., 2017). When the suberin is degraded in a cutinase-expressing mutant, an apoplastic tracer can enter the central cylinder locally at the LRES. The promoter activity of the putative *ANAC058* promoter surrounding LRES strongly indicates that *ANAC058* is involved in this suberin deposition process. In order to further investigate this involvement, experiments with apoplastic tracers can be conducted for the *anac058* mutants.

In summary, it is likely that *ANAC058* is a transcription factor regulating suberin synthesis and deposition at several different sites in the root (developmental suberin in the endodermis and suberin at the site of lateral root emergence) as well as the proposed cutin of the root cap. Several promoter activity patterns (at the embryonic root tip and at the main root base) have to be further investigated to determine the exact gene function at those sites but they are also likely related to suberin and polyester regulation.

4.2.2 The putative promoter of *ANAC058* is induced by wounding and ABA

Suberin deposition is inducible by abiotic and biotic stresses like wounding, salt stress and drought stress (Barberon et al., 2016; Franke et al., 2009; North & Nobel, 1995). Stress signals are often transferred to the site of stress response by abscisic acid (ABA) and several suberin genes are known to be responsive to ABA (Barberon et al., 2016; Yadav et al., 2014).

Wounding response of the putative *ANAC058* promoter was tested with the $Prom_{ANAC058}$*::GUS-GFP* construct in leaves and seeds. Leaves were pierced at several sites with a steel forceps and promoter activity was tested after 3 h, 6 h, 3 d and 7 d. Wounding response was not observed 3 h or 6 h after wounding, but after 3 d GUS activity was visible surrounding the wounding site and to a lesser degree at 7 d after wounding (fig. 3.6). This correlates with the expression of *FAR1*, *FAR4* and *FAR5* for which expression is increased very slightly if at all 1 h after wounding and continued to increase 1 d and 3 d after wounding. *FAR4* and *FAR5* are still strongly expressed 4 d after leaves were wounded (Domergue et al. 2010). Similar, expression of *DAISY* increased only slightly 1 h and 5 h after wounds were induced and expression was stronger 1 d after wounding (Franke et al., 2009). Substantial wounding response with regard to suberin seems to start 1 d after wounding and appears to continue for at least 7 d. It would be interesting to investigate the activity of the putative ANAC058 1 d after wounding. However, it is not or only marginally involved in the responses the first 24 h after wounding. *ANAC058* might not be the only transcription factor involved in regulating suberin genes in response to wounding. Possibly, early *ANAC058* promoter activity is below detection level which can still allow other TFs to regulate the majority of the early stress response. Expression of *ANAC058* in response to wounding was not tested in this work but preliminary work indicates mainly induction of expression 7 d after wounding, not at 3 d (Frenger, 2014). Testing the wounding response with expression analysis and promoter constructs under the same growth conditions could give more detailed results. Part of the early stress response might be the transcription factor *MYB41*, which was characterized as a suberin transcription factor responsive to stress (Kosma et al., 2014). Wounding response of *MYB41* was not tested by Kosma and coworkers but the putative promoter was active in roots 24 h after subjecting seedlings to abiotic stress, implying a fast stress response.

Wounding in different tissues can also have a varying stress response as was visible for the $Prom_{ANAC058}$*::GFP-GUS* construct with regard to wounding of seeds and leaves. GUS activity was visible in seeds stained few minutes after wounding occurred, making the wounding response much faster than in leaves. This might be related to activity of different genes in seeds, which possibly are part of a transcription factor network involving *ANAC058*. Possible candidates are the transcription factors *MYB9* and *MYB107* which were already characterized as seed coat specific suberin transcription factors (Gou et al., 2017; Lashbrooke et al., 2016). Additionally, wounding of seeds can much more severely impact plant development in comparison to leaf wounding. This possibly increases the necessity for fast stress responses.

The phytohormone ABA is known as an important component of the drought and salt stress transduction pathway (Zhang et al., 2006). Expression and promoter activity of various genes associated with suberin change if ABA is applied to plants as was observed for *DAISY* (Lee et al.,

2009b), *ABCG6* (Yadav et al., 2014), *MYB41* (Kosma et al., 2014) and *GPAT5* (Barberon et al., 2016). Suberin deposition increases visibly when staining ABA treated seedlings with Fluorol Yellow 088, as observed by Barberon and coworkers. After application of ABA for 20 h, endodermal suberin is deposited much closer to the root tip than in control plants and additional suberization was observed in the cortex (Barberon et al., 2016).

Responsiveness of the putative *ANAC058* promoter to ABA application was tested as well with the $Prom_{ANAC058}$*::GFP-GUS* construct. Seedlings were transferred to MS plates containing 1 µM and 30 µM ABA. Subsequently, promoter activity was observed under the binocular and the transmitted-light microscope (fig. 3.7). Similar to *GPAT5* expression in ABA treated seedlings (Barberon et al., 2016), activity of the putative *ANAC058* promoter starts closer to the root tip than in control plants. Otherwise, the promoter activity pattern is the same as for control seedlings since the activity decreases towards the root base in the same manner. The effect did not differ between both ABA concentrations, indicating that induced promoter activity does not depend on a specific concentration, at least between 1 µM to 30 µM ABA. Unlike expression of *GPAT5* which was observed after application of 1 µM ABA not only in the endodermis but also in the cortex, putative promoter activity of *ANAC058* seems to be restricted to the endodermis. Induction of *ANAC058* gene expression was also observed in response to 100 µM ABA (Jensen et al., 2010) and mutants overexpressing *ANAC058* were identified in an ABA sensitivity screen (Coego et al., 2014), supporting the observations in this work. The sensitivity screen revealed germination arrest if *ANAC058* overexpression is induced during germination in the presence of 1 µM ABA. Solely induced overexpression without added ABA resulted in wild type germination but growth arrest of seedling roots shortly after germination. The *ANAC058* overexpressing mutant seems to be hypersensitive to ABA. *ANAC058* overexpression in combination with applied ABA may have resulted in strong overexpression of suberin genes during germination, causing ectopic suberin deposition in various tissues and disruption the normal germination process. To elucidate *ANAC058's* role during germination with regard to ABA sensitivity, investigation of putative promoter activity during the germination process would be of interest. Additionally, in-detail examination of germinating *ANAC058* overexpressing lines might be interesting with regard to expression of suberin genes and suberin deposition. Since constitutive overexpression of *ANAC058* did not appear to have an effect on plant development (Frenger, 2014), induction of *ANAC058* overexpression may lead to better results. In order to determine the extent of *ANAC058* conferring ABA signals with regard to suberin, induction of *GPAT5* expression and suberin deposition by ABA application can be investigated in *anac058* mutants. Apical *GPAT5* expression and suberization were observed in the wild type in response to ABA treatment (Barberon et al., 2016). If this effect is reduced, delayed or abolished in the mutant after ABA application, *ANAC058* likely is involved in ABA signaling inducing suberin deposition.

ANAC058's wounding response and promoter activity in roots in response to ABA treatment correlates with similar responses of suberin associated genes under the same conditions. These results support the role of *ANAC058* as a good candidate for a transcription factor which is involved in suberin regulation.

4.3 *ANAC058* function inferred by bioinformatical analyses

4.3.1 NAC binding sequences were found in suberin gene promoters

Potential function and target genes of the *ANAC058* protein can be predicted using databases and bioinformatical analyses. *ANAC058* is one of the transcription factors most prominently co-expressed with suberin associated genes in a multi-species co-expression analysis (Lashbrooke et al., 2016). Close co-expression can indicate direct regulation of suberin genes by *ANAC058* but indirect regulation is also possible. In case of direct expression regulation, transcription factors often bind to characteristic motifs in the promoter of their target genes. For NACs, several of these binding motifs have been experimentally inferred and have been published as NAC binding sites (NACBS1-6, fig. 3.8) (Shao et al., 2015). All NACBS except for NACBS3 were found in sequences 1500 bp upstream of transcription start of suberin genes. Not all of the investigated suberin genes seem to contain the used NACBS in their putative promoters as NACBS were found in 7 of 13 submitted promoters. The absent NACBS3 sequence is very similar to the NACBS6 sequence and is present within NACBS6 occurrences in several promoters. Since NACBS3 is shorter than NACBS6, it is possible that it occurred randomly with high enough probability that the actual motif occurrences did not reach the p-value threshold. In several of the suberin gene promoters more than one NACBS was found, indicating that *FAR1*, *RALPH*, *ABCG20*, *GPAT5* and *GPAT7* are directly regulated by a NAC transcription factor. *HORST* and *FAR5* promoters contain only one NACBS but the co-expression of *FAR5* and *ANAC058* (fig. 3.1) suggests at least for *FAR5* direct regulation. Since only 1500 bp were selected for promoters it is possible that NACBS might be present in some suberin gene promoters outside the selected sequence. Additionally, more NACBS might exist that have not been described yet. Another possibility is that a subset of suberin genes is regulated directly and the rest are indirectly regulated or regulated by a different TF belonging to the potential suberin regulation TF network.

4.3.2 Prediction of *ANAC058's* secondary structure and functionally important protein regions

The NAC proteins bind to the NACBS with the N-terminal DNA binding domain (DBD) which is the defining feature of this gene family and is called the NAC domain. The C-terminal domain regulates transcription of the target genes and is consequently called the transcription regulatory domain (TRD, see also fig. 1.3). Elucidating the potential function of the ANAC058 protein and its domains required identifying the domains, testing for the secondary protein structure and amino acid motifs. The alignment generated for the phylogenetic analysis (phylogenetic trees in 8.7 and 8.13, supp.) displays the sequence conservation in the DBD of NACs, whereas the TRD sequences do not align (data not shown). The tertiary structure of the DBD domain has been determined for *ANAC019* (Ernst et al., 2004) and rice *SNAC1* (Chen et al., 2011). For both proteins the folds were similar, consisting of a seven-stranded twisted antiparallel β-sheet which is flanked by α-helices on either side. Predicting the secondary structure of *ANAC058* (fig. 3.9) did not allow for the detailed results gained by crystallography but the same basic structure applies. DNA binding might be mediated by a loop between two β-strands in combination with the β-sheet, particularly depending on a section rich in basic residues (Ernst et al., 2004; Olsen et al., 2005b). Sequence similarity of the DBD of different

NACs might imply binding of similar target genes. The phylogenetic analysis using the DBD shows *ANAC058* clustering with *ANAC038* (fig. 8.3, supp.) for which an involvement in suberin regulation was implicated (Frenger, 2014), supporting this assumption.

In contrast to the DBD, only one α-helix was predicted in the TRD. The absence of conserved domains and prediction of only few secondary structures in the TRD indicates intrinsic disorder (ID) in this domain. Since ID is well known for transcription factors in general and for the TRD of NACs in specific, the *ANAC058* sequence was tested for ID. The analysis revealed that the complete TRD is intrinsically disordered. As a consequence, the TRD probably does not adopt a well-defined protein structure but an ensemble of conformers. Tertiary structures are absent and secondary structures fluctuate in protein regions with ID (Dyson and Wright, 2005), which allows for high flexibility and possibly binding of several interaction partners. Inferring protein function for intrinsically disordered domains is difficult due to missing conservation and complexity of features. *In silico* prediction of sequence regions with possible functional importance is still feasible using prediction of molecular recognition features (MoRFs), sequence motifs and secondary structures. Interaction of intrinsically disordered proteins often depends on MoRFs. These features are short regions which may form local structures upon binding and can be sequence motifs conserved in proteins with the same binding partner. In literature, predicted MoRFs and α-helices localized in the TRD of NACs were shown to be important for transcriptional activation and protein interaction (O'Shea et al., 2015). This applies specifically to a NAC protein in the same phylogenic group as *ANAC058* (*ANAC046*, see fig. 8.3 for phylogeny, O'Shea et al., 2015). Testing for MoRFs in the TRD of *ANAC058* revealed one MoRF close to the DBD and one at the very C-terminal end of the protein. None coincided with the predicted α-helix, therefore the two MoRFs and the predicted α-helix might indicate three different functionally important protein regions. Additionally to MoRFs, sequence motifs can also signify regions of functional importance. Sequence motifs as inferred by MEME analysis were shown to be characteristic for phylogenetic groups within the NAC gene family (Ooka et al., 2003) and can be essential for transcriptional regulation (Kjaersgaard et al., 2011). The motif found in the TRD of *ANAC058* is the LP motif determined repeatedly in TRD of NACs (Jensen et al., 2010; Kjaersgaard et al., 2011; Ko et al., 2007; Ooka et al., 2003). The LP motif in *ANAC058* might represent another amino acid sequence important for protein function. In order to determine the exact protein regions of ANAC058 essential for protein activity, the four sequences with the predicted MoRFs, α-helix and LP motif are good candidates for further experiments. Truncated proteins excluding the various protein regions can be tested for transcriptional activation function in vitro with yeast-one hybrid systems. Since ANAC058 is a transcription factor, the protein is expected to localize in cells to the nucleus. Still, the exact localization can be investigated with a *35S::ANAC058-GFP* construct. The construct was generated but not investigated in plants due to time constraints.

4.4 *anac058* mutants

In order to investigate phenotypic effects caused by changes in the expression of *ANAC058*, mutants with decreased expression were isolated and generated (see 3.2.1). Scouring two different databases for knock-out mutants for *ANAC058* did not reveal any mutant lines with a complete knock-out of the entire gene (fig. 3.10). One line with a transposon insertion at the end of the last exon (*anac058-1*, fig. 3.11) was determined amidst frequent insertions annotated outside the gene. While the protein in *anac058-1* is truncated, some functionality probably remains (fig. 8.5, supp.). Due to transcriptional knock-out of *ANAC058*, it is referred to as a knock-out line. Two lines with insertions close to the 5' end of the gene in the putative promoter of *ANAC058* were detected and one was isolated and characterized as a strong knock-down mutant (*anac058-2*). The generated amiRNAi lines (*anac058-3 (amiRNAi)* and *anac058-4 (amiRNAi)*) show decreased expression by approximately 50% and served, similar to *anac058-2*, as knock-down lines (fig. 3.11 D and E). The absence of complete knock-out mutants implies the necessity of remaining amounts of the functional ANAC058 protein for plant development. Essential functionality does not seem to require the C-terminal 33 amino acids of the wild-type ANAC058 protein. The insertion towards the 3' end of the coding sequence of *anac058-1* still allows the RNA up until the insertion site to be produced correctly (fig. 8.5, supp.) and consequently the protein from amino acid 1 to 283 is supposedly still functional. Since the insertion site is localized directly downstream of the MEME motif (fig. 3.9, for MEME analysis result, see fig. 8.4, supp.), the final protein misses only the predicted MoRF at the C-terminal protein end (see also 4.3.2). It still contains three of the four presumably important sequences: the predicted MoRF close to the DBD, the predicted α-helix and the MEME motif (compare fig. 3.9). Folding of the protein is probably not significantly affected since the protein is shorter by only 17 amino acids and the intrinsically disordered domain does not adopt complex secondary or tertiary structures. Truncation possibly only decreases binding affinity to interaction partners. Nonetheless, studies with a closely related NAC protein emphasize the importance of a predicted MoRF at the C-terminal end of the protein for transcriptional activation and protein interaction (O'Shea et al., 2015). It is possible that the *ANAC058* protein in the transcriptional knock-out *anac058-1* acts partly like the wild-type protein and only few specific functions are abolished or diminished. For lack of experimental proof regarding the activity of ANAC058 in the mutant, *anac058-1* is still referred to as a knock-out in the following.

4.4.1 Suberin amounts are not affected in whole root systems of *anac058* mutants

The impact of *ANC058* knock-out and knock-down on suberin was investigated by gas chromatographic suberin analysis for *anac058-1* and *-2*.

Samples were either complete root systems of 5 weeks old soil-grown plants (fig. 3.12) or apical sections of root systems collected from hydroponically grown plants of the same age (fig. 3.13).

In whole root systems of soil-grown Col plants, the amounts of the characteristic monomer C18:1 ω-hydroxy fatty acid (7.9 µg mg^{-1}, fig. 3.12) are approximately half the published values (Franke et al., 2005) possibly due to slight differences in growth conditions. The suberin amounts in L*er* roots are lower than for Col, as was also detected before (Frenger, 2014). The composition however is the

same as for Col and similar to published results for *A. thaliana* (Franke et al., 2005). Analyzing the complete root system of *anac058* mutants did not yield the expected result of significantly decreased suberin amounts. Amounts of aliphatic components in total were slightly increased in *anac058-2* by 12 % and decreased in *anac058-1* by 14 % compared to the wild types Col and L*er*, respectively. The decrease was not significant but several monomers in *anac058-2* displayed significantly increased amounts. Since promoter activity of the putative *ANAC058* promoter was observed mainly in apical sections of roots (fig. 3.5), whole root systems might be unsuitable for allowing observation of small changes due to mutations in *ANAC058*. The root might compensate for the lack of suberin in apical sections, which can explain the increased amounts of suberin observed for *anac058-2*.

4.4.2 Suberin amounts are decreased in apical root sections of *anac058* mutants

In order to investigate potential suberin effects in young root parts, apical sections of hydroponically grown *anac058* mutants were investigated as well. Suberin composition was the same as observed for soil-grown plants for all genotypes but amounts were lower in roots of hydroponically grown plants, compared to the soil grown ones. Less suberin in plants grown in hydroponics was observed before (Frenger, 2014) likely related to decreased availability of water and nutrients in soil. Slight short-term and localized drought conditions can occur in between irrigation, leading to increased suberin amounts. A relation between suberization and drought conditions was observed before (North and Nobel, 1998, 1995). Additionally, cell walls of hydroponically grown plants were not treated with cellulase and pectinase in order to reduce loss of material during sample preparation. This causes higher dry weight amounts per identical suberin amounts. Furthermore, different tissues were selected (apical root sections). Consequently, the amount of ω-hydroxy fatty acid in Col was much lower (0.5 µg mg^{-1}) than detected for root systems of soil grown plants (7.9 µg mg^{-1}). Suberin amounts in hydroponically grown L*er* plants showed also lower amounts compared the soil grown plants of the same ecotype. Interestingly, suberin amounts in the hydroponically grown L*er* ecotype were now slightly higher (0.6 µg mg^{-1} for ω-hydroxy fatty acids) than in Col grown under the same conditions. Since L*er* plant development was slightly delayed compared to Col plant growth, root systems were smaller in general. Consequently, collection of sufficient sample material for analysis demanded the use of a larger relative proportion of the total root system. The apical sections of L*er* plants contained older root tissue including more suberin compared to Col apical sections. This possibly explains slightly higher suberin amounts per root dry weight for L*er* compared to Col.

Analyzing the effect of *ANAC058* knock-out and knock-down, a consequent decrease in suberin amounts for both alleles was detected. For *anac058-2* this effect was significant for most detected ω-hydroxy fatty acids and α,ω-dicarboxylic acids. Amounts of both substance classes were decreased each in total by 49 % (ω-hydroxy fatty acids) and 37 % (α,ω-dicarboxylic acids). Monomers of all substance classes and all carbon chain lengths were affected, leading to suberin amounts lowered by 35 % in *anac058-2* apical roots. The effect on *anac058-1* root suberin is not significant but consistent with the *anac058-2* suberin phenotype. Aliphatic suberin amounts are decreased only by 15 % in *anac058-1* even though the production of wild-type *ANAC058* RNA is completely abolished. Presumably, binding of protein interaction partners and transcriptional activation function are only

slightly affected by the alteration of the C-terminal 33 amino acids. Suberin composition in *anac058* mutants did not change and amounts of all substance classes and chain lengths were reduced, supporting the assumption that *ANAC058* is a general regulator of suberin without preference towards specific suberin associated genes. The implicated involvement of *ANAC058* in regulation of most if not all suberin-associated genes seems to be restricted to young roots in *A. thaliana*, as is supported by the promoter activity analysis (3.1.3). In later stages of development, other transcription factors likely are the main regulators of root suberin synthesis and deposition. The strong effect in young root sections of *anac058-2* might cause a compensatory reaction by the plant, resulting in increased suberin amounts in basal root sections. This might lead to higher suberin amounts in total root systems as measured for soil-grown *anac058-2* plants (fig. 3.12). The effect in *anac058-1* apical root sections might be slight enough that the threshold for compensatory suberin deposition is not exceeded and the effect in apical sections and total root sections is similar (fig. 3.12 and 3.13). Whole root systems of hydroponically grown *anac058* plants have yet to be investigated with regard to suberin.

Suberin is also deposited in seed coats but promoter activity implied that *ANAC058* is active in seeds only in response to wounding (fig. 3.6). This indicates wild-type suberin amounts in intact seeds of *anac058* mutants which was also observed previously for *anac058-1* (Frenger, 2014). In general, knock-down and knock-out of *ANAC058* seems to affect specifically suberin in young roots and young root sections.

4.4.3 Suberin deposition is delayed in *anac058* mutants

Investigation of suberin deposition by histochemical staining of 6 d old *anac058* seedlings concentrated the focus on suberin in young roots. Staining suberin with Fluorol Yellow 088 in seedlings allows the observation of developmental suberization of the endodermis along the root. Close to the root tip in very young root sections, no suberin is observed. At a more basal localization, single endodermal cells showed staining resulting in a patchy appearance until, further basal, all endodermal with only few exceptions (passage cells) are suberized (Naseer et al., 2012). This characteristic suberin deposition pattern was observed for both wild type ecotypes and *anac058* mutant alleles (fig. 3.14). Approximately 50 % of the total root length is continuously suberized in Col and approximately 25 % display each patchy or no suberin. When zones of different suberization are measured in 5 d old seedlings by counting the endodermal cells from the hypocotyl to the start of the elongation zone, percentages of sections are similar (Barberon et al., 2016; Pfister et al., 2014). The percentage of the so measured zones was usually at slightly below 50 % for continuous suberin and at approx. 30 % of endodermal cells for patchy and absent suberin. In L*er*, suberization is slightly delayed in comparison to Col, leading to a larger patchy suberin zone and less continuous suberin, whereas the zone without suberin has the same percentage. This might be due to the slightly delayed development of the L*er* ecotype.

When investigating suberization in *anac058* mutants, suberin deposition is clearly delayed. Again, the knock-down mutant *anac058-2* shows the stronger phenotype with a highly significant decrease in percentage of continuous suberin lamella (approx. 30 % of total root length) compared to the wild-type

(approx. 50 % of total root length). Consequently, the percentage of patchy suberin and no suberin is increased significantly. The same effect can be observed for *anac058-1* for which the root section with continuous suberin is decreased significantly as well (25 % of total root length) and the patchy suberin zone is significantly larger. However, the zone without suberin is nearly unchanged. The *anac058-4 (amiRNAi)* seedlings showed also delayed suberin deposition, albeit less strongly compared to *anac058-1* and *-2*. This phenotype correlates well with *ANAC058* transcription levels in this line (fig. 3.11 D) which did not decrease as severely as in *anac058-1* and *-2*. In conclusion, the absence or decreased amounts of a completely functional *ANAC058* protein leads to delayed start of suberin deposition as well as delayed formation of the continuous suberin lamella. A similar effect was observed for the suberin mutants *horst-1* and *horst-3* (Naseer et al., 2012). However, the suberin phenotype in the *horst* mutant is not restricted to apical root sections. Suberin amounts in whole root systems of soil-grown *horst* plants decreased as well (Höfer et al., 2008). This difference might be due to additional transcription factors becoming active with continuing root development, compensating the effect of the *ANAC058* knock-down in the young roots of *anac058-2*. In *horst* mutants, potential compensation of the suberin effect dependant on the functional HORST protein does not occur. Additionally, the compensatory suberin deposition might also be due to stress signals caused by insufficient suberization in *anac058*. In both cases a complex regulatory network or at least an additional transcription factor seems to be involved in suberin regulation. Possible candidates are other unknown NACs which may heterodimerize with *ANAC058* or the transcription factor *MYB41. MYB41* is a stress-induced suberin transcription factor (Kosma et al., 2014). On the other hand, the absence of a knock-out *ANAC058* mutant with a completely non-functional ANAC058 protein suggests that at one point during plant development the effect of a knock-out cannot be compensated and has a lethal impact on the plant. During that developmental stage, the remaining protein in *anac058-2* and the probably still functional partial protein in *anac058-1* might be sufficient for suberization and compensation of a suberin effect appears to be impossible.

4.4.4 Expression of suberin-associated genes is decreased in *anac058* mutants

In *anac058* mutants, knock-out and knock-down of *ANAC058* correlates with decreased suberization (3.2.2 and 3.2.3). This suberin effect suggests decreased expression of suberin associated genes. Accordingly, a decrease in gene expression was observed for the suberin synthesis genes *RALPH*, *GPAT5* and *HORST* in apical root sections of 4-5 weeks old hydroponically-grown *anac58* plants (fig. 3.15). As such, sample material is similar to the material for which an effect on suberin was detected with gas chromatography (fig. 3.13). The decrease of suberin gene expression in *anac058-2* was observed for all three genes, befitting the fact that *anac058-2* is the stronger allel as determined already with suberin analyses (3.2.2 and 3.2.3). In *anac058-1,* a lower expression of *RALPH* and *HORST* was detected, if not as strongly decreased as in *anac058-2*. *GPAT5* expression, on the other hand, is unchanged in *anac058-1*. It is likely that in this case additional signals and transcription factors resulted in wild-type level expression of *GPAT5*. Remaining *GPAT5* levels in *anac058-2* are still at over 50 % compared to the wild type, strengthening the theory that especially *GPAT5* is co-regulated by other transcription factors. Interestingly, the relatively weak knock-down of *ANAC058* in *anac058-3 (amiRNAi)* resulted in the strongest decrease of *RALPH* and *GPAT5* expression

observed in all *anac058* mutant allels. *ANAC058*, *RALPH* and *GPAT5* expression is only 50 % of the wild type expression which might by due to the type of gene regulation. Several NACs are known to be regulated post-transcriptionally by miRNAs (Puranik et al., 2012). Introducing an additional level of regulation with the RNA interference construct might disrupt possible post-transcriptional regulation of *ANAC058* to the extent that *RALPH* and *GPAT5* expression levels are more strongly affected. The suberin phenotype in the *anac058-4 (amiRNAi)* line on the other hand is weaker than in *anac058-1* and *anac058-2* (fig. 3.14). Other suberin associated genes have to be investigated in the amiRNAi lines in order to determine whether all are strongly affected in their expression. Nonetheless, lower expression levels of *ANAC058* correlate with decreased suberin gene expression and delayed suberin deposition.

RBOHF (respiratory burst oxidase homologue F, an NADPH oxidase) was selected as the designated Casparian strip synthesis gene (Lee et al., 2013). Its expression was tested as well and did not correlate with *ANAC058* expression. The Casparian strip (CS), like suberin, is deposited in the apoplast around endodermal cells. Differently from suberin, CS forms a ring around the cells and its formation starts earlier in root development, closer to the root tip. The polymer consists of lignin in *A. thaliana* (Naseer et al., 2012), thus is generated from oxidatively coupled monolignols. For this reaction, *RBOHF* is needed to provide hydrogen peroxide for the peroxidase *PER64* (Lee et al., 2013). *ANAC058*, probably active in the endodermis (3.1.3), could be involved in regulation of CS generation. However, the basically unaltered expression of *RBOHF* indicates that *ANAC058* expression and CS synthesis are unrelated of each other. *RBOHF* has numerous additional functions like generating reactive oxygen species as part of plant defense responses (Torres et al., 2002). It is expressed accordingly in all root cell types of 5 d old seedlings although the protein accumulates in the endodermis in Casparian strip domains (Lee et al., 2013). In *anac058* mutants, *RBOHF* expression is essentially unchanged, if slightly higher compared to the wild type. This slight increase in expression might reflect marginally increased stress levels in the root due to suberization delay.

4.4.5 Physiology of *anac058* mutants

4.4.5.1 Susceptibility of *anac058* mutants to salt stress is increased

Suberin has been implicated in salt and drought stress responses in various species (Barberon et al., 2016; Baxter et al., 2009; Kosma et al., 2014; Krishnamurthy et al., 2011, 2009). Since mutants or cultivars with lower levels of suberin have shown increased sensitivity to salt (Beisson et al., 2007; Krishnamurthy et al., 2009), susceptibility of *anac058* mutants to increased levels of NaCl (50 mM) was tested. For the *GPAT5* mutant line *gpat5-1* with lower amounts of seed coat and root suberin, sensitivity of the mutant during germination to increased levels of ions, including NaCl, was observed (Beisson et al., 2007). Germination rate of *anac058* mutants on the other hand was not affected (data not shown) which correlates well with wild type levels of seed coat suberin observed for *anac058-1* (Frenger, 2014). The absence of any activity of the putative *ANAC058* promoter in intact seeds supports this theory (see fig. 3.6). Additionally to the decreased germination rate of *gpat5-1*, seedling establishment rate was also lower than for the wild type with increasing salt concentrations (Beisson et

al., 2007). The increased rate of aborted seedling growth might be due to accumulation of ions up to toxic levels in the seedlings during and shortly after germination. This effect was also not more frequent in *anac058* mutants compared to the wild type (data not shown). Possibly, delayed suberin deposition is not relevant yet at a developmental stage this early. In *gpat5-1,* the developmental arrest might be again related to seed coats that were more permeable to salts (Beisson et al., 2007).

Further plant development of *anac058* on MS medium with 50 mM NaCl was continuously observed for 5 weeks and root lengths of 10 d old seedlings were measured representatively (fig. 3.16 and fig. 8.7, supp.). Still, no effect of increased salt concentrations specifically on *anac058* mutants was observed. In all genotypes, roots were slightly longer in seedlings growing on increased salt concentrations compared to control conditions. This tendency might be a stress evasion response of the plant to moderate salt stress. On the other hand, the stress evasion response usually entails proliferation of lateral roots instead of root elongation, as was observed in response to 50 mM NaCl before (Zolla et al., 2010). The unexpected main root growth indicates that the applied stress under the respective growth conditions was very mild.

Since suberin amounts have been connected to salt stress susceptibility (Barberon et al., 2016; Krishnamurthy et al., 2011, 2009) and *anac058* seedings show delayed suberin deposition, the lack of an effect on *anac058* is probably due to insufficient severity of stress. This assumption is supported by the used concentration of 50 mM NaCl also having no visible effects on *gpat5-1* under very similar growth conditions (Beisson et al., 2007). Accordingly, a repetition of the experiment with *anac058*, applying increasing NaCl concentrations would be of interest. Additionally, the remaining functional ANAC058 protein in *anac058* mutants might allow salt stressed mutants to deposit sufficient suberin for stress resistance to mild stress. *ANAC058* has been implicated in salt stress response by expression analysis (Frenger, 2014) which raises the question of its importance in salt stressed *anac058* mutants. In order to investigate the severity of the applied salt stress and *ANAC058's* role further, Fluorol Yellow 088 staining of salt treated mutants and respective wild type seedlings would clarify whether suberin deposition delay in mutants is still present under stress conditions.

In order to avoid possible adaptions of mutant and wild type to increased NaCl concentrations during germination and early seedling establishment, 3 d old seedlings were transferred to high salt medium (50 mM NaCl) and root growth was monitored for 5 weeks. In-detail investigation of root length was conducted after 7 d of growth on NaCl medium (fig. 3.17) but no significant growth effect for *anac058* seedlings compared to the wild type was observed at all times. Root length of mutants before the transfer was not visibly different from the respective wild type (data not shown). Transfer of wild type and mutants to control MS medium resulted in no visible differences regarding growth of mutants compared to the respective wild type (observed in different experiments, data not shown). Tendentially, roots of *anac058-2* were slightly shorter than roots of the wild type when growing on salt medium. This was not observed when germinating mutants on increased salt concentrations. Differences were not significant but might represent a slightly higher susceptibility of *anac058* to NaCl when subjected to increased salt concentrations after germination. Decreased tolerance of *gpat5-1* seedlings was also observed when transferring 3 d old seedlings to MS with high NaCl concentration. However, the decrease in tolerance manifested as a high number of bleached *gpat5-1* seedlings

(Beisson et al., 2007). The decreased amounts of root suberin in *gpat5-1* probably negatively affected the barrier function of suberin leading to uptake of toxic amounts of Na^+. A similar effect can be observed for plants with no histochemically detectable suberin (*CASP1::CDEF1* and *ELTP::CDEF1*, Barberon, 2017). In leaves of these mutants, high amounts of NaCl were measured even though the plants were grown under control conditions. The absence of a clear effect in *anac058* mutants on the other hand might be due to the low concentration of applied NaCl. Again, higher concentrations of NaCl were applied to *gpat5-1* than to *anac058* mutants and remaining suberin in *anac058* mutants in combination with remaining functional ANAC058 protein and other TFs might allow sufficient salinity tolerance.

Application of salt stress by hydroponic culture on the other hand revealed a clear effect of 50 mM NaCl on *anac058* (fig. 3.18). Plants were grown for 25 d in hydroponics and salt treatment was conducted for 2 weeks. A distinct effect on plant health was observed after 2 weeks for all genotypes. Premature senescence was visible in old leaves of wild types and mutants as chlorosis at the leaf margins. Measurement of fresh and dry weight supported this observation with significantly decreased root and shoot weight for plants subjected to NaCl treatment compared to control plants (fig. 3.18 and fig. 8.8, supp.). Generally, *A. thaliana* is a salt sensitive species (Munns and Tester, 2008) but differences between *A. thaliana* ecotypes exist. The L*er* ecotype was observed by Jha and coworkers to be less sensitive to salt stress than Col (Jha et al., 2010). In the present work, the L*er* ecotype displayed a smaller plant size compare to Col. However, this difference was not related to salt stress but appeared also under control conditions. Instead, ecotype differences in response to salt treatment were observed as different effects on shoot and root. For L*er*, the shoot is predominantly affected (fresh weight decreases by approx. 40 % compared to approx. 12 % decrease in Col) and in Col the effect of salt is stronger on the root (approx. 30 % fresh weight decrease compared to approx. 10 % in L*er*, fig. 3.18). The ecotype differences might be due to developmental variation since development of L*er* plants is delayed compared to Col. Another possibility is the different strategies employed by ecotypes when dealing with excess salt. Na^+ accumulates in L*er* predominantly in the shoot and in Col predominantly in the root (Jha et al., 2010), which correlates well with the organ-specific fresh weight decrease. Less suberin amounts in whole roots systems of L*er* plants compared to Col, albeit measured in plants grown on soil, might also have an impact (fig. 3.12). In Col, the Na^+ ions accumulating in the root might be explained by a higher amount of suberin resulting in accumulation of some Na^+ outside the endodermal barrier. Consequently, less Na^+ enters the xylem. In L*er*, Na^+ ions might pass the endodermis more easily and subsequently accumulate in the shoot. Suberin has been repeatedly shown to be deposited in response to salt stress (Barberon et al., 2016; Franke et al., 2009), indicating a protective function. Additionally, expression of Na^+ uniporters in roots might be different in ecotypes in response to salt stress (Jha et al., 2010). Possibly, several stress responses such as suberin barriers, ion exclusion and transporters work in tandem and depend on each other's feedback response. In order to investigate the salt stress response in detail, analysis of transporter activity and localization of Na^+ ion accumulation in roots might be of interest. Cell-type specific potassium accumulation has been investigated with laser ablation-inductively coupled plasma-mass spectrometry (LA-ICP-MS) (Persson et al., 2016) and the method might serve well for the same analysis with regard to Na^+.

Fittingly, if suberin amounts are decreased as in *anac058*, the detrimental effect of salt stress on plants is amplified. Morphology of plants was more affected in mutants than in wild type as the *anac058* plants retained only few fully turgid leaves. Shoot fresh weight was decreased due to NaCl by 70 % in *anac058-1* and by 50 % in *anac058-2* compared to L*er* (40 % decrease) and Col (12 % decrease), respectively (fig. 3.18). As observed for the wild type ecotypes, the effect is in general stronger for the shoot in *anac058-1* (L*er* background) and stronger in the root in *anac058-2* (Col background). Thus, the organ-specific effect can be related to the ecotype background.

Since the *anac058* mutants, compared to the wild types, are affected more strongly with regard to viability and biomass production by salt stress, lower amounts of suberin seem to increase salt sensitivity. Biomass production is lower and water content in plants has been affected as well. The fresh weight:dry weight ratio decreases for both mutants in general, indicating a stronger impact of NaCl application on the fresh weight than on the dry weight and consequently on the water content (fig. 8.8, supp.). This might be related to the osmotic pressure of NaCl and the insufficient suberin barrier not being able to retain water in the mutants over a time period of 2 weeks. The strong impact of salt stress on mutants compared to the wild type, appearing as significantly less biomass emphasizes the importance of the intact suberin barrier during salt stress.

It should be taken into consideration that under control conditions, *anac058-2* plants already contained slightly less biomass than the respective wild type, though the difference is not significant (fig. 8.8, supp.). Since *anac058-2* is the stronger allel with respect to decreased suberin amounts, suberin barrier functions might already be slightly affected under control conditions. Still, the difference due to salt stress between *anac058-2* and its wild type is significantly more pronounced. Additionally, nearly all differences between salt stressed *anac058* mutants and respective wild types are significant, supporting increased salt stress susceptibility of mutants. Only the decrease of *anac058-1* root fresh weight is not significant. However, this might be due to *anac058-1* being the weaker allel or higher inherent tolerance of L*er* (Jha et al., 2010). More distinct differences might be obtained by applying more severe salt stress in a repetition of the experiment. While 50 mM NaCl can be expected to have a negative effect on biomass production since 40 mM NaCl is known to have a detrimental effect on L*er* (Cramer, 2002; Munns and Tester, 2008), this concentration is not supposed to be lethal. Volkov and colleagues observed that *A. thaliana* is not able to complete its life circle at NaCl concentration above 80 mM, whereas the plants survived 50 mM NaCl for 5 weeks at least (Volkov et al., 2004). The fact that *anac058* mutants are severely affected by 50 mM NaCl already indicates uptake of high amounts of ions and likely accumulation of Na^+ in the shoot. The observed necrotic spots and senescence of leaves are associated with salt toxicity due to high concentrations of ions in the leaf (Munns and Tester, 2008). Cation transporters like *SOS1* are proposed as a major factor in uptake of Na^+ (Demidchik et al., 2002; Volkov et al., 2004). For the uptake by the transporters, NaCl has to be able to reach the plasmamembrane. Since the suberin lamella covers the plasmamembrane it probably affects the accessibility of the transporters. Thus, in plants with less suberized endodermal cells, NaCl supposedly can enter the endodermis in an easier manner. That probably leads to elevated Na^+ concentration in plants with no detectable suberin even under control growth conditions (Barberon, 2017) and confirms suberin as a transcellular barrier, as was proposed by Barberon in

2017. During salt stress, increased suberization is expected. The increase might be smaller in *anac058* mutants, additional to the suberization delay under control conditions. In order to investigate the salt susceptibility of the *anac058* mutants further, measurement of the suberin amounts in roots of salt-stressed hydroponically-gown mutants would be of interest. Additionally, dried shoot and root material was collected for dry weight measurements (fig. 3.18) and measurement of ionomic composition might reveal changes in ion accumulation and their localization in mutants. Furthermore, the effectiveness of the endodermal barrier in *anac058* would be interesting to investigate by measuring Na^+ in different cell layers of the root with LA-ICP-MS, as mentioned before. Possibly, Na^+ accumulates outside the endodermis in the wild type but not in the mutants. Since root hydraulic conductivity (L_{pr}) decreases in response to salt stress within 1 hour after salt treatment start (Boursiac et al., 2005; Martínez-Ballesta et al., 2003), measurement of L_{pr} of salt-stressed *anac058* and wild type roots might reveal whether early plant responses to salt stress differ in the mutants.

Incidentally, transpiration is an important factor in salt stress (Munns and Tester, 2008; Volkov et al., 2004) and a sharp drop of transpiration in *A. thaliana* was observed after application of 100 mM NaCl (Volkov et al., 2004). Transpiration rates might be connected to amounts of root suberin (Baxter et al., 2009) and were not measured for *anac058* mutants. As *ANAC058* also seems to be also inducible by ABA, ABA signaling related to transpiration and suberization might be affected in the mutants. Consequently, transpiration measurements would be of interest. Transpiration might also explain the absence of effects when growing seedlings on MS medium with 50 mM NaCl. As plates are a closed system, relative air humidity is probably at nearly 100 % and transpiration therefore minimal. Under these nontranspiring conditions, salt-stressed *A. thaliana* plants are probably predominantly subjected to osmotic stress instead of ion toxicity (Munns and Tester, 2008; Zhu et al., 1998). Hydroponically grown plants on the other hand were subjected to average 47 % relative humidity during the day, supposedly resulting in higher transpiration rates and increased delivery of Na^+ to the shoot. Additionally, differences in the used media might also have an impact. Availability of other ions like calcium has also been implicated in salt tolerance (Lahaye and Epstein, 1969) and might differ in differently composed media with various grades of solidity.

4.4.5.2 Susceptibility of *anac058* mutants and wild type to osmotic stress is the same

Salt induced stress has two components: the osmotic stress caused by high amounts of ions in close vicinity of the root decreasing soil water potential and the toxic amounts of ions accumulating in the shoot. In order to separate the impact of osmotic stress and Na^+ toxicity on mutants with decreased amounts of root suberin amounts, growth of *anac058* in solutions with low water potential was investigated. Plants were grown in hydroponics for 2 weeks and transferred to a PEG solution with a water potential of - 0.49 MPa. After 4 d of PEG treatment plant health was severely affected (fig. 3.19). For all genotypes loss of leaf turgor was observed as well as violet coloring, probably due to enhanced anthocyan production. Consequently, negative water potential induced strong osmotic stress which was not observed for the NaCl treatment. Salt-stressed plants appeared healthy 4 d after treatment start (data not shown). However, the water potential of the applied salt solution was less negative (- 0.36 MPa) than of the PEG solution even if still distinctly below control solution water potential

(- 0.09 MPa). Loss of turgor in response to PEG was reflected in a decrease of fresh weight for root and shoot of all genotypes (fig. 3.19). This effect was especially severe for the Columbia ecotype with shoot and root fresh weight decreased by 78 % and 76 %, respectively. In comparison, L*er* shoot and root fresh weight decreased by 13 % and 35 %, respectively. Root:shoot ratio calculated from dry weigh on the other hand increased for both ecotypes, indicating a stronger detrimental effect on shoot than on root biomass production (fig. 3.19). Possibly the plant is concentrating its growth efforts on the root in order to find a new, suitable growth medium (Yamaguchi and Sharp, 2010). When subjected to short-term osmotic stress, Col appears to be more tolerant which was reflected by the absence of necrotic spots on leaves. These necoses were observed, on the other hand, at the leaf margins of *L*er and *anac058-1* plants. Tolerance might be related to better drought tolerance of Col (Meyre et al., 2001) but possibly might also be due to transpiration and aquaporin activity. Both transpiration and aquaporin activity were not measured for the ecotypes during these growth conditions. Another factor might be the delayed development of *L*er which can make the plants more susceptible to stress.

Suberin, on the other hand, seems to have no significant effect on short term osmotic stress tolerance in *A. thaliana*, at least under the applied growth conditions. The *anac058* mutants with decreased amounts of suberin did not appear to be more sensitive to osmotic stress than the respective wild type. Root fresh weight of PEG-treated *anac058-2* plants decreased significantly less than for Col but this effect was not observed for *anac058-1* and is therefore probably unrelated to suberin levels. The same lack of effect was shown for the suberin mutant *gpat5* when treated with 400 mM PEG or mannitol for 12 d (Beisson et al., 2007). However, expression of several suberin associated genes increased when subjected to osmotic stress (Franke et al., 2009; Lee et al., 2009b; Yadav et al., 2014), suberin amounts in maize increased after growth in 30 % PEG solution for 4 d (Schreiber et al., 1999) and ectopic suberin is able to provide enhanced drought tolerance (Baxter et al., 2009). Osmotic stress probably induces production of stress related suberin which might protect *A. thaliana* during long term drought stress. Measurement of root suberin in *anac058* mutants subjected to osmotic stress would clarify whether differences between mutants and wild type observed under control conditions are still present. Since changes in transpiration might partly compensate the effect of PEG, its measurement for *anac058* and wild types during osmotic stress would be of interest.

In summary, *anac058* seem to be more susceptible to salt stress under conditions where plants transpire. The susceptibility seems to be related predominantly to the accumulation of toxic ion concentrations in the plants instead to osmotic stress. In order to verify this, the PEG treatment might be repeated using a PEG solution with the same water potential as the stress inducing NaCl solution.

4.4.5.3 Root hydraulic conductivity of *anac058* mutants

Changes in root hydraulic conductivity (L_{p_r}) have been related in *A. thaliana* mainly to aquaporin activity (Tournaire-Roux et al., 2003) but also to suberin amounts (Ranathunge and Schreiber, 2011). Especially under stress conditions, higher suberin amounts were linked to decreased L_{p_r} values for crops (Barrios-Masias et al., 2015; Krishnamurthy et al., 2011, 2009; Zimmermann and Steudle, 1998). L_{p_r} measurements for L*er* (120 ml g^{-1} h^{-1} MPa^{-1}) and Col (143 ml g^{-1} h^{-1} Mpa^{-1}, fig. 3.20) are similar to previously measured root hydraulic conductivity under control conditions (Boursiac et al.,

2005; Shahzad et al., 2016). Water permeability of Col roots appears slightly higher than for L*er*, even though suberin amounts in Col roots are higher, at least for soil grown plants (fig. 3.12). Suberin amounts in complete root systems of hydroponically grown plants have yet to be tested and might be different. Since L_{p_r} is strongly dependent on aquaporin expression, differences between ecotypes might also be aquaporin-related.

The reduced amounts of suberin in the *anac058* mutants did not have a consistent effect on L_{p_r}. L_{p_r} of *anac058-2* is significantly decreased, L_{p_r} of *anac058-4 amiRNAi* is slightly decreased as well, whereas L_{p_r} of *anac058-1* is slightly increased. Decreased hydraulic conductivity in *anac058-2* roots might be related to increased amounts of suberin, as was observed in total root systems (fig. 3.12). Since suberin deposition is delayed in young roots, compensatory suberin might be deposited in basal root sections as a stress response, decreasing water permeability. This stress response might additionally entail less open aquaporin channels which also results in increased L_{p_r} values. Suberin deposition in *anac058-4 amiRNAi* seedlings is slightly delayed (fig. 3.14) but L_{p_r} is not significantly affected, only slightly decreased compared to Col. Possibly, compensatory suberin deposition is also present in *anac058-4 amiRNAi* plants or the suberin effect is not distinct enough for an effect on L_{p_r}. Suberin in root systems of *anac058-4 amiRNAi* plants grown hydroponically for 3 weeks has yet to be analyzed but might be close to wild type levels. L_{p_r} of *anac058-1* is also not affected and water permeability seems to be slightly higher even, if not significantly different. Absence of significant differences might be due to *anac058-1* being the weaker allel (fig. 3.13 and fig. 3.14). Additionally, suberin amounts in whole root systems were lower in *anac058-1* than in the respective wild type, indicating no compensating suberin deposition. It is possible that the slight suberin deposition delay in *anac058-1* (fig. 3.14) results in marginally higher water permeability. However, suberin amounts of total root systems were only measured for soil grown plants and should also be investigated in plants grown in hydroponics.

Still, in contrast to water uptake, uptake of NaCl seems to depend on a different uptake pathway since both mutants are significantly more sensitive to increased NaCl concentrations. The long term salt stress response might be impaired in *anac058* while water permeability is only slightly affected. In order to separate aquaporin activity from apoplastic water flow, L_{p_r} measurement after inhibition of aquaporins in *anac058* would be of interest.

4.5 Overexpression of *ANAC058*

4.5.1 Endodermal-specific overexpression of *ANAC058* delays suberin deposition

In knock-out and knock down mutants, phenotypic effects might be partly or entirely masked be compensatory plant responses. In case this applies to *anac058* mutants, overexpression plants were generated. Constitutive overexpression of *ANAC058* yielded no visible effects (Frenger, 2014), possibly caused by silencing of overexpression in roots due to its detrimental developmental effects (Coego et al., 2014). Consequently, $Prom_{RALPH}$*::ANAC058* overexpression plants were generated

which overexpress *ANAC058* specifically in the endodermis. Additionally, overexpression is restricted to developmental stages during which suberin in synthesized since *RALPH/CYP86B1* is a suberin synthesis gene. *ANAC058* seems to be slightly overexpressed in two of three $Prom_{RALPH}$*::ANAC058* lines but the *GPAT5* and *RALPH* expression pattern does not correlate to *ANAC058* expression. Overexpression of *ANAC058* is expected to induce increased expression of suberin genes as was observed in leaves of *35S::ANAC058* plants (Frenger, 2014). Possibly, *ANAC058* as a transcription factor binding to the promoter of *RALPH* is inducing itself in $Prom_{RALPH}$*::ANAC058* plants, creating a strong feed-forward loop. Since suberin synthesis and deposition seem to be tightly regulated in a stress dependent, as well as a developmental and a tissue-dependent manner, several regulatory fail-safe mechanisms might exist. These might silence the construct or decrease *ANAC058* transcript or protein amounts post-translationally or -transcriptionally.

When investigating the suberin deposition histochemically by staining suberin of 6 d old seedlings with Fluorol Yellow 088, a suberin deposition delay was observed for $Prom_{RALPH}$*::ANAC058* plants (fig. 3.22). This is in contrast to the slight overexpression of *ANAC058* as seen in fig. 3.21 in the respective lines. On the other hand, the suberin deposition delay is in accordance with the expression pattern of *RALPH* and *GPAT5* in $Prom_{RALPH}$*::ANAC058* which seem to be unchanged or down-regulated. A possible explanation is a regulatory network decreasing levels of ANAC058 protein post-translationally to wild type levels which would not be detected by RT-PCR. Additionally, NACs have been observed to be post-transcriptionally regulated by miRNAs (Puranik et al., 2012) which would explain the *ANAC058* transcript levels in $Prom_{RALPH}$*::ANAC058* being close to wild type levels. Since expression of only few suberin-associated genes has been tested in the overexpression plants, down-regulation of other genes might be more severe to result in significant suberin deposition delay. To further elucidate the result of the overexpression of *ANAC058* under the putative *RALPH* promoter, testing of *ANAC058* protein levels and investigation of further suberin associated genes would be relevant. Additionally, further investigation of *35S::ANAC058* with regard to suberin gene expression in roots and histochemical suberin investigation might help elucidate effects caused by *ANAC058* overexpression.

4.5.2 Conditional overexpression of *ANAC058* in roots results in suberin effects

4.5.2.1 Conditional overexpression of *ANAC058* results in ectopic suberin deposition

In order to avoid the response of regulatory networks to overexpression which might protect the plant by reducing overexpression effects, a conditional overexpression construct was employed. As provided by the TRANSPLANTA project (Coego et al., 2014), the *ANAC058* coding sequence was cloned behind a β-estradiol inducible promoter and introduced into *A. thaliana* wild type plants by Coego and coworkers. The obtained two lines *TPT.D* and *TPT.G* were tested for induced overexpression of *ANAC058* which was especially distinct for *TPT.G* (fig. 3.23). *TPT.G* plants were grown hydroponically and overexpression was induced by the transfer of plants to a β-estradiol containing solution. In order to investigate suberin amounts with gas chromatography, apical sections of root systems were selected since they showed a suberin effect in *ANAC058* knock-out and

knock-down plants. Additionally, application of the overexpression inducer likely has the strongest effect on newly generated root material.

Unexpectedly, analysis of suberin in apical sections of plants after induced *ANAC058* overexpression for 1 week did not show any consistent differences (fig. 3.24). Suberin amounts were similar to those measured previously under comparable conditions (fig. 3.13). Treatment of the *TPT.G* line with mock solution resulted in tendentially more suberin compared to Col, as seen for total aliphatic suberin amounts. Since the increase is insignificant for all monomers and the total suberin amount, mock treated TPT.G plants can be treated as control plants. For β-estradiol induced TPT.G plants, two monomers increased significantly, the C22 alcohol and the C24 ω-hydroxy fatty acid. In *ANAC058* knock-out and knock-down plants most monomers were affected which indicates that the same should apply to overexpression. Possibly, within 1 week the effect of induced overexpression has been reversed or preventative mechanisms were activated. Another possibility is suberin degradation due impaired nutrient availability. Degradation of suberin under iron deficiency conditions was shown before (Barberon et al., 2016). Accordingly, difference in nutrient access due to increased suberin amounts closing apoplastic uptake pathways might start a degradation process, leading to approximately wild type suberin levels.

Histochemical investigation of suberin in induced TPT plants might reveal small changes not detected with gas chromatography. Accordingly, a transfer experiment has been conducted with TPT.G and Col seedlings. 4 d old seedlings were transferred to MS supplemented with β-estradiol and overexpression was induced for 2 d after which suberin was stained with Fluorol Yellow 088. Beforehand, induced overexpression was observed by transferring *TPT.G* seedlings to MS with β-estradiol and measuring *ANAC058* transcript levels after 6 h (fig. 8.11, supp.). Induction for 2 d and successive suberin staining revealed a distinct effect on suberin (fig. 3.25 and fig. 3.26). Suberin deposition started very close to the root tip, significantly earlier than in the wild type or in mock treated *TPT.G* seedlings. In control seedlings, the section without suberin makes up approximately 40 % whereas in β-estradiol induced seedlings it amounts to only 14 % of total root length. Similar values were measured for lines with ectopic suberin, *esb1* and *casp1casp3* (Pfister et al., 2014). Additionally, the patchy suberization zone in which single endodermal cells are suberized but no continuous suberin lamella has been developed yet does not exist in induced *ANAC058* overexpressing seedlings. The suberization close to the root tip is very similar to ectopic suberin deposition observed in *esb1* seedlings. The *esb1* mutant also displayed the tendency towards shorter and rounder cells (Baxter et al., 2009; Hosmani et al., 2013) as was observed for *ANAC058* overexpressing seedlings. In case of *esb1*, suberin deposition is increased as a response to defective Casparian strips (CSs) (Hosmani et al., 2013). CSs in induced *TPT.G* plants were not investigated but were intact in *anac058* mutants (Christopher Millàn Hidalgo, University of Bonn, Germany, personal communication). No direct link between *ANAC058* and CS generation was uncovered. In contrast to apical root sections, the deposition in basal root sections in induced *TPT.G* plants is unchanged, side roots are present and passage cells were observed. Whether the same applies to *esb1* is not clear.

Overexpression of *ANAC058* leads to earlier ectopic suberin deposition as observed histochemically but this effect seems to be diminished by the plant itself after 1 week. At that time point, gas

chromatography analysis uncovered only slightly, insignificantly increased suberin amounts in apical sections of root systems of induced *TPT.G* plants. In case differences in suberin are too small to detect in apical root sections of root systems, induction of overexpression in seedlings for 1 week and subsequent Fluorol Yellow 088 staining would be of interest. Another explanation for no visible effects after 1 week of overexpression might be the detrimental effect of the overexpression. It might cause protective measures in the plant and subsequently wild type suberin levels. Detrimental effects can be related to ectopic suberin deposition which may hinder cell elongation. Other options are the plant adapting to nutrient deficiency which may be caused by ectopic suberin or an additional unknown function of *ANAC058,* related to ectopic overexpression in all cells.

Since suberin was not deposited outside the endodermis even though *ANAC058* was overexpressed in all cell types, additional factors are necessary for suberin deposition in other root tissues. As NACs can form heterodimers, the necessary dimerization partner might be present only in the endodermis. The *ANAC038* gene has been associated with suberin but knock-out of the gene resulted in increased suberin amounts in roots and the putative promoter appears to be active in the central cylinder instead of the endodermis (Frenger, 2014). Consequently, *ANAC038* providing the dimerization partner for *ANAC058* is unlikely. Since overexpression of only *ANAC058* causes a suberin effect, any additionally needed factors for suberin synthesis and deposition have to be present in the endodermis but not in any other cell layers. Accordingly, the suberin generation machinery which is necessary for ectopic and stress induced suberin is present and inducible by *ANAC058* in the endodermis.

4.5.2.2 Conditional overexpression of *ANAC058* results in increased expression of suberin-associated genes

To investigate induced expression of suberin associated genes by conditional *ANAC058* overexpression, quantitative RT-PCR was employed. Apical root sections of hydroponically grown *TPT.G* plants treated with β-estradiol for 1 week were collected and strong overexpression of *ANAC058* compared to mock treated *TPT.G* plants was observed (fig. 3.27). Thus, expression of several published suberin genes was tested as well. An increase in expression for all investigated suberin genes, *RALPH*, *GPAT5*, *HORST*, *ASFT* and *ABCG6*, was observed. In combination with down-regulation of suberin associated genes in *ANAC058* knock-out and knock-down plants, this correlation of suberin gene and *ANAC058* expression indicates strongly that *ANAC058* regulates suberin-associated genes.

4.5.2.3 Conditional overexpression of *ANAC058* affects expression of CS and lignin-associated genes, not cutin-associated genes

Since the Casparian strip (CS) is located to the endodermis, expression of several CS specific genes was investigated as well. Interestingly, *RBOHF*, *ESB1* and *PER64* (Hosmani et al., 2013; Lee et al., 2013) are upregulated as well (fig. 3.27). Possibly, *ANAC058* also regulates CS synthesis and deposition. This is unlikely, however, since no indication of an effect on CS in *anac058* mutants or any instances of co-expression of *ANAC058* and CS genes were observed previously. Another option is possibly increased cell division in *ANAC058* overexpressing plants since a tendency towards shorter

and rounder cells was observed. Cell elongation may be hindered by ectopic suberin deposition close to root tip or due to an unknown effect *ANAC058* overexpression has on root development. Since the root has to maintain growth cell division might increase, especially as ectopic suberin might cause a decrease in nutrient uptake (Barberon, 2017; Baxter et al., 2009) and nutrient deficiency signals might induce root growth. This potential effect has to be researched further, especially if it is connected to enhanced suberin deposition. If the cell number increases, CS generation would have to increase as well. Since *A. thaliana* CS consists of lignin (Naseer et al., 2012), upregulation of lignin biosynthesis gene *CAD5* (Fraser and Chapple, 2011) correlates with increased expression of *ESB1*, *RBOHF* and *PER64*. Upregulation of *CAD5* might also be associated with suberin since it was observed to be upregulated when overexpressing another TF, *MYB41*. This TF likely regulates stress induced suberin deposition and causes accumulation of suberin and lignin when overexpressed (Kosma et al., 2014). However, the connection between the two polymers suberin and lignin is not entirely clear.

The similarity of cutin composition to suberin raises the question, whether *ANAC058* might also be involved in its synthesis. Expression of two cutin-associated genes, *GPAT4* and *CYP86A2* (Li et al., 2007a; Xiao et al., 2004) is unchanged in *ANAC058* overexpressing plants, indicating no involvement in cutin regulation for *ANAC058*.

4.5.2.4 Conditional overexpression of *ANAC058* affects expression of an aquaporin gene slightly

Since ecotypic suberin deposition has an effect on water uptake or loss (Baxter et al., 2009), uptake of water into the root was investigated further with regard to transporters. Bulk water uptake as measured by root hydraulic conductivity relies heavily on aquaporin water transport (Tournaire-Roux et al., 2003). Accordingly, expression of the aquaporin gene *PIP2;2* was discovered to be increased slightly in *ANAC058* overexpressing plants (fig. 3.27). This gene is predominantly expressed in the endodermis and in a few outer cell layers of the central cylinder (Javot et al., 2003). This change in expression can be related to the disruption of water relations and ion homeostasis by ectopic suberin deposition or by changes in root development. In order to test whether water uptake is de- or increased in *ANAC058* overexpressing plants, hydraulic conductivity has to be measured. To separate the effect of the enhanced suberin barrier from aquaporin influence, an aquaporin blocker might be added to the measurements.

4.5.2.5 Conditional overexpression of *ANAC058* affects expression of various TFs

ANAC058 might not necessarily bind to promoters of suberin genes directly but might be a super-regulator of suberin biosynthesis or deposition. Thus, possible transcription factors active downstream of *ANAC058* were investigated. Expression of four different MYB transcription factors was analyzed and found to be elevated in all cases (fig. 3.27). *MYB41* was published as a stress-induced suberin transcription factor (Kosma et al., 2014). Its expression is only slightly increased which might be stress induced due to ectopic suberin instead of directly *ANAC058* related. *MYB41* is ABA responsive which in turn is a signal for drought stress. Provided transpiration is not or only slightly affected in induced *TPT.G* plants, the regular transpiration in combination with decreased water

uptake due to enhanced suberization might induce a drought stress response. *MYB41* does not appear to be localized upstream of *ANAC058* in a TF network since overexpression of *MYB41* did not induce *ANAC058* expression (Cominelli et al., 2008).

Expression of the transcription factors *MYB93*, *MYB9* and *MYB107* is strongly increased, stronger than the expression of the tested suberin genes even. *MYB93* has been associated with regulation of lateral root development and its promoter is active in endodermal cells overlying lateral root primordia (Gibbs et al., 2014; Gibbs and Coates, 2014). Possibly, regulation of suberin deposition and lateral root development is tightly co-regulated. Suberin has been shown to be responsible for maintaining apoplastic barriers when developing lateral roots break through the endodermis (Li et al., 2017). Expression of the *ANAC058* ortholog increases in response to *MdMYB93* overexpression (Legay et al., 2016) and the reverse is also true; *MYB93* expression increases due to *ANAC058* overexpression (fig. 3.27). A possible explanation is co-regulation or a feed-forward loop involving *MYB93* and *ANAC058*. Suberin amounts in *myb93* were not investigated (Gibbs et al., 2014) which would be of interest. *MYB9* and *MYB107* have been published as transcription factors of seed coat suberin (Gou et al., 2017; Lashbrooke et al., 2016) and might be located downstream of *ANAC058* in a transcription factor network present in roots. They also appear in the co-expression network with several suberin genes and *ANAC058* (fig. 3.1), indicating close co-regulation. No changes in root suberin were detected in *myb7*, which were possibly compensated by *MYB9* (Gou et al., 2017). As observed by Lashbrooke and coworkers, both MYBs appear to control seed coat suberin together. Additionally, a complex suberin regulation network seems to exist in roots. This leads to the conclusion that a possible suberin phenotype of suberin transcription factor knock-out mutants will always be at least partly compensated by the plant's suberin regulation network.

In order to elucidate the exact role of *ANAC058* and its binding targets, a ChIP assay or a yeast-one hybrid assay has to be conducted. Possible targets are either all suberin associated genes, only those with NAC binding sequences in the promoters (fig. 3.8), potential MYBs which act downstream of *ANAC058*, or a combination of these possibilities. Suberin appears to be regulated in a complex manner, possibly similar to the regulation of secondary cell walls (Ko et al., 2014; Zhong et al., 2008) or the cuticle (Nawrath et al., 2013). The regulatory network of those has not been completely elucidated but models include NACs, MYBs as well as positive and negative feed-forward and feedback regulation.

4.5.3 Conditional overexpression of *ANAC058* in leaves has no effect on leaf wax

Overexpression of *ANAC058* in leaves instead of roots allows observation of expression entirely due to the induction whereas in roots the basic wild type expression has to be taken into account. In *35S::ANAC058* leaves, overexpression of *ANAC058* correlated with increased expression of *GPAT5*, *RALPH*, *HORST*, *KCS17* and *ASFT* (Frenger 2014). By applying β-estradiol to leaves, *ANAC058* overexpression was induced in leaves of both TRANSPLANTA lines *TPT.D* and *TPT.G* (Shrestha, 2016) with the strongest effect in *TPT.G* (fig. 3.28). Accordingly, expression of *GPAT5* increased in this line after induction (Shrestha, 2016). Since overexpression of *GPAT5* in leaves was observed to lead to altered composition of wax in the cuticle (Li et al., 2007b), cuticular wax was investigated in

leaves of plants with induced *ANAC058* overexpression. Composition of epicuticular leaf wax is similar to published *A. thaliana* leaf wax (Kurdyukov, 2006), though in general less short chain monomers and more long chain monomers were detected in this work (fig. 3.29). Slight differences to literature might be due to different growth parameters or detection methods. No typical suberin monomers were detected in the wax of plants in which *ANAC058* overexpression was induced. Possibly, a necessary component of the suberin machinery is missing in leaves as well as in non-endodermal cells in roots. Apparently, overexpression of *ANAC058* only leads to increased suberin amounts in tissues where suberin is developmentally deposited, specifically in roots. Whether developmental seed coat suberin is affected is not known and has yet to be investigated. Supporting the observation of suberin effects which are restricted to tissues with developmental suberin is the phenotype of the *35S::ANAC058* line (Frenger, 2014). Expression of *ANAC058* and suberin genes is increased in leaves but the shoot developed normally. Overexpression of *MYB41* and subsequent deposition of suberin and lignin in leaves on the other hand resulted in a strong growth phenotype (Cominelli et al., 2008; Kosma et al., 2014). This indicates that no or nearly no suberin components are deposited in the apoplast of *35S::ANAC058* leaves. The cuticle in these leaves was not investigated but its analysis with gas chromatography would elucidate the presence of suberin and lignin. A microarray conducted for *35S::ANAC058* might clarify the differences to *35S::MYB41* plants with regard to gene expression. The results might explain why suberin is deposited in leaves due to overexpression of one TF (*MYB41*) but not the other (*ANAC058*).

The lack of suberin in leaves of *ANAC058* overexpressing plants might be due to an unknown component of the suberin export machinery which is missing in leaves. This component may be necessary for monomer and dimer transport to the extracellular space but is not regulated by *ANAC058*. Furthermore, the timespan between *ANAC058* induction and wax extraction (2 weeks) might have been too large and small effects are covered by the regular wax production. *ANAC058* expression peaks at 24 h after induction (Shrestha, 2016) and normal wax accumulation, if it was changed at all, probably resumes shortly after. Analysis of free lipids in the cells shortly after induction will allow clarification whether production of suberin monomers increases and if they accumulate inside cells. Some components should be able to reach the apoplastic space nonetheless shortly after induction, since cutin export machinery is in place. Single suberin monomers generated by overexpression of *GPAT5* as well as *HORST* and *GPAT5* together accumulate in the leaf wax of the respective overexpressing plants after all (Li et al., 2007a; Li et al., 2007b).

In general, *ANAC058* was revealed as a transcription factor of suberin, necessary but not sufficient for suberin synthesis and deposition except in the root endodermis. The function in suberin regulation is supported by the potato orthologue of *ANAC058* (fig. 8.13, supp.), *StNAC103*. This gene has also been shown to regulate suberin but serves as a negative regulator (Verdaguer et al., 2016). Since sequence similarity of *ANAC058* and *StNAC103* applies only to the DNA binding domain, target genes can be expected to be similar. The transcription regulatory domain varies distinctly and transcriptional regulation might therefore be entirely different. Promoter activity patterns in roots also differ between *StNAC103* and *ANAC058*. The putative promoter of *StNAC103* is active in the root meristem, the

promoter of *ANAC058* in the endodermis and root cap cells. This difference is possibly due to their opposed role in transcription regulation.

Furthermore, *ANAC058* appears to be crucial for plant development since apparently no knock-out with a completely non-functional ANAC058 protein exists. If the generation of a complete knock-out mutant with the CRISPR-Cas9 method is also impossible, this crucial function would be confirmed. Plant development is also disrupted by overexpression of *ANAC058* in all cells during germination (Coego et al., 2014) and expression and possibly protein levels in roots seem to be tightly regulated. *ANAC058* seem to regulate various suberin synthesis and deposition genes but whether this regulation is direct or indirect has to be elucidated still. By conducting a microarray of *anac058* or induced overexpression mutants, changes in gene expression of previously not characterized genes might be detected. These genes might be previously unkown suberin genes. Several transcription factors that are overexpressed in *ANAC058* overexpressing roots indicate indirect regulation, as they may operate downstream of *ANAC058*. Investigation of their expression in *anac058* mutants should reveal downregulation if they are indeed located downstream of *ANAC058* in a signaling cascade. As shown for secondary cell wall regulation, transcription factors might also regulate target genes directly and indirectly simultaneously (Ko et al., 2014). Suberin barrier function with regard to salt stress is impaired in *anac058* mutants. However, the effect of increased suberization on salt stress tolerance still has to be investigated employing induced overexpression of *ANAC058*.

5 Summary

Aim of this work was the investigation of *ANAC058*'s role in regulation of suberin synthesis and deposition. The transcription factor *ANAC058* was found to be a regulator of developmental root suberin in young roots, necessary and sufficient for regulation in the endodermis but apparently not in other plant tissues. Characterization of the gene revealed promoter activity, expression and mutant phenotype to be typical for a suberin-associated gene. The expression of *ANAC058* is restricted to roots under no-stress conditions and the putative promoter is specifically active in the root endodermis of young root sections. Knock-out as well as knock-down mutants showed delayed root suberization. Overexpression of *ANAC058* resulted in ectopic suberin deposition in roots but only in response to overexpression which was induced for a short period of time. In both *anac058* mutants as well as induced overexpression mutants, expression of suberin-associated genes correlated with *ANAC058* expression. Whether regulation of suberin genes is achieved by direct binding of the *ANAC058* protein to the respective promoters is not known yet. However, NAC binding sequences were found in putative promoter sequences of some suberin genes.

Involvement of *ANAC058* in Casparian strip formation on the other hand seems absent or marginal. In *anac058* mutants Casparian strips appear functional and the expression of a Casparian strip synthesis gene is unaffected. Putative *ANAC058* promoter activity also starts in greater distance from the root tip than Casparian strip formation. However, Casparian strip genes are upregulated after induction of *ANAC058* overexpression. This might be related to an indirect effect of the overexpression on root development or an unknown interaction of suberin lamella and Casparian strips.

Expression of *ANAC058* at wild type levels in roots appears to be crucial for correct plant development. The single knock-out mutant found for this gene is suspected to contain a partly functional *ANAC058* protein. Additionally, neither constitutive overexpression nor overexpression driven by a suberin gene promoter resulted in a phenotype different from the wild type. This function of *ANAC058* in plant development might be related to suberin but can also be an additional, still unknown, function of the gene. The absence of complete knock-out mutants might be due to the strongly affected suberin barrier resulting in lethal changes in ion homeostasis during early plant development. Overexpression instead might affect cell development with the ectopically deposited apoplastic barrier preventing cell elongation. Accordingly, induced overexpression seemed to affect root development slightly.

Additional to *ANAC058*'s involvement in endodermal suberization, putative *ANAC058* promoter activity indicates several other functions. The promoter is active in the root cap cells after the root reaches a specific development stage. The activity was tentatively related to a proposed root cap cuticle. The putative promoter of *ANAC058* is also active at sites of lateral root emergence. Its activity was observed in the endodermis at the root base of lateral roots as well as in surrounding endodermal cells of the main root. Since suberin appears to close the apoplastic pathway when lateral roots break through the endodermis, a respective involvement of *ANAC058* is likely. In the main root, activity of the putative *ANAC058* promoter was also observed at the root base, directly at the root-shoot junction. Promoter activity at the root base is present in the subepidermal cell layer which correlates with

localization of peridermal suberin. Peridermal suberin is present in roots sections entering secondary root growth, specifically in outer-most cell layers. This indicates a function of *ANAC058* in peridermal suberization regulation.

Regulation of developmentally deposited root suberin, despite characterization of *ANAC058* is still in need of further research. Several observations indicate that *ANAC058* is part of a transcription factor network which regulates suberin. The putative *ANAC058* promoter is active in young root sections whereas during further root development, other transcription factors seem to regulate suberin genes. Effects on suberin observed in young roots and apical root sections of *anac058* mutants were not present in whole root systems of plants grown on soil, indicating a compensatory suberin deposition. A network might relate stress signals due to insufficient suberization. Unknown transcription factors or *MYB41* might cause upregulation of suberin genes resulting in wild type suberin amounts. Transcription factors downstream of *ANAC058* might be *MYB9*, *MYB107* and *MYB93* since their expression was particularly elevated after induced overexpression of *ANAC058*. Lack of a suberin effect in *ANAC058* overexpressing plants except in case of induced overexpression might also be the result of suberin degradation.

ANAC058 also appears to have a function in the plant's response to stress. Promoter activity is induced by wounding of leaves as activity was observed at the wounding sites. Furthermore, ABA application changes the promoter activity in roots. When seedlings are grown on medium containing elevated ABA levels, the activity of the putative promoter is present in endodermal cells closer to the root tip compared to control plants. Suberin is involved in the stress response of plants and ABA is a stress signal transducer as well as involved in suberization. Both imply that *ANAC058* is also involved in regulation of stress induced suberization.

Physiological effects of the delayed suberization in *anac058* roots were observed in response to salt stress, but not in response to osmotic stress. Growth and plant health was more severely affected in the salt-stressed mutants than in the wild type. On the other hand, hydraulic conductivity of the mutant's roots was tendentially decreased. This emphasized the function of suberin as a barrier involved in ion uptake. Impact of increased suberization on water uptake and stress resistance was not investigated but is of further scientific interest.

6 Zusammenfassung

Das Ziel dieser Arbeit war die Untersuchung der Funktion des Gens *ANAC058* in Hinblick auf die Regulation von Suberin. *ANAC058* ist ein Transkriptionsfaktor, der unter Anderem involviert ist in die Regulation des entwicklungsbedingten Suberins von jungen *Arabidopsis thaliana* Wurzeln. Es wurde gezeigt, dass *ANAC058* notwendig und ausreichend für die Suberinisierung der Endodermis ist. Dies scheint nicht für andere Pflanzengewebe zu gelten. Die Charakterisierung von *ANAC058* zeigt, dass die Promoteraktivität des putativen *ANAC058*-Promoters, das Expressionsmuster und der Phänotyp der Insertions-Mutanten typisch für ein Suberin-assoziiertes Gen sind. Bei Abwesenheit von Stress wurde die Expression des Gens in Wurzeln aber nicht in Blättern beobachtet. Der putative *ANAC058*-Promoter ist spezifisch in der Endodermis von jungen Wurzelabschnitten aktiv. Darüber hinaus konnte in Mutanten, in denen das *ANAC058*-Gen transkriptionell ausgeschaltet oder runterreguliert ist eine Verzögerung der Suberinisierung beobachtet werden. Diese Verzögerung manifestiert sich in den *anac058* Mutanten in Form einer größeren Distanz von der Wurzelspitze bis zu erstem Auftreten von Suberin im Vergleich zum Wildtyp. Ebenso konnte bei den Mutanten eine verringerte Suberinmenge in apikalen Wurzelabschnitten mittels Gaschromatographie nachgewiesen werden.

Die Überexpression von *ANAC058* resultiert in verstärkter Suberinisierung von Wurzeln, aber nur bei kurzzeitig induzierter Überexpression. In diesem Fall kann Suberin in der Endodermis deutlich näher an der Wurzelspitze histologisch beobachtet werden. In beiden *anac058* Mutanten wie auch in der induzierten Überexpressionsmutante korreliert die Expression von *ANAC058* und Suberin-assoziierten Genen. Ob *ANAC058* die Suberingene direkt reguliert und ANAC058 in den Promotoren dieser Gene bindet ist nicht bekannt. Allerdings wurden NAC Bindestellen (NACBS, NAC binding sites) in putativen Promotersequenzen einiger Suberingene gefunden.

Dagegen scheint *ANAC058* nicht oder nur minimal an der Bildung des Casparischen Streifens beteiligt zu sein. In *anac058* bleibt die Expression eines Gens, das in die Synthese des Caparischen Streifens involviert ist, unverändert. Darüber hinaus ist der Casparische Streifen in *anac058* intakt. Ebenso startet die Bildung des Casparischen Streifens näher an der Wurzelspitze als die Aktivität des *ANAC058* Promoters. Nur im Fall von induzierter Überexpression von *ANAC058* korreliert die Expression von Genen, die mit dem Casparischer Streifen assoziiert sind und die *ANAC058*-Expression. Dies könnte allerdings auch auf eine indirekte Auswirkung der Überexpression von *ANAC058* auf die Wurzelentwicklung oder auf eine noch unbekannte Interaktion der Suberinlamelle und des Casparischen Streifens zurückgehen.

Für die erfolgreiche Entwicklung der Pflanze scheint die Erhaltung des Wildtyp-Expressionslevels von *ANAC058* eine essentielle Voraussetzung zu sein. Bei der einzigen *ANAC058* Insertionsmutante mit transkriptionellem Knock-out wird vermutet, dass das ANAC058 Protein zum großen Teil noch aktiv ist. Die restlichen *anac058* Mutanten zeigen statt eines Knock-outs nur eine verringerte Expression von *ANAC058*. Auch hat weder eine konstitutive Überexpression noch eine Überexpression unter der Kontrolle des Promoters eines Suberinsynthesegens einen erkennbar veränderten Phänotyp verursacht. Diese essentielle Funktion von *ANAC058* kann mit Suberin in Verbindung gebracht werden, kann aber auch eine zusätzliche, noch unbekannte Funktion des Gens sein. Falls in

Insertionsmutanten das *ANAC058* Protein vollständig abwesend wäre, könnte eine stark beeinträchtigte Suberinbarriere daraus resultieren. Dies könnte wiederum zu letalen Veränderungen in der Ionen-Homöostase während der frühen Pflanzenentwicklung führen. Überexpression und ektopische Suberinisierung dagegen könnte die Zellentwicklung beeinflussen. Falls das apoplastische Suberin die Plasmamembran von sich noch entwickelnden Zellen auf allen Seiten zu bedeckt könnte so die Zellelongation behindert werden. Dies kann auch die Erklärung für leicht veränderte Wurzelentwicklungen nach induzierter Überexpression von *ANAC058* sein.

Zusätzlich zur Funktion von *ANAC058* in endodermalen Suberinisierung deutet die Aktivität des putativen Promoters auf weitere Funktionen hin. Der Promoter ist aktiv in Wurzelhaubenzellen ab einem gewissen Entwicklungsstadium der Wurzeln. Diese Aktivität könnte mit einer potentiellen Wurzelhauben-Kutikel in Verbindung gebracht werden. Der putative Promoter ist darüber hinaus an Stellen, an denen Seitenwurzeln aus der Hauptwurzel heraustreten, aktiv. Diese Aktivität ist präsent in Enodermiszellen an der Wurzelbasis von Seitenwurzeln sowie in den umgebenden Endodermiszellen der Hauptwurzel. Suberin scheint eine Funktion im Verschließen des apoplastischen Weges an den Stellen an denen die Seitenwurzel durch die Endodermis bricht einzunehmen. Daher mag *ANAC058* für diese Funktion relevant sein. Darüber hinaus ist der putative Promoter in der Wurzelbasis der Hauptwurzel aktiv. Der Aktivität des Promoters ist in der subepidermalen Zellschicht sichtbar und korreliert daher mit der Lokalisation von peridermalen Suberin. Dieses existiert in Wurzelabschnitten mit sekundärem Dickenwachstum und schließt die Wurzel zur Umwelt hin ab. Daher lässt sich eine Funktion von *ANAC058* bei der Regulation von peridermalen Suberin vermuten.

Die Regulation des entwicklungsbedingten Suberins bedarf, trotz Charakterisierung von *ANAC058*, weiterer Untersuchungen. Verschiedene Beobachtungen weisen drauf hin, dass *ANAC058* Teil eines Transkriptionsfaktor-Netzwerks ist. Da der putative Promoter von *ANAC058* nur in apikalen Wurzelabschnitten aktiv ist, müssen andere Transkriptionsfaktoren die Regulation von Suberingenen während der späteren Entwicklung übernehmen. Auch der Effekt auf Suberin, der bei apikalen Wurzelabschnitten und in jungen Wurzeln beobachtet wurde, konnte nicht in gesamten Wurzelsystemen gefunden werden. Dies deutet auf eine Suberinisierung in, die den Effekt in Mutanten kompensiert. Ein Netzwerk könnte Stressignale aufgrund von unzureichender Suberiniserung weitergeben. Daraufhin würden noch unbekannte Transkriptionsfaktoren oder *MYB41* Suberingene hochregulieren. Die Transkriptionsfaktoren, die in dem Netzwerk *ANAC058* nachgeschaltet sind, könnten *MYB9*, *MYB107* und *MYB93* sein. Diese sind nach induzierter Überexpression von *ANAC058* in ihrer Expression besonders hochreguliert. Die Abwesenheit eines Suberineffekts in anderen *ANAC058* überexprimierenden Pflanzen, die nicht das Induktionssystem benutzen, könnte auch auf den Abbau von übermäßigen Suberin zurückzuführen sein.

Zusätzlich zur Aktivität von *ANAC058* während der Pflanzenentwicklung konnte auch eine Rolle in der Stressantwort von Pflanzen beobachtet werden. Die Promoteraktivität von *ANAC058* ist induziert durch Verwundung und ist präsent an entsprechenden Stellen. Außerdem verändert die ABA-Applikation das Aktvitätsmuster des Promoters in Wurzeln. Suberin ist Teil der Antwort von Pflanzen auf unterschiedlichen Stress; ABA ist sowohl ein Botenstoff der Stressantwort als auch involviert in

Suberinisierung. Beides impliziert, dass *ANAC058* auch in die Regulation von Stress-induzierter Suberinisierung involviert ist.

Der physiologische Effekt der verzögerten Suberinisierung in Wurzeln von *anac058* wurde bei Salzstress beobachtet, aber nicht bei osmotischem Stress. Die Mutanten, die dem Salzstress ausgesetzt waren, zeigten eine starke Beeinträchtigung des Wachstums und der Vitalität, während der Wildtyp weniger stark betroffen war. Hydraulische Konduktivität in Wurzeln von *anac058* ist dagegen tendentiell verringert. Diese Ergebnisse verdeutlichen die Funktion von Suberin als eine Barriere für Ionenaufnahme. Wasserfluss und Schutz vor osmotischen Stress dagegen hängen zumindest unter angewandten Bedingungen scheinbar nicht mit der Suberinmenge in den Wurzeln zusammen. Der Einfluss von verstärkter Suberinisierung durch Überexpression von *ANAC058* auf Wasseraufnahme und Stressresistenz wurde nicht untersucht, ist aber weiterhin von wissentschaftlichem Interesse.

7 Lists and References

Bibliography

Aida, Mitsuhiro, Ishida, Tetsuya, Fukaki, Hidehiro, Fujisawa, Hisao, Tasaka, M., 1997. Genes involved in organ separation in Arabidopsis: an analysis of the *cup-shaped cotyledon* mutant. Plant Cell 9, 841–857.

Alonso, J.M., Stepanova, A.N., Leisse, T.J., Kim, C.J., Chen, H., Shinn, P., Stevenson, D.K., Zimmerman, J., Barajas, P., Cheuk, R., Gadrinab, C., Heller, C., Jeske, A., Koesema, E., Meyers, C.C., Parker, H., Prednis, L., Ansari, Y., Choy, N., Deen, H., Geralt, M., Hazari, N., Hom, E., Karnes, M., Mulholland, C., Ndubaku, R., Schmidt, I., Guzman, P., Aguilar-Henonin, L., Schmid, M., Weigel, D., Carter, D.E., Marchand, T., Risseeuw, E., Brogden, D., Zeko, A., Crosby, W.L., Berry, C.C., Ecker, J.R., 2003. Genome-wide insertional mutagenesis of *Arabidopsis thaliana*. Science 301, 653–657.

Andersen, T.G., Barberon, M., Geldner, N., 2015. Suberization-the second life of an endodermal cell. Curr. Opin. Plant Biol. 28, 9–15.

Aoki, Y., Okamura, Y., Tadaka, S., Kinoshita, K., Obayashi, T., 2016. ATTED-II in 2016: A plant coexpression database towards lineage-specific coexpression. Plant Cell Physiol. 57, e5.

Arvidsson, S., Kwasniewski, M., Riaño-Pachón, D.M., Mueller-Roeber, B., 2008. QuantPrime - A flexible tool for reliable high-throughput primer design for quantitative PCR. BMC Bioinformatics 9, doi:10.1186/1471-2105-9-465.

Bailey, T.L., Boden, M., Buske, F.A., Frith, M., Grant, C.E., Clementi, L., Ren, J., Li, W.W., Noble, W.S., 2009. MEME Suite: Tools for motif discovery and searching. Nucleic Acids Res. 37, doi: 10.1093/nar/gkp335.

Bailey, T.L., Elkan, C., 1994. Fitting a mixture model by expectation maximization to discover motifs in biopolymers. Proc. Second Int. Conf. Intell. Syst. Mol. Biol. 28–36.

Barberon, M., 2017. The endodermis as a checkpoint for nutrients. New Phytol. 213, 1604–1610.

Barberon, M., Vermeer, J.E.M., De Bellis, D., Wang, P., Naseer, S., Andersen, T.G., Humbel, B.M., Nawrath, C., Takano, J., Salt, D.E., Geldner, N., 2016. Adaptation of Root Function by Nutrient-Induced Plasticity of Endodermal Differentiation. Cell 164, 447–459.

Barrios-Masias, F.H., Knipfer, T., McElrone, A.J., 2015. Differential responses of grapevine rootstocks to water stress are associated with adjustments in fine root hydraulic physiology and suberization. J. Exp. Bot. 66, 6069–6078.

Bartel, D.P., 2004. MicroRNAs: Genomics, Biogenesis, Mechanism, and Function. Cell 116, 281–297.

Baxter, I., Hosmani, P.S., Rus, A., Lahner, B., Borevitz, J.O., Muthukumar, B., Mickelbart, M. V., Schreiber, L., Franke, R.B., Salt, D.E., 2009. Root suberin forms an extracellular barrier that affects water relations and mineral nutrition in Arabidopsis. PLoS Genet. 5, e1000492.

Beisson, F., Li, Y., Bonaventure, G., Pollard, M., Ohlrogge, J.B., 2007. The Acyltransferase GPAT5 Is Required for the Synthesis of Suberin in Seed Coat and Root of *Arabidopsis*. Plant Cell Online 19, 351–368.

Berhin, A., De Bellis, D., Humbel, B.M., Nawrath, C., 2017. Characterization of the root cap cuticle of *Arabidopsis thaliana*. Conf. Plant Apoplastic Diffus. Barriers 2017, Pereira, C. S., Graça, J., Miguel C. M.

Berman, H.M., Westbrook, J., Feng, Z., Gilliland, G., Bhat, T.N., Weissig, H., Shindyalov, I.N., Bourne, P.E., 2000. The protein data bank. Nucleic Acids Res. 28, 235–242.

Bernards, M.A., 2002. Demystifying suberin. Can. J. Bot. 80, 227–240.

Bernards, M.A., Lopez, M.L., Zajicek, J., Lewis, N.G., 1995. Hydroxycinnamic acid-derived polymers constitute the polyaromatic domain of suberin. J. Biol. Chem. 270, 7382–7386.

Bird, D., Beisson, F., Brigham, A., Shin, J., Greer, S., Jetter, R., Kunst, L., Wu, X., Yephremov, A., Samuels, L., 2007. Characterization of Arabidopsis ABCG11/WBC11, an ATP binding cassette (ABC) transporter that is required for cuticular lipid secretion. Plant J. 52, 485–498.

Boerjan, W., Ralph, J., Baucher, M., 2003. Lignin Biosynthesis. Annu. Rev. Plant Biol. 54, 519–546.

Boher, P., Serra, O., Soler, M., Molinas, M., Figueras, M., 2013. The potato suberin feruloyl transferase FHT which accumulates in the phellogen is induced by wounding and regulated by abscisic and salicylic acids. J. Exp. Bot. 64, 3225–3236.

Boursiac, Y., Chen, S., Luu, D.-T., Sorieul, M., Van Den Dries, N., Maurel, C., Dries, N. Van Den, Maurel, C., 2005. Early effects of salinity on water transport in Arabidopsis roots . Molecular and cellular features of Aquaporin expression. Plant Physiol. 139, 790–805.

Brands, M., 2014. Functional genomics of At1g68850 provides evidence for the involvement of peroxidases in suberin deposition in the root endodermis and the seed coat. Master Thesis, Univ. Bonn.

Breeze, E., Harrison, E., McHattie, S., Hughes, L., Hickman, R., Hill, C., Kiddle, S., Kim, Y. -s., Penfold, C.A., Jenkins, D., Zhang, C., Morris, K., Jenner, C., Jackson, S., Thomas, B., Tabrett, A., Legaie, R., Moore, J.D., Wild, D.L., Ott, S., Rand, D., Beynon, J., Denby, K., Mead, A., Buchanan-Wollaston, V., 2011. High-Resolution Temporal Profiling of Transcripts during Arabidopsis Leaf Senescence Reveals a Distinct Chronology of Processes and Regulation. Plant Cell 23, 873–894.

Brundrett, M.C., Kendrick, B., Peterson, C.A., 1991. Efficient lipid staining in plant material with Sudan Red 7B or Fluoral Yellow 088 in polyethylene glycol-glycerol. Biotech. Histochem. 66, 111–116.

Bryson, K., McGuffin, L.J., Marsden, R.L., Ward, J.J., Sodhi, J.S., Jones, D.T., 2005. Protein structure prediction servers at University College London. Nucleic Acids Res. 33, 36–38.

Buchan, D.W.A., Minneci, F., Nugent, T.C.O., Bryson, K., Jones, D.T., 2013. Scalable web services for the PSIPRED Protein Analysis Workbench. Nucleic Acids Res. 41, 349–357.

Caspary, R., 1865. Bemerkungen über die Schutzscheide und die Bildung des Stammes und der Wurzel. Jahrbücher für wissenschaftliche Bot. 4.

Chaumont, F., Moshelion, M., Daniels, M.J., 2005. Regulation of plant aquaporin activity. Biol. Cell 97, 749–764.

Chen, Q., Wang, Q., Xiong, L., Lou, Z., 2011. A structural view of the conserved domain of rice stress-responsive NAC1. Protein Cell 2, 55–63.

Clough, S.J., Bent, A.F., 1998. Floral dip: a simplified method for *Agrobacterium*-mediated transformation of Arabidopsis thaliana. Plant J. 16, 735–743.

Coego, A., Brizuela, E., Castillejo, P., Ruíz, S., Koncz, C., del Pozo, J.C., Piñeiro, M., Jarillo, J.A., León, J., TRANSPLANTA-Consortium, 2014. The TRANSPLANTA collection of Arabidopsis lines: A resource for functional analysis of transcription factors based on their conditional overexpression. Plant J. 77, 944–953.

Cominelli, E., Sala, T., Calvi, D., Gusmaroli, G., Tonelli, C., 2008. Over-expression of the Arabidopsis *AtMYB41* gene alters cell expansion and leaf surface permeability. Plant J. 53, 53–64.

Compagnon, V., Diehl, P., Benveniste, I., Meyer, D., Schaller, H., Schreiber, L., Franke, R., Pinot, F., 2009. CYP86B1 Is Required for Very Long Chain ω-Hydroxyacid and α,ω-Dicarboxylic Acid Synthesis in Root and Seed Suberin Polyester. Plant Physiol. 150, 1831–1843.

Cramer, G.R., 2002. Response of abscisic acid mutants of Arabidopsis to salinity. Funct. Plant Biol. 29, 561–567.

Curtis, M.D., Grossniklaus, U., 2003. A Gateway cloning vector set for high-throughput functional analysis of genes in planta. Breakthr. Technol. 133, 462–469.

DeBono, A., Yeats, T.H., Rose, J.K.C., Bird, D., Jetter, R., Kunst, L., Samuels, L., 2009. *Arabidopsis* LTPG is a Glycosylphosphatidylinositol-Anchored Lipid Transfer Protein required for export of lipids to the plant surface. Plant Cell 21, 1230–1238.

Demidchik, V., Davenport, R.J., Tester, M., 2002. Nonselective cation channels in plants. Annu. Rev. Plant Biol. 53, 67–107.

Disfani, F.M., Hsu, W.L., Mizianty, M.J., Oldfield, C.J., Xue, B., Keith Dunker, A., Uversky, V.N., Kurgan, L., 2012. MoRFpred, a computational tool for sequence-based prediction and characterization of short disorder-to-order transitioning binding regions in proteins. Bioinformatics 28, 75–83.

Doblas, V.G., Smakowska-Luzan, E., Fujita, S., Alassimone, J., Barberon, M., Madalinski, M., Belkhadir, Y., Geldner, N., 2017. Root diffusion barrier control by a vasculature-derived peptide binding to the SGN3 receptor. Science 355, 280–284.

Dolan, L., Janmaat, K., Willemsen, V., Linstead, P., Poethig, S., Roberts, K., Scheres, B., 1993. Cellular organisation of the Arabidopsis thaliana root. Development 119, 71–84.

Domergue, F., Vishwanath, S.J., Joubes, J., Ono, J., Lee, J.A., Bourdon, M., Alhattab, R., Lowe, C., Pascal, S., Lessire, R., Rowland, O., 2010. Three Arabidopsis Fatty Acyl-Coenzyme A Reductases, FAR1, FAR4, and FAR5, Generate Primary Fatty Alcohols Associated with Suberin Deposition. Plant Physiol. 153, 1539–1554.

Dyson, H.J., Wright, P.E., 2005. Intrinsically unstructured proteins and their functions. Nat. Rev. Mol. Cell Biol. 6, 197–208.

Edgar, R.C., 2004. MUSCLE: Multiple sequence alignment with high accuracy and high throughput. Nucleic Acids Res. 32, 1792–1797.

Ernst, H.A., Nina Olsen, A., Skriver, K., Larsen, S., Lo Leggio, L., 2004. Structure of the conserved domain of ANAC, a member of the NAC family of transcription factors. EMBO Rep. 5, 297–303.

Fendrych, M., Van Hautegem, T., Van Durme, M., Olvera-Carrillo, Y., Huysmans, M., Karimi, M., Lippens, S., Guérin, C.J., Krebs, M., Schumacher, K., Nowack, M.K., 2014. Programmed cell death controlled by ANAC033/SOMBRERO determines root cap organ size in *Arabidopsis*. Curr. Biol. 24, 931–940.

Franke, R., Briesen, I., Wojciechowski, T., Faust, A., Yephremov, A., Nawrath, C., Schreiber, L., 2005. Apoplastic polyesters in *Arabidopsis* surface tissues - A typical suberin and a particular cutin. Phytochemistry 66, 2643–2658.

Franke, R., Höfer, R., Briesen, I., Emsermann, M., Efremova, N., Yephremov, A., Schreiber, L., 2009. The *DAISY* gene from *Arabidopsis* encodes a fatty acid elongase condensing enzyme involved in the biosynthesis of aliphatic suberin in roots and the chalaza-micropyle region of seeds. Plant J. 57, 80–95.

Fraser, C.M., Chapple, C., 2011. The phenylpropanoid pathway in Arabidopsis. Arab. B. 9, e0152.

Frenger, M.S., 2014. Untersuchungen zur Regulation und Biosynthese apoplastischer Polyester in höheren Pflanzen. PhD Thesis, Univ. Bonn.

Fuda, N.J., Ardehali, M.B., Lis, J.T., 2009. Defining mechanisms that regulate RNA polymerase II transcription in vivo. Nature 461, 186–192.

Gibbs, D.J., Coates, J.C., 2014. *AtMYB93* is an endodermis-specific transcriptional regulator of lateral root development in Arabidopsis. Plant Signal. Behav. 9, e29808.

Gibbs, D.J., Voß, U., Harding, S. a, Fannon, J., Moody, L. a, Yamada, E., Swarup, K., Nibau, C., Bassel, G.W., Choudhary, A., Lavenus, J., Bradshaw, S.J., Stekel, D.J., Bennett, M.J., Coates, J.C., 2014. *At*MYB93 is a novel negative regulator of lateral root development in Arabidopsis. New Phytol. 203, 1194–1207.

Gou, M., Hou, G., Yang, H., Zhang, X., Cai, Y., Kai, G., Liu, C.-J., 2017. The MYB107 transcription factor positively regulates suberin biosynthesis. Plant Physiol. 173, 1045–1058.

Graça, J., Santos, S., 2006. Glycerol-derived ester oligomers from cork suberin. Chem. Phys. Lipids 144, 96–107.

Graça, J., Santos, S., 2007. Suberin: A biopolyester of plants' skin. Macromol. Biosci. 7, 128–135.

Grant, C.E., Bailey, T.L., Noble, W.S., 2011. FIMO: Scanning for occurrences of a given motif. Bioinformatics 27, 1017–1018.

Greve, K., Cour, T. LA, Jensen, M.K., Poulsen, F.M., Skriver, K., 2003. Interactions between plant RING-H2 and plant-specific NAC (*NAM/ATAF1/2/CUC2*) proteins: RING-H2 molecular specificity and cellular localization. Biochem. J. 371, 97–108.

Griffiths-Jones, S., 2004. The microRNA Registry. Nucleic Acids Res. 32, 109–111.

Heredia, A., 2003. Biophysical and biochemical characteristics of cutin, a plant barrier biopolymer. Biochim. Biophys. Acta 1620, 1–7.

Höfer, R., Briesen, I., Beck, M., Pinot, F., Schreiber, L., Franke, R., 2008. The *Arabidopsis* cytochrome P450 *CYP86A1* encodes a fatty acid ω-hydroxylase involved in suberin monomer biosynthesis. J. Exp. Bot. 59, 2347–2360.

Hoffmann-Benning, S., Kende, H., 1994. Cuticle Biosynthesis in Rapidly Growing Internodes of Deepwater Rice. Plant Physiol. 104, 719–723.

Hosmani, P.S., Kamiya, T., Danku, J., Naseer, S., Geldner, N., Guerinot, M.L., Salt, D.E., 2013. Dirigent domain-containing protein is part of the machinery required for formation of the lignin-based Casparian strip in the root. Proc. Natl. Acad. Sci. 110, 14498–14503.

Jakobson, L., Lindgren, L.O., Verdier, G., Laanemets, K., Brosché, M., Beisson, F., Kollist, H., 2016. BODYGUARD is required for the biosynthesis of cutin in Arabidopsis. New Phytol. 211, 614–626.

Javot, H., Lauvergeat, V., Santoni, V., Martin-laurent, F., Güçlü, J., Vinh, J., Heyes, J., Franck, K.I., Schäffner, A.R., Bouchez, D., Maurel, C., 2003. Role of a single aquaporin isoform in root water uptake. Plant Cell 15, 509–522.

Jeffree, C.E., 2006. The fine structure of the plant cuticle. In: Biology of the Plant Cuticle, Riederer, M. and Müller, C., Eds (Oxford: Blackwell Publishing), pp. 11–125.

Jensen, M.K., Kjaersgaard, T., Nielsen, M.M., Galberg, P., Petersen, K., O'Shea, C., Skriver, K., 2010. The *Arabidopsis thaliana* NAC transcription factor family: structure–function relationships and determinants of ANAC019 stress signalling. Biochem. J. 426, 183–196.

Jetter, R., Schäffer, S., Riederer, M., 2000. Leaf cuticular waxes are arranged in chemically and mechanically distinct layers: Evidence from *Prunus laurocerasus* L. Plant, Cell Environ. 23, 619–628.

Jha, D., Shirley, N., Tester, M., Roy, S.J., 2010. Variation in salinity tolerance and shoot sodium accumulation in *Arabidopsis* ecotypes linked to differences in the natural expression levels of transporters involved in sodium transport. Plant, Cell Environ. 33, 793–804.

Jones, D.T., 1999. Protein secondary structure prediction based on position-specific scoring matrices. J. Mol. Biol. 292, 195–202.

Joubès, J., Raffaele, S., Bourdenx, B., Garcia, C., Laroche-Traineau, J., Moreau, P., Domergue, F., Lessire, R., 2008. The VLCFA elongase gene family in *Arabidopsis thaliana*: phylogenetic analysis, 3D modelling and expression profiling. Plant Mol. Biol. 67, 547–566.

Kamiya, T., Borghi, M., Wang, P., Danku, J.M.C., Kalmbach, L., Hosmani, P.S., Naseer, S., Fujiwara, T., Geldner, N., Salt, D.E., 2015. The MYB36 transcription factor orchestrates Casparian strip formation. Proc. Natl. Acad. Sci. 112, 10533–10538.

Karimi, M., Inze, D., Depicker, A., 2002. GATEWAY vectors for *Agrobacterium*-mediated plant transformation. Trends Plant Sci. 7, 193–195.

Kjaersgaard, T., Jensen, M.K., Christiansen, M.W., Gregersen, P., Kragelund, B.B., Skriver, K., 2011. Senescence-associated barley NAC (NAM, ATAF1,2, CUC) transcription factor interacts with radical-induced cell death 1 through a disordered regulatory domain. J. Biol. Chem. 286, 35418–35429.

Ko, J.H., Jeon, H.W., Kim, W.C., Kim, J.Y., Han, K.H., 2014. The MYB46/MYB83-mediated transcriptional regulatory programme is a gatekeeper of secondary wall biosynthesis. Ann. Bot. 114, 1099–1107.

Ko, J.H., Yang, S.H., Park, A.H., Lerouxel, O., Han, K.H., 2007. ANAC012, a member of the plant-specific NAC transcription factor family, negatively regulates xylary fiber development in *Arabidopsis thaliana*. Plant J. 50, 1035–1048.

Koressaar, T., Remm, M., 2007. Enhancements and modifications of primer design program Primer3. Bioinformatics 23, 1289–1291.

Kosma, D.K., Molina, I., Ohlrogge, J.B., Pollard, M., 2012. Identification of an Arabidopsis fatty alcohol:caffeoyl-Coenzyme A acyltransferase required for the synthesis of alkyl hydroxycinnamates in root waxes. Plant Physiol. 160, 237–48.

Kosma, D.K., Murmu, J., Razeq, F.M., Santos, P., Bourgault, R., Molina, I., Rowland, O., 2014. AtMYB41 activates ectopic suberin synthesis and assembly in multiple plant species and cell types. Plant J. 80, 216–229.

Krishnamurthy, P., Ranathunge, K., Franke, R., Prakash, H.S., Schreiber, L., Mathew, M.K., 2009. The role of root apoplastic transport barriers in salt tolerance of rice (*Oryza sativa* L.). Planta 230, 119–134.

Krishnamurthy, P., Ranathunge, K., Nayak, S., Schreiber, L., Mathew, M.K., 2011. Root apoplastic barriers block Na^+ transport to shoots in rice (*Oryza sativa* L.). J. Exp. Bot. 62, 4215–4228.

Kurdyukov, S., 2006. The Epidermis-Specific Extracellular BODYGUARD Controls Cuticle Development and Morphogenesis in *Arabidopsis*. Plant Cell 18, 321–339.

Lahaye, P.A., Epstein, E., 1969. Salt toleration by plants: enhancement with calcium. Science 166, 395–396.

Lashbrooke, J., Cohen, H., Levy-Samocha, D., Tzfadia, O., Panizel, I., Zeisler, V., Massalha, H., Stern, A., Trainotti, L., Schreiber, L., Costa, F., Aharoni, A., 2016. MYB107 and MYB9 homologs regulate suberin deposition in angiosperms, The Plant Cell 28, 2097-2116.

Lee, S.B., Go, Y.S., Bae, H.-J., Park, J.H., Cho, S.H., Cho, H.J., Lee, D.S., Park, O.K., Hwang, I., Suh, M.C., 2009. Disruption of glycosylphosphatidylinositol-anchored lipid transfer protein gene altered cuticular lipid composition, increased plastoglobules, and enhanced susceptibility to infection by the fungal pathogen *Alternaria brassicicola*. Plant Physiol. 150, 42–54.

Lee, S.B., Jung, S.J., Go, Y.S., Kim, H.U., Kim, J.K., Cho, H.J., Park, O.K., Suh, M.C., 2009. Two Arabidopsis 3-ketoacyl CoA synthase genes, *KCS20* and *KCS2/DAISY*, are functionally redundant in cuticular wax and root suberin biosynthesis, but differentially controlled by osmotic stress. Plant J. 60, 462–475.

Lee, Y., Rubio, M.C., Alassimone, J., Geldner, N., 2013. A mechanism for localized lignin deposition in the endodermis. Cell 153, 402–412.

Legay, S., Guerriero, G., André, C., Guignard, C., Cocco, E., Charton, S., Boutry, M., Rowland, O., Hausman, J.F., 2016. MdMyb93 is a regulator of suberin deposition in russeted apple fruit skins. New Phytol. 212, 977–991.

Legay, S., Guerriero, G., Deleruelle, A., Lateur, M., Evers, D., André, C.M., Hausman, J.F., 2015. Apple russeting as seen through the RNA-seq lens: strong alterations in the exocarp cell wall. Plant Mol. Biol. 88, 21–40.

Lemon, B., Tjian, R., 2000. Orchestrated response: A symphony of transcription factors for gene control. Genes Dev. 14, 2551–2569.

Lenz, H., Dombinov, V., Dreistein, J., Reinhard, M.R., Gebert, M., Knoop, V., 2013. Magnesium deficiency phenotypes upon multiple knockout of *Arabidopsis thaliana* MRS2 clade B genes can be ameliorated by concomitantly reduced calcium supply. Plant Cell Physiol. 54, 1118–1131.

Li-Beisson, Y., Shorrosh, B., Beisson, F., Andersson, M.X., Arondel, V., Bates, P.D., Baud, S., Bird, D., DeBono, A., Durrett, T.P., Franke, R.B., Graham, I.A., Katayama, K., Kelly, A.A., Larson, T., Markham, J.E., Miquel, M., Molina, I., Nishida, I., Rowland, O., Samuels, L., Schmid, K.M., Wada, H., Welti, R., Xu, C., Zallot, R., Ohlrogge, J., 2013. Acyl-Lipid Metabolism. Arab. B. 11, e0161.

Li, B., Kamiya, T., Kalmbach, L., Yamagami, M., Yamaguchi, K., Shigenobu, S., Sawa, S., Danku, J.M.C., Salt, D.E., Geldner, N., Fujiwara, T., 2017. Role of *LOTR1* in Nutrient Transport through Organization of Spatial Distribution of Root Endodermal Barriers. Curr. Biol. 27, 758–765.

Li, Y., Beisson, F., Koo, A.J.K., Molina, I., Pollard, M., Ohlrogge, J., 2007. Identification of acyltransferases required for cutin biosynthesis and production of cutin with suberin-like monomers. Proc. Natl. Acad. Sci. 104, 18339–18344.

Li, Y., Beisson, F., Ohlrogge, J., Pollard, M., 2007. Monoacylglycerols Are Components of Root Waxes and Can Be Produced in the Aerial Cuticle by Ectopic Expression of a Suberin-Associated Acyltransferase. Plant Physiol. 144, 1267–1277.

Lulai, E., Corsini, D., Crop, N., 1998. Differential deposition of suberin phenolic and aliphatic domains and their roles in resistance to infection during potato tuber (*Solanum tuberosum* L .) wound-healing. Physiol. Mol. Plant Pathol. 53, 209–222.

Lulai, E.C., Freeman, T.P., 2001. The importance of phellogen cells and their structural characteristics in susceptibility and resistance to excoriation in immature and mature potato tuber (*Solanum tuberosum* L.) periderm. Ann. Bot. 88, 555–561.

Ma, F., Peterson, C. a., 2000. Plasmodesmata in onion (Allium cepa L.) roots: a study enabled by improved fixation and embedding techniques. Protoplasma 211, 103–115.

Martin, R.E., Crist, J.B., 1970. Elements of bark structure and terminology. Wood Fiber Sci. 2, 269–279.

Martínez-Ballesta, M.C., Aparicio, F., Pallás, V., Martínez, V., Carvajal, M., 2003. Influence of saline stress on root hydraulic conductance and PIP expression in Arabidopsis. J. Plant Physiol. 160, 689–697.

McLean, B.G., Hempel, F.D., Zambryski, P.C., 1997. Plant intercellular communication via plasmodesmata. Plant Cell 9, 1043–1054.

McLeay, R.C., Bailey, T.L., 2010. Motif Enrichment Analysis : a unified framework and an evaluation on ChIP data. BMC Bioinformatics 11, doi: 10.1186/1471-2105-11-165.

Meyre, D., Leonardi, A., Brisson, G., Vartanian, N., 2001. Drought-adaptive mechanisms involved in the escape / tolerance strategies of *Arabidopsis* Landsberg *erecta* and Columbia ecotypes and their F1 reciprocal progeny. J. Plant Physiol. 158, 1145–1152.

Miguel, A., Milhinhos, A., Novák, O., Jones, B., Miguel, C.M., 2016. The *SHORT-ROOT*-like gene *PtSHR2B* is involved in *Populus* phellogen activity. J. Exp. Bot. 67, 1545–1555.

Mittler, R., Blumwald, E., 2010. Genetic Engineering for Modern Agriculture: Challenges and Perspectives. Annu. Rev. Plant Biol. 61, 443–462.

Molina, I., Li-Beisson, Y., Beisson, F., Ohlrogge, J.B., Pollard, M., 2009. Identification of an Arabidopsis Feruloyl-Coenzyme A Transferase Required for Suberin Synthesis. Plant Physiol. 151, 1317–1328.

Munns, R., Tester, M., 2008. Mechanisms of Salinity Tolerance. Annu. Rev. Plant Biol. 59, 651–681.

Murashige, T., Skoog, F., 1962. A Revised Medium for Rapid Growth and Bio Assays with Tobacco Tissue Cultures. Physiol. Plant. 15, 473–497.

Mustroph, A., Zanetti, M.E., Jang, C.J.H., Holtan, H.E., Repetti, P.P., Galbraith, D.W., Girke, T., Bailey-Serres, J., 2009. Profiling translatomes of discrete cell populations resolves altered cellular priorities during hypoxia in Arabidopsis. Proc. Natl. Acad. Sci. 106, 18843–18848.

Nagahashi, G., Thomson W.W., Leonard, R.T., 1974. The Casparian Strip as a Barrier to the Movement of Lanthanum in Corn Roots. Science 183, 670–671.

Nakashima, K., Tran, L.S.P., Van Nguyen, D., Fujita, M., Maruyama, K., Todaka, D., Ito, Y., Hayashi, N., Shinozaki, K., Yamaguchi-Shinozaki, K., 2007. Functional analysis of a NAC-type transcription factor OsNAC6 involved in abiotic and biotic stress-responsive gene expression in rice. Plant J. 51, 617–630.

Nakayama, T., Shinohara, H., Tanaka, M., Baba, K., Ogawa-Ohnishi, M., Matsubayashi, Y., 2017. A peptide hormone required for Casparian strip diffusion barrier formation in Arabidopsis roots. Science 355, 284–286.

Naseer, S., Lee, Y., Lapierre, C., Franke, R., Nawrath, C., Geldner, N., 2012. Casparian strip diffusion barrier in *Arabidopsis* is made of a lignin polymer without suberin. Proc. Natl. Acad. Sci. 109, 10101–10106.

Nawrath, C., Schreiber, L., Franke, R.B., Geldner, N., Reina-Pinto, J.J., Kunst, L., 2013. Apoplastic diffusion barriers in Arabidopsis. Arab. B. 11, e0167.

Ng, S., Ivanova, A., Duncan, O., Law, S.R., Van Aken, O., De Clercq, I., Wang, Y., Carrie, C., Xu, L., Kmiec, B., Walker, H., Van Breusegem, F., Whelan, J., Giraud, E., 2013. A membrane-bound NAC transcription factor, ANAC017, mediates mitochondrial retrograde signaling in *Arabidopsis*. Plant Cell 25, 3450–3471.

Nicholas, K.B., Nicholas, H.B.J., 1997. GeneDoc: a tool for editing and annotating multiple sequence alignments. Distrib. by author. http//www.psc.edu/biomed/genedoc.

Nieminen, K., Blomster, T., Helariutta, Y., Mahonen, A.P., 2015. Vascular Cambium Development. Arab. B. 13, e0177.

North, G.B., Nobel, P.S., 1995. Hydraulic conductivity of concentric root tissues of *Agave deserti* Engelm. under wet and drying conditions. New Phytol. 130, 47–57.

North, G.B., Nobel, P.S., 1998. Water uptake and structural plasticity along roots of a desert succulent during prolonged drought. Plant, Cell Environ. 21, 705–713.

Nosbüsch, D., 2009. Untersuchung des β-Ketoacyl-CoA Synthase-Gens At4g34510 in *Arabidopsis t*haliana. diploma thesis, Univ. Bonn.

O'Malley, R.C., Huang, S.C., Song, L., Lewsey, M.G., Bartlett, A., Nery, J.R., Galli, M., Gallavotti, A., Ecker, J.R., 2016. Cistrome and epicistrome features shape the regulatory DNA landscape. Cell 165, 1280–1292.

O'Shea, C., Kryger, M., Stender, E.G.P., Kragelund, B.B., Willemoës, M., Skriver, K., 2015. Protein intrinsic disorder in *Arabidopsis* NAC transcription factors: transcriptional activation by ANAC013 and ANAC046 and their interactions with RCD1. Biochem. J. 465, 281–294.

Olsen, A.N., Ernst, H.A., Leggio, L. Lo, Skriver, K., 2005. NAC transcription factors: structurally distinct, functionally diverse. Trends Plant Sci. 10, 79–87.

Olsen, A.N., Ernst, H.A., Leggio, L. Lo, Skriver, K., 2005. DNA-binding specificity and molecular functions of NAC transcription factors. Plant Sci. 169, 785–797.

Ooka, H., Ooka, H., Satoh, K., Satoh, K., Doi, K., Doi, K., Nagata, T., Nagata, T., Otomo, Y., Otomo, Y., Murakami, K., Murakami, K., Matsubara, K., Matsubara, K., Osato, N., Osato, N., Kawai, J., Kawai, J., Carninci, P., Carninci, P., Hayashizaki, Y., Hayashizaki, Y., Suzuki, K., Suzuki, K., Kojima, K., Kojima, K., Takahara, Y., Takahara, Y., Yamamoto, K., Yamamoto, K., Kikuchi, S., Kikuchi, S., 2003. Comprehensive analysis of NAC family genes in *Oryza sativa* and *Arabidopsis thaliana*. DNA Res. 10, 239–247.

Ossowski, S., Schwab, R., Weigel, D., 2008. Gene silencing in plants using artificial microRNAs and other small RNAs. Plant J. 53, 674–690.

Panikashvili, D., Shi, J.X., Bocobza, S., Franke, R.B., Schreiber, L., Aharoni, A., 2010. The *Arabidopsis* DSO/ABCG11 transporter affects cutin metabolism in reproductive organs and suberin in roots. Mol. Plant 3, 563–575.

Pereira, H., 1988. Chemical composition and variability of cork from *Quercus suber* L. Wood Sci. Technol. 22, 211–218.

Persson, D.P., Chen, A., Aarts, M.G.M., Salt, D.E., Schjoerring, J.K., Husted, S., 2016. Multi-element bioimaging of *Arabidopsis thaliana* roots. Plant Physiol. 172, 835–847.

Peterson, C.A., Cholewa, E., 1998. Structural modifications of the apoplast and their potential impact on ion uptake. Zeitschrift Für Pflanzenernährung Und Bodenkd. 161, 521–531.

Peterson, C. a, Enstone, D.E., 1996. Functions of passage cells in the endodermis and exodermis of roots. Physiol. Plant. 97, 592–598.

Pfister, A., Barberon, M., Alassimone, J., Kalmbach, L., Lee, Y., Vermeer, J.E.M., Yamazaki, M., Li, G., Maurel, C., Takano, J., Kamiya, T., Salt, D.E., Roppolo, D., Geldner, N., 2014. A receptor-like kinase mutant with absent endodermal diffusion barrier displays selective nutrient homeostasis defects. elife 3, e03115.

Piovesan, D., Tabaro, F., Mičetić, I., Necci, M., Quaglia, F., Oldfield, C.J., Aspromonte, M.C., Davey, N.E., Davidović, R., Dosztányi, Z., Elofsson, A., Gasparini, A., Hatos, A., Kajava, A. V., Kalmar, L., Leonardi, E., Lazar, T., Macedo-Ribeiro, S., Macossay-Castillo, M., Meszaros, A., Minervini, G., Murvai, N., Pujols, J., Roche, D.B., Salladini, E., Schad, E., Schramm, A., Szabo, B., Tantos, A., Tonello, F., Tsirigos, K.D., Veljković, N., Ventura, S., Vranken, W., Warholm, P., Uversky, V.N., Dunker, A.K., Longhi, S., Tompa, P., Tosatto, S.C.E., 2017. DisProt 7.0: A major update of the database of disordered proteins. Nucleic Acids Res. 45, 219–227.

Puranik, S., Sahu, P.P., Srivastava, P.S., Prasad, M., 2012. NAC proteins: regulation and role in stress tolerance. Trends Plant Sci. 17, 369–381.

Rains, M.K., Gardiyehewa de Silva, N.D., Molina, I., 2017. Reconstructing the suberin pathway in poplar by chemical and transcriptomic analysis of bark tissues. Tree Physiol. 1–22.

Ranathunge, K., Lin, J., Steudle, E., Schreiber, L., 2011. Stagnant deoxygenated growth enhances root suberization and lignifications, but differentially affects water and NaCl permeabilities in rice (*Oryza sativa* L.) roots. Plant, Cell Environ. 34, 1223–1240.

Ranathunge, K., Schreiber, L., 2011. Water and solute permeabilities of *Arabidopsis* roots in relation to the amount and composition of aliphatic suberin. J. Exp. Bot. 62, 1961–1974.

Ranathunge, K., Thomas, R.H., Fang, X., Peterson, C.A., Gijzen, M., Bernards, M.A., 2008. Soybean root suberin and partial resistance to root rot caused by *Phytophthora sojae*. Phytopathology 98, 1179–1189.

R Development Core Team, R.C.T., 2008. R: A language and environment for statistical computing. R Found. Stat. Comput. Vienna, Austria. ISBN 3-900051-07-0, URL http//www.R-project.org.

Renault, H., Alber, A., Horst, N.A., Basilio Lopes, A., Fich, E.A., Kriegshauser, L., Wiedemann, G., Ullmann, P., Herrgott, L., Erhardt, M., Pineau, E., Ehlting, J., Schmitt, M., Rose, J.K.C., Reski, R., Werck-Reichhart, D., 2017. A phenol-enriched cuticle is ancestral to lignin evolution in land plants. Nat. Commun. 8, 14713.

Riechmann, J.L., Heard, J., Martin, G., Reuber, L., -Z., C., Jiang, Keddie, J., Adam, L., Pineda, O., Ratcliffe, O.J., Samaha, R.R., Creelman, R., Pilgrim, M., Broun, P., Zhang, J.Z., Ghandehari, D., Sherman, B.K., -L. Yu, G., 2000. *Arabidopsis* transcription factors: genome-wide comparative analysis among eukaryotes. Science 290, 2105–2110.

Ronquist, F., Huelsenbeck, J.P., 2003. MrBayes 3: Bayesian phylogenetic inference under mixed models. Bioinformatics 19, 1572–1574.

Roppolo, D., Boeckmann, B., Pfister, A., Boutet, E., Rubio, M.C., Denervaud-Tendon, V., Vermeer, J.E.M., Gheyselinck, J., Xenarios, I., Geldner, N., 2014. Functional and Evolutionary Analysis of the CASPARIAN STRIP MEMBRANE DOMAIN PROTEIN Family. Plant Physiol. 165, 1709–1722.

Roppolo, D., De Rybel, B., Tendon, V.D., Pfister, A., Alassimone, J., Vermeer, J.E.M., Yamazaki, M., Stierhof, Y.D., Beeckman, T., Geldner, N., 2011. A novel protein family mediates Casparian strip formation in the endodermis. Nature 473, 381–384.

Roy, S.J., Negrão, S., Tester, M., 2014. Salt resistant crop plants. Curr. Opin. Biotechnol. 26, 115–124.

RStudio Team, 2015. RStudio: Integrated Development for R. RStudio, Inc., Boston, MA URL http//www.rstudio.com/.

Sabba, R.P., Lulai, E.C., 2002. Histological analysis of the maturation of native and wound periderm in potato (*Solanum tuberosum* L.) tuber. Ann. Bot. 90, 1–10.

Samuels, L., Kunst, L., Jetter, R., 2008. Sealing Plant Surfaces: Cuticular Wax Formation by Epidermal Cells. Annu. Rev. Plant Biol. 59, 683–707.

Schmid, M., Davison, T.S., Henz, S.R., Pape, U.J., Demar, M., Vingron, M., Schölkopf, B., Weigel, D., Lohmann, J.U., 2005. A gene expression map of *Arabidopsis thaliana* development. Nat. Genet. 37, 501–506.

Schreiber, L., Franke, R., Hartmann, K.D., Ranathunge, K., Steudle, E., 2005. The chemical composition of suberin in apoplastic barriers affects radial hydraulic conductivity differently in the roots of rice (*Oryza sativa* L. cv. IR64) and corn (*Zea mays* L. cv. Helix). J. Exp. Bot. 56, 1427–1436.

Schreiber, L., Hartmann, K., Skrabs, M., Zeier, J., 1999. Apoplastic barriers in roots: chemical composition of endodermal and hypodermal cell walls. J. Exp. Bot. 50, 1267–1280.

Shahzad, Z., Canut, M., Tournaire-Roux, C., Martinière, A., Boursiac, Y., Loudet, O., Maurel, C., 2016. A Potassium-Dependent Oxygen Sensing Pathway Regulates Plant Root Hydraulics. Cell 167, 87–98.

Shao, H., Wang, H., Tang, X., 2015. NAC transcription factors in plant multiple abiotic stress responses: progress and prospects. Front. Plant Sci. 6, 1–8.

Shen, H., Yin, Y., Chen, F., Xu, Y., Dixon, R.A., 2009. A bioinformatic analysis of NAC genes for plant cell wall development in relation to lignocellulosic bioenergy production. Bioenergy Res. 2, 217–232.

Shiono, K., Ogawa, S., Yamazaki, S., Isoda, H., Fujimura, T., Nakazono, M., Colmer, T.D., 2011. Contrasting dynamics of radial O2-loss barrier induction and aerenchyma formation in rice roots of two lengths. Ann. Bot. 107, 89–99.

Shrestha, S., 2016. Chemische und molekulare Charakterisierung trangener Arabidopsis thaliana Pflanzen, die den Transkriptionsfaktor ANAC058 überexprimieren. Hausarbeit, Univ. Siegen.

Sieber, P., Schorderet, M., Ryser, U., Buchala, A., Kolattukudy, P., Métraux, J.-P., Nawrath, C., 2000. Transgenic Arabidopsis Plants Expressing a Fungal Cutinase Show Alterations in the Structure and Properties of the Cuticle and Postgenital Organ Fusions. Plant Cell 12, 721–737.

Soler, M., Serra, O., Molinas, M., García-Berthou, E., Caritat, A., Figueras, M., 2008. Seasonal variation in transcript abundance in cork tissue analyzed by real time RT-PCR. Tree Physiol. 28, 743–751.

Soler, M., Serra, O., Molinas, M., Huguet, G., Fluch, S., Figueras, M., 2007. A Genomic Approach to Suberin Biosynthesis and Cork Differentiation. Plant Physiol. 144, 419–431.

Souer, E., Van Houwelingen, A., Kloos, D., Mol, J., Koes, R., 1996. The *No Apical Meristem* gene of Petunia is required for pattern formation in embryos and flowers and is expressed at meristem and primordia boundaries. Cell 85, 159–170.

Steudle, E., 2000. Water uptake by plant roots: an integration of views. Plant Soil 226, 45–56.

Stöver, B.C., Müller, K.F., 2010. TreeGraph 2: Combining and visualizing evidence from different phylogenetic analyses. BMC Bioinformatics 11, doi:10.1186/1471-2105-11-7.

Sundaresan, V., Springer, P., Volpe, T., Haward, S., Jones, J.D.G., Dean, C., Ma, H., Martienssen, R., 1995. Patterns of gene action in plant development revealed by enhancer trap and gene trap transposable elements. Genes Dev. 9, 1797–1810.

Szczuka, E., Szczuka, A., 2003. Cuticle fluorescence during embryogenesis of *Arabidopsis thaliana* (L.) Heynh. Acta Biol. Cracoviensia Ser. Bot. 45, 63–67.

Torii, K.U., 1996. The Arabidopsis *ERECTA* Gene Encodes a Putative Receptor Protein Kinase with Extracellular Leucine-Rich Repeats. Plant Cell 8, 735–746.

Torres, M.A., Dangl, J.L., Jones, J.D.G., 2002. Arabidopsis gp91^{phox} homologues *AtrbohD* and *AtrbohF* are required for accumulation of reactive oxygen intermediates in the plant defense response. Proc. Natl. Acad. Sci. 99, 517–522.

Tournaire-Roux, C., Sutka, M., Javot, H., Gout, E., Gerbeau, P., Luu, D.T., Bligny, R., Maurel, C., 2003. Cytosolic pH regulates root water transport during anoxic stress through gating of aquaporins. Nature 425, 393–397.

Tran, L.P., Nakashima, K., Sakuma, Y., Simpson, S.D., Fujita, Y., Maruyama, K., Fujita, M., Seki, M., Shinozaki, K., Yamaguchi-shinozaki, K., 2004. Isolation and Functional Analysis of Arabidopsis Stress-Inducible NAC Transcription Factors That Bind to a Drought-Responsive cis -Element in the *early responsive to dehydration stress 1* Promoter. Plant Cell 16, 2481–2498.

Tsuwamoto, R., Fukuoka, H., Takahata, Y., 2008. *GASSHO1* and *GASSHO2* encoding a putative leucine-rich repeat transmembrane-type receptor kinase are essential for the normal development of the epidermal surface in Arabidopsis embryos. Plant J. 54, 30–42.

Untergasser, A., Cutcutache, I., Koressaar, T., Ye, J., Faircloth, B.C., Remm, M., Rozen, S.G., 2012. Primer3-new capabilities and interfaces. Nucleic Acids Res. 40, e115.

Vacic, V., Oldfield, C.J., Mohan, A., Radivojac, P., Cortese, M.S., Uversky, V.N., Dunker, a K., 2007. Characterization of Molecular Recognition Features , MoRFs , and their binding partners. J. Proteome Res. 6, 2351–2366.

Verdaguer, R., Soler, M., Serra, O., Garrote, A., Fernández, S., Company-Arumí, D., Anticó, E., Molinas, M., Figueras, M., 2016. Silencing of the potato *StNAC103* gene enhances the accumulation of suberin polyester and associated wax in tuber skin. J. Exp. Bot. 67, 5415–5427.

Vishwanath, S.J., Delude, C., Domergue, F., Rowland, O., 2015. Suberin: biosynthesis, regulation, and polymer assembly of a protective extracellular barrier. Plant Cell Rep. 34, 573–586.

Volkov, V., Wang, B., Dominy, P.J., Fricke, W., Amtmann, A., 2004. *Thellungiella halophila*, a salt-tolerant relative of *Arabidopsis thaliana*, possesses effective mechanisms to discriminate between potassium and sodium. Plant, Cell Environ. 27, 1–14.

Xiao, F., Goodwin, S.M., Xiao, Y., Sun, Z., Baker, D., Tang, X., Jenks, M.A., Zhou, J.M., 2004. *Arabidopsis CYP86A2* represses *Pseudomonas syringae* type III genes and is required for cuticle development. EMBO J. 23, 2903–2913.

Xie, Q., Frugis, G., Colgan, D., Chua, N.H., 2000. *Arabidopsis* NAC1 transduces auxin signal downstream of TIR1 to promote lateral root development. Genes Dev. 14, 3024–3036.

Xie, Q., Guo, H.S., Dallman, G., Fang, S., Weissman, A.M., Chua, N.H., 2002. SINAT5 promotes ubiquitin-related degradation of NAC1 to attenuate auxin signals. Nature 419, 167–170.

Yadav, V., Molina, I., Ranathunge, K., Castillo, I.Q., Rothstein, S.J., Reed, J.W., 2014. ABCG Transporters Are Required for Suberin and Pollen Wall Extracellular Barriers in Arabidopsis. Plant Cell 26, 3569–3588.

Yamaguchi, M., Sharp, R.E., 2010. Complexity and coordination of root growth at low water potentials: Recent advances from transcriptomic and proteomic analyses. Plant, Cell Environ. 33, 590–603.

Yang, R., Jarvis, D.E., Chen, H., Beilstein, M.A., Grimwood, J., Jenkins, J., Shu, S., Prochnik, S., Xin, M., Ma, C., Schmutz, J., Wing, R.A., Mitchell-Olds, T., Schumaker, K.S., Wang, X., 2013. The reference genome of the halophytic plant *Eutrema salsugineum*. Front. Plant Sci. 4, 1–14.

Yang, W., Simpson, J.P., Li-Beisson, Y., Beisson, F., Pollard, M., Ohlrogge, J.B., 2012. A Land-Plant-Specific Glycerol-3-Phosphate Acyltransferase Family in Arabidopsis: Substrate Specificity, *sn*-2 Preference, and Evolution. Plant Physiol. 160, 638–652.

Yeats, T.H., Huang, W., Chatterjee, S., Viart, H.M.F., Clausen, M.H., Stark, R.E., Rose, J.K.C., 2014. Tomato Cutin Deficient 1 (CD1) and putative orthologs comprise an ancient family of cutin synthase-like (CUS) proteins that are conserved among land plants. Plant J. 77, 667–675.

Yeats, T.H., Martin, L.B.B., Viart, H.M.-F., Isaacson, T., He, Y., Zhao, L., Matas, A.J., Buda, G.J., Domozych, D.S., Clausen, M.H., Rose, J.K.C., 2012. The identification of cutin synthase: formation of the plant polyester cutin. Nat. Chem. Biol. 8, 609–611.

Zeier, J., Schreiber, L., 1997. Chemical composition of hypodermal and endodermal cell walls and xylem vessels isolated from *Clivia miniata*: identification of the biopolymers lignin and suberin. Plant Physiol. 113, 1223–1231.

Zeier, J., Schreiber, L., 1999. Fourier transform infrared-spectroscopic characterisation of isolated endodermal cell walls from plant roots: Chemical nature in relation to anatomical development. Planta 209, 537–542.

Zhang, J., Jia, W., Yang, J., Ismail, A.M., 2006. Role of ABA in integrating plant responses to drought and salt stresses. F. Crop. Res. 97, 111–119.

Zhong, R., Lee, C., Ye, Z.H., 2010. Global analysis of direct targets of secondary wall NAC master switches in *Arabidopsis*. Mol. Plant 3, 1087–1103.

Zhong, R., Lee, C., Zhou, J., McCarthy, R.L., Ye, Z.-H., 2008. A Battery of Transcription Factors Involved in the Regulation of Secondary Cell Wall Biosynthesis in *Arabidopsis*. Plant Cell Online 20, 2763–2782.

Zhu, J.-K., Liu, J., Xiong, L., 1998. Genetic Analysis of Salt Tolerance in Arabidopsis: Evidence for a Critical Role of Potassium Nutrition. Plant Cell 10, 1181–1191.

Zimmermann, H.M., Steudle, E., 1998. Apoplastic transport across young maize roots: effect of the exodermis. Planta 206, 7–19.

Zolla, G., Heimer, Y.M., Barak, S., 2010. Mild salinity stimulates a stress-induced morphogenic response in *Arabidopsis thaliana* roots. J. Exp. Bot. 61, 211–224.

List of Figures

List of Tables

8 Supplemental

8.1 Solutions and media

Plant growth		
Seed sterilization solution	2.0 mL	NaHClO (12 %)
	12.5 mL	ethanol (100 %)
	10.5 mL	H_2O_{deion}
1/2 - 1 MS agar (Murashige and Skoog, 1962)	0.5 - 1 % (v/v)	Murashige & Skoog medium without vitamins (Duchefa Biochemie B.V, Haarlem, Netherlands)
	0.65 - 0.8 % (v/v)	agar
		H_2O_{deion}
		autoclave
Hydroponics nutrient solution	0.05 %	FloraGro (3-1-6) (General hydroponics, Santa Rosa, CA, USA)
	0.05 %	FloraBloom (0-4-5) (General hydroponics, Santa Rosa, CA, USA)
	0.05 %	FloraMicro (Softwater 5-0-1) (General hydroponics, Santa Rosa, CA, USA)
		H_2O_{deion}
Hydroponics nutrient solution for root hydraulic conductivity measurements (Lp_r)	1.25 mM	KNO_3
	0.75 mM	$MgSO_4$
	1.5 mM	$Ca(NO_3)_2$
	0.5 mM	KH_2PO_4
	50 mM	FeEDTA
	100 mM	Na_2SiO_3
	50 mM	H_3BO_3
	12 mM	$MnSO_4$
	0.7 mM	$CuSO_4$
	1 mM	$ZnSO_4$
	0.24 mM	MoO_4Na_2
		H_2O_{deion}
Soil irrigation solution	approx. 0.9 g/L	EUFLOR Flory3 NPK-Dünger mit Magnesium und Spurennährstoff 15 + 10 + 15 (+2)
	approx 0.2 g/L	Confidor (Bayer, Leverkusen, Germany)

Media for microbial cultures

LB medium	20 g/L	LB medium (Carl Roth) autoclave
LB agar	35 g/L	LB agar (Carl Roth) autoclave
Inoculation media	5 % (w/v) 0.05 % (v/v)	Sucrose Silwet L-77

Solutions for molecular biology

Agarose gel	1 g 100 mL approx 0.05 %	agarose TAE buffer Ethidium Bromide
TAE buffer	4.84 g/L 1.142 mL/L 1 mM	Tris base acetic acid EDTA pH 8 H_2O_{deion}
TE buffer	10 mM 1 mM	Tris-HCl pH 7.5 EDTA H_2O_{deion} sterile filter

Solutions for staining and histological sample preparation

GUS assay staining solution	0.1 M 0.1 M 0.01 M 0.003 M 1 mM 0.1 %	NaH_2PO_4 Na_2HPO_4 EDTA $K_3[Fe(CN)_6]$ H_2O_{deion} pH 7 X-Gluc (Biochemical DIRECT, UK) Triton X-100
Fixation solution	137 mM 2.4 mM 10 mM 2 mM 0.037 % (v/v)	NaCl KCl Na_2HPO_4 KH_2PO_4 formaldehyde H_2O_{deion}
Fluorol Yellow 088 dye	0.01 % (w/v)	Fluorol Yellow 088 lactic acid
Anniline Blue dye	0.5 % (w/v)	Anniline Blue H_2O_{deion}

Solutions for gas chromatography sample preparation		
Enzyme solution for cell wall digestion	0.5 % (w/v)	cellulase
	0.5 % (w/v)	pectinase
	10 mM	citric acid
	1 mM	NaN_3
		H_2O_{deion}
		pH 3
Borax buffer	0.01 M	borate
		H_2O_{deion}
		pH 9
Lipid extraction solution	50 %	chloroform
	50 %	methanol
Derivatization solution	20 µL	BSTFA
	20 µL	pyridine
	up to 200 µL	sample dissolved in chloroform

8.2 Primers used in this work

8.2.1 Primer generation

Primers were generated with Primer3 (Koressaar and Remm, 2007; Untergasser et al., 2012) for all applications except quantitative RT-PCR for which QuantPrime (Arvidsson et al., 2008) was employed. Primers not generated for this thesis were supplied by the Ecophysiology laboratory (University of Bonn, Germany).

8.2.2 Calculation of primer melting temperature

$$T_m = 69.3 + 41\left(\frac{\sum G + \sum C}{\sum bases}\right) - \left(\frac{650}{\sum bases}\right) \quad (3)$$

T_m: melting temperature [°C], ∑*G*: sum of guanine bases of respective primer, ∑*C*: sum of cytosine bases of respective primer, ∑*bases*: sum of bases of respective primer

8.2.3 List of used primers

Target	no.	Sequence (5' - 3')	Primer description	T_m
At3g18780 (*ACTIN2*)	LS218	GGCTCCTCTTAACCCAAAGG	Forward primer for expression study with RT-PCR. Use with LS219. Amplicon size 393 bp (RNA/cDNA) and 471 bp (DNA)	59.35
At3g18780 (*ACTIN2*)	LS219	TTCTCGATGGAAGAGCTGGT	Reverse primer for expression study with RT-PCR. Use with LS218. Amplicon size 393 bp (RNA/cDNA) and 471 bp (DNA)	57.30
At3g18400 (*ANAC058*)	LS997	CGGGCAACAGAAGCTGGTTA	Forward primer for expression study with RT-PCR. Use with LS1085. Amplicon size 643 bp (RNA/cDNA) and 911 bp (DNA)	59.35
At3g11430 (*GPAT5*)	LS1221	TCGGTCGTGTCAGAGTTTGA	Forward primer for expression study with RT-PCR. Use with LS1222. Amplicon size 594 bp (RNA/cDNA) and 853 bp (DNA)	57.30
At3g11430 (*GPAT5*)	LS1222	GTGGTTGTAGTTCTCCGGGA	Reverse primer for expression study with RT-PCR. Use with LS1221. Amplicon size 594 bp (RNA/cDNA) and 853 bp (DNA)	59.35
At5g23190 (*CYP86B1/ RALPH*)	LS331	TCCATCAGGAAATACGTCGTC	Forward primer for expression study with RT-PCR. Use with LS332. Amplicon size 528 bp (RNA/cDNA) and 1030 bp (DNA)	57.87
At5g23190 (*CYP86B1/ RALPH*)	LS332	CCTACTTGCGTGTGGAAGTTC	Reverse primer for expression study with RT-PCR. Use with LS331. Amplicon size 528 bp (RNA/cDNA) and 1030 bp (DNA)	59.82
At3g18400 (*ANAC058*)	LS567	GAGGAATGGGTAGTGTGTAG	Forward primer for genotyping of ET11247 (Enhancer Trap, anac058-1) line. Use with LS568 and LS569. Product size: 889 bp (WT) and 471 bp (ET11247)	57.30
At3g18400 (*ANAC058*)	LS568	CCCGTCGAAGTAATAATTTTCTTA	Reverse primer for genotyping of ET11247 (Enhancer Trap, anac058-1) line. Use with LS567 and LS569. Product size: 889 bp (WT) and 471 bp (ET11247)	55.88
pWS31 vector transposon	LS569	AAATCGGTTATACGATAACGGTC	Reverse primer for genotyping of ET11247 (Enhancer Trap, anac058-1) line. Use with LS567 and LS568. Product size: 889 bp (WT) and 471 bp (ET11247)	57.08
At3g18400 (*ANAC058*)	LS1190	GGCAAATCCCAAGGTTCACA	Forward primer for genotyping of SALK-84913 (T-DNA insertion, anac058-2) line. Use with LS1191 and LS1192. Product size: 1069 bp (WT) and 814 bp (ET11247)	57.30
At3g18400 (*ANAC058*)	LS1191	CGCAACGCAATCTGATCTCA	Reverse primer for genotyping of SALK-84913 (T-DNA insertion, anac058-2) line. Use with LS1190 and LS1192. Product size: 1069 bp (WT) and 814 bp (ET11247)	57.30
pBIN-pROK2 T-DNA	LS1192	ATTAAGTTGTCTAAGCGTCAA	Reverse primer for genotyping of SALK-84913 (T-DNA insertion, anac058-2) line. Use with LS1190 and LS1191. Product size: 1069 bp (WT) and 814 bp (ET11247)	52.01
At3g18400 (*ANAC058*)	LS1296	ggggacaagtttgtacaaaaaagcaggctta GAGTTAGGGGACCTTTCTCTTCA	Forward primer (with attB1 GATEWAY attachment site) for amplification of At3g18400 promotor and first exon sequence. Use with LS1297. Amplicon size 2781 bp.	75.49
At3g18400 (*ANAC058*)	LS1297	ggggaccactttgtacaagaaagctgggta GGCAAATCCCAAGGTTCACA	Forward primer (with attB1 GATEWAY attachment site) for amplification of At3g18400 promotor and first exon sequence. Use with LS1296. Amplicon size 2781 bp.	76.80
lacZ gene	M13_For	GTAAAACGACGGCCAGT	Forward primer for genotyping of organisms containing a pMDC vector. Use with M13_Rev. Product size depending on vector insert.	52.77
lacZ gene	M13_Rev	CAGGAAACAGCTATGAC	Reverse primer for genotyping of organims containing a pMDC vector. Use with M13_For, LS1216 or LS1229. Product size depending on vector insert.	50.36
35S promotor	LS1216	CCAACCACGTCTTCAAAGCA	Forward primer for genotyping organisms containing a construct with 35S promoter. Use with M13_rev. Amplicon size depends on construct.	57.30
At5g23190 (*CYP86B1/ RALPH*), putative promoter	LS1229	TCTCCTGATAGCCAAAGTTT	Forward primer for genotyping organisms containing a construct with $Prom_{RALPH}$. Use with M13_rev. Amplicon size depends on construct.	53.20
GFP gene	LS1086	CAAGGGCGAGGAGCTGTT	Forward primer for genotyping of organisms containing a construct with the GFP gene. Use with LS1087. Product size 708 bp.	58.24
GFP gene	LS1087	TTGTACAGCTCGTCCATGC	Reverse primer for genotyping of organisms containing a construct with the GFP gene. Use with LS1086. Product size 708 bp.	56.67
GUS gene	LS313	TTGGGGTTTCTACAGGACGTAAC	Forward primer for genotyping of organisms containing a construct with the GFP and GUS genes. Use with LS1086. Product size 740 bp.	60.65

GUS gene	LS1086	CAAGGGCGAGGAGCTGTT	Reverse primer for genotyping of organisms containing a construct with the GFP and GUS genes. Use with LS313. Product size 740 bp.	58.24
Hygromycin resistance gene (*Hph*)	Hygromy-cin for	TGCGCCCAAGCTGCATCATC	Forward primer for genotyping of organisms containing a construct with theHygromycin resistance gene gene. Use with Hygromycin rev. Product size 843 bp.	61.40
Hygromycin resistance gene (*Hph*)	Hygromy-cin rev	GTCTGTCGAGAAGTTTCTGATCG	Reverse primer for genotyping of organisms containing a construct with the Hygromycin resistance gene. Use withHygro for. Product size 843 bp.	60.65
At1g13440 (*GAPDH*)	LS602	TTGGTGACAACAG GTCAAGCA	Forward primer for expression study with qRT-PCR. Use with LS603. Amplicon size 62 bp (RNA/cDNA)	57.87
At1g13440 (*GAPDH*)	LS603	AAACTTGTCGCTCAATGCAATC	Forward primer for expression study with qRT-PCR. Use with LS602. Amplicon size 62 bp (RNA/cDNA)	56.53
At5g23190 (*RALPH/ CYP86B1*)	LS604	TCCCGTGGATCACAAAGAGGTTC	Forward primer for expression study with qRT-PCR. Use with LS605. Amplicon size 112 bp (RNA/cDNA)	62.43
At5g23190 (*RALPH/ CYP86B1*)	LS605	AGCTTCCATACGACCCATTGCG	Forward primer for expression study with qRT-PCR. Use with LS604. Amplicon size 112 bp (RNA/cDNA)	62.12
At5g58860 (*HORST/ CYP86A1*)	LS606	GTTTACCTCAAGGCTGCTTTGGC	Forward primer for expression study with qRT-PCR. Use with LS607. Amplicon size 64 bp (RNA/cDNA)	62.43
At5g58860 (*HORST/ CYP86A1*)	LS607	TGAAAT CCTGAGGCACAGAAGGG	Forward primer for expression study with qRT-PCR. Use with LS606. Amplicon size 64 bp (RNA/cDNA)	62.43
At5g41040 (*ASFT*)	LS610	ACGATGTCGTAGACGCCAAGAAC	Forward primer for expression study with qRT-PCR. Use with LS611. Amplicon size 60 bp (RNA/cDNA)	62.43
At5g41040 (*ASFT*)	LS611	TAGTC ACCTGAGCGGTAACAGG	Forward primer for expression study with qRT-PCR. Use with LS610. Amplicon size 60 bp (RNA/cDNA)	62.12
At2g24430 (*ANAC038*)	LS624	GTCGGGATGAAGAAGACTTTGGTC	Forward primer for expression study with qRT-PCR. Use with LS625. Amplicon size 134 bp (RNA/cDNA)	62.72
At2g24430 (*ANAC038*)	LS625	ACTACCCACTCGTCTTGCT TGG	Forward primer for expression study with qRT-PCR. Use with LS624. Amplicon size 134 bp (RNA/cDNA)	62.12
At5g16770 (*MYB9*)	LS626	TGGACCAACTACTTGAGACCTGAC	Forward primer for expression study with qRT-PCR. Use with LS627. Amplicon size 111 bp (RNA/cDNA)	62.72
At5g16770 (*MYB9*)	LS627	GGCTATCGACGACCAC TTGTTTCC	Forward primer for expression study with qRT-PCR. Use with LS626. Amplicon size 111 bp (RNA/cDNA)	64.43
At3g11430 (*GPAT5*)	LS638	ACGGATAGGATTGTTCCGGTTGC	Forward primer for expression study with qRT-PCR. Use with LS639. Amplicon size 60 bp (RNA/cDNA)	62.43
At3g11430 (*GPAT5*)	LS639	TGTAGTCGCGTGGAAGAATCCG	Forward primer for expression study with qRT-PCR. Use with LS638. Amplicon size 60 bp (RNA/cDNA)	62.12
At1g34670 (*MYB93*)	LS670	GCTCG CAGATTTGAATAGGTGTGG	Forward primer for expression study with qRT-PCR. Use with LS671. Amplicon size 135 bp (RNA/cDNA)	62.72
At1g34670 (*MYB93*)	LS671	TTCCCGAGAATGGAGTGGAGATGG	Forward primer for expression study with qRT-PCR. Use with LS670. Amplicon size 135 bp (RNA/cDNA)	64.43
At3g02940 (*MYB107*)	LS672	TAAACCGGTGTGGGAAGAGTTGC	Forward primer for expression study with qRT-PCR. Use with LS673. Amplicon size 148 bp (RNA/cDNA)	62.43
At3g02940 (*MYB107*)	LS673	TGACCAGCTATAGACGACCACTTG	Forward primer for expression study with qRT-PCR. Use with LS672. Amplicon size 148 bp (RNA/cDNA)	62.72
At5g13580 (*ABCG6*)	LS684	AAGAACGTCTTGGATGCTTCGC	Forward primer for expression study with qRT-PCR. Use with LS685. Amplicon size 61 bp (RNA/cDNA)	60.25
At5g13580 (*ABCG6*)	LS685	GCATCTGCGCAAGTGTAGAACG	Forward primer for expression study with qRT-PCR. Use with LS684. Amplicon size 61 bp (RNA/cDNA)	62.12
At1g01610 (*GPAT4*)	LS1060	TGAAAGAGTTCGGCGATGACTCAC	Forward primer for expression study with qRT-PCR. Use with LS1061. Amplicon size 99 bp (RNA/cDNA)	62.72
At1g01610 (*GPAT4*)	LS1061	CATGCACCATGTAACCTTCCTTGC	Forward primer for expression study with qRT-PCR. Use with LS1060. Amplicon size 99 bp (RNA/cDNA)	62.72
At3g18400 (*ANAC058*)	LS1084	CTTATAGTTTCCCAAAAGAGATGATCC	Forward primer for expression study with qRT-PCR. Use with LS1085. Amplicon size 80 bp (RNA/cDNA)	60.41
At3g18400 (*ANAC058*)	LS1085	CATTTTGGATCATATTGGAGACTCCTT	Forward primer for expression study with qRT-PCR. Use with LS1084. Amplicon size 80 bp (RNA/cDNA)	60.41
AT1G64060 (*RBOHF*)	LS1352	TCGGTTCGACTGCTTAAGGTTGC	Forward primer for expression study with qRT-PCR. Use with LS1353. Amplicon size 127 bp (RNA/cDNA)	62.43

AT1G64060 (*RBOHF*)	LS1353	ATGGCGAAACCGCAGGACATTG	Forward primer for expression study with qRT-PCR. Use with LS1352. Amplicon size 127 bp (RNA/cDNA)	62.12
At2g28670 (*ESB1*)	LS1354	ATGTCCCTTTCCTCGTTGGA	Forward primer for expression study with qRT-PCR. Use with LS1355. Amplicon size 101 bp (RNA/cDNA)	57.30
At2g28670 (*ESB1*)	LS1355	GCCACTAGCAACAGGGAAACC	Forward primer for expression study with qRT-PCR. Use with LS1354. Amplicon size 101 bp (RNA/cDNA)	61.78
At5g42180 (*PER64*)	LS1356	ACCCAACACTAAACCCCTCATTC	Forward primer for expression study with qRT-PCR. Use with LS1357. Amplicon size 90 bp (RNA/cDNA)	60.65
At5g42180 (*PER64*)	LS1357	CATCCATGTTCGATCCAGCAT	Forward primer for expression study with qRT-PCR. Use with LS1356. Amplicon size 90 bp (RNA/cDNA)	57.87
At4G28110 (*MYB41*)	LS1396	AAGACCGGACATCAAGAGAGGAAG	Forward primer for expression study with qRT-PCR. Use with LS1397. Amplicon size 100 bp (RNA/cDNA)	62.72
At4G28110 (*MYB41*)	LS1397	AGCGGCTATTGCTGACCACTTG	Forward primer for expression study with qRT-PCR. Use with LS1396. Amplicon size 100 bp (RNA/cDNA)	62.12
At4G34230 (*CAD5*)	LS1400	TCACTCCTCTGCTTATGCTTGGG	Forward primer for expression study with qRT-PCR. Use with LS1401. Amplicon size 78 bp (RNA/cDNA)	62.43
At4G34230 (*CAD5*)	LS1401	GCATCTCCTCTGTCTCCTTCATGC	Forward primer for expression study with qRT-PCR. Use with LS1400. Amplicon size 78 bp (RNA/cDNA)	64.43
At4G00360 (*ATT1/ CYP86A2*)	LS1402	CGCTCTTGAATTCACCACCAGGAC	Forward primer for expression study with qRT-PCR. Use with LS1403. Amplicon size 101 bp (RNA/cDNA)	64.43
At4G00360 (*ATT1/ CYP86A2*)	LS1403	TCTGAGCCGTTTCGAGAATTGGAC	Forward primer for expression study with qRT-PCR. Use with LS1402. Amplicon size 101 bp (RNA/cDNA)	62.72
At2G37170 (*PIP2;2*)	LS1473	TCTCTAGCAGACGGCTACAACAC	Forward primer for expression study with qRT-PCR. Use with LS1474. Amplicon size 122 bp (RNA/cDNA)	62.43
At2G37170 (*PIP2;2*)	LS1474	ACGTGGGAGTCTCTAGCGTTAC	Forward primer for expression study with qRT-PCR. Use with LS1473. Amplicon size 122 bp (RNA/cDNA)	62.12

8.3 *In silico* co-expression analysis

Table 8.1 Annotated genes co-expressed with *GPAT5*, *FAR4* and *RALPH/CYP86B1*

Co-expressed genes were inferred with the NetworkDrawer tool of the ATTED-II database ver. 8.0 (http://atted.jp, (Aoki et al., 2016)), last accessed 04. 01. 2016. Genes involved in suberin synthesis and deposition are shown with a red background next to their respective publication. Genes used as guide genes for the co-expression analysis (three genes on top) are bolded; remaining genes are sorted according to their protein function. Co-expression network is shown in fig. 3.1.

AGI locus	function	publication
At3g11430	**glycerol-3-phosphate acyltransferase 5**	Beisson et al. (2007)
At3g44540	**fatty acid reductase 4**	Domergue et al. (2010)
At5g23190	**cytochrome P450, family 86, subfamily B, polypeptide 1**	Compagnon et al. (2009)
At3g44550	fatty acid reductase 5	Domergue et al. (2010)
At3g53510	ABC-2 type transporter family protein	Yadav et al. (2014)
At2g37360	ABC-2 type transporter family protein	Yadav et al. (2014)
At5g13580	ABC-2 type transporter family protein	Yadav et al. (2014)
At1g53270	ABC-2 type transporter family protein	
At5g19410	ABC-2 type transporter family protein	
At5g16770	myb domain protein 9	Lashbrooke et al. 2016
At3g02940	myb domain protein 107	Lashbrooke et al. 2016
At4g34510	3-ketoacyl-CoA synthase 17	
At5g08250	Cytochrome P450 superfamily protein	
At5g44550	CASPL1B1	
At4g33610	glycine-rich protein	
At1g55990	glycine-rich protein	
At5g13900	Bifunctional inhibitor/lipid-transfer protein/seed storage 2S albumin superfamily protein	
At2g48140	Bifunctional inhibitor/lipid-transfer protein/seed storage 2S albumin superfamily protein	
At1g05450	Bifunctional inhibitor/lipid-transfer protein/seed storage 2S albumin superfamily protein	
At4g36610	alpha/beta-Hydrolases superfamily protein	
At3g50400	GDSL-like Lipase/Acylhydrolase superfamily protein	
At1g74460	GDSL-like Lipase/Acylhydrolase superfamily protein	
At2g23540	GDSL-like Lipase/Acylhydrolase superfamily protein	
At5g09520	hydroxyproline-rich glycoprotein family protein	
At5g09530	hydroxyproline-rich glycoprotein family protein	
At4g38080	hydroxyproline-rich glycoprotein family protein	
At5g09480	hydroxyproline-rich glycoprotein family protein	
At5g10230	annexin 7	
At4g16640	Matrixin family protein	
At5g14130	Peroxidase superfamily protein	
At1g68850	Peroxidase superfamily protein	
At2g35380	Peroxidase superfamily protein	
At2g43390	unknown protein	
At1g56320	unknown protein	
At2g16760	Calcium-dependent phosphotriesterase superfamily protein	
At5g37690	SGNH hydrolase-type esterase superfamily protein	
At3g18400	NAC domain containing protein 58	

8.4 *In silico* organ and tissue-specific expression

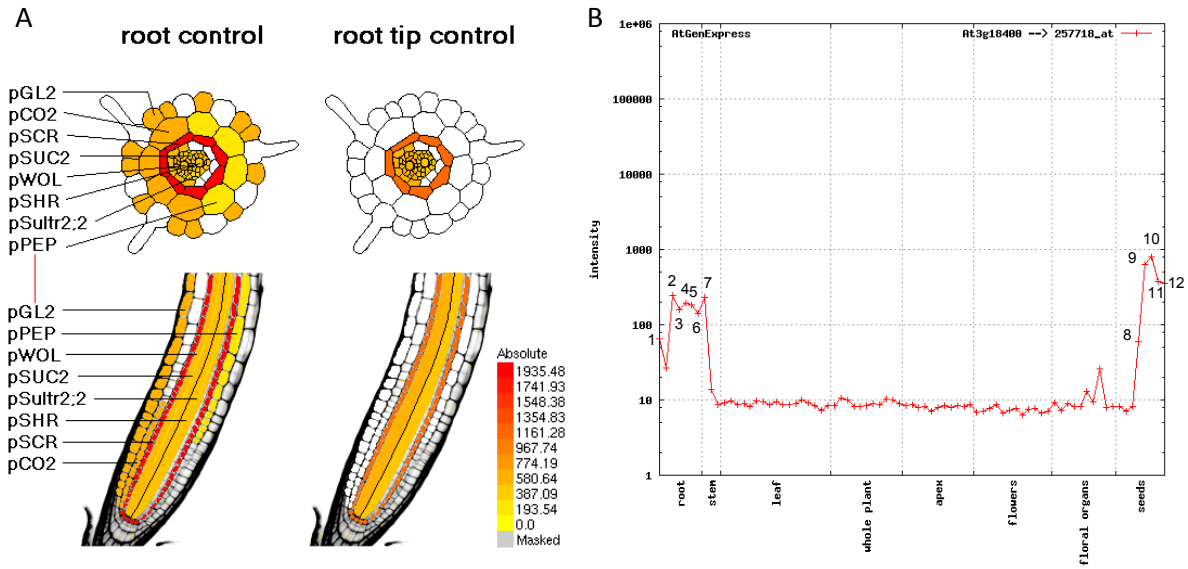

Fig. 8.1 *In silico* expression pattern of *ANAC058*

Tissue-specific expression pattern according to the Cell Type Specific Arabidopsis eFP Browser (A) (Mustroph et al., 2009) and organ-specific expression according to AtGenExpress Visualization Tool (AVT, B) (Schmid et al., 2005). Data points in AtGenExpress graph with expression values over 50 are labeled 1 - 12 from left to right. Corresponding sample information can be found in table 8.2, supp.

Table 8.2 AtGenExpress (Schmid et al., 2005) expression values for organ-specific expression of *ANAC058*

Of all available samples only organs with *ANAC058* expression values above 50 were selected. The data point labels correspond to the labeled data points in fig. 8.1 B, supp..

data point label	tissue cluster	tissue	genotype	age	expression value for At3g18400
1	root	roots	Wt	7 days	64.176
2	root	root	Wt	15 days	241.1692
3	root	root	Wt	8 days	160.2778
4	root	root	Wt	8 days	191.328
5	root	root	Wt	21 days	184.8697
6	root	root	Wt	21 days	139.6281
7	stem	hypocotyl	Wt	7 days	229.8255
8	seeds	seeds, stage 6, w/o siliques; mid to late torpedo embryos	Wt	8 wk	59.5732
9	seeds	seeds, stage 7, w/o siliques; late torpedo to early walking-stick embryos	Wt	8 wk	625.3634
10	seeds	seeds, stage 8, w/o siliques; walking-stick to early curled cotyledons embryos	Wt	8 wk	793.0977
11	seeds	seeds, stage 9, w/o siliques; curled cotyledons to early green cotyledons embryos	Wt	8 wk	376.6842
12	seeds	seeds, stage 10, w/o siliques; green cotyledons embryos	Wt	8 wk	356.4891

8.5 *ANAC058's* putative promoter activity

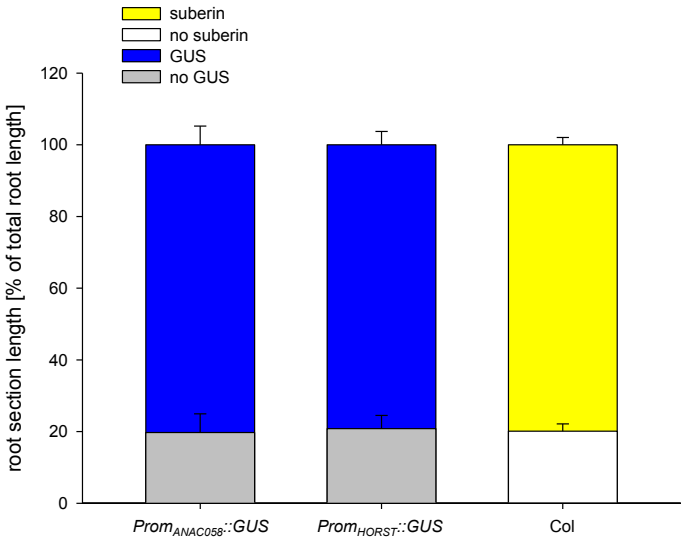

Fig. 8. 2 Start of promoter activity *in* $Prom_{ANAC058}$*::GPF-GUS*, in $Prom_{HORST}$*::GUS* and start of suberin deposition along root length

Distance from root tip to start of GUS activity in $Prom_{ANAC058}$*::GPF-GUS* and $Prom_{HORST}$*::GUS* plants as well as distance to start of Fluorol Yellow 088 stained suberin in Col was determined. Length of root sections without and with staining was measured and set in relation to total root length. n=14 for $Prom_{ANAC058}$*::GFP-GUS*, n=3 for $Prom_{HORST}$*::GUS* and n=7 for Col stained with Fluorol Yellow 088 (independent seedlings). Respective values can be found in table 8.12, supp..

8.6 NAC binding sites (NACBS) in promoters of suberin-associated genes

Table 8.3 NACBS in putative promoters of suberin-associated genes

NACBS were identified in promoters (1500 - 1 bp upstream of transcription start) in suberin genes using the Find Individual Motif Occurrence (FIMO) tool (Grant et al., 2011), of the MEME Suite web portal (http://meme-suite.org/), last accessed 30. 09. 2017.

Motif	promoter	Strand	Start	End	p-value	q-value	Matched Sequence
NACBS4	ABCG20	-	1352	1376	9.79E-06	0.198	AGAATTTCTCCTTGCACATGTATGT
NACBS4	ABCG20	+	1337	1361	1.04E-05	0.198	AGAAATTCGTGACATACATACATGT
NACBS2	FAR1	-	1019	1034	2.19E-05	0.707	AGTCGTGCAAGGTAAG
NACBS1	FAR1	+	1019	1034	3.76E-05	0.89	CTTACCTTGCACGACT
NACBS2	CYP86B1/RALPH	-	344	359	4.59E-05	0.741	TTACGTACAAAGGACG
NACBS6	CYP86A1/HORST	+	565	573	5.38E-05	0.713	TGGCGTGAT
NACBS6	ABCG20	+	1170	1178	5.38E-05	0.713	TAGCGTGCT
NACBS4	GPAT5	+	666	690	5.55E-05	0.706	GGAGAGGCTTTGTAAACACGCAAGT
NACBS1	CYP86B1/RALPH	+	344	359	5.68E-05	0.89	CGTCCTTTGTACGTAA
NACBS6	ABCG20	-	978	986	8.35E-05	0.713	TGGCGTGTT
NACBS6	GPAT5	+	1414	1422	8.35E-05	0.713	TGACGTGCA
NACBS4	GPAT7	+	1051	1075	8.47E-05	0.747	ACACATTCCAAATGTACGCGCATAC
NACBS2	FAR5	+	708	723	9.68E-05	1	AATAGTGTAAGGCAAG
NACBS4	FAR1	-	1403	1427	9.78E-05	0.747	ACAACTTCTTCATCTACCCGCATTG
NACBS5	GPAT7	+	13	31	9.94E-05	1	TGACCTACGGATTACGGAT

Table 8.4 List of suberin-associated genes used in NACBS search

AGI code	Locus	publication
At1g04220	*KCS2/DAISY*	Franke et al., 2009
At5g43760	*KCS20*	Lee et al., 2009b
At5g22500	*FAR1*	Domergue et al., 2010
At3g44540	*FAR4*	Domergue et al., 2010
At3g44550	*FAR5*	Domergue et al., 2010
At5g23190	*CYP86B1/RALPH*	Compagnon et al., 2009
At5g58860	*CYP86A1/HORST*	Höfer et al., 2008
At3g11430	*GPAT5*	Beisson et al., 2007
At5g06090	*GPAT7*	Yang et al., 2012
At5g41040	*ASFT*	Molina et al., 2009
At2g37360	*ABCG2*	Yadav et al., 2014
At5g13580	*ABCG6*	Yadav et al., 2014
At3g53510	*ABCG20*	Yadav et al., 2014

8.7 Phylogeny of the NAC family

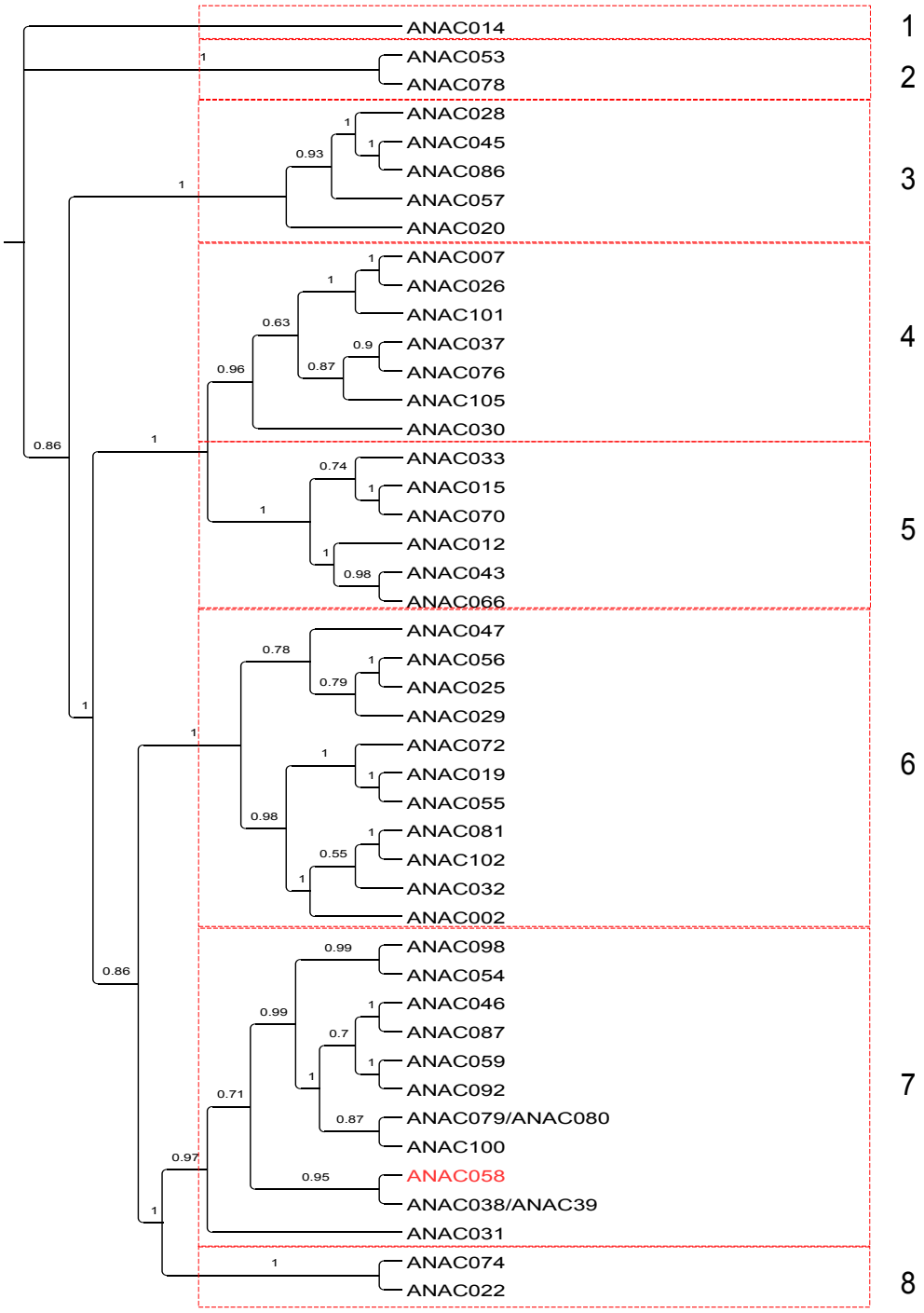

Fig. 8.3 Phylogenetic tree of *ANAC058* paralogs in *A. thaliana*

Phylogeny was inferred with Bayesian analysis (MrBayes version 3.1.2). Posterior probabilities of the nodes are given with 1 for 100 % support. *ANAC058* is emphasized with red letters. The different clades are separated into 8 groups according to Ooka et al., 2003 and Jensen et al., 2010. For AGI code for genes see table 8.5, sup..

Table 8.5 List of genes used in phylogenetic analysis of *ANAC058* paralogs in *A. thaliana*

ANAC058 paralogs were extracted from the *A. thaliana* genome with the TAIR database BLAST tool (for details see 2.1.3)

AGI code	Locus	Score (bits)	e-value
AT3G18400.1	*ANAC058*	598	e-171
AT2G24430.1	*ANAC038/39*	253	9.00E-68
AT5G61430.1	*ANAC100*	252	2.00E-67
AT5G07680.1	*ANAC079/80*	251	3.00E-67
AT5G53950.1	*ANAC098, CUC2*	250	7.00E-67
AT5G39610.1	*ANAC092, NAC2, ORE1, NAC6*	239	2.00E-63
AT5G18270.1	*ANAC087*	237	1.00E-62
AT3G04060.1	*ANAC046*	235	2.00E-62
AT1G76420.1	*ANAC031, CUC3, NAC368*	234	7.00E-62
AT3G29035.1	*ANAC059, NAC3*	228	3.00E-60
AT3G15170.1	*ANAC054, CUC1, NAC1*	226	1.00E-59
AT1G56010.2	*ANAC022, NAC1*	208	4.00E-54
AT4G27410.2	*ANAC072, RD26*	204	8.00E-53
AT1G12260.1	*ANAC007, VND4, EMB2749*	203	1.00E-52
AT1G71930.1	*ANAC030, VND7*	201	8.00E-52
AT1G62700.1	*ANAC026, VND5*	200	1.00E-51
AT5G62380.1	*ANAC101, VND6*	199	3.00E-51
AT3G15500.1	*ANAC055, NAC3*	197	7.00E-51
AT2G18060.1	*ANAC037, VND1*	197	8.00E-51
AT4G36160.1	*ANAC076, VND2*	196	1.00E-50
AT1G52890.1	*ANAC019*	195	3.00E-50
AT1G65910.1	*ANAC028*	195	3.00E-50
AT4G10350.1	*ANAC070, BRN2*	194	5.00E-50
AT2G46770.1	*ANAC043, NST1, EMB2301*	191	5.00E-49
AT5G66300.1	*ANAC105, VND3*	191	7.00E-49
AT3G03200.1	*ANAC045*	190	1.00E-48
AT3G61910.1	*ANAC066, NST2*	190	1.00E-48
AT1G33280.1	*ANAC015, BRN1*	189	2.00E-48
AT4G28530.1	*ANAC074*	188	4.00E-48
AT3G10500.1	*ANAC053*	187	9.00E-48
AT1G01720.1	*ANAC002, ATAF1*	187	1.00E-47
AT5G04410.1	*ANAC078, NAC2*	186	1.00E-47
AT3G17730.1	*ANAC057*	186	2.00E-47
AT3G04070.1	*ANAC047*	185	3.00E-47
AT5G17260.1	*ANAC086*	185	3.00E-47
AT1G61110.1	*ANAC025*	184	1.00E-46
AT1G79580.1	*ANAC033, SMB*	182	3.00E-46
AT5G63790.1	*ANAC102*	182	3.00E-46
AT5G08790.1	*ANAC081, ATAF2*	181	6.00E-46
AT1G77450.1	*ANAC032*	180	9.00E-46
AT1G32770.1	*ANAC012, SND1, NST3*	180	1.00E-45
AT3G15510.1	*ANAC056, NARS1, NAC2*	178	3.00E-45
AT1G54330.1	*ANAC020*	178	5.00E-45
AT1G69490.1	*ANAC029, NAP*	177	7.00E-45
AT1G33060.1	*ANAC014*	177	1.00E-44

8.8 Conserved motifs specific for the TRD of phylogenetic NAC group with *ANAC058*

A

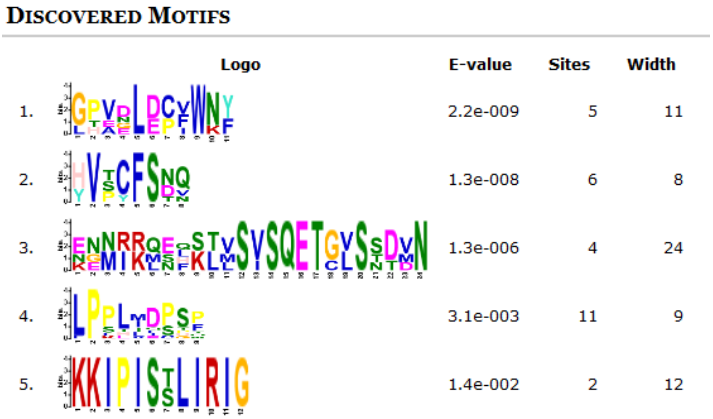

B

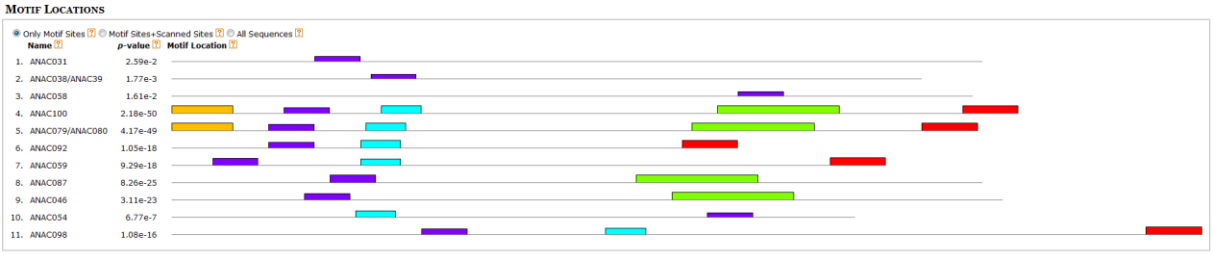

Fig. 8.4 Motifs discovered in the TRD of NACs within phylogenetic group 7 (fig. 8.3, supp.)

Multiple EM of Motif Elicitation (MEME) tool (Bailey et al., 2009) of the MEME Suite web page (http://meme-suite.org/), last accessed 30. 09. 2017 was employed. Individual identified motifs and their symbols (A) are depicted and location of the motifs within the tested sequences (B, *ANAC058* is the third gene from the top, *ANAC038/ANAC039* the second)). Number of motifs was restricted to 5. The same analysis was conducted for TRD sequences of genes in phylogenetic group 6 (fig. 8.3, supp.) and none of the motifs identified for group 7 (A) were found (data not shown).

8.9 Characterization of anac058 protein in *anac058-1*

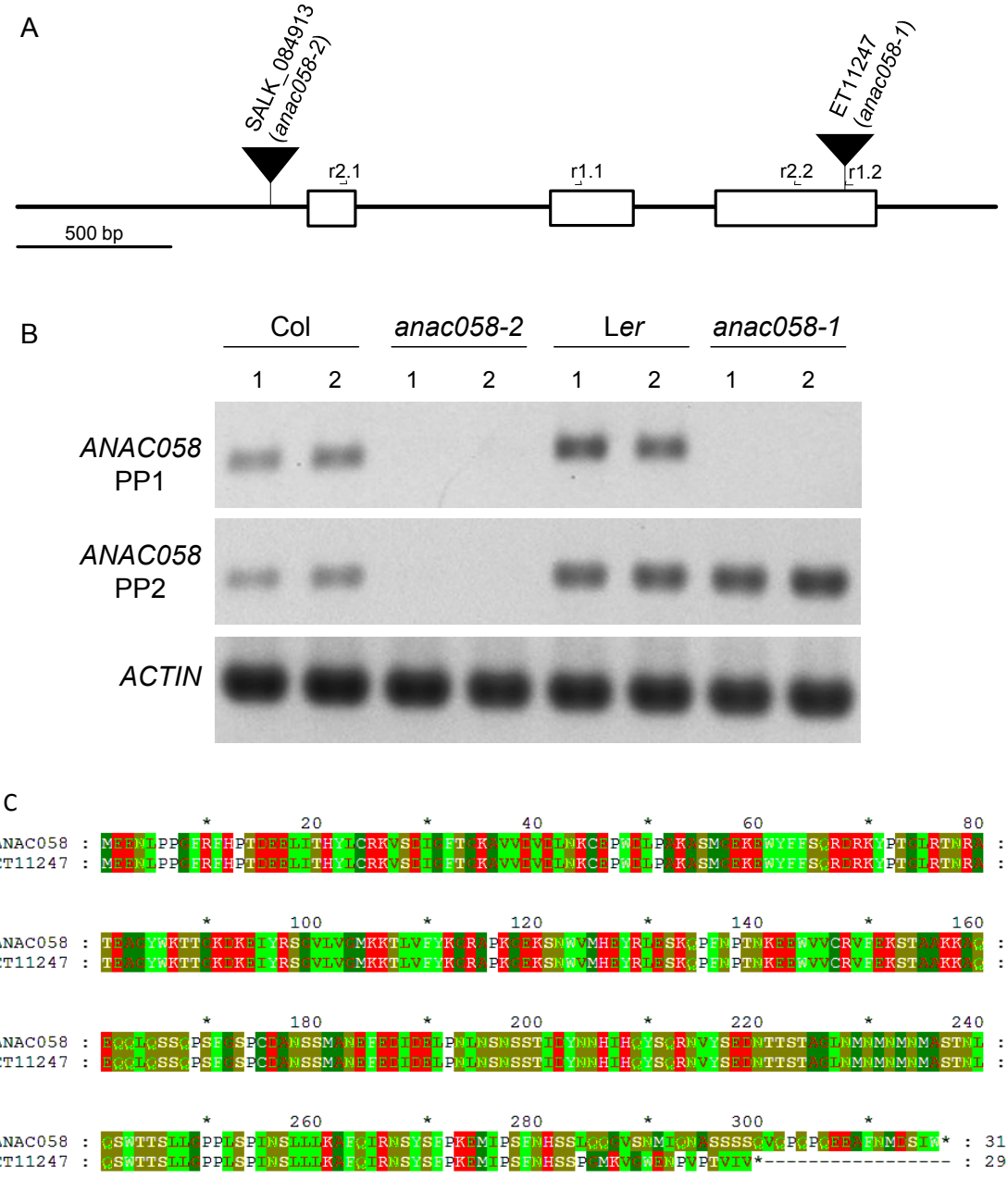

Fig. 8.5 *ANAC058* RNA and protein in *anac058-1*

The transcript of *ANAC058* in *anac058-1* was amplified using primer pair 1 (PP1, primers r1.1 and r1.2 in A) which flanks the insertion site, as well as primer pair 2 (PP2, primers r2.1and r2.2 in A) which binds entirely upstream of the insertion site (A). RT-PCR for two plants of each genotype (1 and 2) with PP1 shows no remaining transcript of *ANAC058*, whereas upstream of insertion site transcript amounts were at wild type level (B). Translation of wild type (*ANAC058*) and *anac058-1* (ET11247) *ANAC058* sequence revealed a protein shorter by 17 aa in *anac058-1*. The insertion changes the C-terminal 33 aa of the wild type *ANAC058* protein. Insertion site was verified by sequencing.

8.10 Suberin deposition in *anac058* mutants

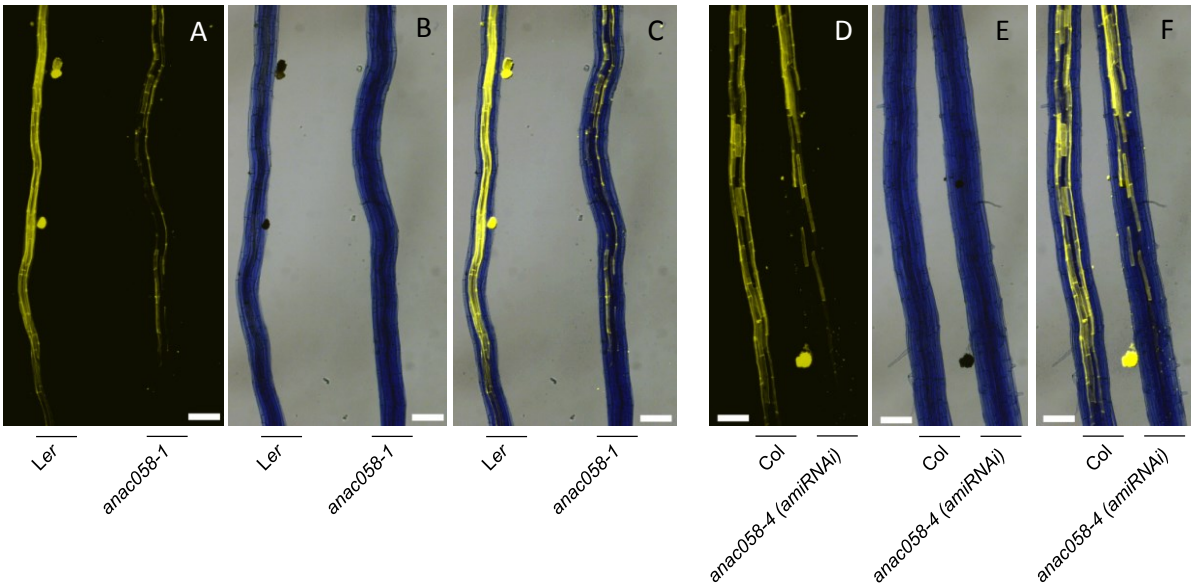

Fig. 8.6 Suberin deposition in *anac058* seedlings stained with Fluorol Yellow 088 compared to the wild type

Suberin was stained with Fluorol Yellow 088 in 6 d old seedlings grown on MS plates. Depicted are representative pictures showing roots of the same length at a position where delay of suberin deposition is visible in *anac058-1* (A and C) and in *anac0058-4 (amiRNAi)* (D and F) compared to the respective wild type. Corresponding measurements of root sections without suberin, with patchy and continuous suberin can be found in fig. 3.14. Fluorescence was observed with a fluorescence microscope employing a standard GFP filter, bright field pictures of the same root section was taken (B and E) and an overlay of both pictures was generated in ImageJ (C and F).

8.11 Salt and osmotic stress treatment of *anac058* mutants in comparison to control plants

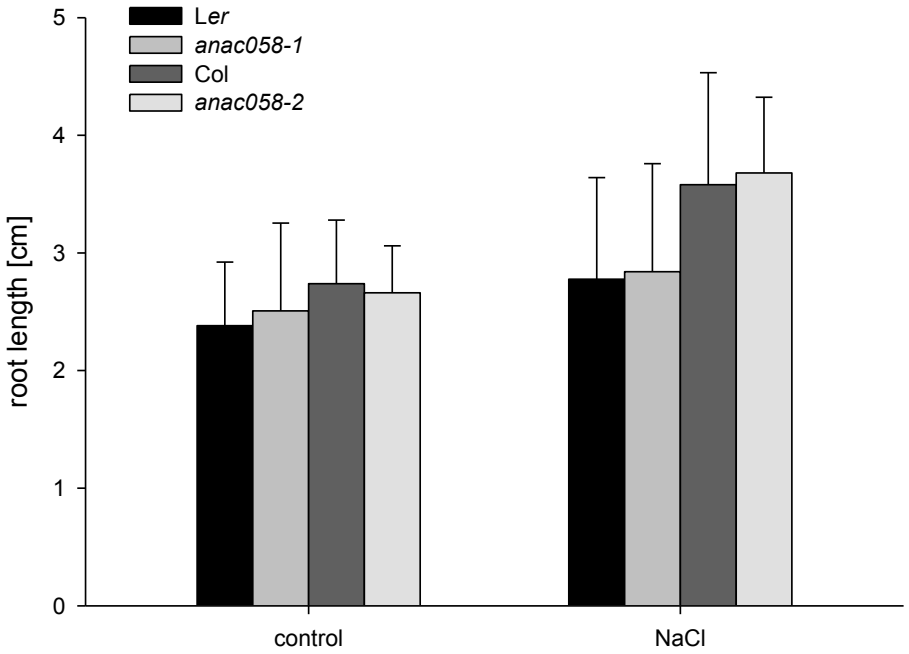

Fig. 8.7 Germination of *anac058* mutants and respective wild types on 50 mM NaCl

Total main root length of seedlings grown for 10 d on control (1/2 MS) and 50 mM NaCl media was measured representatively for root growth observed over 5 weeks. Mean values and standard deviation represented by error bars were calculated from 22 (Col), 21 (*anac058-2*), 15 (L*er*) and 11 (*anac058-1*) independent seedlings for control conditions and from 26 (Col), 39 (*anac058-2*), 19 (L*er*) and 10 (*anac058-1*) independent seedlings for salt conditions. For respective values, see table 8.8, supp..

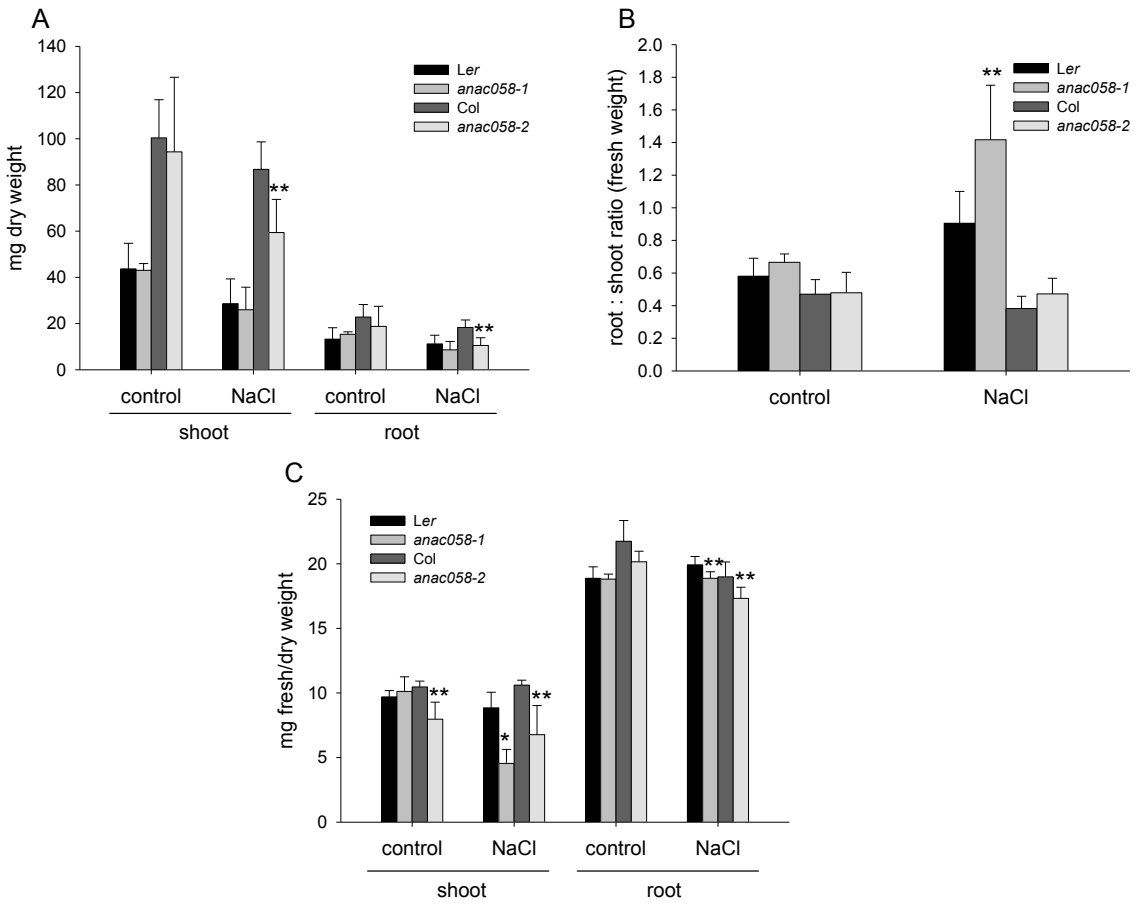

Fig. 8.8 Growth of *anac058* mutants and respective wild types in 50 mM NaCl solution

Plants were grown for 25 d in hydroponics and were transferred to new hydroponics solution (control) or hydroponics solution supplemented with 50 mM NaCl. Plant biomass was investigated after 2 weeks of NaCl treatment. Root and shoot fresh weight (fig. 3.18 C) and dry weight (A) was measured and root:shoot ratio was calculated from fresh weight (B) and dry weight (fig. 3.18 D). The ratio fresh:dry weight is depicted in C. Mean values and standard deviations as represented by error bars were calculated from 5 (Col), 4 (*anac058-2*), 6 (L*er*) and 3 (*anac058-1*) independent seedlings for control conditions and from 7 (Col), 9 (*anac058-2*), 7 (L*er*) and 8 (*anac058-1*) independent seedlings for salt conditions. All related values are present in table 8.20, supp..

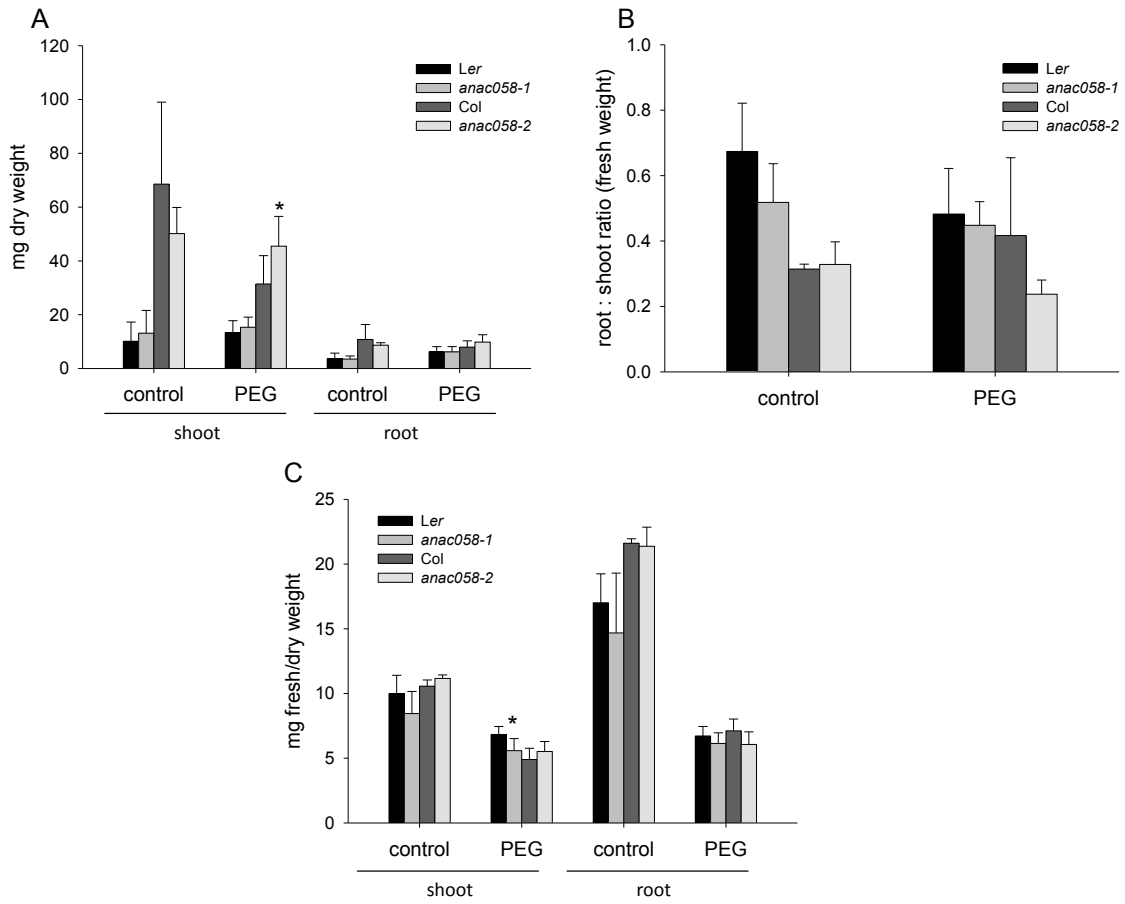

Fig. 8.9 Growth of *anac058* mutants and respective wild types in 1.73 % PEG solution

Plants were grown for 25 d in hydroponics and were transferred to new hydroponics solution (control) or hydroponics solution supplemented with 1.73 % PEG (173 g/l H_20, water potential Δ -0.4 MPa). Plant biomass was investigated after 4 d of PEG treatment. Root and shoot fresh weight (fig. 3.19 C) and dry weight (A) was measured and root:shoot ratio was calculated from fresh weight (B) and dry weight (fig. 3.19 D). The ratio fresh/dry weight is depicted in C. Mean values and standard deviations represented by error bars were calculated from 3 (Col, *anac058-2*, L*er*, *anac058-1*) independent seedlings for control conditions and from 6 (Col), 7 (*anac058-2* and L*er*) and 8 (*anac058-1*) independent seedlings for PEG conditions. All related values are present in table 8.21, supp..

8.12 Overexpression of *ANAC058*

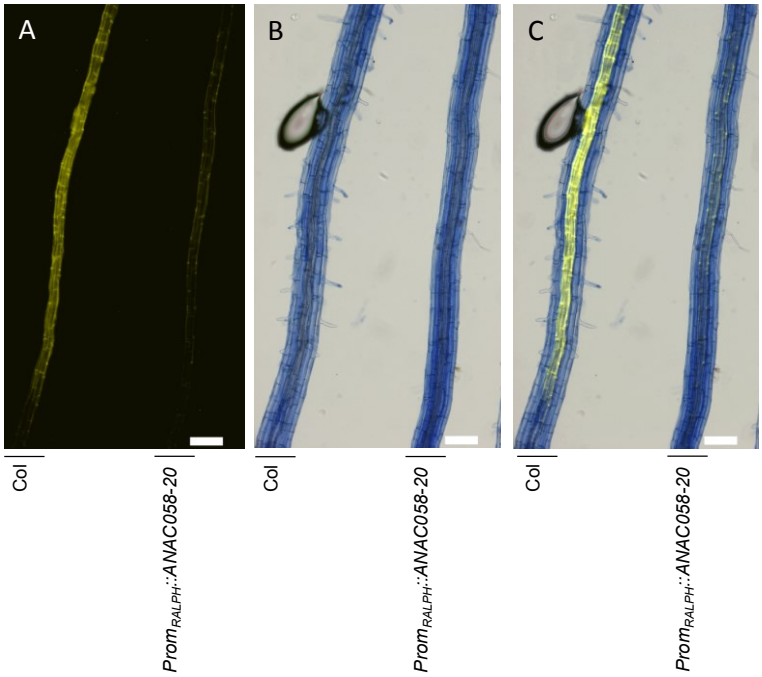

Fig. 8.10 Suberin deposition in *Prom$_{RALPH}$::ANAC058-20* seedlings stained with Fluorol Yellow 088 in comparison to the wild type

Suberin was stained with Fluorol Yellow 088 in 6 d old seedlings grown on MS plates. Depicted are representative pictures showing roots of the same length at a position where delay of suberin deposition is visible in *Prom$_{RALPH}$::ANAC058*-20 (A and C) compared to the respective wild type. Corresponding measurements of root sections without suberin, with patchy and continuous suberin can be found in fig. 3.22. Fluorescence was observed with a fluorescence microscope employing a standard GFP filter, bright field pictures of the same root section was taken (B) and an overlay of both pictures was generated in ImageJ (C).

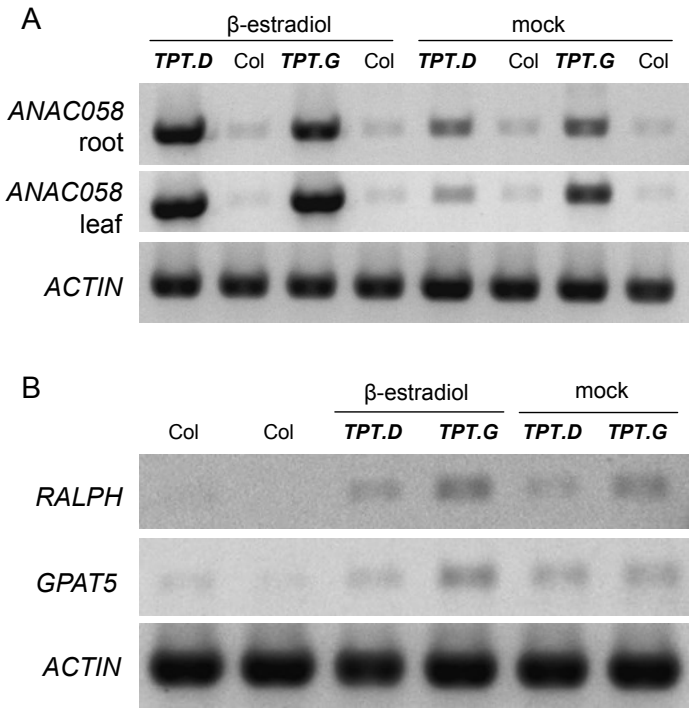

Fig. 8.11 Expression of *ANAC058* and suberin genes in roots and leaves of induced *TPT.D* and *TPT.G* seedlings

11 d old seedlings grown on MS, treated for 6 h with β-estradiol by transferring seedlings to MS with 10 µM β-estradiol and mock medium were used. Roots and leaves of several seedlings were collected and pooled for each sample. Col seedlings grown on the same plate as the TPT lines, depicted to the right of the corresponding line, were tested as well. *ANAC058* was measured by RT-PCR in root and leaf samples (A). Suberin gene *RALPH/CYP86B1* and *GPAT5* expression was tested by RT-PCR for leaf samples (B). *ACTIN* was used as the control.

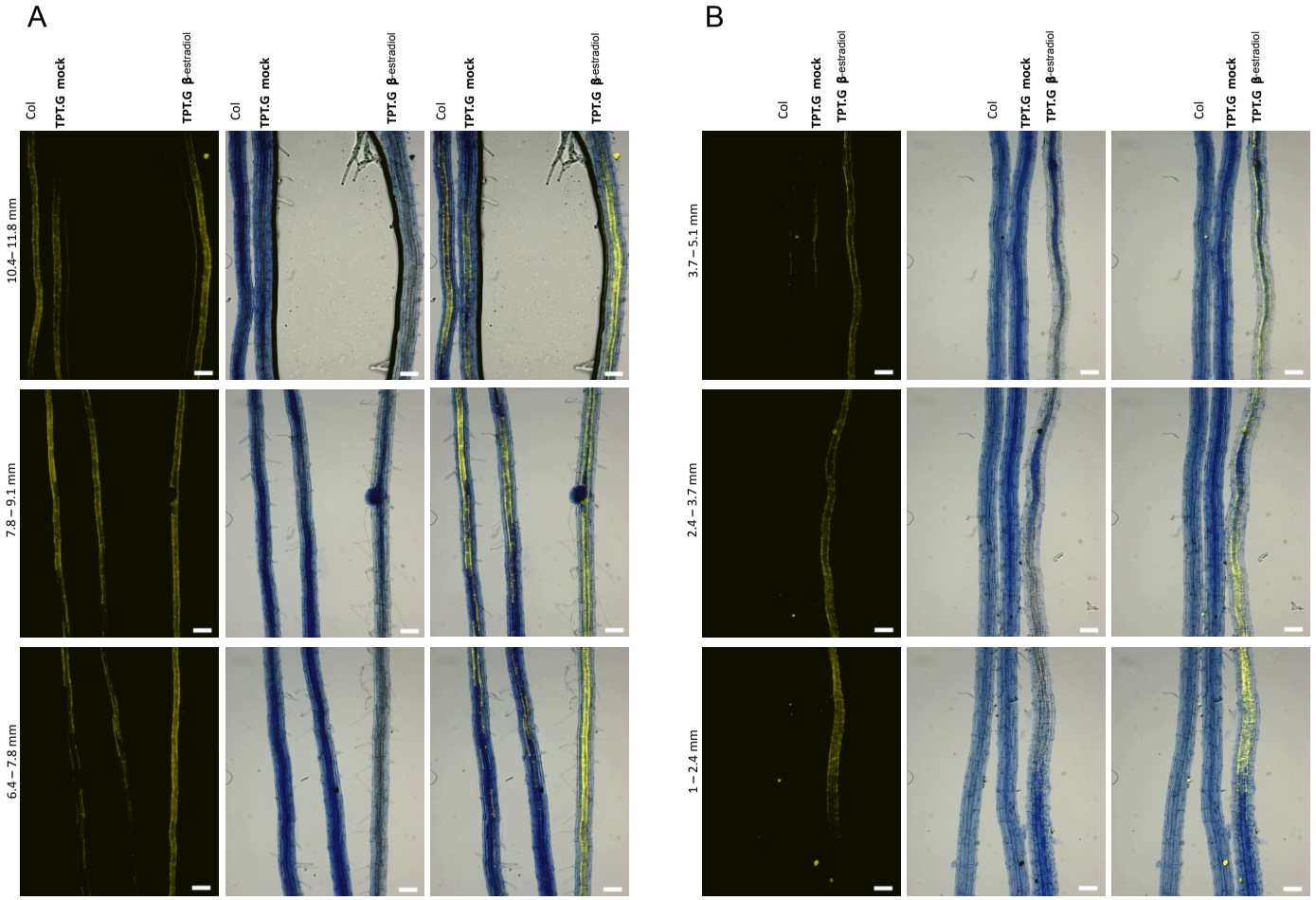

Fig. 8.12 Suberin deposition in induced *TPT.G*, mock treated *TPT.G* and wild-type seedlings

Suberin was stained with Fluorol Yellow 088 in 6 d old seedlings grown for 4 d on MS plates and transferred to MS supplemented with 10 µM β-estradiol or mock solution. Depicted are representative pictures showing the basal (A) and apical (B) root of *TPT.G* and Col seedlings, treated either mock or β-estradiol treated. Roots have similar root length. Distance from the root tip is given in mm. Fluorescence was observed with a fluorescence microscope employing a standard GFP filter, bright field pictures of the same root section were taken and an overlay of both pictures was generated in ImageJ. Scale bars signify 100 µM.

8.13 Phylogenetic relation of *StNAC103* within the *A. thaliana* NAC gene family

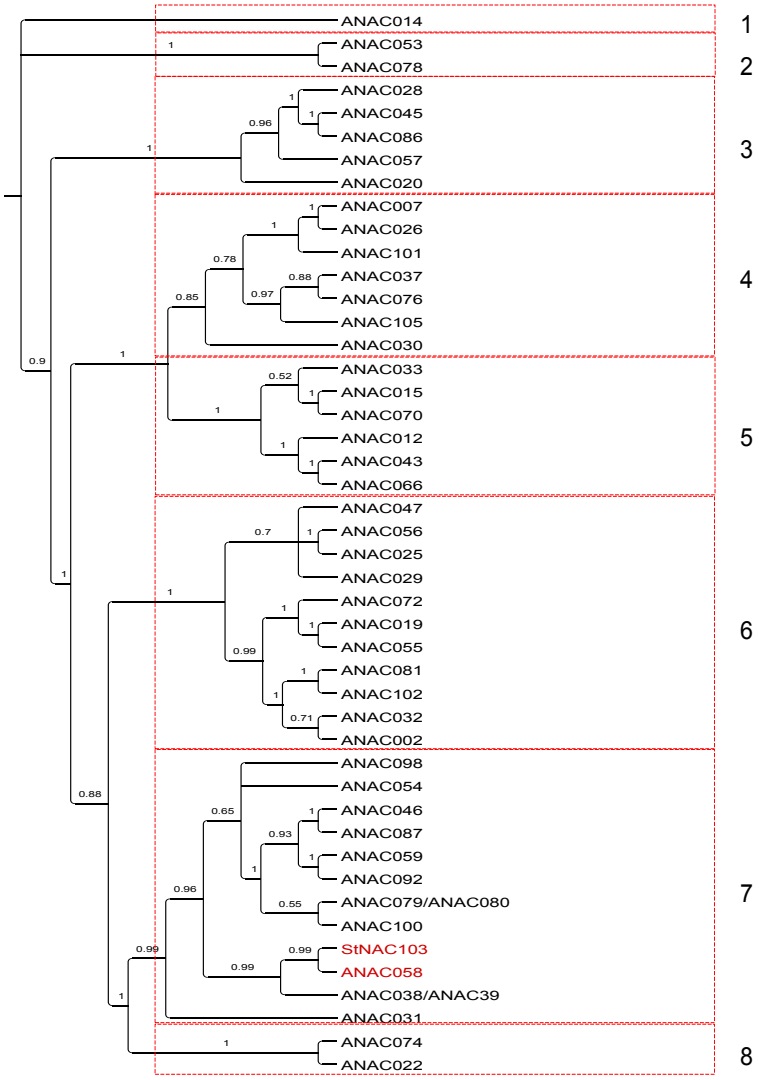

Fig. 8.13 Phylogenetic tree of *ANAC058* paralogs and *StNAC103*

Phylogeny was inferred with Bayesian analysis (MrBayes version 3.1.2). Posterior probabilities of the nodes are given with 1 for 100 % support. *ANAC058* and *StNAC103* are emphasized with red letters. The different clades are separated into 8 groups according to Ooka et al., 2003 and Jensen et al., 2010. For AGI code of *A. thaliana* genes see table 8.5, supp..

8.14 Generation of transgenic *A. thaliana*

8.14.1 Genotyping of potentially transgenic plants

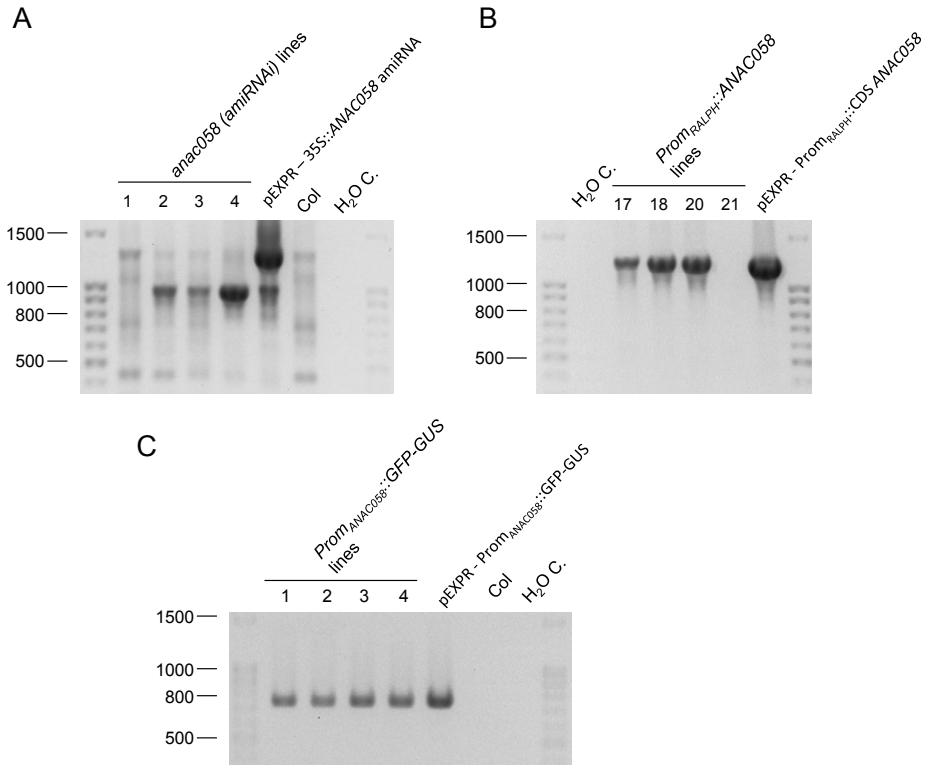

Fig. 8.14 Genotyping of T1 plants from T0 plants transformed with 35S::ANAC058 amiRNA, $Prom_{RALPH}$::CDS ANAC058 and $Prom_{ANAC058}$::GFP-GUS constructs

The plants generated with the construct 35S::ANAC058 amiRNA (A, plasmid map fig. 8.22, supp.) were subsequently referred to as *anac058 (amiRNAi)* lines, plants generated with the construct $Prom_{RALPH}$::CDS ANAC058 (B, plasmid map fig. 8.23, supp)) were subsequently referred to as *$Prom_{RALPH}$::ANAC058* lines. Plasmid map of pEXPR - $Prom_{ANAC058}$::GFP-GUS is depicted in fig. 8.24, supp..

8.14.2 Vector maps

8.14.2.1 Donor vectors

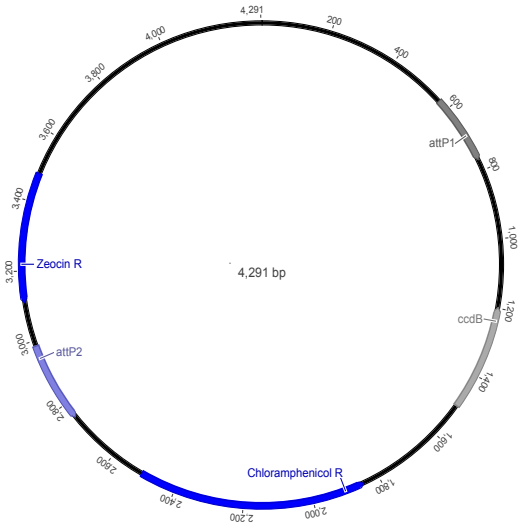

Fig. 8.15 Vector map of the donor vector pDONR ™ / Zeo used to generate most entry clones

attP1 and attP2: recombination sites, Zeocin R: resistance gene conferring resistance to the antibiotic Zeocin, Chloramphenicol R: resistance gene conferring resistance to the antibiotic Chloramphenicol, *ccd*B: gene inhibiting the bacterial DNA gyrase.

8.14.2.2 Destination vectors

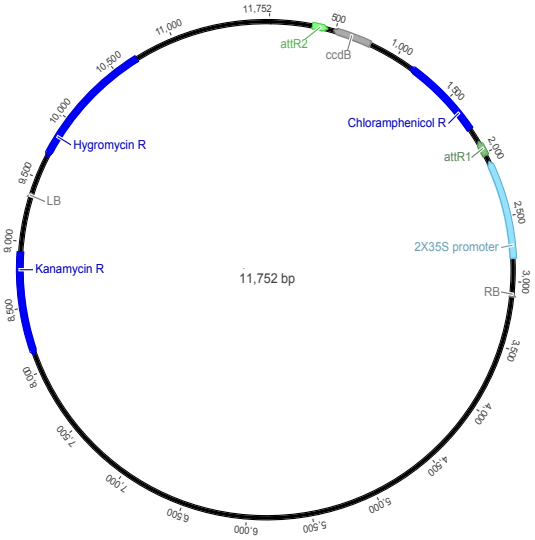

Fig. 8.16 Vector map of the destination vector pMDC32 (Curtis and Grossniklaus, 2003) used to generate expression clones

attR1 and attR2: recombination sites, Hygromycin R: resistance gene conferring resistance to the antibiotic Hygromycin, Chloramphenicol R: resistance gene conferring resistance to the antibiotic Chloramphenicol, Kanamycin R: resistance gene conferring resistance to the antibiotic Kanamycin, LB and RB: left border and right border, respectively, for T-DNA transfer, *ccd*B: gene inhibiting the bacterial DNA gyrase, 2x35S promoter: 35S CMV promoter sequence, twice.

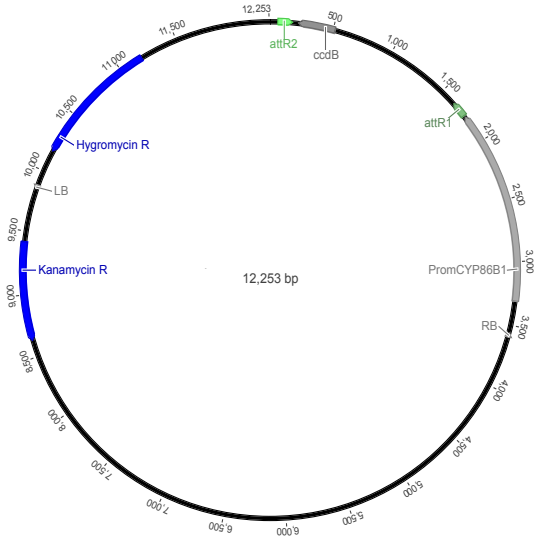

Fig. 8.17 Vector map of the destination vector <u>pMDC99-Prom$_{RALPH}$</u>, used to generate expression clones

Vector derived from pMDC99 (Curtis and Grossniklaus, 2003) featuring the putative promoter region of *CYP86B1/RALPH* (*PromCYP86B1*) generated by Daniela Nosbüsch (Laboratory Ecophysiology, University of Bonn, Germany) based on a vector by Curtis and Grossniklaus, 2003.

attR1 and attR2: recombination sites, Hygromycin R: resistance gene conferring resistance to the antibiotic Hygromycin, Kanamycin R: resistance gene conferring resistance to the antibiotic Kanamycin, LB and RB: left border and right border, respectively, for T-DNA transfer, *ccd*B: gene inhibiting the bacterial DNA gyrase.

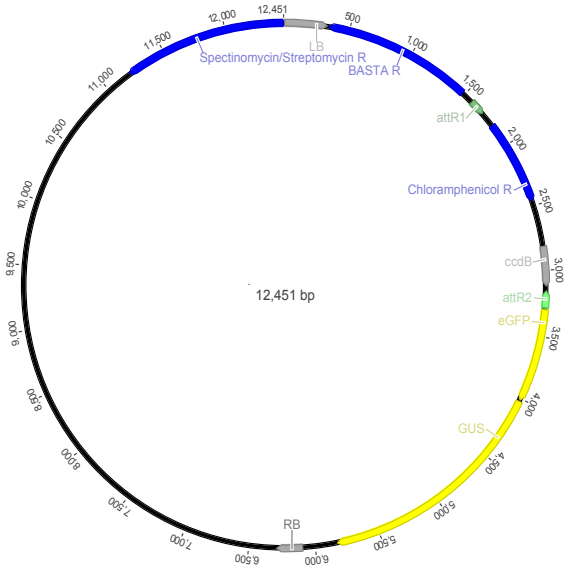

Fig. 8.18 Vector map of the destination vector <u>pBGWFS7</u> (Karimi et al., 2002), used to generate expression clones

attR1 and attR2: recombination sites, BASTA R: gene bar conferring resistance to the herbicide BASTA with the active ingredient Phosphinothricin, Chloramphenicol R: resistance gene conferring resistance to antibioticum Chloramphenicol, Spectinomycin/Streptomycin R: gene conferring resistance to antibiotics Spectinomycin, Streptomycin, LB and RB: left border, right border, respectively, *ccd*B: gene inhibiting the bacterial DNA gyrase. Obtained from VIB vzw (Gent, Belgium).

8.14.2.3 Entry clones

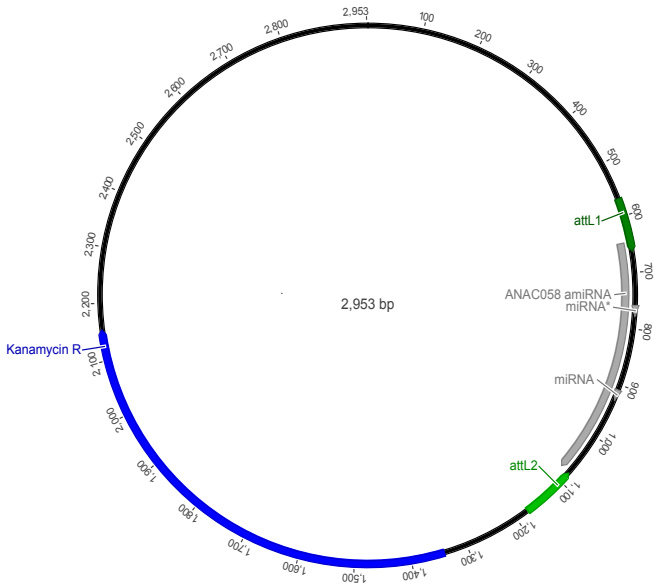

Fig. 8.19 Vector map of the entry clone <u>pENTR - *ANAC058* amiRNA</u>, used to generate expression clones
Vector with the backbone of pDONR221 and the *ANAC058* amiRNA construct, generated by GeneArt, Thermo Fisher Scientific according to own *in silico* cloning.
attL1 and attL2: recombination sites, Kanamycin R: resistance gene conferring resistance to the antibioticum Kanamycin, *ANAC058* amiRNA: synthetic sequence consisting of the endogenous micro RNA precursor MIR319a and *ANAC058-amiRNA* sequences in forward (miRNA) and reverse (miRNA*) direction at specific locations inside MIR319a (see 2.5.3).

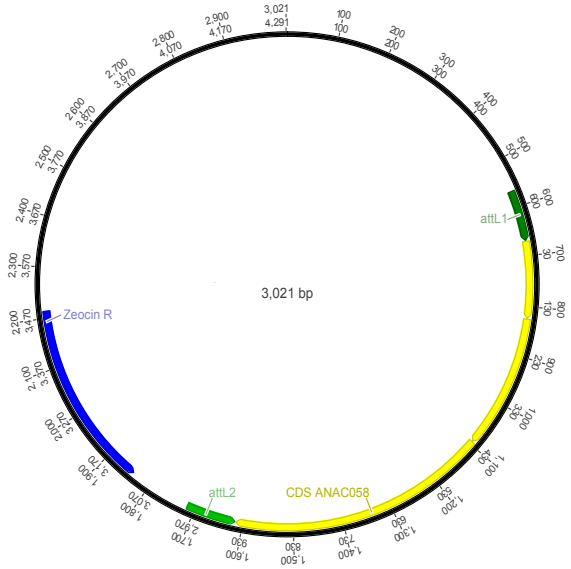

Fig. 8.20 Vector map of the entry clone <u>pENTR - CDS *ANAC058*</u>, used to generate expression clones
Vector with the backbone of pDONR ™ /Zeo and the CDS of *ANAC058*.
attL1 and attL2: recombination sites, Zeocin R: resistance gene conferring resistance to the antibioticum Zeocin, *ANAC058-CDS*: coding sequence of *ANAC058*.

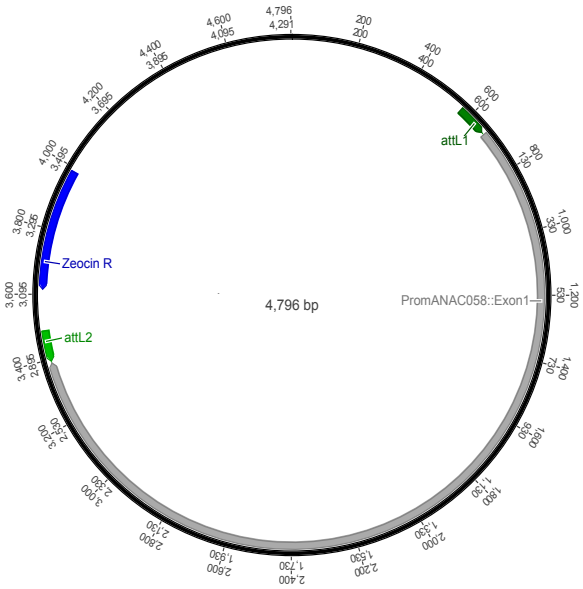

Fig. 8.21 Vector map of the entry clone <u>pENTR - Prom$_{ANAC058}$</u>, used to generate expression clones

Vector with the backbone of pDONR TM /Zeo and Prom$_{ANAC058}$::Exon1.

attL1 and attL2: recombination sites, Zeocin R: resistance gene conferring resistance to the antibioticum Zeocin, *PromANAC058::EXON1*: putative promoter of *ANAC058* including exon 1

8.14.2.4 Expression clones

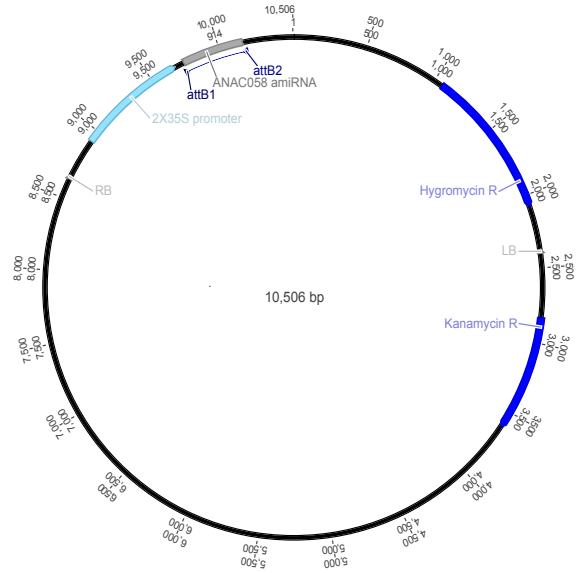

Fig. 8.22 Vector map of the expression clone <u>pEXPR - 35S::*ANAC058* amiRNA</u>

Vector with the backbone of pMDC32 and the *ANAC058* amiRNA construct.

attB1 and attB2: recombination sites, Hygromycin R: resistance gene conferring resistance to the antibioticum Hygromycin, LB and RB: left border and right border, respectively, for T-DNA transfer, 2x35S promoter: 35S CMV promoter sequence, twice, *ANAC058* amiRNA: synthetic sequence consisting of the endogenous micro RNA precursor MIR319a and *ANAC058-amiRNA* sequences in forward (miRNA) and reverse (miRNA*) direction at specific locations inside MIR319a (see 2.5.3).

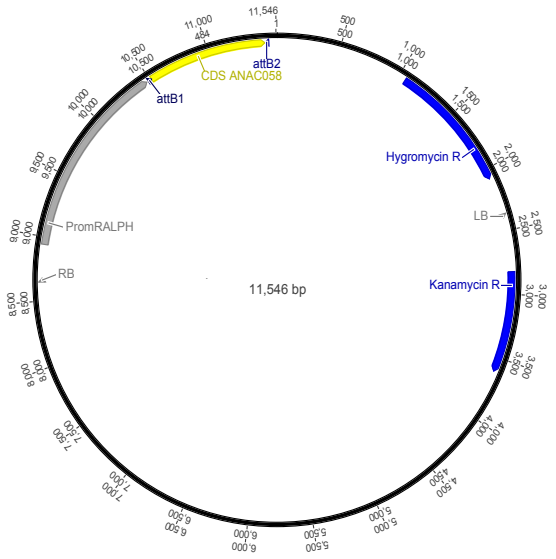

Fig. 8.23 Vector map of the expression clone pEXPR - Prom$_{RALPH}$::CDS *ANAC058*

Vector with the backbone of pMDC99-Prom$_{RALPH}$ and the CDS of *ANAC058*.

attB1 and attB2: recombination sites, Hygromycin R: resistance gene conferring resistance to the antibioticum Hygromycin, LB and RB: left border and right border, respectively, for T-DNA transfer, *ANAC058-CDS*: coding sequence of *ANAC058*, subsequently referred to as *ANAC058* in context of this construct.

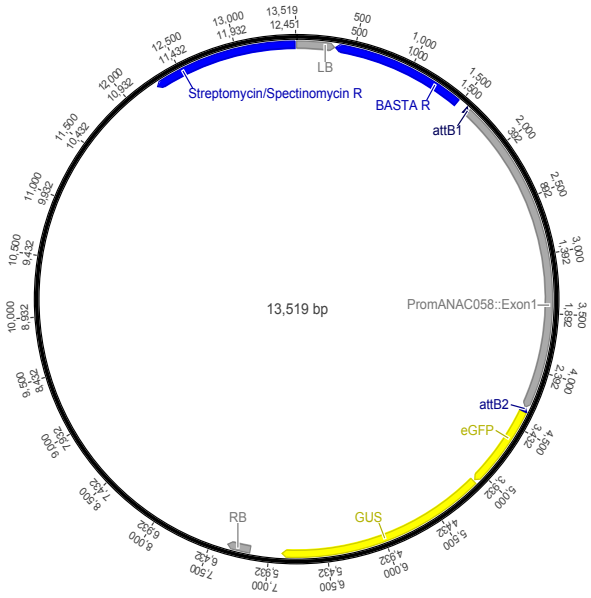

Fig. 8.24 Vector map of the expression clone pEXPR - Prom$_{ANAC058}$::GFP-GUS

Vector with the backbone of pBGWFS7 and the Prom$_{ANAC058}$::Exon1.

attB1 and attB2: recombination sites, BASTA R: gene bar conferring resistance to the herbicide BASTA with the active ingredient Phosphinothricin, Chloramphenicol R: resistance gene conferring resistance to the antibioticum Chloramphenicol, Spectinomycin/Streptomycin R: gene conferring resistance to the antibiotics Spectinomycin and Streptomycin, LB and RB: left border and right border, respectively, for T-DNA transfer, *PromANAC058::EXON1*: putative promoter of *ANAC058* including exon 1.

8.15 Tables with values used to generate diagrams

8.15.1 qRT-PCR measurement

Table 8.6 Gene expression in apical root sections of *anac058* mutants

Gene expression was measured with hydroponically grown plants (*anac058-1*, *anac058-2* and respective wild type grown for 5 weeks, *anac058-3 (amiRNAi)* and respective wild type grown for 4 weeks). Apical 6 cm (*anac058-2* and respective wild type), 4 cm (*anac058-1* and respective wild type and 3 cm (*anac058-3 (amiRNAi)* and respective wild type) were collected. Wild type values were set to one and the expression values in *anac058* mutants are the -fold expression compared to their respective wild type. *GAPDH* was used as the endogenous control. Means and standard deviations were calculated from three technical replicates. For diagram, see fig. 3.15.

	L*er*	*anac058-1*	Col	*anac058-2*	Col (amiRNAi)	*anac058-3 (amiRNAi)*
	[Fold difference in expression level relative to control ± SD]	[Fold difference in expression level relative to control ± SD]	[Fold difference in expression level relative to control ± SD]	[Fold difference in expression level relative to control ± SD]	[Fold difference in expression level relative to control ± SD]	[Fold difference in expression level relative to control ± SD]
ANAC058	1.000± 0.030	0.002± 0.000	1.000± 0.033	0.033± 0.017	1.000± 0.063	0.467± 0.014
RALPH	1.000± 0.022	0.601± 0.032	1.000± 0.046	0.539± 0.054	1.000± 0.025	0.421± 0.014
GPAT5	1.000± 0.116	1.001± 0.022	1.000± 0.018	0.734± 0.007	1.000± 0.027	0.433± 0.008
HORST	1.000± 0.117	0.762± 0.023	1.000± 0.021	0.474± 0.020		
RBOHF	1.000± 0.116	1.146± 0.015	1.000± 0.024	1.269± 0.024		

Table 8.7 Expression of suberin, Casparian strip, lignin, cutin, aquaporin and various MYB genes in induced *TPT.G* plants

Apical root sections (apical 6 cm) of 4 weeks old, hydroponically grown plants, 2 for each genotype, were investigated. Plants were either treated with a 10 µM β-estradiol solution or a mock solution for 8 d before harvest. *GAPDH* was used as endogenous control and results were normalized to the expression in *ANAC058.TPT.G* mock which was set to 1. Means and standard deviations were calculated from three technical replicates. For diagram, see fig. 3.27.

	TPT.G mock [Fold difference in expression level relative to control ± SD]	***TPT.G*** β-estradiol [Fold difference in expression level relative to control ± SD]
ANAC058	1.000 ± 0.112	172.107 ± 0.777
RALPH	1.000 ± 0.011	3.051 ± 0.075
GPAT5	1.000 ± 0.097	2.418 ± 0.013
HORST	1.000 ± 0.099	2.791 ± 0.037
ASFT	1.000 ± 0.028	2.599 ± 0.147
ABCG6	1.000 ± 0.054	2.285 ± 0.204
ANAC038	1.000 ± 0.156	2.361 ± 0.318
RBOHF	1.000 ± 0.080	2.212 ± 0.011
ESB1	1.000 ± 0.109	1.783 ± 0.022
PER64	1.000 ± 0.113	1.658 ± 0.251
CAD5	1.000 ± 0.125	2.239 ± 0.035
GPAT4	1.000 ± 0.165	1.273 ± 0.315
CYP86A2	1.000 ± 0.124	0.962 ± 0.032
PIP2.2	1.000 ± 0.040	2.086 ± 0.139
MYB41	1.000 ± 0.134	1.655 ± 0.277
MYB93	1.000 ± 0.044	2.885 ± 0.195
MYB107	1.000 ± 0.064	2.778 ± 0.261
MYB9	1.000 ± 0.075	4.075 ± 0.266

8.15.2 Chemical analyses

Table 8.8 Root suberin composition in *anac058-1* and wild type

Total root systems of 5 weeks old, soil grown plants were investigated. Depicted are amounts of aliphatic suberin monomers in µg per mg root dry weight sorted according to substance classes and carbon chain length (fatty acids (acids), primary alcohols (alcohols), ω-hydroxy fatty acids (ω-OH acids) and α,ω-dicaorboxylic acids (α,ω-diacids)). Mean values and standard deviations were calculated from 4 independent samples of mutant and wild type each. Significant differences were determined by student t-test. For diagram, see fig. 3.12.

monomers	L*er* [µg mg^{-1} ± SD]		*anac058-1* [µg mg^{-1} ± SD]		*t*-test
ALIPHATICS	**19.439 ±**	**4.367**	**16.694 ±**	**2.258**	**0.307**
acids	**4.204 ±**	**0.920**	**2.539 ±**	**1.288**	**0.080**
COOH C18	0.272 ±	0.108	0.201 ±	0.069	0.310
COOH C20	0.656 ±	0.157	0.580 ±	0.069	0.411
COOH C22	3.248 ±	0.725	3.049 ±	0.467	0.661
COOH C24	0.300 ±	0.046	0.281 ±	0.031	0.508
alcohols	**1.845 ±**	**0.527**	**2.869 ±**	**0.911**	**0.100**
OH C18	0.747 ±	0.226	0.654 ±	0.066	0.459
OH C20	0.729 ±	0.209	0.539 ±	0.080	0.140
OH C22	0.369 ±	0.094	0.291 ±	0.043	0.182
ω-OH acids	**8.466 ±**	**1.929**	**5.418 ±**	**1.594**	**0.051**
ω-OH C16	1.397 ±	0.377	1.191 ±	0.136	0.345
ω-OH C18	0.518 ±	0.128	0.419 ±	0.061	0.215
ω-OH C18:1	3.519 ±	0.763	2.953 ±	0.458	0.251
ω-OH C20	0.583 ±	0.159	0.478 ±	0.073	0.279
ω-OH C22	2.277 ±	0.618	1.909 ±	0.259	0.314
ω-OH C24	0.173 ±	0.012	0.163 ±	0.010	0.213
α,ω-diacids	**4.925 ±**	**1.034**	**6.697 ±**	**1.655**	**0.119**
diacid C16	1.558 ±	0.334	1.366 ±	0.183	0.353
diacid C18	0.691 ±	0.222	0.553 ±	0.082	0.289
diacid C18:1	2.200 ±	0.430	1.888 ±	0.314	0.286
diacid C22	0.211 ±	0.035	0.179 ±	0.027	0.187
AROMATICS	**1.869 ±**	**0.390**	**1.521 ±**	**0.081**	**0.131**
Coumaric acid	1.167 ±	0.311	0.887 ±	0.062	0.127
Ferulic acid	0.701 ±	0.111	0.634 ±	0.095	0.393

Table 8.9 Root suberin composition in *anac058-2* and wild type

Total root systems of 5 weeks old, soil grown plants were investigated. Depicted are amounts of aliphatic suberin monomers in µg per mg root dry weight sorted according to substance classes and carbon chain length (fatty acids (acids), primary alcohols (alcohols), ω-hydroxy fatty acids (ω-OH acids) and α,ω-dicaorboxylic acids (α,ω-diacids)). Mean values and standard deviations were calculated from 4 independent samples of mutant and wild type each. Significant differences were determined by student t-test. For diagram, see fig. 3.12.

monomers	Col		*anac058-2*		*t*-test
	[µg mg^{-1} ± SD]		[µg mg^{-1} ± SD]		
ALIPHATICS	**30.791 ±**	**3.460**	**34.915 ±**	**6.533**	**0.307**
acids	**4.706 ±**	**0.436**	**6.911 ±**	**1.139**	**0.011**
COOH C18	0.118 ±	0.047	0.171 ±	0.126	0.457
COOH C20	0.954 ±	0.128	0.881 ±	0.196	0.560
COOH C22	3.324 ±	0.272	5.262 ±	0.839	0.005
COOH C24	0.429 ±	0.049	0.768 ±	0.125	0.002
alcohols	**2.304 ±**	**0.351**	**2.211 ±**	**0.380**	**0.733**
OH C18	0.871 ±	0.128	0.827 ±	0.161	0.682
OH C20	0.871 ±	0.164	0.803 ±	0.112	0.516
OH C22	0.561 ±	0.064	0.581 ±	0.116	0.774
ω-OH acids	**15.706 ±**	**1.839**	**17.364 ±**	**3.402**	**0.424**
ω-OH C16	2.051 ±	0.224	1.996 ±	0.433	0.827
ω-OH C18	0.612 ±	0.370	0.794 ±	0.135	0.392
ω-OH C18:1	7.904 ±	0.808	8.532 ±	1.775	0.543
ω-OH C20	1.053 ±	0.166	0.943 ±	0.169	0.388
ω-OH C22	3.732 ±	0.312	4.575 ±	0.849	0.112
ω-OH C24	0.353 ±	0.042	0.525 ±	0.066	0.005
α,ω-diacids	**8.076 ±**	**0.858**	**8.429 ±**	**1.628**	**0.715**
diacid C16	2.037 ±	0.229	2.131 ±	0.435	0.716
diacid C18	1.104 ±	0.158	0.984 ±	0.191	0.371
diacid C18:1	4.158 ±	0.436	4.609 ±	0.863	0.388
diacid C22	0.268 ±	0.063	0.257 ±	0.055	0.796
AROMATICS	**4.252 ±**	**1.221**	**4.083 ±**	**0.701**	**0.819**
Coumaric acid	2.556 ±	0.983	2.277 ±	0.282	0.606
Ferulic acid	1.696 ±	0.248	1.806 ±	0.458	0.686

Table 8.10 Root suberin composition in apical root sections of *anac058-1* and wild type

Apical root sections (apical 7 cm) of 5 weeks old, hydroponically grown plants were investigated. Depicted are amounts of aliphatic suberin monomers in µg per mg root dry weight sorted according to substance classes and carbon chain length (fatty acids (acids), primary alcohols (alcohols), ω-hydroxy fatty acids (ω-OH acids) and α,ω-dicaorboxylic acids (α,ω-diacids)). Mean values and standard deviations were calculated from 4 independent samples of mutant and wild type each. Significant differences were determined by student t-test. For diagram, see fig. 3.13.

monomers	L*er* [µg mg^{-1} ± SD]		*anac058-1* [µg mg^{-1} ± SD]		*t*-test
ALIPHATICS	**3.958 ±**	**0.924**	**3.350 ±**	**0.204**	**0.815**
acids	**0.798 ±**	**0.148**	**0.744 ±**	**0.013**	**0.491**
COOH C18	0.273 ±	0.081	0.346 ±	0.072	0.139
COOH C20	0.072 ±	0.021	0.063 ±	0.002	0.447
COOH C22	0.540 ±	0.097	0.512 ±	0.004	0.582
COOH C24	0.186 ±	0.031	0.169 ±	0.007	0.307
alcohols	**0.651 ±**	**0.152**	**0.582 ±**	**0.078**	**0.448**
OH C18	0.139 ±	0.033	0.122 ±	0.013	0.369
OH C20	0.455 ±	0.113	0.409 ±	0.068	0.506
OH C22	0.057 ±	0.008	0.052 ±	0.008	0.367
ω-OH acids	**1.271 ±**	**0.349**	**1.032 ±**	**0.067**	**0.227**
ω-OH C16	0.174 ±	0.053	0.148 ±	0.009	0.358
ω-OH C18	0.021 ±	0.009	0.021 ±	0.004	0.932
ω-OH C18:1	0.605 ±	0.165	0.483 ±	0.024	0.194
ω-OH C20	0.065 ±	0.030	0.037 ±	0.009	0.131
ω-OH C22	0.354 ±	0.082	0.289 ±	0.018	0.179
ω-OH C24	0.052 ±	0.022	0.053 ±	0.010	0.959
α,ω-diacids	**1.238 ±**	**0.298**	**0.992 ±**	**0.070**	**0.161**
diacid C16	0.268 ±	0.062	0.214 ±	0.014	0.139
diacid C18	0.255 ±	0.102	0.207 ±	0.067	0.461
diacid C18:1	0.619 ±	0.129	0.500 ±	0.009	0.118
diacid C22	0.052 ±	0.013	0.038 ±	0.012	0.163
AROMATICS	**0.799 ±**	**0.149**	**0.804 ±**	**0.063**	**0.954**
Coumaric acid	0.149 ±	0.027	0.138 ±	0.029	0.595
Ferulic acid	0.650 ±	0.124	0.666 ±	0.040	0.815

Table 8.11 Root suberin composition in apical root sections of *anac058-2* and wild type

Apical root sections (apical 6.5 cm) of 5 weeks old, hydroponically grown plants were investigated. Depicted are amounts of aliphatic suberin monomers in µg per mg root dry weight sorted according to substance classes and carbon chain length (fatty acids (acids), primary alcohols (alcohols), ω-hydroxy fatty acids (ω-OH acids) and α,ω-dicaorboxylic acids (α,ω-diacids)). Mean values and standard deviations were calculated from 4 independent samples of mutant and wild type each. Significant differences were determined by student t-test. For diagram, see fig. 3.13.

monomers	Col [µg mg^{-1} ± SD]		*anac058-2* [µg mg^{-1} ± SD]		*t*-test
ALIPHATICS	**3.041 ±**	**0.370**	**1.983 ±**	**0.202**	**0.004**
acids	**0.833 ±**	**0.032**	**0.617 ±**	**0.063**	**0.001**
COOH C18	0.437 ±	0.051	0.368 ±	0.114	0.306
COOH C20	0.050 ±	0.006	0.032 ±	0.007	0.006
COOH C22	0.289 ±	0.033	0.233 ±	0.036	0.064
COOH C24	0.494 ±	0.028	0.352 ±	0.097	0.031
alcohols	**0.569 ±**	**0.109**	**0.438 ±**	**0.101**	**0.130**
OH C18	0.100 ±	0.017	0.093 ±	0.030	0.705
OH C20	0.298 ±	0.060	0.228 ±	0.059	0.146
OH C22	0.171 ±	0.034	0.118 ±	0.016	0.032
ω-OH acids	**0.870 ±**	**0.181**	**0.441 ±**	**0.060**	**0.004**
ω-OH C16	0.094 ±	0.019	0.044 ±	0.015	0.006
ω-OH C18	0.010 ±	0.003	0.005 ±	0.002	0.050
ω-OH C18:1	0.451 ±	0.098	0.202 ±	0.028	0.003
ω-OH C20	0.081 ±	0.012	0.063 ±	0.013	0.093
ω-OH C22	0.201 ±	0.042	0.106 ±	0.014	0.005
ω-OH C24	0.033 ±	0.015	0.021 ±	0.006	0.176
α,ω-diacids	**0.770 ±**	**0.117**	**0.487 ±**	**0.087**	**0.008**
diacid C16	0.128 ±	0.021	0.063 ±	0.005	0.001
diacid C18	0.231 ±	0.027	0.144 ±	0.063	0.045
diacid C18:1	0.361 ±	0.071	0.231 ±	0.018	0.012
diacid C22	0.024 ±	0.003	0.019 ±	0.004	0.082
AROMATICS	**1.019 ±**	**0.065**	**0.917 ±**	**0.165**	**0.293**
Coumaric acid	0.199 ±	0.066	0.174 ±	0.030	0.518
Ferulic acid	0.820 ±	0.022	0.743 ±	0.155	0.362

Table 8.12 Root suberin composition in apical root sections of induced *TPT.G* and control plants

Apical root sections (apical 6 cm) of 4 weeks old, hydroponically grown plants were analyzed. Plants were either treated with a 10 µM β-estradiol solution or a mock solution for 8 d before harvest. Depicted are amounts of aliphatic suberin monomers in µg per mg root dry weight sorted according to substance classes and carbon chain length (fatty acids (acids), primary alcohols (alcohols), ω-hydroxy fatty acids (ω-OH acids) and α,ω-dicaorboxylic acids (α,ω-diacids)). Mean values and standard deviations were calculated from independent 4 samples (Col and *TPT.G* mock) or 3 samples (*TPT.G* b-estradiol). Significant differences were determined by student t-test. For diagram, see fig. 3.24.

monomers	Col		***TPT.G*mock**		***TPT.G*β-estradiol**		*t*-test		
	[µg mg^{-1} ± SD]		[µg mg^{-1} ± SD]		[µg mg^{-1} ± SD]		Col - ***TPT.G*mock**	Col - ***TPT.G*β**	***TPT.G*mock - *TPT.G*β**
ALIPHATICS	**1.365 ±**	**0.535**	**1.573 ±**	**0.415**	**1.716 ±**	**0.208**	**0.560**	**0.339**	**0.615**
acids	**0.415 ±**	**0.207**	**0.442 ±**	**0.097**	**0.562 ±**	**0.064**	**0.815**	**0.297**	**0.127**
COOH C18	0.153 ±	0.069	0.189 ±	0.065	0.174 ±	0.037	0.482	0.656	0.746
COOH C20	0.022 ±	0.008	0.026 ±	0.005	0.026 ±	0.003	0.507	0.483	0.926
COOH C22	0.245 ±	0.155	0.253 ±	0.080	0.335 ±	0.084	0.922	0.409	0.247
COOH C24	0.148 ±	0.046	0.164 ±	0.024	0.201 ±	0.045	0.570	0.191	0.214
alcohols	**0.169 ±**	**0.037**	**0.185 ±**	**0.025**	**0.216 ±**	**0.020**	**0.500**	**0.104**	**0.139**
OH C18	0.054 ±	0.016	0.053 ±	0.004	0.069 ±	0.011	0.957	0.232	0.050
OH C20	0.091 ±	0.018	0.104 ±	0.026	0.104 ±	0.006	0.459	0.315	0.990
OH C22	0.024 ±	0.008	0.027 ±	0.008	0.043 ±	0.009	0.523	0.025	0.048
ω-OH acids	**0.424 ±**	**0.181**	**0.533 ±**	**0.213**	**0.505 ±**	**0.073**	**0.463**	**0.506**	**0.835**
ω-OH C16	0.041 ±	0.022	0.058 ±	0.022	0.063 ±	0.012	0.312	0.175	0.725
ω-OH C18	0.007 ±	0.003	0.007 ±	0.005	0.008 ±	0.003	0.984	0.872	0.925
ω-OH C18:1	0.205 ±	0.095	0.249 ±	0.110	0.200 ±	0.024	0.566	0.939	0.495
ω-OH C20	0.017 ±	0.006	0.018 ±	0.006	0.019 ±	0.002	0.816	0.660	0.831
ω-OH C22	0.110 ±	0.046	0.157 ±	0.060	0.135 ±	0.024	0.259	0.427	0.590
ω-OH C24	0.045 ±	0.013	0.045 ±	0.015	0.080 ±	0.017	0.999	0.028	0.035
α,ω-diacids	**0.357 ±**	**0.122**	**0.413 ±**	**0.102**	**0.433 ±**	**0.075**	**0.512**	**0.389**	**0.779**
diacid C16	0.047 ±	0.026	0.065 ±	0.023	0.078 ±	0.022	0.360	0.158	0.468
diacid C18	0.085 ±	0.034	0.090 ±	0.023	0.069 ±	0.018	0.817	0.512	0.251
diacid C18:1	0.174 ±	0.068	0.216 ±	0.070	0.213 ±	0.040	0.421	0.414	0.961
diacid C22	0.007 ±	0.004	0.010 ±	0.003	0.009 ±	0.003	0.274	0.487	0.721
AROMATICS	**0.536 ±**	**0.128**	**0.537 ±**	**0.066**	**0.550 ±**	**0.016**	**0.991**	**0.862**	**0.755**
Coumaric acid	0.075 ±	0.030	0.088 ±	0.032	0.080 ±	0.027	0.533	0.751	0.719
Ferulic acid	0.461 ±	0.124	0.449 ±	0.048	0.470 ±	0.006	0.859	0.911	0.472

Table 8.13 Leaf wax composition in apical root sections of induced *TPT.D*, *TPT.G* and control plants

5 replicates for each genotype and treatment of 6 weeks old soil grown plants were analyzed 2 weeks after β-estradiol induction. Depicted are amounts of wax monomers in µg per mg leaf dry weight sorted according to substance classes and carbon chain length (fatty acids (acids COOH), primary alcohols (OH), secondary alcohols (2-OH), aldehydes (CH_2O) and alkanes (H)). Mean values and standard deviations were calculated from 5 independent samples each. Significant differences were determined by ANOVA Tukey test. For diagram, see fig. 3.29.

monomers	Col		*TPT.D* mock		*TPT.D* β-estradiol		*TPT.G* mock		*TPT.G* β-estradiol		ANOVA - Tukey					
	[µg mg^{-1} ± SD]		[µg mg^{-1} ± SD]		[µg mg^{-1} ± SD]		[µg mg^{-1} ± SD]		[µg mg^{-1} ± SD]		Col-*TPT.D*mock	Col-*TPT.D*β	Col-*TPT.G*mock	Col-*TPT.G*β	*TPT.D*mock-*TPT.D*β	*TPT.G*mock-*TPT.G*β
ALIPHATICS	**2.000 ±**	**0.477**	**2.283 ±**	**0.141**	**1.807 ±**	**0.330**	**1.974 ±**	**0.265**	**1.879 ±**	**0.290**						
acids	**0.314 ±**	**0.078**	**0.327 ±**	**0.050**	**0.286 ±**	**0.058**	**0.281 ±**	**0.039**	**0.327 ±**	**0.057**						
COOH C32	0.123 ±	0.020	0.118 ±	0.033	0.125 ±	0.017	0.116 ±	0.014	0.119 ±	0.014	0.992	1.000	0.984	0.997	0.978	1.000
COOH C34	0.191 ±	0.059	0.209 ±	0.028	0.162 ±	0.042	0.164 ±	0.029	0.208 ±	0.043	0.955	0.802	0.852	0.967	0.401	0.494
alcohols	**0.550 ±**	**0.123**	**0.653 ±**	**0.077**	**0.570 ±**	**0.115**	**0.586 ±**	**0.079**	**0.623 ±**	**0.099**						
OH C27	0.038 ±	0.011	0.074 ±	0.023	0.089 ±	0.044	0.097 ±	0.007	0.098 ±	0.053	0.445	0.149	0.072	0.069	0.953	1.000
OH C28	0.077 ±	0.020	0.123 ±	0.040	0.077 ±	0.022	0.096 ±	0.027	0.062 ±	0.013	0.065	1.000	0.759	0.905	0.066	0.277
OH C30	0.059 ±	0.011	0.068 ±	0.015	0.066 ±	0.013	0.064 ±	0.009	0.071 ±	0.012	0.761	0.883	0.973	0.559	0.999	0.885
OH C32	0.067 ±	0.013	0.058 ±	0.023	0.061 ±	0.011	0.055 ±	0.007	0.064 ±	0.011	0.831	0.950	0.657	0.995	0.997	0.861
OH C34	0.059 ±	0.014	0.044 ±	0.022	0.043 ±	0.008	0.043 ±	0.006	0.052 ±	0.015	0.425	0.370	0.394	0.928	1.000	0.846
OH C36	0.035 ±	0.011	0.051 ±	0.016	0.032 ±	0.012	0.040 ±	0.011	0.024 ±	0.008	0.198	0.998	0.937	0.626	0.119	0.226
2-OH C30	0.044 ±	0.010	0.049 ±	0.009	0.052 ±	0.007	0.051 ±	0.006	0.051 ±	0.007	0.903	0.519	0.000	0.649	0.950	0.000
2-OH C32	0.171 ±	0.049	0.185 ±	0.045	0.149 ±	0.036	0.139 ±	0.019	0.201 ±	0.033	0.974	0.887	0.650	0.727	0.564	1.000
aldehydes	**0.258 ±**	**0.064**	**0.191 ±**	**0.043**	**0.154 ±**	**0.036**	**0.154 ±**	**0.045**	**0.172 ±**	**0.057**						
CH_2O C30	0.059 ±	0.018	0.056 ±	0.009	0.046 ±	0.008	0.047 ±	0.013	0.054 ±	0.016	0.999	0.622	0.660	0.974	0.770	0.939
CH_2O C32	0.108 ±	0.021	0.078 ±	0.022	0.068 ±	0.016	0.064 ±	0.017	0.075 ±	0.024	0.162	0.036	0.020	0.118	0.936	0.902
CH_2O C34	0.091 ±	0.025	0.057 ±	0.013	0.039 ±	0.013	0.043 ±	0.018	0.043 ±	0.019	0.049	0.002	0.004	0.004	0.570	1.000
alkanes	**0.877 ±**	**0.228**	**1.113 ±**	**0.148**	**0.797 ±**	**0.158**	**0.953 ±**	**0.174**	**0.757 ±**	**0.176**						
H C29	0.247 ±	0.062	0.327 ±	0.029	0.330 ±	0.096	0.340 ±	0.054	0.277 ±	0.124	0.526	0.488	0.374	0.972	1.000	0.727
H C31	0.445 ±	0.117	0.564 ±	0.110	0.329 ±	0.060	0.443 ±	0.097	0.341 ±	0.056	0.279	0.298	1.000	0.401	0.005	0.422
H C33	0.185 ±	0.053	0.222 ±	0.039	0.138 ±	0.021	0.170 ±	0.026	0.139 ±	0.016	0.450	0.222	0.951	0.234	0.007	0.606

8.15.3 Fluorol Yellow 088 and GUS staining measurements

Table 8.14 Start of promoter activity in *Prom$_{ANAC058}$::GPF-GUS*, in *Prom$_{HORST}$::GUS* and start of suberin deposition along root length

Distance from root tip to start of GUS activity in *Prom$_{ANAC058}$::GPF-GUS* and *Prom$_{HORST}$::GUS* plants and distance to start of Fluorol Yellow 088 stained suberin in Col was determined. Length of root section without (no GUS or no suberin) and with staining (GUS or suberin) was measured and set in relation to total root length. n=14 for *Prom$_{ANAC058}$::GFP-GUS*, n=3 for *Prom$_{HORST}$::GUS* and n=7 for Col stained with Fluorol Yellow 088 (FY) for calculation of mean and standard deviations (independent samples). For diagram, see fig. 8.2, supp..

	Prom$_{ANAC058}$::GFP-GUS [% ± SD]	*Prom$_{HORST}$::GUS* [% ± SD]	Col, stained with FY [% ± SD]
no GUS/suberin	19.745 ± 5.217	20.798 ± 3.723	20.114 ± 2.031
GUS/suberin	80.255 ± 5.217	79.202 ± 3.723	79.886 ± 2.031

Table 8.15 Suberin deposition in *anac058-1* and wild type seedlings

Suberin was stained with Fluorol Yellow 088 in 6 d old seedlings grown on MS plates. Measuring the length of root sections with different suberization states (no suberin, patchy, continuous) allows the calculation of root section length as percentage of total root length. Mean values and standard deviations were calculated from 5 (L*er* and *anac058-1*) independent seedlings. Significant differences were determined by student t-test. For diagram, see fig. 3.14.

	L*er* [%] ± SD	*anac058-1* [%] ± SD	*t*-test
no suberin	21.554 ± 2.864	24.399 ± 1.054	0.071
patchy	38.526 ± 5.615	51.901 ± 5.477	0.005
continous	39.920 ± 8.270	23.700 ± 6.066	0.008

Table 8.16 Suberin deposition in *anac058-2* and wild type seedlings

Suberin was stained with Fluorol yellow 088 in 6 d old seedlings grown on MS plates. Measuring the length of root sections with different suberization states (no suberin, patchy, continuous) allows the calculation of root section length as percentage of total root length. Mean values and standard deviations were calculated from 6 (*anac058-2*) and 7 (Col) independent seedlings. Significant differences were determined by student t-test. For diagram, see fig. 3.14.

	Col [%] ± SD	*anac058-2* [%] ± SD	*t*-test
no suberin	20.114 ± 2.031	31.696 ± 7.114	0.002
patchy	25.451 ± 6.083	36.976 ± 6.598	0.007
continous	54.435 ± 5.657	31.328 ± 5.346	0.000

Table 8.17 Suberin deposition in *anac058-4 (amiRNAi)* and wild type seedlings

Suberin was stained with Fluorol Yellow 088 in 6 d old seedlings grown on MS plates. Measuring the length of root sections with different suberization states (no suberin, patchy, continuous) allows the calculation of root section length as percentage of total root length. Mean values and standard deviations were calculated from 10 (*anac058-4 (amiRNAi)* and Col) independent seedlings. Significant differences were determined by student t-test. For diagram, see fig. 3.14.

	Col	*anac058-4 (amiRNAi)*	*t*-test
	[%] ± SD	[%] ± SD	
no suberin	17.762 ± 5.296	26.081 ± 7.649	0.011
patchy	26.131 ± 10.427	32.449 ± 8.197	0.149
continous	56.106 ± 13.422	41.471 ± 10.763	0.015

Table 8.18 Suberin deposition in *Prom$_{RALPH}$::ANAC058* and wild type seedlings

Suberin was stained with Fluorol Yellow 088 in 6 d old seedlings grown on MS plates. Measuring the length of root sections with different suberization states (no suberin, patchy, continuous) allows the calculation of root section length as percentage of total root length. Mean values and standard deviations were calculated from 9 (*Prom$_{RALPH}$::ANAC058-20*), 10 (*Prom$_{RALPH}$::ANAC058-17*) or 19 (Col) independent seedlings. Significant differences were determined by student t-test. For diagram, see fig. 3.22.

	Col	*Prom$_{RALPH}$::ANAC058-17*	*Prom$_{RALPH}$::ANAC058-20*	*t*-test	
	[%] ± SD	[%] ± SD	[%] ± SD	*Prom$_{RALPH}$:: ANAC058-17*	*Prom$_{RALPH}$:: ANAC058-20*
no suberin	40.558 ± 6.480	57.774 ± 19.554	50.981 ± 20.025	0.001	0.047
patchy	22.178 ± 5.389	20.617 ± 14.717	21.312 ± 10.405	0.680	0.772
continous	37.263 ± 7.472	21.609 ± 19.238	27.708 ± 12.860	0.004	0.019

Table 8.19 Suberin deposition in induced *TPT.G* and control seedlings

Suberin was stained with Fluorol Yellow 088 in 6 d old seedlings grown for 4 d on MS plates and transfered to MS supplemented with 10 µM β-estradiol or mock solution. Measuring the length of root sections with different suberization states allows the calculation of root section length as percentage of total root length. Mean values and standard deviations were calculated from 3 (Col), 11 (*TPT.G* mock) or 12 (*TPT.G* β-estradiol) independent seedlings. Significant differences were determined by student t-test. For diagram, see fig. 3.26.

	Col	***TPT.G*** mock	***TPT.G*** β-estradiol	*t*-test		
	[%] ± SD	[%] ± SD	[%] ± SD	Col - ***TPT.G***mock	Col - ***TPT.G***β	***TPT.G***mock - ***TPT.G***β
no suberin	38.075 ± 6.144	41.202 ± 6.587	13.788 ± 5.212	0.436	0.000	0.000
patchy	31.093 ± 8.114	27.411 ± 3.848	0.000 ± 0.000	0.224	0.000	0.000
continous	30.832 ± 8.353	31.386 ± 8.210	86.212 ± 5.212	0.888	0.000	0.000

8.15.4 Physiology of *anac058* mutants

Table 8.20 Germination of *anac058* mutants and wild type on 50 mM NaCl

Root length measurement of seedlings grown for 10 d on 1/2 MS and 1/2 MS supplemented with 50 mM NaCl. Mean values and standard deviations were calculated from 22 (Col, control), 21 (*anac058-2*, control), 15 (L*er*, control), 11 (*anac058-1*, control), 26 (Col, NaCl), 39 (*anac058-2*, NaCl), 19 (L*er*, NaCl) and 10 (*anac058-1*) independent seedlings. Significant differences were determined by student t-test. For diagram, see fig. 8.7, supp..

conditions	L*er*	*anac058-1*	Col	*anac058-2*	*t*-test	
	[cm ± SD]	[cm ± SD]	[cm ± SD]	[cm ± SD]	L*er* - *anac058-1*	Col - *anac058-2*
control	2.381 ± 0.540	2.507 ± 0.746	2.738 ± 0.540	2.661 ± 0.399	0.623	0.601
NaCl	2.776 ± 0.863	2.841 ± 0.919	3.580 ± 0.952	3.680 ± 0.644	0.854	0.614

Table 8.21 Growth of *anac058* and wild type seedlings on 50 mM NaCl

Root length measurement of seedlings transferred after 3 d growth on MS and grown for 7 d on 1/2 MS with 50 mM NaCl. Root tip position directly after the transfer was marked with a black dot and total root length of the main root as well as main root length grown only on NaCl medium (dot to root tip) was measured. Mean values and standard deviations were calculated from 23 (Col), 24 (*anac058-2*), 16 (L*er*) and 14 (*anac058-1*) independent seedlings. Significant differences were determined by student t-test. For diagram, see fig. 3.17.

	L*er*	*anac058-1*	Col	*anac058-2*	*t*-test	
	[cm ± SD]	[cm ± SD]	[cm ± SD]	[cm ± SD]	L*er* - *anac058-1*	Col - *anac058-2*
whole root length	3.903 ± 1.537	3.630 ± 1.199	4.679 ± 0.752	4.417 ± 0.691	0.596	0.219
root growth on NaCl	3.571 ± 1.457	3.287 ± 1.111	3.946 ± 0.708	3.801 ± 0.617	0.558	0.455

Table 8.22 Growth of *anac058* mutants and wild type in 50 mM NaCl solution

Plants were grown for 25 d in hydroponics and were transferred to new hydroponics solution (control) or hydroponics solution supplemented with 50 mM NaCl. Plant health was investigated after 2 weeks of NaCl treatment. Root and shoot fresh weight (FW) and dry weight (DW) were measured and root:shoot ratio was calculated from fresh weight and dry weight as well as the fresh:dry weight ratio. Mean values and standard deviations were calculated from 5 (Col), 4 (*anac058-2*), 6 (L*er*) and 3 (*anac058-1*) independent seedlings for control conditions and from 7 (Col), 9 (*anac058-2*), 7 (L*er*) and 8 (*anac058-1*) independent seedlings for salt conditions. Significant differences were determined by student t-test. For diagrams, see fig. 3.18 and fig. 8.8, supp..

plant organ	conditions	L*er*	*anac058-1*	Col	*anac058-2*	*t*-test	
		[mg ± SD]	[mg ± SD]	[mg ± SD]	[mg ± SD]	L*er* - *anac058-1*	Col - *anac058-2*
shoot FW	control	427.967 ± 129.625	433.833 ± 19.621	1051.340 ± 178.422	814.133 ± 351.440	0.942	0.078
shoot FW	NaCl	262.057 ± 131.727	124.700 ± 64.163	923.057 ± 150.974	410.022 ± 176.189	0.021	0.000
root FW	control	252.250 ± 100.681	288.267 ± 15.128	497.720 ± 131.828	383.667 ± 182.690	0.570	0.108
root FW	NaCl	223.571 ± 76.499	164.625 ± 71.878	350.586 ± 81.986	181.722 ± 57.352	0.148	0.000
root/shoot FW	control	0.580 ± 0.110	0.666 ± 0.051	0.470 ± 0.089	0.479 ± 0.125	0.254	0.504
root/shoot FW	NaCl	0.905 ± 0.195	1.417 ± 0.334	0.382 ± 0.075	0.472 ± 0.096	0.004	0.061
shoot DW	control	43.683 ± 11.067	43.067 ± 2.928	100.400 ± 16.504	94.333 ± 32.291	0.929	0.296
shoot DW	NaCl	28.614 ± 10.731	25.975 ± 9.753	86.771 ± 11.870	59.422 ± 14.321	0.626	0.001
root DW	control	13.267 ± 4.933	15.333 ± 1.079	22.800 ± 5.447	18.800 ± 8.663	0.510	0.140
root DW	NaCl	11.200 ± 3.774	8.650 ± 3.619	18.329 ± 3.222	10.522 ± 3.340	0.205	0.000
root/shoot DW	control	0.298 ± 0.051	0.357 ± 0.031	0.228 ± 0.051	0.200 ± 0.066	0.111	0.177
root/shoot DW	NaCl	0.396 ± 0.062	0.329 ± 0.047	0.212 ± 0.031	0.176 ± 0.034	0.035	0.045
shoot FW/DW	control	9.699 ± 0.487	10.125 ± 1.125	10.470 ± 0.447	7.973 ± 7.973	0.437	0.005
shoot FW/DW	NaCl	8.852 ± 1.205	4.549 ± 1.079	10.607 ± 0.380	6.769 ± 6.769	0.000	0.001
root FW/DW	control	18.877 ± 0.892	18.817 ± 0.385	21.747 ± 1.606	20.159 ± 0.817	0.917	0.118
root FW/DW	NaCl	19.924 ± 0.642	18.882 ± 0.507	18.991 ± 1.151	17.324 ± 0.864	0.004	0.005

Table 8.23 Growth of *anac058* mutants and wild type in 1.73 % PEG solution

Plants were grown for 25 d in hydroponics (A) and were transferred to new hydroponics solution (control) or hydroponics solution supplemented with 1.73 % PEG (173 g/l H_20, water potential Δ -0.4 MPa). Plant health was investigated after 4 d of PEG treatment. Root and shoot fresh weight (FW) and dry weight (DW) were measured and root:shoot ratio was calculated from fresh weight and dry weight as well as the fresh/dry weight ratio. Mean values and standard deviations were calculated from 3 (Col, *anac058-2*, L*er*, *anac058-1*) independent seedlings for control conditions and from 6 (Col), 7 (*anac058-2* and L*er*) and 8 (*anac058-1*) independent seedlings for PEG conditions. Significant differences were determined by student t-test. For diagrams, see fig. 3.19 and fig. 8.9, supp..

plant organ	conditions	L*er*	*anac058-1*	Col	*anac058-2*	*t*-test	
		[mg ± SD]	[mg ± SD]	[mg ± SD]	[mg ± SD]	L*er* - *anac058-1*	Col - *anac058-2*
shoot FW	control	104.533 ± 74.673	120.500 ± 96.572	731.900 ± 342.382	553.950 ± 104.461	0.833	0.372
shoot FW	PEG	91.343 ± 32.173	87.025 ± 30.456	158.800 ± 62.121	251.600 ± 79.642	0.794	0.041
root FW	control	63.667 ± 40.360	54.833 ± 32.535	233.133 ± 118.216	178.450 ± 14.004	0.783	0.473
root FW	PEG	41.200 ± 11.197	38.238 ± 13.322	55.317 ± 12.728	59.743 ± 20.428	0.652	0.656
root/shoot FW	control	0.674 ± 0.148	0.518 ± 0.118	0.314 ± 0.015	0.329 ± 0.069	0.231	0.451
root/shoot FW	PEG	0.482 ± 0.140	0.448 ± 0.072	0.417 ± 0.238	0.238 ± 0.043	0.551	0.074
shoot DW	control	10.100 ± 7.151	13.133 ± 8.442	68.533 ± 30.473	50.150 ± 9.703	0.660	0.278
shoot DW	PEG	13.357 ± 4.421	15.313 ± 3.761	31.400 ± 10.562	45.457 ± 11.089	0.371	0.040
root DW	control	3.600 ± 2.100	3.500 ± 1.153	10.800 ± 5.551	8.650 ± 0.929	0.946	0.458
root DW	PEG	6.229 ± 1.884	6.188 ± 1.952	7.950 ± 2.322	9.800 ± 2.765	0.968	0.223
root/shoot DW	control	0.396 ± 0.091	0.313 ± 0.114	0.154 ± 0.013	0.175 ± 0.026	0.377	0.164
root/shoot DW	PEG	0.484 ± 0.114	0.412 ± 0.100	0.267 ± 0.078	0.215 ± 0.025	0.214	0.123
shoot FW/DW	control	10.002 ± 1.403	8.446 ± 1.710	10.567 ± 0.477	11.165 ± 0.271	0.290	0.132
shoot FW/DW	PEG	6.833 ± 0.625	5.583 ± 0.935	4.900 ± 0.871	5.520 ± 0.770	0.010	0.200
root FW/DW	control	17.012 ± 2.232	14.683 ± 4.621	21.608 ± 0.344	21.380 ± 1.474	0.476	0.806
root FW/DW	PEG	6.720 ± 0.734	6.139 ± 0.822	7.113 ± 0.915	6.064 ± 0.973	0.175	0.072

Table 8.24 Root hydraulic conductivity of *anac058* mutants and wild type

Seedlings were grown for 10 d on 1/2 MS, transferred to hydroponics and measured at 3 weeks old. *L*pr is calculated from root sap flow [ml h^{-1}] per applied pressure (MPa) related to root dry weight [g] (for details, see 2.2.4). Depicted are mean values and standard deviations were calculated from 20 (L*er*), 21 (*anac058-1*), 19 (Col and *anac058-4 (amiRNAi)*) and 18 (*anac058-2*) independent plants. Significant differences were determined by Tukey test and p-values for the respective mutants in comparison to their wild type (L*er* and *anac058-1*, Col and *anac058-2*, *anac058-4 (amiRNAi)*) are depicted. For the respective diagram, see fig. 3.20.

	Lp_r	
	[ml g^{-1} h^{-1} MPa^{-1} ± SD]	Tukey test (Lp_r-genotype)
L*er*	119.645 ± 42.714	
anac058-1	128.846 ± 39.712	1.000
Col	143.224 ± 36.228	
anac058-2	97.897 ± 43.752	0.031
anac058-4 (amiRNAi)	137.370 ± 43.394	1.000

Curriculum vitae

Acknowledgment

Special thanks go to Prof. Dr. Lukas Schreiber and Dr. Rochus Franke for admitting me into the research group (Ökophysiology, IZMB, University of Bonn), supporting me during my work on this thesis and always being present with advice and help if needed. I am very grateful to Dr. Rochus Franke for his extensive support in the laboratory and outside, help with experimental setups and result interpretation. Also, giving me the opportunity to attend conferences, international meetings and to work in the INRA institute in France was invaluable.

A lot of gratitude goes to Prof. Dr. Christophe Maurel for allowing me to conduct root hydraulic conductivity measurements in his laboratory (Aquaporin group, INRA institute, Montpellier, France). Also, many thanks go to Dr. Yann Boursiac and Dr. Monica Calvo-Polanco of the same group for incredible help in and outside the lab as well as making this laboratory visit abroad possible, successful and enjoyable. I also want to thank the whole Aquaporin group for the wonderful working atmosphere.

Many thanks go to the Zellbiology group of the IZMB institute (University Bonn, Germany) which allowed me to use their confocal microscope. Especially Dr. Boris Voigt and Claudia Heym were invaluable whenever I had technical questions.

The Ökophysiology group always provided a really pleasant atmosphere, help was always available and many pleasant evenings were spent together. Special thanks go to Dr. Friedrich Waßmann who taught me a lot about laboratory work, was quick to answer every question and was a steady source of fun conversations. I also want to thank Christopher Millán Hidalgo who examined Casparian strips in my *anac058* mutants during his stay in Prof. David Salt's laboratory, Nottingham University, UK. Furthermore, I want to thank Jonas Neblik who documented the growth of my seedlings for 1 month. Many thanks also go to every present and former member in the Ökophysiology group for helping me with laboratory questions and appliances whenever I was at a loss, also for watering my plants whenever I couldn't. Additional thanks go to former colleague Dr. Marc Frenger, who did the preliminary research on this topic and left me such a challenging and interesting project. And a heartfelt thank you also goes to the proof-readers Dr. Viktoria Zeisler, Christopher Millán Hidalgo, Charlotte Petruschke and Tino Kreszies – thank you so much!

The research group Molekulare Evolution, (IZMB, University of Bonn) was always incredibly helpful whenever I had specialized cloning or molecular biology questions and organized great get-togethers – many thanks!

The members of the RootBarriers project which I saw every 6 months for almost 3 years were a joy to meet and provided great input during the early stages of my project. A lot of gratitude goes to all people I talked with during these meetings for interesting and pleasant discussions – scientific, as well as non-scientific ones.

And finally, so much gratitude goes to my family and friends. I am grateful for every time you made me laugh or commiserated with me. Special thanks go to Melanie Brunke, for teaching me so much!

Special thanks also go to my family, which was so great, supportive, incredibly patient and also helped with proof-reading.

Thank you, everyone!